

▲  
**3D  
PRINT  
CANAL  
HOUSE**



*The Structural Feasibility of 3D-printing houses using printable polymers*



A.C. van der Veen  
November 2014

**Cover image:** Artist Impression of the 3D Print Canal House located at the Ranonkelkade in Amsterdam, which is its possible destination. [source: DUS Architects]

# **MSc Thesis – Interim Report**

***“The structural feasibility of 3D-printing houses using printable polymers”***

***“De constructieve haalbaarheid van het 3D-printen van huizen  
gebruikmakend van printbare polymeren”***

**Department of Design and Construction  
Faculty of Civil Engineering and Geosciences  
Delft University of Technology**

**Author:**

A.C. (Arnaud) van der Veen

Student number: 1290452

e-mail: [arnaudvanderveen@gmail.com](mailto:arnaudvanderveen@gmail.com)

**Graduation committee:**

Prof.Ir. R. Nijse, Delft University of Technology

Dr. Ir. F.A. Veer, Delft University of Technology

Dr. Ir. J.L. Coenders, Delft University of Technology

Ir. R. Houtman, Tentech B.V.

Ir. J. Schönwälder, Tentech B.V.

[r.nijse@tudelft.nl](mailto:r.nijse@tudelft.nl)

[f.a.veer@tudelft.nl](mailto:f.a.veer@tudelft.nl)

[j.l.coenders@tudelft.nl](mailto:j.l.coenders@tudelft.nl)

[rogier@tentech.nl](mailto:rogier@tentech.nl)

[julia@tentech.nl](mailto:julia@tentech.nl)

## Preface

This document forms the final report of my graduation study for the Master of Science program of Civil Engineering at the Delft University of Technology. In this report the research to the material properties of a 3D-printable polymer is described, together with a study to the structural behavior geometries that entirely consist of this printing polymer. Based on the performed study, the feasibility of printing a house with polymers can be judged and recommendations for the structural design of printable geometries can be given. As this thesis study forms the first research around the 3D Print Canal House Project, the outcome of this research can serve as a stepping stone for further studies on this topic. For this reason I have tried to uncover the main obstacles within this project which have led to recommendations for the next research steps to perform. Although it seems to be a long road towards the desired end-goal of a fully 3d-printed house, I hope a respectable leap has been taken by the performance of this thesis study.

For me personally, it was a new and enjoyable experience to perform an elaborate research like this. I hope it will be enjoyable to read the outcome of my efforts as well.

Arnaud van der Veen  
Delft  
November 2014

## Acknowledgements

The research that is described within this interim report is carried out in cooperation with the Delft University of Technology, DUS Architects, Henkel and Tentech B.V. At first and foremost, I want to thank Tentech that they offered me the opportunity to work on such an inspiring and challenging project.

Within Tentech, I want to thank Rogier Houtman for his kind interaction and the comfortable working conditions he provided. The freedom and responsibility that was given to me to represent an engineering firm within a building project, was instructive and special for me.

I also especially want to thank Julia Schönwälder for taking up the role of my daily supervisor and fulfilling this role with gusto. No matter how busy she was, she always took the time for me when I was at Tentech, to ask about my progress and help me with specific questions I had. Also thanks for the multiple rides back to Delft after having meetings in Amsterdam.

From the TU Delft, most of my thanks go to Fred Veer. This, because as being the material expert within my committee, he was the closest involved to this thesis in which material research formed the essential part. Because material research only formed a minimum part within my study program of Civil Engineering, performing material research was almost completely new for me. Therefore the guidance Fred Veer gave me throughout the project was really helpful.

Subsequently I want to thank Jeroen Coenders for being part of my committee. Although my research might went in another direction then where his expertise and interests lie, Jeroen Coenders stayed continuously interested and helpful in the progress and improvement of my research. I hope that my research formed a stepping stone for other graduation students to relate computational design topics to 3d printing, as this forms a promising link.

Furthermore I want to thank Rob Nijse for being the chair of my committee. He repeatedly reminded me what my role as a graduating Structural Engineer within a design project should be. Also his shown willingness for supporting me in a rapid execution of my graduation project is something I am thankful for.

From DUS Architects, my thanks go to Hans Vermeulen for his bravery to think beyond the current limits and for organizing meetings together with Tentech and Heijmans on a regular basis. The input I got during this meetings was helpful for the improvement of my thesis. Also, I especially want to thank Sven de Haan for being my contact within DUS Architects. The cooperation with you for fabricating the specimens and blocks went really well and you were willing to defend the need for printing these samples within DUS Architects.

I want to thank Luca Marchese of Henkel for exchanging ideas with me on how to improve the performance of the material and Jordy Vos from Heijmans for interchanging some ideas as well.

I also thank Bob de Vogel, Frans Oostrum and Pieter Droppert for assisting me respectively with the strength-temperature test, creep test and DSC-test and especially Ton Riemslog for assisting me in several tests.

And last but not least, I would like to thank my family and friends for their support during my graduation period.

## Summary

At this point in time, 3D-printing techniques in general, but especially applied for the building industry, still are in a phase of early experiments. One of the experimental attempts is to print a full-scale, three-story high, house in Amsterdam, using an up scaled version of a FDM-printer that is able to print blocks of 1.8 x 1.8 x 3.0 meters using printable polymers. This thesis report focuses on answering the initial structural question that appears around this project, which is a research to the behavior of the currently applied printing material. The outcome of this research will be used to give recommendations for the structural design of printable geometries.

The material research emphasis on obtaining the material properties that are most essential to be known for this particular printing material and the application of the material within this particular building project. These basically are the mechanical (strength) properties of the material and its thermal behavior. Since the FDM-printer lays down the material layer by layer, the hypothesis was that the material would show anisotropic behavior. Therefore the strength properties are researched in different orientations relative to the direction of the printed lines. Furthermore, it was expected that the strength properties would differ for the horizontal plane and vertical plane in which there can be printed, as the resolutions in both planes differ as well.

As a part of this research, there is experimented with two innovative production methods for creating test specimens of complex forms, which are direct 3D-printing and laser-cutting of test specimens. It turns out that direct 3D-printing of test specimens can be a good and quick method for producing complex test specimens, in case the resolution of the applied 3D-printer is accurate enough. For the applied printer within this case study project, it turns out that laser cutting test specimens is the best option, as it leads to a higher dimensional accuracy and a more uniform specimen thickness.

For the vertical printing plane, the material indeed shows clear anisotropic behavior, as the tensile, shear and flexural strength values and the failure modes parallel and perpendicular to the printing direction differ significantly. Material that is printed within the horizontal printing plane shows more isotropic behavior than material that is printed in the vertical plane, due to more and better adhesive connections between the different layers. For the compressive strength it holds that not much difference is noticed between the different orientations, especially because the tested samples are composed of multiple printed layers in both the horizontal and vertical plane. This result leads to an important recommendation to compose printable building-blocks out of 3D-elements instead of only 2D-plate elements, which so far has been the case. This actually leads to a stronger, more isotropic, more homogeneous and therefore better predictable material behavior. Throughout the research this recommendation is further confirmed by outcomes of the absorption test, geometry tests and insulation requirements. The absorption test shows that the material becomes watertight in case multiple printing layers are applied in the horizontal direction. The performed bending and pressure tests on printed geometries demonstrate that geometries, which are build up by a single layer, fail due to local effects: they either fail on local buckling or local bending of an individual member of the geometry or they fail at the location of local inaccuracies, which often occur within printed geometries. The stress level at which these failure modes take place can be significantly increased by composing individual geometry members out of multiple printed layers. Finally, to meet the requirements for heat and sound insulation, a certain wall and floor thickness is required which only can be achieved by printing multiple layers within the horizontal printing direction.

The performed temperature-strength test and DSC-test show that current thermal behavior of the material is the most important point of concern regarding the applied printing material. The material is applied in the rubber phase, it softens at 60 degrees Celsius and already at a surface temperature of 40 degrees Celsius, the material has lost already about 70% of the material strength it has at room temperature. It is obvious that further research on the improvement of the temperature behavior of the building material is essential to make printable polymers suitable for structural applications. Also the comparison with general structural materials and polymers applied in the construction practice, confirms that the printing material in its current form, is not structurally applicable. Furthermore, the comparison shows that the stiffness of the material needs to be improved, as the Young's Modulus is relatively low.

Although the essence of further research should lie on the improvement of the printing material, it still can be valuable to continue the structural design process parallel to the material development. Based on the performed material research, recommendations are given for design improvements. These recommendations can be used as a starting point for a possible future study to the structural design of printable geometries, chambers and complete houses.

**Key words:** 3D-printing, additive manufacturing, FDM-printing, polymers, printable polymers, structural polymers, housing, building engineering, structural design, material research, specimen production, 3D printed specimens, mechanical material properties, thermal properties, material behavior, canal house, 3D print house



# Table of Contents

1.	Introduction.....	1
1.1	Introduction to the project: 3D Print Canal House .....	1
1.2	Reading Guide .....	3
2.	Research Plan .....	5
2.1	Problem Definition .....	5
2.2	Scope of the research.....	6
2.3	Research Objectives .....	7
2.4	Research Question .....	7
2.5	Research Methodology .....	7
3.	Required Material Properties and Research Methods.....	9
3.1	Relevant Conditions .....	9
3.2	Expected Material Behavior .....	13
3.3	Required Material Properties.....	15
3.4	Testing Methods.....	19
4.	Printed and Laser-cut Test Specimens .....	25
4.1	Required Test Specimens .....	25
4.2	Innovative Production Methods for Test Specimens .....	28
5.	Material Tests – Elementary Level .....	35
5.1	Tensile Test.....	35
5.2	Shear Test .....	46
5.3	Compressive Test .....	58
5.4	Determination of the Young’s moduli .....	65
5.5	Determination Density .....	69
5.6	Absorption and Drying Test.....	71
5.7	Temperature – Strength Test .....	74
5.8	Differential Scanning Calorimetry Test .....	81
5.9	Creep Test.....	87
6.	Material Tests – Block/Geometry level .....	97
6.1	Compressive/Buckling Tests.....	97
6.2	Bending Tests .....	111
7.	Overview of Test Results, Grading and Qualification.....	135
7.1	Overview of Test Results .....	135

7.2	Strength Grading and Safety Factors.....	136
7.3	Comparison with other (building) materials .....	139
7.4	Other important properties .....	144
8.	Design Recommendations.....	146
9.	Discussion .....	151
9.1	Scope and limitations of overall Research .....	151
9.2	Usefulness of Individual Research Results .....	151
9.3	Future potential of printing houses in polymers.....	154
9.4	Next steps.....	155
10.	Conclusions and Recommendations .....	159
10.1	Conclusions.....	159
10.2	Recommendations .....	160
	Appendices .....	163
	Appendix I – Determination method average value, characteristic value and standard deviation of test results.....	163
	Appendix II –Inaccuracies in dimension measurements.....	164
	Appendix III – Obtained Material Properties .....	166
	Bibliography.....	175
	List of Figures.....	177
	List of Tables.....	183

# 1. Introduction

These days, there is a growing attention for 3D-printing (or Additive Manufacturing) techniques [3D Printwereld, 2014] [Mobiel.nu, 2014]. While these techniques are already applied for years in the mechanical industry, the development of relatively cheap consumer 3D-printers has given additive manufacturing techniques a new boost. A lot of people nowadays expect a great future for 3D-printing. Some experts believe that these techniques can cause a new industrial revolution and others say that in the future, our buildings and construction works will be printed on the building site.

In spite of these very promising stories about 3D printing in general and 3D printing in the building industry in particular, it seems that these stories so far mainly are based on general progressive belief instead of being founded by research to the actual possibilities of 3D printing in the Construction Industry.

When taking a closer look to the current state of additive manufacturing techniques it becomes obvious that some huge steps need to be taken on technical side before one arrives at a point that printing (parts) of buildings or construction works becomes feasible. Disruptive innovations will be needed both for the 3D-printing techniques itself as in the field of materials science, to give additive manufacturing a future in the building industry. Once printing (parts) of constructions actually would become technically feasible, then still the question remains whether these techniques add value to or reduce costs of building projects.

In all cases, it is clear that large amounts of research and development need to be performed to take further steps. Long-term developments like this require a combination of theoretical and practical studies, for which both theoretical researchers as more practical engineers are needed parallel to each other. At this moment, 3D-printing techniques in general, but especially applied for the building industry, still are in a phase of early experiments. At different places around the world first attempts are made to print houses with the use of a 3D-printer. These first 3D-printed houses probably will not meet all the requirements of general housing and therefore will not function as an actual house, but more as an experimental building or pavilion. These practical and experimental attempts have two main functions: one is that experimenting leads to new knowledge and insights, such that the techniques can be further evolved and another important function is that techniques need certain exposing and imaginative milestones in order to attract enough attention, enthusiasm, people and money to set further steps. Printing a full-scale house is such a milestone that triggers the imagination. One of the experimental attempts to print a full scale house is situated in Amsterdam, where the goal is to print a full-scale, three-story high Canal House. Where in other places around the world there are experiments in printing houses with sand or concrete [D-shape, 2014] [Contour crafting, 2014], the aim in Amsterdam is to print a house out of polymers. Although this is quite an unusual material when it comes to building structures, the choice for this material is made because the conclusion was drawn that 3D-printing techniques currently are most evolved for printing with plastics. Therefore, an up scaled version of an Ultimaker Printer, which is a consumer FDM printer, is build, a building site is furnished and the attempt to reach the milestone of a printed canal house is started.

This thesis study strives to contribute to this particular experiment that is currently ongoing in Amsterdam, by performing early technical research for this 3D-printed housing project. Although technically contributing to one particular test case forms only a small research area, it hopefully is a helpful step within the overall development of what at least is a promising innovative technique.

## 1.1 Introduction to the project: 3D Print Canal House

The Amsterdam architectural firm DUS Architects currently develops together with different partners a Canal House which needs to be made by 3D-printing techniques (Additive Manufacturing techniques). In case of a successful course and outcome, this canal house might become one of the first 3D-printed buildings ever made.

Although in the building industry, one usually only starts with building after the completion of a definite architecture and structural design, this canal house is developed in an iterative way. This means that design and execution go hand in hand and in an experimental way the building will be realized. In this process, DUS closes partnerships with external parties to fill existing knowledge gabs and to be able to set next steps in the project. To bring in knowledge of structural design, a partnership is closed with the Utrecht design- and consulting firm Tentech. They will contribute to the issues in this project that are related to the load bearing structure of this building.

Because so far no structural engineer has studied the structure of this design project yet, all the structural

questions that surround this project are still open. For this reason, this thesis report will focus on answering the initial structural questions that appear around this project.

### 1.1.1 Composition of Canal House

The 3D-printer that is used, which is called the 'De Kamermaker' (English: The Chamber-maker), is capable to print elements with the maximum dimensions of about 1.8 x 1.8 x 3.0 m. Although this certainly is big for a 3D printer, these dimensions are not sufficient to be able to print the house as a whole in one print. Also rooms in these dimensions are not very useful.

For this reason the idea is to build up a chamber out of multiple printable plate- or 3D-elements that together will form a chamber. This implies that it is intended to have as much freedom in shapes and dimensions of the chambers as possible, such that the design freedom is as big as possible and the functional arrangement of the house can be realized in an infinite number of ways. This fact could for example lead to a future situation where every individual will be able to arrange his or her own house to his/her own wishes.

The Canal House will not be delivered completely at one time, but will be built up in phases, chamber by chamber. Furthermore it is desirable that the house is transportable towards every place in the world. On the picture below, the composition of the house in chambers and printable blocks/elements is clarified:

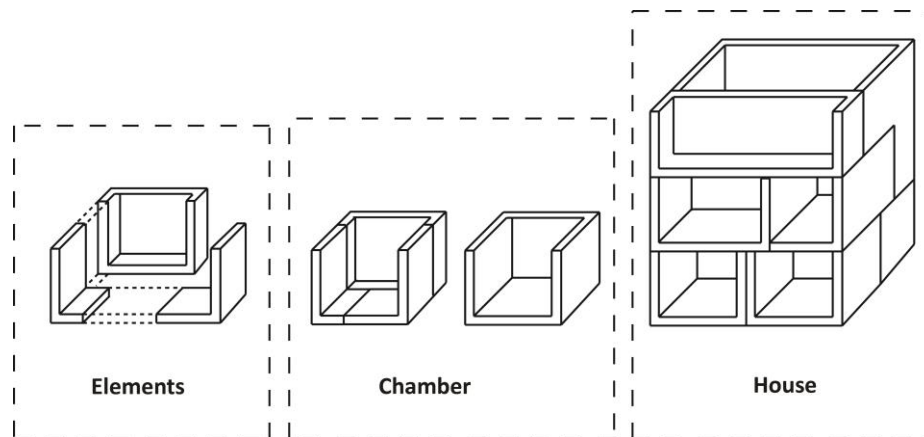


Fig. 1 Composition of the building out of Chambers and printable Blocks/Elements

The main difficulty for this project in structural field, lies in the material use. Because the 'Kamermaker' can only print in (mixes of) plastics, the building will be made in a material that is unusual for the building industry and of which not a lot of knowledge is available concerning the structural behavior and properties.

What makes the current situation even more complex is the fact that the research and development of the ideal applicable printing material is ongoing during the course of this thesis project. This means that at the start of this thesis project, no definite decision has been made on the applied material and its properties.

It may speak for itself that probably even more than in case of other materials, there is an important desire to minimise the use of material, since the costs, building speed and the environment will benefit from this. For this reason it is highly undesirable to apply floor- and wall-elements that are complete solid, so there has to be looked for alternatives. DUS Architects has come with a (provisional) solution in the form of a Honeycomb-structure and relief in the planes (see Figure 2). This current design has to be checked structurally and an exploration needs to be carried out to find out if this design can be further optimized for the purpose of material savings.



Fig. 2 Provisional Block Design in the form of a Honeycomb structure [source: DUS Architects]

## 1. Introduction

### 1.1.2 Integration structure with material and architecture

Within DUS Architects there is an ongoing research on the functional and architectural optimization of the elements/chambers and the building as a whole, so the architectural design is not a fixed given. As mentioned in the previous subparagraph, the applied material is not fixed either. Since the structural solutions should harmonize with the architecture and material use, which are flexible entities, some flexibility should be included in the proposed structural solution as well. This because the structure needs to be applicable as well within the whole range of architectural and material variations.

Exactly because of these expected changes during the project on the domains of architecture and material use, DUS Architects in the end wants to come to an integrated computer model where architecture, material and structure are linked in such a way that in case of a change in the architectural or material parameters, the consequences on the structure are immediately visible, and vice versa.

### 1.1.3 Overview of Structural products/objectives – 3D Canal House Project

To summarize this introduction to the project, the following general overview can be given of end products that should be realised on structural side within the complete 3D Canal House Project:

- Structural Design of the printable Elements
- Structural Design of the Chambers
- Structural Design of the House
- Structural link to an integrated computer model

## 1.2 Reading Guide

After the research plan, that is presented in chapter 2, the actual research starts in chapter 3 with a research to and a definition of the material properties that are required to be known for the purpose of structurally designing a printed house. This chapter ends with a description of the tests that need to be performed in order to obtain the required properties. The output of chapter 3, a definition and selection of the material properties and testing methods, forms the input of chapter 4. Based on the defined testing methods and required properties, the form and dimensions of the required test specimens are determined. After this, an elaborate description is given of the two innovative production methods, 3D-printing and laser-cutting, that are used for creating the required test specimens of complex forms.

In chapter 5, the actual performed elementary material tests are described. Testing methods are given, test results are shown and conclusions based on the results are drawn. After the performed research of chapter 5, the required elementary material properties are known. Next, in chapter 6, material tests will be performed on geometries composed of the printing material. In this way it can be studied whether the elementary results of chapter 5 can be extrapolated to printed geometries and more insight will be gained on failure modes of printed geometries. In chapter 7, first an overview of the test results of chapter 5 and 6 is given. After that these results are further analysed by grading them and comparing them to the characteristics of other materials. Chapter 8 contains design recommendations that are based on the outcomes of the performed material research.

Chapter 9 is the discussion chapter. In this chapter, the performed research is evaluated, limitations are mentioned and the usefulness of results is judged. Also, the future potential of 3D printing houses in polymers is assessed and recommendations for next (research) steps to perform, are presented. Finally, in chapter 10, conclusions of the overall research are drawn and the most important recommendations for design and further research are given.

**This page has been left blank intentionally**

## 2. Research Plan

### 2.1 Problem Definition

By studying the state of the 3D Print Canal House Project at the start of this research, an analysis is made of the problems that are present in the project on structural side. This analysis starts at the overall problem of the project and by zooming in still some further, more tangible sub-problems are obtained. The sub-problems that are discovered in this way, form a good starting point for defining the objectives and scope of this research.

#### 2.1.1 Main Structural problem of 3D Print Canal House Project

The reason DUS Architects has closed a partnership with Tentech in this project, is simply to validate their plans for a 3D-printed Canal House on structural side and to receive structural advice that can be used as input for the further design of the house. This overall problem of verifying the structural design of the Canal House, can be subdivided into the following two main problems:

1. Every Chamber should individually be capable of transferring the loads that are working on it towards the ground/foundation. This, because the building will be build up chamber by chamber.
2. Chambers together should cooperate in such a way that the building as a whole is capable of transferring the loads that are working on it to the ground/foundation.

Important remarks allied to these main problems:

- Since the dimensions of printable elements are limited to 1.8 x 1.8 x 3.0 m, an individual chamber is build up by elements, since these dimensions are not sufficient for printing a whole room in one print.
- It is desired that the house is detachable, on the level of chambers, or even on the level of printable elements.
- It is desired that the house is build up out of printable elements/parts as much as possible. Only there where use of the printer is not sufficient to arrive at a solution that meet the structural requirements, supporting materials and elements can be used to come to a structural satisfactory solution.
- DUS Architects desires to come towards an integrated computer model in which the architecture, material use and structure are coupled in such a way that modifications made in the architectural design or material use automatically leads to changes on structural side, and vice versa.
- There is a wish to, if possible, combine the printable building elements with service ducts.
- As mentioned in paragraph 1.1, the house is designed and built in an iterative way. Therefore, it is important to offer structural solutions that allow some flexibility in choices on the side of architecture and material use.

#### 2.1.2 Further subdivision of the problem

The two main problems that are given in the previous paragraph, resisting the load on chamber-level and on house-level, can be further divided into a list of sub-problems. This list with sub-problems makes the overall problem, and the steps that need to be taken to arrive at the end solution to this overall problem, clearer and more tangible. Notice that the list below contains all structural problems/objectives that exist around the complete 3D Print Canal House Project.

1. Find out the Material-properties/-parameters by performing theoretical and practical material research.
2. Design the optimal (=material minimization) composition of a printable vertical element (wall-element).
3. Design the optimal (=material minimization) composition of a printable horizontal element (floor-element)
4. Mechanically verify the designed horizontal and vertical element
5. Design a printable coupling between vertical and horizontal element.
6. Design a representative printable 3D-element, with a seamless connection between 2d-oriented elements.
7. Determine if supporting materials/elements are required for making the 3D-element.
8. Mechanically verify the designed representative 3D-element.
9. Realize a printable horizontal and vertical span, which means this span is limited to 3.0 m
10. Design connections between printable (3.0 x 1.8 x 1.8) elements, such that rooms can be formed.

11. Realize horizontal and vertical spans  $> 3.0$  m, so these are spans that include a connection between elements.
12. Verify the mechanical behavior of a room composed of independent printed elements.
13. Design connections between individual chambers.
14. Realize the Structural design of the building as a whole, so make sure the linked rooms work together.
15. Verify the mechanical behavior of the building as a whole.
16. Design the foundation of the building.
17. Look for the possibilities to integrate service ducts within the building elements
18. Realize a structural link to an integrated computer model

## 2.2 Scope of the research

Because this research forms the first structural research that has been performed on the overall project, this research focuses on the initial steps that has to be taken in the Canal House project on structural side.

The research has to be started with elementary material research by all means, because without knowing the material properties, designing and analyzing the structure is not possible. So the initial step that needs to be set is easily defined. When the elementary material properties are known, it is important to study whether the obtained properties can be extrapolated towards the blocks/geometries that are designed and printed. Therefore, the second step of this research is to test the behavior of printed geometries and to study their failure modes. The conclusions that are drawn on the basis of this combination of material research on elementary-level and geometry-level, are used to give recommendations for the design of printable geometries and connections between those geometries. Furthermore based on the performed research, a founded judgment can be given of the current and future feasibility of printing structures using printable polymers. As the feasibility of the project is judged, recommendations can be given for the most important directions for future research.

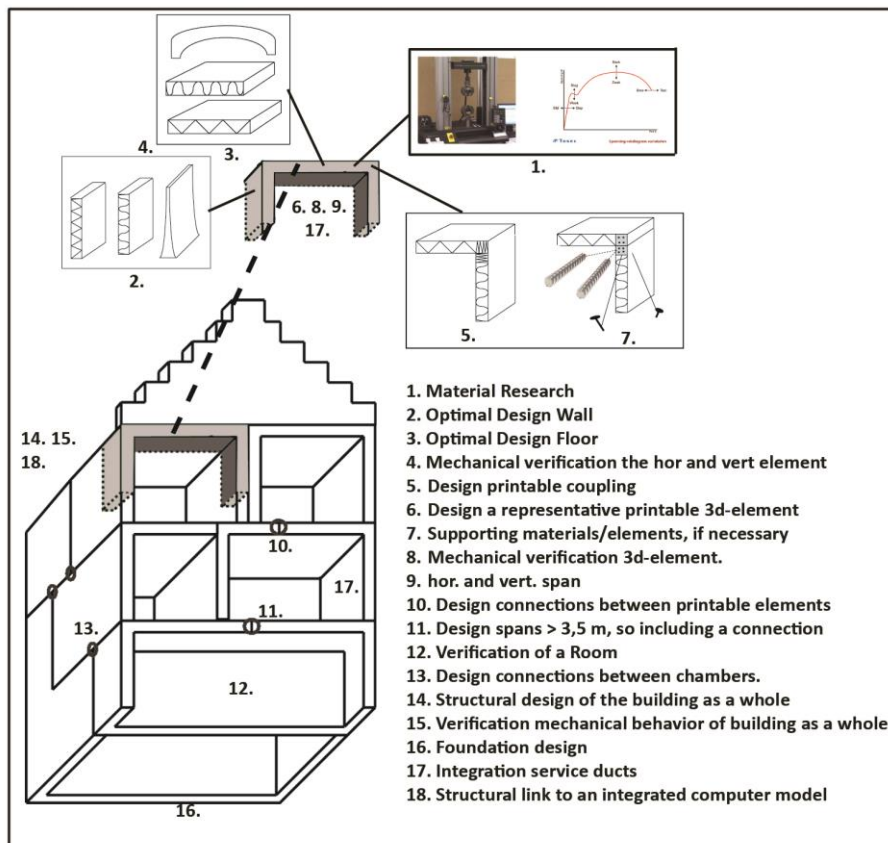


Fig. 3 Visualisation of the structural problems within the Building project



## 2. Research Plan

### 2.3 Research Objectives

With the boundaries of the research area set, the steps which have been taken within the scope of the research can be put under three main objectives:

- Find the elementary properties of the printing material, that are required for structural design with this material.
- Test the behavior of the material on the level of printed blocks/geometry.
- Give recommendations for structural design of an optimal printable, two-dimensional wall- and floor-element and a possible coupling between those two.

### 2.4 Research Question

From the main objectives mentioned in paragraph 2.3, the following three sub-questions for this research follow logically:

1. What are the numerical values of the fundamental material properties of the applied printing material?
2. How does the material behave on the level of blocks/geometry?
3. How does a structurally feasible form and composition of a printable wall, floor and a possible coupling between those two look like?

Answering these three sub-questions will lead to the answer of the main question of this research:

***In what way is it structurally feasible to 3D-print wall- and floor-structures, using printable polymers?***

### 2.5 Research Methodology

In the figure on the next page, the research methodology is presented. At the start of this project, there were plenty of unknowns around the overall 3D Canal House project and especially about the structural questions in this project. Therefore it was essential that the project started with an analysis and definition of the problem, the scope of the research and the main objectives. The research plan, which forms the outcome of this problem analysis, is composed on basis of interviews and meetings with the people around the project and by reading through the (news-)publications that are written about this project.

After the definition of the research plan, the actual research is started. The main objective of the first part of this research is to find the mechanical parameters of the applied printing material. This is done by testing specimens of the material in the laboratory.

The output of the Material-Research part forms the input of the second part, where the elementary material properties are compared to tests results that are obtained by testing printed geometries. By testing printed blocks/geometries, it can be validated whether the elementary material properties can be extrapolated to and used for judgment of printed geometries. Furthermore, the failure modes of the tested geometries enable proper insights in the general structural behavior of printable geometries.

A proper evaluation of the performed research on both elementary level as on geometry level is essential, because the conclusions and recommendations that are drawn based on this research will form the starting point for further studies on this topic. As this thesis forms the first study to 3d-printing of constructions by means of polymers, it is important that the outcome of this research gives direction for future research around this topic.

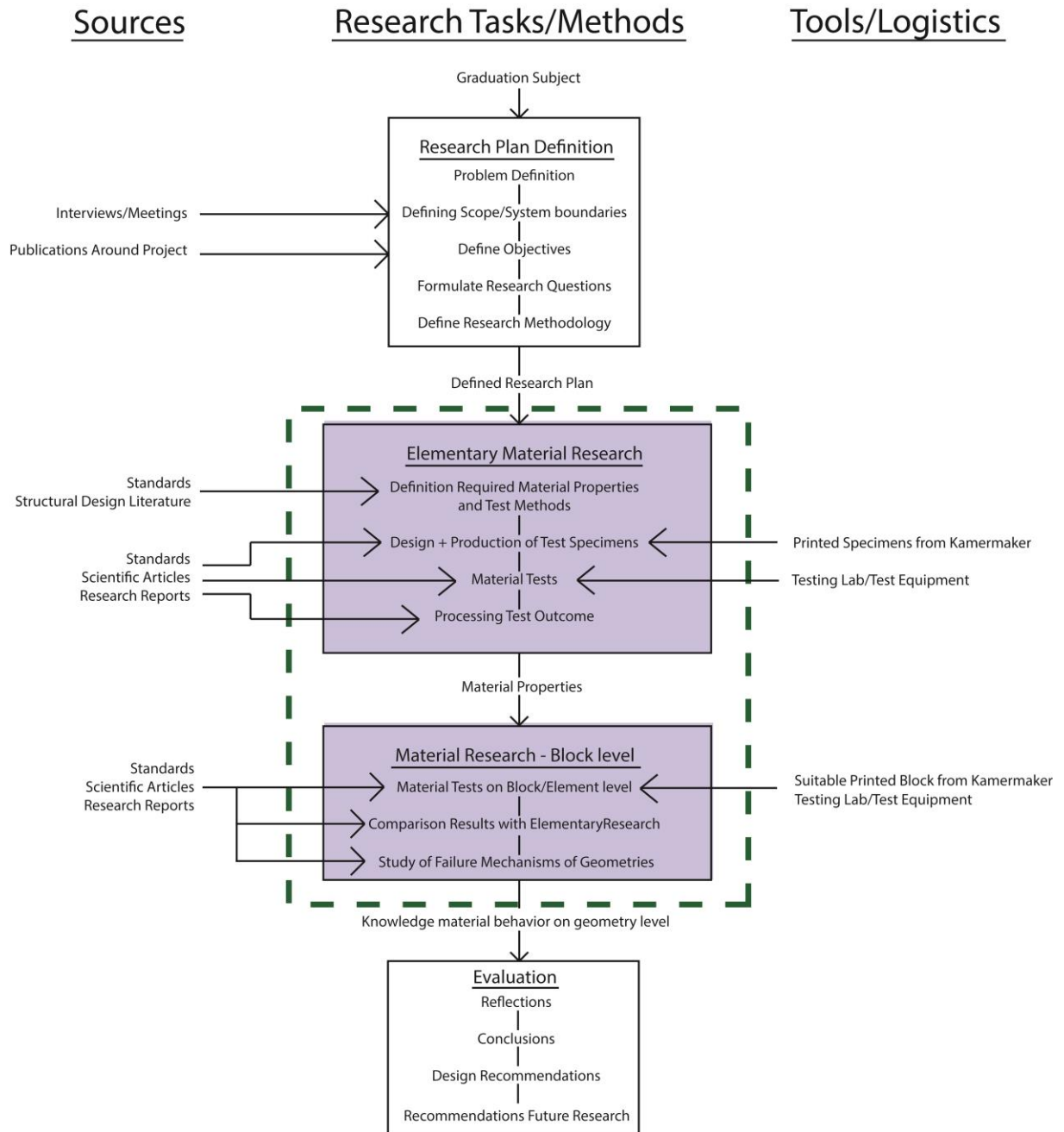


Fig. 4 Research Methodology

## 3. Required Material Properties and Research Methods

As explained in chapter 1 and 2 this research thesis supports an existing building project of which the execution is already ongoing. This means speed (time) and applicability are important factors in this research, which leads to a research approach that will be quite goal-oriented.

For the material properties of the printing material, this means that because of the limited available time and resources, not all existing material properties can be searched for. Instead, a choice needs to be made for the properties that are most essential to be known to suit the aim of this research project and of the overall 3D Print Canal House Project.

The aim of this chapter is to make this choice well-founded and come to a list of parameters that need to be found within this Material Research part. Furthermore the research methods to actually find these material properties are defined.

### 3.1 Relevant Conditions

#### 3.1.1 Function/destination Canal House

In most cases the user function of a completed building forms the essential property, since this is the whole reason one initially decides to develop the building. In the 3D printed Canal House project however, the biggest aim is to experiment with, learn from and develop further the innovative construction method of 3D-printing. Furthermore gaining exposure, exhibiting the building process and final building and involving a lot of parties are important sub-goals which, in turn, further stimulate the technical development of the technique again.

From this it can be concluded that the path towards the final building seems to be more important in this project than the function/destination of the building itself. For the structural analysis and execution of the building it however is necessary to define a certain destination of the building, because the destination influences and defines different rules and regulations in these areas.

The problem that arises here is that there has not been made a well-defined choice yet for the destination of the house and the architect want to leave the options open. In such cases one would normally design the building according to maximum requirements, such that it suits every user function. However, especially this project demands for requirements that are as low as possible because it already will be a challenge to meet the minimum requirements with the used material and construction method. For this reason, in consultation with DUS Architects and contractor Heijmans, it is decided to approach this project in two phases: for the rooms/parts of the building that will be built on a short term, the function defined as “other user functions” is chosen. For the short term, this will be sufficient, since the first rooms of the building will only serve as a small exhibition, comparable to a small pavilion. This choice will lead to the lowest requirements according to the “Bouwbesluit”. For the longer term, the ‘temporary residential function’ (temporary housing) is chosen, which leads to larger, but still relatively low structural requirements and enables the possibility to use the building for more purposes than just a pavilion. The building then for example could be used to let people stay over the night and offers the opportunity to serve as a feasible prototype for new housing instead of being just an exhibition place.

The separation in these two phases is possible, since the building will be realized in an iterative way. So the first rooms that initially serve as an exhibition, will be rebuilt when building up the whole house, such that they meet the higher requirements that are connected to housing.

To summarize:

- On short term, the first rooms will serve as an exhibition place (pavilion), for which the definition “other user functions” from the “Bouwbesluit” can be used.
- On long term, the building will have a temporary residential (housing) function.

### 3.1.2 Context and Circumstances

The circumstances to which the building will be exposed already give a good direction for the material properties that need to be obtained, because the material properties are a numerical expression of the behavior of the material under different conditions.

The Canal House will be developed at the building site in Amsterdam North, at the Badhuiskade 11. So primarily, the building will be exposed to the local circumstances there. When the building is completed, there is the desire to move the building towards a place alongside the nearby Ranonkelkade (such that it actually becomes a Canal House).

The transportability of the house also enables the future possibility to move the house towards expositions all over the world, which makes it hard to predict the exact future circumstances the house will be exposed to.

Because currently there is nothing clear yet about the future possibilities and desire to transport the house towards other places in the world, for now the circumstances of the building site and the first standing place alongside the Ranonkelkade, form the assumed conditions.

This means, that in case the building will be moved towards another place in the world, one should check if the building material/house can resist the local conditions there as well.

At the building site and first stand in Amsterdam the building will be (possibly) exposed to the conditions that are listed below. For every condition, the material property/properties that are linked to the particular condition are directly given.

Conditions	Related Material Properties
Natural Conditions	
Wind	Wind-tightness, mechanical properties (to resist wind load)
Rain	Water absorption, water resistance, corrosion resistance, influence acid rain
Hail	Water absorption, Robustness
Snow	Water absorption, mechanical properties (to resist snow load)
Frost	Mechanical properties under freezing temperatures
Spurting water from river	Water absorption, water resistance
Solar radiation	Radiation absorption, discoloration
Ground Settlements	Deformability/Strain
Vegetation and mould	Mechanical Properties, deformability and Mould resistance
Time	Creep
Temperature differences from -30 to 80 degrees	Mechanical properties under material temperatures from -30 to 80 degrees [Krusche et al., 1982]
Temperature differences inside and outside	Deformability/Strain
Usage Conditions	
People using the building for its purpose (exhibition or housing)	Mechanical Properties (to resist variable loads)
People standing on roof of the building	Mechanical Properties (to resist variable loads)
Furniture and other stuff required to fulfill the function of the building	Mechanical Properties (to resist variable loads)

Special conditions	
Fire	Melting point, glass transition temperature, crystallization temperature, specific heat, heat capacity
Special Loads during construction and usage (e.g. collision, explosion)	Mechanical properties
Other conditions	
Own weight of building	Density, Mechanical properties

**Table 1** Conditions to which the building material will be exposed to and the properties that describe the behavior of the material under these conditions

From the conditions listed in Table 1 it can be concluded that it becomes especially important to study the material reaction to loads, moisture and different temperatures.

### 3.1.3 Influence printing method on properties

The printing process of the 3D Printer will probably lead to different material properties in different directions. Therefore, the printing process and the possible consequential direction-dependent behavior are explained in this subparagraph.

First, since it is a 3D-printer which is used here, there are 3 directions in which there can be printed, the x-, y- and z-direction, and two planes: the xy-plane and the xz-plane.

The possible printing resolution-ranges differ in these two planes, for the reason that when laying down the material, the material will spread due to gravity, before it is hardened. Due to this spreading of the material, the printed lines will become thicker in the xy-direction than in the xz-direction, which lead to less lines per meter in the xy-plane than in the xz-plane and therefore a lower resolution in the xy-plane than in the xz-plane.

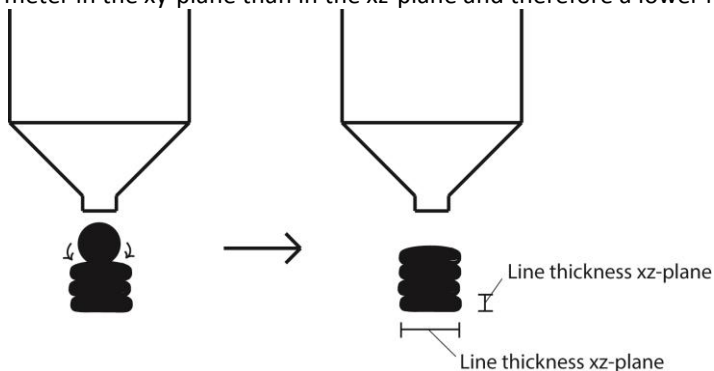


**Fig. 5** Due to gravity and consequential spreading of the material, different line thicknesses and resolutions are obtained in the xy-plane and the xz-plane

The possible adjustable resolution range in the xy-plane is 3.0-6.0 mm, while the line-thickness in the xz-plane is 1.7-2.7 mm. For smaller resolutions the printer head will stick to the material of the previous printed line, which leads to a messy print. Larger resolutions than within the given ranges lead to insufficient connectivity between the layers.

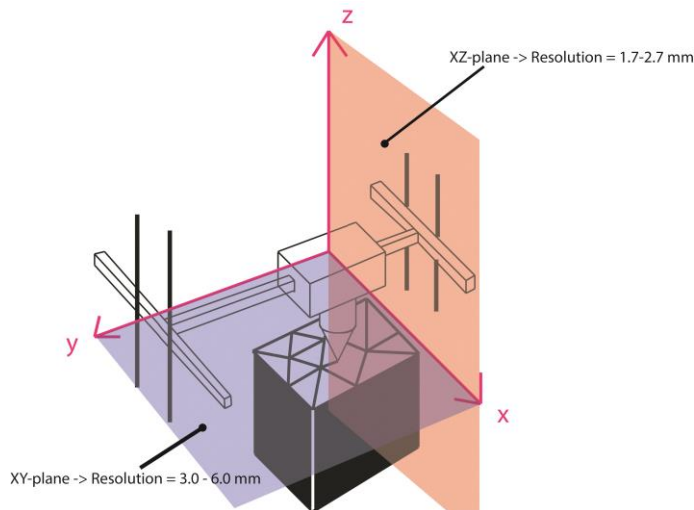


**Fig. 6** The thickness of printed lines can be varied between 1.7 and 2.7 mm in the xz-plane and between 3.0 and 6.0 mm in the xy plane

For a better understanding of these resolutions it probably is useful to explain that setting the resolution in this printer is not just a matter of entering a desired number of millimeters. In fact, there are three parameters that can be set, printing speed, pressure and height of the printer-head, which together determine the line thickness and thereby resolution in which there is printed.

The people of DUS Architects, by trial-and-error, found an optimum resolution in the xz-plane of 2.1 mm. For the xy-plane such a research is not performed, since so far, it never have been the case that two parallel lines in xy-direction are printed in such a way that they connect with each other.

The optimum resolution in the xz-plane was determined, taking into account an optimised compromise between speed maximization, maximization of connectivity between the layers and minimization of the failure chance (failures are: printer head sticks to material or sliding of layers over each other which leads to undesired curvatures and holes in the printed elements).

However, from structural perspective a resolution which is as low as possible, would probably be better, since it is quite likely that the material strength will be higher if the resolution is lower. This consideration was not taken into account during the determination of the optimum printing resolution, so it might be valuable to research the influence of resolution minimisation on the strength of the material.

Apart from the difference in resolution, also differences in connectivity can be expected between the two different directions. Due to gravity, the layers might better connect in the xz-plane, since the gravity force pushes the layers on each other, which is not the case in the xy-plane.

On the other hand also the hardening process might play a role here. When a line is not solidified yet before the line next to it or on top of it will be printed, than the two lines will better connect than in case that the previous line is already solidified. In the xy-direction it is more likely that a line is not solidified yet before the new line next to it will be printed out, because the printer head first prints everything in xy-direction, before it moves in the z-direction to a higher level. What also can have an influence is the end connectivity between the lines which is present in the xy-direction and not in the xz-direction. This will also be advantageous for the strength in xy-direction.

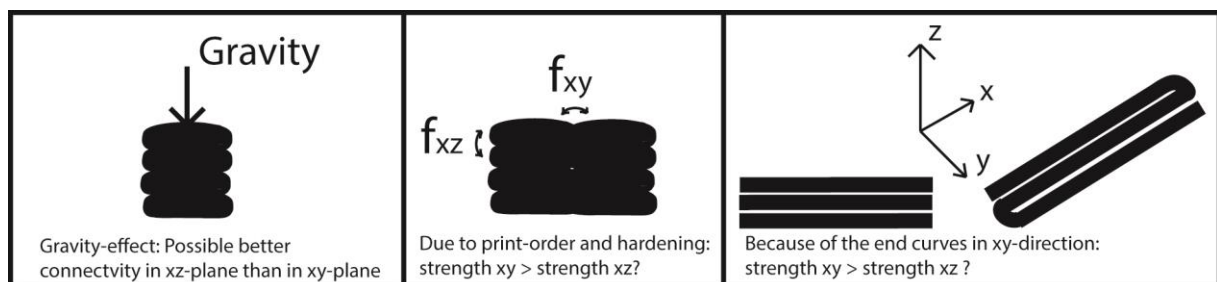


**Fig. 7** These three processes probably cause a difference in layer-connectivity between the xy-plane and the xz-plane

### 3. Required Material Properties and Research Methods

Because of the difference in resolution and the difference in connectivity between the xz-plane and the xy-plane, a difference between the strength in the xz-plane and the xy-plane can be expected.

The hypothesis is that the strength of the material in xz-plane will be higher than in the xy-plane, because it is expected that the higher resolution in the xz-plane and the connectivity between the layers due to gravity will play a bigger role than the other mentioned effects that seemed to be advantageous for the strength in the xy-direction.

Then, within a single plane, also a direction dependent behavior can be expected: Because the printer prints line by line or layer by layer, different strength capacities can be expected in the direction parallel to the printed lines and the direction perpendicular to the printed lines. So the material is expected to be anisotropic within both of the 2D-planes.

So, to summarize: A difference in mechanical properties can be expected between the two planes (xy- and xz-plane) in which there can be printed. Furthermore, within both of the planes it holds that there probably will be an anisotropic behavior.

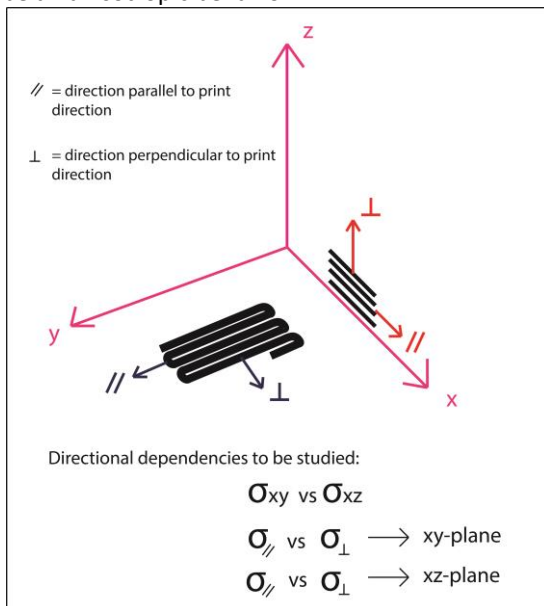


**Fig. 8** A difference in strength properties is expected between the two printed planes and between the 'grain directions'

These directional dependencies all should be taken into account during the material tests, which means for most of the mechanical properties that they have to be obtained for the different directions/configurations.

## 3.2 Expected Material Behavior

### 3.2.1 Particular Printing Material

In paragraph 3.1.3 there was already concluded that the printing material probably will display anisotropic behavior and plane-dependent-behavior. Both properties are caused by the way the material is processed by the 3D-printer.

The fact that a 3D-printer is used that processes the material, also lead to some other predictable material aspects. The 3D-printer works according to the so-called Fused Deposition Modeling (FDM) technique, which processes the material as follows: The printing-material is supplied in granular form and the grains are added to the 3D-printer. The extruder of the 3D-printer subsequently melts the material and by means of a nozzle at the end of the extruder, the material is laid down layer by layer, to become solid again when it is exposed to the open air.

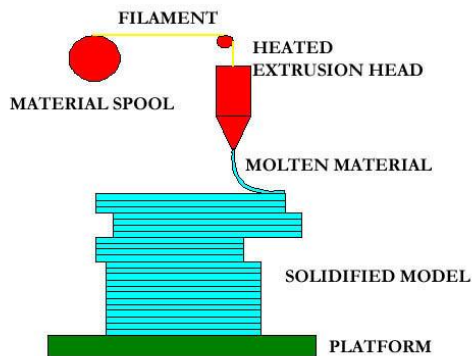


**Fig. 9 Principle of the FDM-technique, which is the applied 3D-printing technique in the Canal House Project [Mechmecca blogspot, 2014]**

This printing process implies that the used material is thermoplastic, with a melting temperature which should be relatively low to enable a fast, smooth and damage-free extrusion/printing process. Because a low melting temperature possibly can lead to quick structural failure due to fire or even already due to sun ray, it is essential to look into the thermal properties of the printed material and also have a look on the influence of the temperature on the mechanical properties.

### 3.2.2 Similarities with other Building Materials

While in other industries like the industrial product design industry, the use of thermoplastic materials is common, the building industry is not familiar with the use of this material type, especially not for structural purposes. To be able to better understand the behavior and properties of the printing material when applied for building engineering, it might be useful to compare certain properties of the printing material, with properties of materials that are commonly used in the building industry.

The anisotropic behavior which is expected for the printed material, is also an important property of timber. So for a good prediction and formulation of the anisotropic properties, it might be helpful to have a look on the anisotropic behavior of timber and make a comparison here.

Like a lot of polymers, it can also be expected that the applied printing material will show visco-elastic creep behavior at room temperature.

For Multiplex plate materials in the timber manufacturing industry, the anisotropic effects often are neutralized by adding multiple layers on top of each other cross-wise. Since directional dependent effects can be expected for 3D printing as well, using multiple layers cross-wise on top of each other perhaps can be a usefully applicable technique as well for the 3D printed material.

From the building industry creep behavior is a known phenomenon, but often not at room temperature already. For steel and glass it holds that the material first needs to be heated up significantly (up to about 500°C), before it shows creep behavior, so under normal circumstances these materials will not creep. Concrete and Timber do creep at room temperature, but unlike polymers, steel and glass, this effect is mainly caused by changes in the water content over time instead of changes in the molecular structure of the material. [Meyers 1999, McCrum 2003]

So the creep behavior of polymers is comparable to glass and steel when looking at the cause of the creep, but comparable to concrete and wood for the circumstances under which creep occurs (normal circumstances). Since the influence of temperature on the mechanical properties will already be studied, it is particularly interesting to study the creep behavior under normal circumstances (so under a constant room temperature), because then it can be checked if creep indeed occurs under any circumstance, instead of only under high temperatures.



### 3. Required Material Properties and Research Methods

The way the material is produced/processed by the 3D-printer is also comparable to the production of glass and steel. Like for glass and steel, the material is heated up to liquefy it, put in the right form and after that becomes solid again when exposed to room temperature.

As is the case for glass and steel, this enables for the printed material the opportunity to give it almost every desirable form which is ideal for architectural and structural configurations. An advantage of 3D-printing compared to the way in which steel and glass are put into the desired forms, is that with 3D-printing, no molds are needed, which makes an quicker, cheaper and tailor-made design possible. A disadvantage of using a 3D-printer instead of casting the liquefied material into a mold, is that the used FDM-technique (line by line printing) in a way also limits the possible form designs, since this production method leads to anisotropic directional behavior as earlier explained, while molded glass and steel are isotropic.

The biggest difference between the printed material and glass and steel of course is the big difference in softening/melting temperatures. While glass and steel only will soften under long exposure to extreme (fire) conditions, the printed material will soften at significant lower temperatures, since the melting and softening point are considerably lower than for glass and certainly for steel.

In general, it is also useful to compare the printing material to other available polymers, because that can help to select or develop a polymer-type that has the optimum properties regarding both the processing-technique of 3D-printing as the application of the material for housing constructions.

To summarize, the following comparisons can be made between the printing material and other, for the building industry common, materials:

Characteristic Printing Material	Material(s) with comparable characteristic
Anisotropic behavior	Timber
Production method cross wise stacked anisotropic layers	Multiplex
Visco- elastic creep behavior	Glass, Steel, Timber and Concrete
From liquid to solid by cooling down towards room temperature	Steel and Glass
General	Other polymers

### 3.3 Required Material Properties

#### 3.3.1 General Required Properties of Building Materials

In paragraph 3.1.1 and 3.1.2 an analysis is made of the function of the building respectively the circumstances to which the material will be exposed. Furthermore, in paragraph 3.2 the printing material is analysed.

Based on these analyzes, a list of material properties is composed for all of which it would be useful to obtain the numerical value by performing material research.

This, because for all of these material properties it actually holds that the value or behavior should be known to be able to guarantee a safe application of the material within a housing project.

Required parameter	Unit
<b>Chemical Properties</b>	
Corrosion Voltage	V
Corrosion Current	A
Acidity	PH
Surface Energy	J/m <sup>2</sup>
<b>Physical Properties</b>	
Specific Mass (density)	kg/m <sup>3</sup>
Melting Point	°C of K
Softening Point (Glass transition Temperature)	°C of K
Heat distortion Temperature	°C of K
Specific heat Capacity	J /m <sup>3</sup> K
Thermal Conductivity	W/(m·K)
Boiling Point	°C of K
Coefficient of Thermal Expansion	-
Released Gases at boiling point	-
Flammability	-
Smoke Number	-
Heat of combustion	J/kg
Flash Point	°C of K
Viscosity	Pa .s
Thermal coefficient of expansion	10 <sup>-6</sup> m/m .K
Vapor Pressure	Pa
Vicat softening point	°C of K
Equilibrium moisture content	%
Water absorption	%
Drying capacity	%
Water Permaebility	m/s
Elongation or shrinkage caused by moisture	Δ l/l
Sound Absorption coefficient	(-)
Light Absorptivity	m <sup>2</sup> /mol
Color	nm
Reflectivity	%
Refractive index	(-)
Polarizability	C·m <sup>2</sup> ·V <sup>-1</sup>
Transmittance	%
<b>Mechanical Properties</b>	
Tensile Strength (ultimate, yield and breaking)	N/mm <sup>2</sup>
Compressive Strength (ultimate, yield and breaking)	N/mm <sup>2</sup>
Tensile Strain/Elongation (at yield, at break, at ultimate strength)	%
Compressive Strain/Elongation (at yield, at break, at ultimate strength)	%

Fatigue Limit	N/mm <sup>2</sup>
Bending Strength	N/mm <sup>2</sup>
Buckling Strength	N/mm <sup>2</sup>
Hardness	KJ/m <sup>2</sup>
Poisson's ratio	(-)
Resilience	J·m <sup>-3</sup>
Shear strength (ultimate, yield and breaking)	N/mm <sup>2</sup>
Shear strain/Elongation	%
Shear Modulus	N/mm <sup>2</sup>
Specific Weight	kN/m <sup>3</sup>
Toughness	J/m <sup>3</sup>
Creep	%/tjtd
Young's Modulus	N/mm <sup>2</sup>
Elastic Limit (Tensile, compressive and shear)	N/mm <sup>2</sup>
Hardening time	time-unit
<b>Dimensional Properties</b>	
Roughness	μ m
Preferred orientation irregularities	-
<b>Electrical Properties</b>	
Dielectric Constant (Permittivity)	F/m
Dielectric Strength	V/m
Electrical Conductivity	S/m
Electromagnetic Permeability	N·A <sup>-2</sup>
Seebeck Coefficient	V/K
<b>Manufacturing Properties</b>	
Embodied energy	J/kg
Embodied Water	m <sup>3</sup> /kg
Reusability	%
Extruding temperature	J/kg
Extruding Pressure	m <sup>3</sup> /kg
Reusability	%
Maximum Printing Speed	m/s

**Table 2** Material Properties that actually should be known in order to guarantee a safe application of the material [Verver et al 2004, McCrum 2003, Kenneth et al 2009]

In paragraph 3.1.3 there was concluded that it is necessary to research possible existing differences of the mechanical properties between the two planes (xy- and xz-plane) in which there can be printed. Also, within both of the planes the possible anisotropic mechanical behavior should be studied. This means for the

### 3. Required Material Properties and Research Methods

mechanical properties from the above table that these properties should be obtained in the 0°, 90° - and 45° - degrees 'grain direction' for material printed in both the xy-plane as the xz-plane.

Next to that, from paragraph 3.2.1 it is concluded that it is essential to research the influence of the temperature on the mechanical properties. This because the low melting temperature of the applied printing material, which is required to make the printing process possible, leads to the hypothesis that the strength of the material may already decline under normal (natural) thermal conditions.

#### 3.3.2 Properties known from Henkel factsheet

The applied printing material is developed by the adhesives/additives-branch of the German company Henkel. Their research for new materials with optimized characteristics for the particular purpose of a 3D-printed house is an iterative and ongoing process over the course of the whole Canal House project.

The particular material that is applied during the execution of this research is called Macromelt 6900E. Before the start of this research till the end of the material research, Macromelt 6900E was the material that was commonly applied on the building site. This material was already developed by Henkel and therefore is not especially made for the application within this 3D Print Canal House project. Based on the knowledge that will be acquired by applying Macromelt 6900E on the building site, by performing material research on Macromelt 6900E within the scope of this Thesis Report and by own further research performed by Henkel, the intention is to improve the Macromelt material or develop new materials with optimized characteristics for the purpose of a 3D-printed house.

For the Macromelt 6900E material, a factsheet is made available containing the following material properties:

Macromelt 6900 E	
Termination	Acid
Bio-based content (%)	77
Softening point (°C)	135 – 145
Heat distortion temperature (°C)	< 35
Melt viscosity (MPas)	–
Melt flow index (g/10 min)	10
Low temperature flexibility (°C)	- 10
Glass transition temperature (DSC) (°C)	5
Tensile strength (N/m <sup>2</sup> )	12.0
Elongation (%)	600
Shore Hardness (A)	90
Impact toughness, un-notched specimen (kJ/m <sup>2</sup> )	No fracture
Density 0.98g/cm <sup>3</sup> , water absorption < 0.5%	

**Table 3 Henkel factsheet for the Macromelt 6900E polymer [Henkel, 2011]**

Although this factsheet already gives an idea of the mechanical material behavior and behavior when exposed to high temperatures, the amount of available properties is insufficient for performing a proper structural analysis on a house or to structurally design a house.

Furthermore, the material is tested by Henkel in another form than in which the material will leave the 3D printer. For example, the dumbbell-formed specimens that are used by Henkel to determine the tensile strength properties, are made by heating up, softening and compressing the material in granulate form

between two steel plates. By this, isotropic (non-directional) material samples are obtained [Marchese, 2014]. This while the material leaves the 3D-printer layer by layer, which means that anisotropic behavior can be expected in practice. Also for other tests it is expected that the material after being printed, will demonstrate other behavior and property-values than in the granular form as it is tested by Henkel.

For these reasons, it is essential to perform a material research on the material in its printed form, before a structural analysis of the printed house can be performed. The available data of the Macromelt 6900E that is mentioned on the factsheet of Henkel will be used throughout this research to compare the values that are obtained within this research with. By this comparison, it will also become possible for future applied materials to give a prediction of the material behavior of the material in printed form, based on the performed research by Henkel on the material in its granulate form.

### 3.3.3 Selection of properties

From all the properties that are mentioned under paragraph 3.3.1 it would be useful to obtain the value, since for all these parameters holds that the value should be known to be able to guarantee a safe and predictable behavior of the material within the housing project. However, for a faster evolution of 3d-printing within construction contexts, it is desired to set steps as quick as possible. Research should not be unnecessarily in-depth in early phases of development. This, because the long duration of in-depth research can lead to a loss in value of this research for practical applications, as the practice might be evolved quicker. Theoretical and practical developments should go hand-in-hand as much as possible, especially during the conceptual phases of a new technique. Therefore, there is chosen to emphasis this material research on the material properties that are most essential to be known for this particular material and the application of the material within the particular project of the 3D Print Canal House. Based on the results of the material research, it should be possible to give a proper advice to the designing parties and to take next steps both practically as theoretically.

Of course the basic mechanical properties of the material, which are the tensile strength, the shear strength and the compressive strength, are essential to be known when using the material for making a structural design. Furthermore in paragraph 3.1.3 it is explained that the material might have different mechanical properties for the xy-printing-plane and the xz-printing plane and within both printing planes also a different mechanical behavior is expected parallel to the direction of the printed lines and perpendicular to this print direction. Since this orientation behavior can really influence the application of the material and the designs, it is essential to study the relations between the mechanical properties and those orientations.

Then, explanation of the FDM-printing-technique in paragraph 3.2.1 teaches us that for this material it is important as well to study the relationship between the mechanical properties and the temperature, since it is expected that the temperature behavior of the material might be critical. This because the printing process demands for a quick softening and melting material, which can mean that the strength of the material degrades already at low temperatures as well.

To obtain more precise values of the temperatures at which the material starts to soften and melt, a DSC-test also need to be performed, because else it stays vague what kind of behavior can be expected in case of high and extreme temperatures.

Because a building often is exposed to long-term loadings, the mechanical creep behavior should be mapped as well. A basic physical property to obtain is the material density, as this value is used in the mechanical calculations.

Finally, because the material will be exposed to rain and snow, the water resistance or absorption of the material is studied.

The tables below give an overview of the properties that are found to be essential for this material and project and therefore are studied within this material research:

3. Required Material Properties and Research Methods

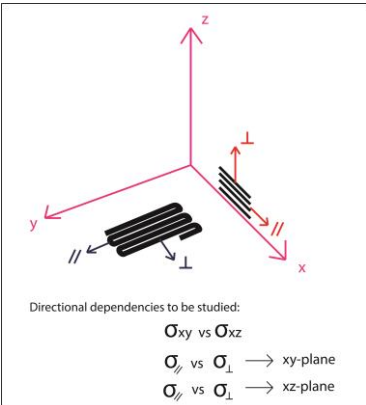
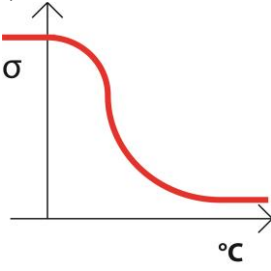
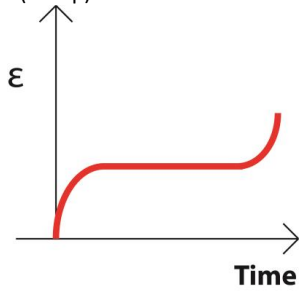
Mechanical Properties	Unit	Required Test	Studied Parameters of influence	Required Test
Tensile Strength	MPa	Tensile test	<p>Different Orientations:</p>  <p>Directional dependencies to be studied:  <math>\sigma_{xy}</math> vs <math>\sigma_{xz}</math>  <math>\sigma_{//}</math> vs <math>\sigma_{\perp}</math> → xy-plane  <math>\sigma_{//}</math> vs <math>\sigma_{\perp}</math> → xz-plane</p>	Regular Tensile, Shear and Compressive Tests
Tensile Breaking Strength	MPa	Tensile test		
Tensile Yield Strength	MPa	Tensile test		
Elongation at Tensile Strength	%	Tensile test		
Elongation at Break	%	Tensile test		
Young's Modulus	MPa	Tensile test with Extensometer		
Shear Strength	MPa	Shear Test		
Compressive Strength	MPa	Compressive Test		
Compressive Yield Strength	MPa	Compressive Test		
Compressive Strain	%	Compressive Test		
			<p>Temperature:</p>  <p>Time (Creep):</p> 	<p>Temperature-Strength Test</p> <p>Creep Test</p>

Table 4 Overview of mechanical material properties that are essential to be known for this building project

Physical Properties	Unit	Required Test
Density	g/cm <sup>3</sup>	Density Test
Water Absorption	weight %]	Absorption and Dry Test
Melting Point	°C	DSC
Softening Point (Glass transition temperature)	°C	DSC
Specific Heat Capacity	J/m <sup>3</sup> K	DSC

Table 5 Overview of physical material properties that are essential to be known for this building project

3.4 Testing Methods

### 3.4.1 Tensile Test

The goal of the tensile test will be to find the different tensile properties, which are the ultimate tensile strength, the tensile breaking strength, the yield strength and the elongation of the material at its maximum stress point and at the breaking point.

All these properties need to be found both for material that is printed in the xz-direction as for material printed in the xy-direction. Furthermore within both printing planes, also the difference needs to be researched between the tensile strengths in the 'grain direction' and perpendicular to this grain direction.

For performing a tensile test, test specimens in the form of a dumbbell need to be used. Common dimensions [NEN-EN 12814-2, ch. 6, p. 10-12] for these plastic dumbbell-samples are:

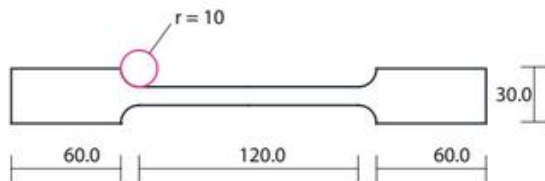


Fig. 10 Common dimensions for a dumbbell specimen [NEN-EN 12814-2, ch. 6, p. 10-12]

Due to the low printing resolution and therefore thick printing lines, using the dimensions of the displayed sample above, would lead to an unsatisfactory sample quality. Therefore there is chosen to increase some of the dimensions, as can be seen on the picture below that shows the definite dimensions:

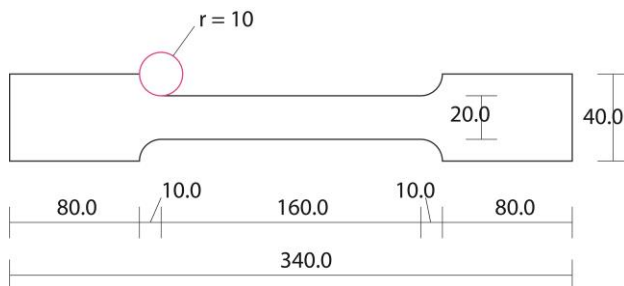


Fig. 11 Due to the low printing resolution, the dimensions of the specimen shown in Figure 10 are enlarged to obtain more satisfactory specimen results

The test specimen will be clamped over the width parts of the sample, within a tensile testing machine. The computer program that is connected to the machine, will register and plot the applied tensile force against the displacement of the upper head of the machine. By adding the dimensions of the particular test specimen, this force-displacement curve can be converted into a stress-strain curve. Then, from this stress-strain curve the required tensile material properties can be obtained.

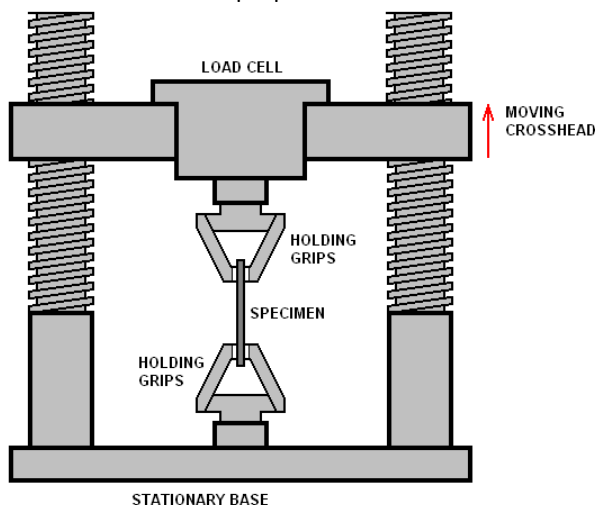


Fig. 12 Test setup of the tensile test [Engineering archives, 2014]

### 3. Required Material Properties and Research Methods

#### 3.4.2 Shear Test

As the name of the test already reveals, the aim of this test is to find the shear strength of the printing material. Like is the case for the tensile test, again the shear strength properties should be studied for material printed in both the printing planes. Also the shear strengths need to be found both parallel as perpendicular to the 'grain'-direction.

It is most common to use one of the following kinds of test samples for the performance of a shear test:

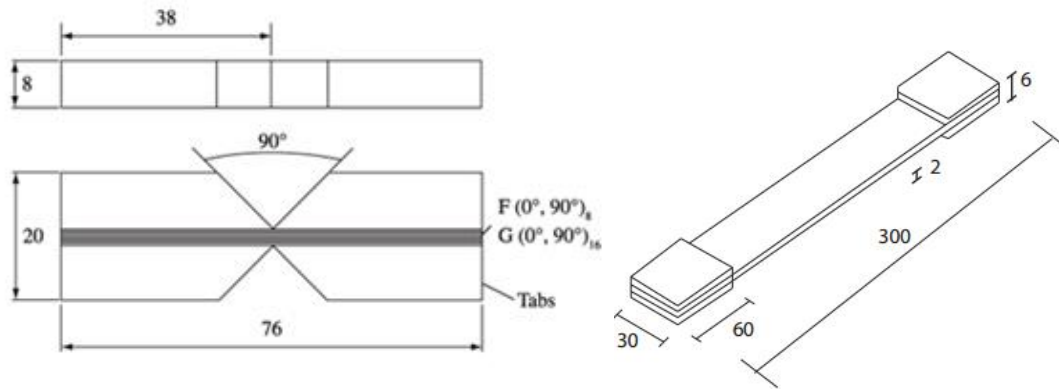


Fig. 13 Common used specimens in a shear test [Scielo Brazil, 2014]

A big disadvantage of these kinds of samples however is that they require a specific and complex testing setup with multiple required attachments for the testing machine:

#### *Interlaminar V-notched shear test*

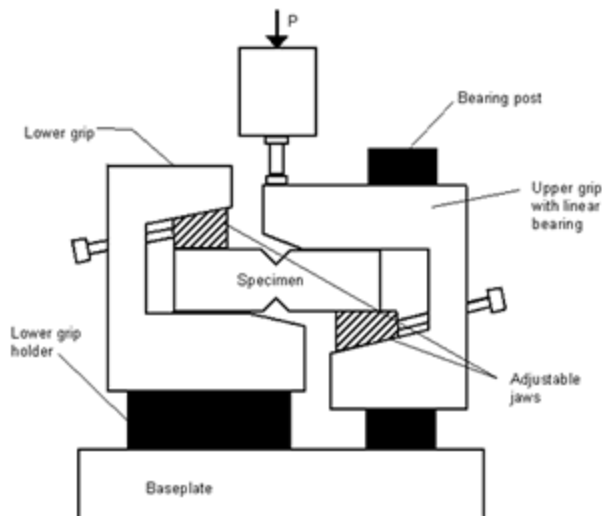


Fig. 14 Applying the usual shear specimens requires specific and complex tools [Vircon Composites, 2014]

From [Bao et al, 2004], the following kind of sample with a butterfly gauge-section is known, which requires a much easier test setup, since it can be simply clamped in a testing machine like is done for tensile specimens:

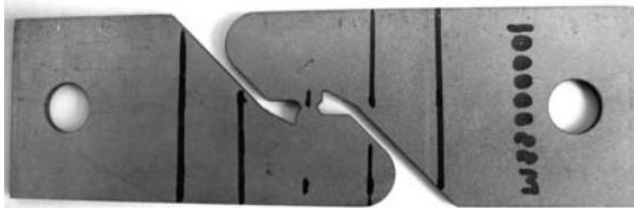


Fig. 15 Alternative shear specimen with a butterfly formed shear area. This specimen can be tested within a regular tensile test device, without the need of complex tools [Tarigopula, 2008]

The disadvantage of these kinds of samples usually is, that it is hard to obtain samples within this specific sample-form. Therefore, in practice, often still is chosen for the easier sample forms and more complex testing method.

However, the innovative production method of 3D-printing enables the opportunity to easily fabricate samples in every desired form. So the mentioned disadvantage seems to be eliminated by using 3D-printing, while the advantage, a simpler test setup, remains intact.

For that reason, there is chosen to make the samples in the form and dimensions according to the sample-dimensions as used in [Reyes, 2009], that are shown on fig. 16.

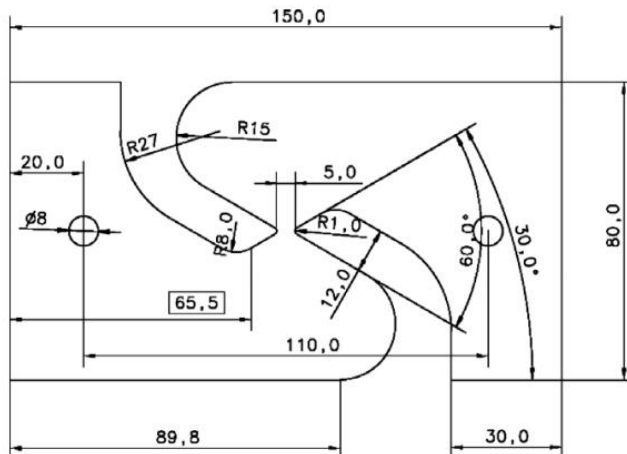


Fig. 16 Dimensions of the shear test specimen [Reyes, 2009]

Because of this specimen form, it now should be possible to easily clamp these specimens in the same testing machine as is used for the tensile test. By doing this, the shear test can be performed and the stress-strain curve including the shear strengths can be obtained in the same way as is done for the tensile test.

### 3.4.3 Compressive Test

The goal of the compressive test is to obtain the compressive strengths of the material. For performing a compressive test, a three-dimensional sample needs to be used. For that reason, this time not the distinction is made between the two-dimensional xz- and xy-plane. Instead, a 3D sample will be printed that needs to be tested on strength differences in all of the three directions.

Because it is useful to be able to use the same kind of sample for testing all three of the directions, a sample with the same dimensions in every direction is desirable. Therefore a cubical sample of 50x50x50 mm is used.

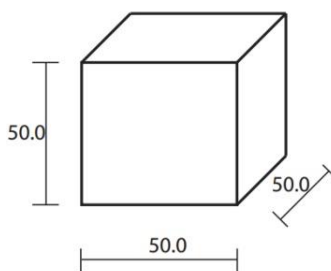


Fig. 17 Solid cube test specimen for the Compressive Test

The sample will be tested in a compressive machine with a head that moves downstairs and that can deliver a compressive force to the sample via a compressive plate.



### 3. Required Material Properties and Research Methods

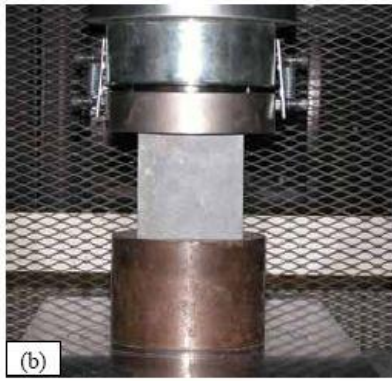


Fig. 18 Test setup for the compressive test [Federal Highway Administration, 2014]

#### 3.4.4 Tensile Test with Extensometer

The stress-strain curves of the regular tensile and compressive tests probably will not be accurate enough for determining the Young's Modulus from the linear-elastic part of the graph. Therefore extra tensile tests are performed using an extensometer. This extensometer measures the elongation over a small gauge length very accurately, such that more reliable results for the determination of the Young's Modulus, can be obtained.

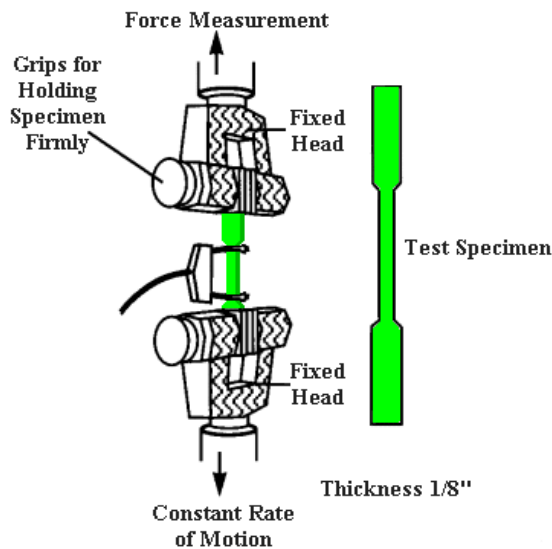


Fig. 19 Test setup for the determination of the Young's Modulus. An extensometer is applied to perform an accurate measurement over the gauge area [Mathweb, 2014]

This test has been performed for the different printing planes and for specimen parallel and perpendicular to the grain, such that the Young's Modulus will be obtained for all these different orientations.

#### 3.4.5 Absorption and Dry Test

The Absorption and Dry test are performed to find the water absorption percentage and drying ability of the printing material. Both the absorption and drying ability are expressed in a percentage against time.

The absorption test is performed by putting a cubical sample in a bucket and fill the bucket with water, until the water level reaches half the height of the sample. After this, the mass of the sample is weight every 24 hours [NEN-EN 15801, ch. 8, p. 7] such that the absorption percentage over the time can be studied.

The drying test is done by entirely immersing a sample during a week, such that it becomes fully saturated with water, if possible. After this week, the sample is dried and the mass is measured every 24 hours. By this, the drying percentage over time is obtained.

#### 3.4.6 Determination Density

The density is determined by making use of Archimedes' law, by immersing a test sample in a glass that is filled to the brim. By doing this, an amount of water equal to the volume of the test sample will flow over the edges of the glass and will be collected by a bucket in which the glass is placed. By using measuring cylinders, now the

amount of overflowed water can be measured and by dividing the mass of the tested sample by this water volume, the density is obtained.

### 3.4.7 Temperature-Strength Test

As mentioned in paragraph 3.2.1, in particular for this material, it is important to have a look at the influence the temperature has on the mechanical properties of the material. When this temperature influence would be studied for all the mechanical properties, this test would become unnecessarily elaborate. Therefore the choice is made to only look at the influence of the temperature on the tensile strength of the material. By this, it already is possible to obtain a good impression about the influence the temperature will have on the strength of the material in general.

This test is performed by using 12 of the same rectangular samples and clamp them within a tensile testing machine. This time, a tensile machine is used in which the specimen and clamps are situated within an oven. The tensile test will be performed for all of the 12 samples under a different temperature, such that 12 different stress-strain curves will be obtained. By changing the oven temperature with constant intervals, it is possible to obtain a graph in which the tensile strength can be plotted against the temperature.

From [Virginia edu, 2014] the hypothesis is obtained that such a graph probably will have a form like this:

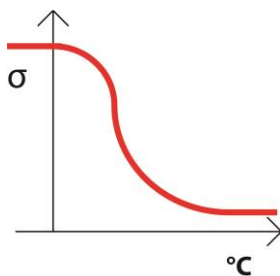


Fig. 20 Common form of a temperature-strength curve

### 3.4.8 Creep Test

The creep test is performed to study the deformation of the material under a constant load over time. Although the hypothesis is, that the tensile creep probably can cause bigger problems than the compressive creep, it can be interesting to both look at the creep behavior under a constant compressive load as under a constant tensile load. Therefore, for both loading cases an available test set-up should be used that enables the opportunity to apply a constant and permanent load on the sample during a considerable period of time.

The form of the test specimens will then be entirely dependent on the particular test setups that are available. In all cases the creep effect can be measured by measuring the material elongation or shortening after certain (often logarithmic) time intervals. Intervals of 1, 10, 100, 1000 and 10.000 minutes will be used here. The deformation can be measured using strain gauges, an extension meter, or less accurate, using a caliper gauge.

The creep test probably leads to a result like is displayed in the graph below [Betten, 2008]:

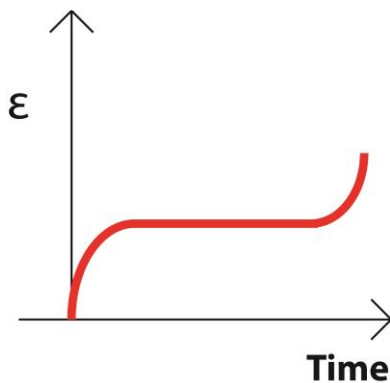


Fig. 21 Common form of a creep curve

## 4. Printed and Laser-cut Test Specimens

### 4.1 Required Test Specimens

#### 4.1.1 Basic forms

In paragraph 3.4 the different test methods and required test specimens are mentioned. An overview of the required test specimens is given on the picture below:

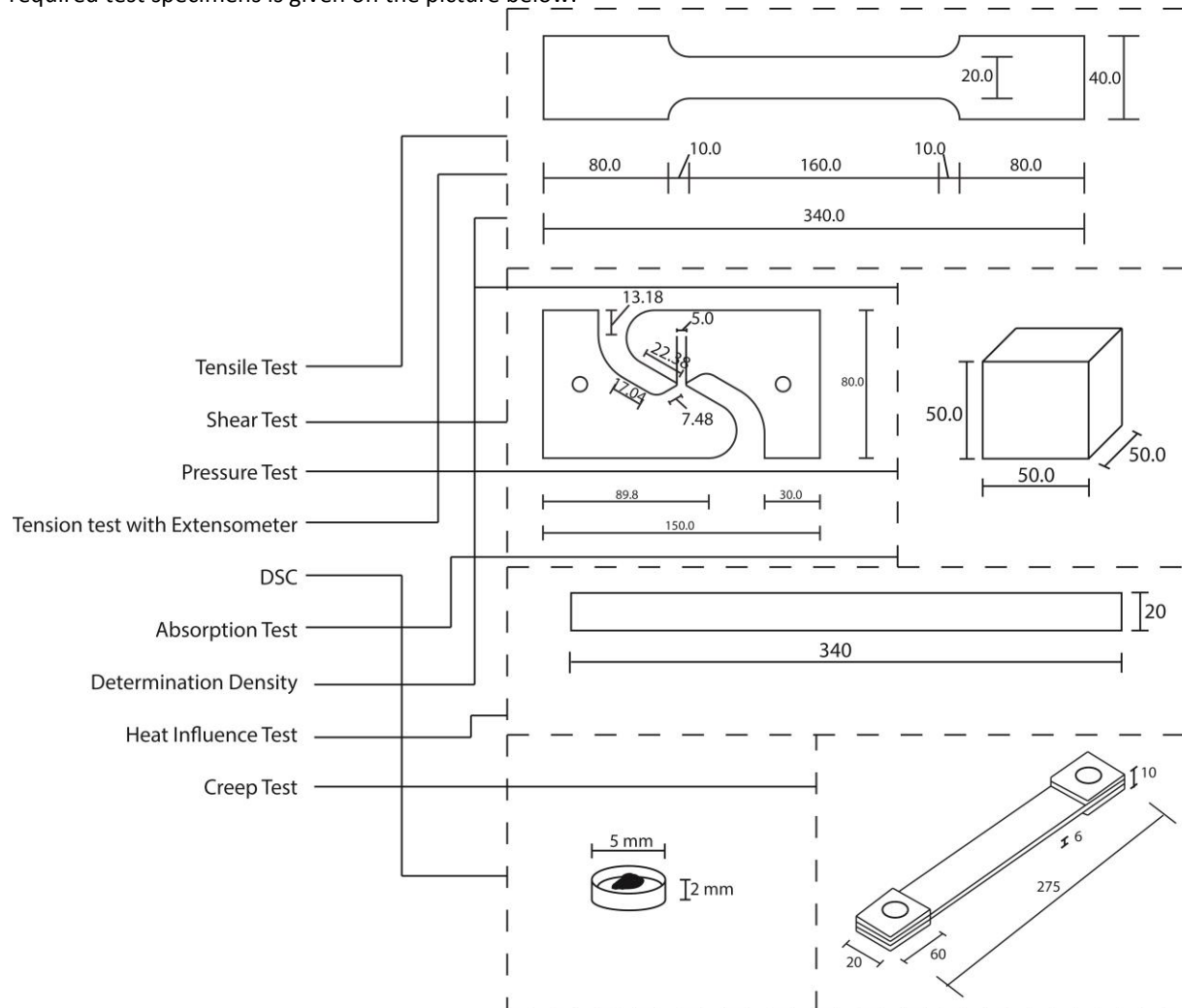


Fig. 22 Overview of the required specimens for the different tests

As already explained under paragraph 3.4, for the tensile test there is chosen for the well-known dumbbell-shaped-sample and for the pressure test for a common cube-formed sample. The reason that for the shear test, there is chosen for this quite unfamiliar and complex-shaped sample is because this sample requires a much simpler test setup. Since the innovative production method of 3D-printing enables the opportunity to fabricate samples in every desired form, 3D printing offers the advantage that complex sample-forms can be easily fabricated such that the testing method for the shear test can be simplified.

#### 4.1.2 Variation of printing parameters

In paragraph 3.1.3 it is explained that the printing method leads to the following parameters that possibly have an influence on the mechanical behavior of the material:

- A difference in mechanical properties is expected between the xy- and xz-plane in which there can be printed.
- The material probably will show anisotropic behavior.
- Different resolutions can be set.

To test if these three factors indeed influence the mechanical behavior, the properties of some of the test

specimen that are drawn in paragraph 4.1.1 should be varied such that these three possible parameters of influence will be included. So at first, this means that the samples used to test the directional dependencies should be printed both in the xy- and the xz-plane and within these both planes, also with a grain-direction of 0°, 90° and 45°. Furthermore it is desired that the print resolution is varied.

Based on the three printer parameters (plane-direction, grain-direction and resolution) the following different specimen-variations should be made for the tensile- and shear-test samples, in order to be able to test the influence of these three factors on the mechanical properties of the material:

1. Printing Plane

2. 'Grain'-direction

3. Resolution

			max. resolution: line thickness = 3.0 mm
			'perfect' resolution: line thickness = 4.2 mm
			min. resolution: line thickness = 6.0 mm
			max. resolution: line thickness = 3.0 mm
			'perfect' resolution: line thickness = 4.2 mm
			min. resolution: line thickness = 6.0 mm
			max. resolution: line thickness = 3.0 mm
			'perfect' resolution: line thickness = 4.2 mm
			min. resolution: line thickness = 6.0 mm
			max. resolution: line thickness = 1.7 mm
			'perfect' resolution: line thickness = 2.1 mm
			min. resolution: line thickness = 2.7 mm
			max. resolution: line thickness = 1.7 mm
			'perfect' resolution: line thickness = 2.1 mm
			min. resolution: line thickness = 2.7 mm
			max. resolution: line thickness = 1.7 mm
			'perfect' resolution: line thickness = 2.1 mm
			min. resolution: line thickness = 2.1 mm

**Table 6** Different specimen-variations that should be made for the tensile- and shear-test in order to test the influence of the printing plane, the grain-direction and the resolution on the mechanical properties of the material

Since, the compressive test-samples have the form of 3-dimensional cubes, there is no question of a printing plane in which the samples are print. Furthermore, the grain direction can be varied, by just turning the cube-sample 90 degrees. What should be varied however, are the different resolutions in which the samples can be printed. The following resolution-variations can be important to study for this matter:

	<b>Resolution xy-plane</b>	<b>Resolution xz-plane</b>
	'perfect' resolution: line thickness = 4.2 mm	'perfect' resolution: line thickness = 2.1 mm
	'perfect' resolution: line thickness = 4.2 mm	min. resolution: line thickness = 2.7 mm
	'perfect' resolution: line thickness = 4.2 mm	max. resolution: line thickness = 1.7 mm
	min. resolution: line thickness = 6.0 mm	'perfect' resolution: line thickness = 2.1 mm
	min. resolution: line thickness = 6.0 mm	min. resolution: line thickness = 2.7 mm
	max. resolution: line thickness = 3.0 mm	'perfect' resolution: line thickness = 2.1 mm
	max. resolution: line thickness = 3.0 mm	max. resolution: line thickness = 1.7 mm

**Table 7** The following resolution-variations should be studied for the compressive samples, in order to study the influence of the resolution on the compressive strength

## 4. Printed and Laser-cut Test Specimens

### 4.1.3 Considerations concerning the parameter-variations

To obtain proper test results, multiple samples should be made of all of these different sample-variations. However, the problem here is that the 'Kamermaker'-3D-printer is only made available for a limited amount of printing hours, because the printer also needs to be used to print out building blocks for architectural studies and for expositions on the building site. Also, adapting the resolutions was mentioned by DUS as undesirable, since it is time-consuming to vary the printer properties all the time and the chance would be quite high that using unusual resolution-properties would lead to failed and unusable specimen-results. For these reasons, in consultation with DUS Architects, it is decided to not vary the resolution of the specimens, such that the amount of specimens that needs to be printed, reduces significantly. Instead, the resolutions in both directions that were found by DUS as being optimal (see paragraph 3.1.3), are chosen for all the specimens.

Given the fact that this resolution is optimum taking into account the printing speed, minimization of the failure chance and also connectivity (which has a direct relationship with the strength), it is quite likely that these optimum DUS-resolutions indeed are the best resolutions to print in. So the choice that is made to not test different resolutions might not be critical.

Still, it is important to be aware of the fact that the exact quantitative relationship between resolution and strength is an unknown factor in this project, which means no statement can be made about the exact change in mechanical behavior when the decision is made to increase or decrease the resolution in which the material is printed. Only hypotheses can be made here.

Because the resolution in the xy-plane was considered not to be sufficient to obtain proper specimens for the shear-test in the dimensions as given under paragraph 4.1.1 (4-6 mm), the decision is made to increase all the dimensions of the shear-test-samples by a factor of 2, which leads to the dimensions as shown in figure 23. Using a smaller 3D-printer with a higher resolution instead of the Kamermaker, for example a regular Ultimaker printer, unfortunately was not possible, since the obtained result in that case would not be representative for the printing process within this project.

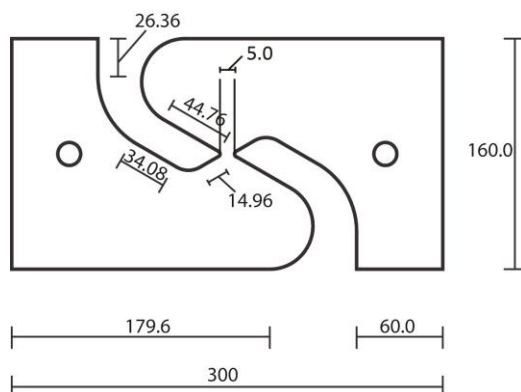


**Fig. 23** The original dimensions of the shear-specimens are doubled for the specimens that are printed within the xy-direction, since the resolution of the printer was not sufficient for printing the specimens in their original size

### 4.1.4 Production methods

To fabricate these test samples it was desired that all the test-samples would be printed out in the desired form directly, such that no further manual operations would be needed afterwards. Unfortunately the 3D-printer is not able to print spans/cantilevers, since the printing material always needs to be supported by the printed layers underneath. In xy-direction this doesn't form a problem, because the samples are printed out in the horizontal floor-plane, which of course doesn't require spans. In the xz-direction however, it obviously is not possible to directly print-out the samples in the desired forms, since both the dumbbell-samples as the shear-samples contain unsupported/cantilevering parts.

This problem is solved by printing out a number of plates in the vertical direction where later on, the samples can be cut out from.

These two different production methods are further described in the following paragraph.

## 4.2 Innovative Production Methods for Test Specimens

### 4.2.1 Production Method 1: Printing Test Specimens

As explained before, the use of a 3D-printer seems to be ideal for manufacturing test specimens since the 3D-printer offers the big advantage that almost every desired sample form can easily be created. Since more complex sample forms can lead to easier test setups, using a 3D-printer for creating test samples could be a good opportunity to simplify and optimize the overall material testing process.

Furthermore also more standard specimen-forms could be obtained easier than usual, because the sample can be directly printed in the desired form without the need of any further manual operations.

Since using a 3D-printer to manufacture test samples is done very little before, this forms quite an unexplored field. Given the opportunities that this fabrication method can have for improving and optimising the testing process, it is really worth it to try out this innovative method of printing out test specimens.

As explained before, only in the xy-plane it is possible to directly print out the test samples. This, because in contrast to the xz-plane, printing in the xy-plane doesn't require unprintable spans or cantilevers to be obtained, since the print is made in the flat horizontal plane that is supported by a floor plate.

Therefore from the specimens that are mentioned under paragraph 4.1.2, only the samples in the xy-plane are created according to the production method of direct 3D printing.

To obtain the final samples by direct 3D printing, the following steps need to be taken:

**Step 1:** Drawing of the different sample-forms in CAD-program that enables the option to export the file with a .stl-extension (e.g. AutoCAD, Rhinoceros)



**Fig. 24** 3D-cad designs of the test specimens

**Step 2:** Drawing in the printing-paths within the sample-outlines using the same CAD-program but a different drawing-layer. By this, the printing direction, and thus the grain direction of the sample can be set. In this phase it of course is important to take into account the feasible resolution, since this determines the amount of printing lines that are possible in both directions within the sample.

This particular 3D-printer, prints continuously and doesn't enable the possibility to have intervals in which it doesn't print. Therefore, the only option to directly obtain single samples would be, to create a different printing file for every single sample. This would be a very time-consuming process for the fact that setting up the printer cost for a new printing round cost quite a lot of time. Therefore connective lines between the samples are added such that all the samples can be printed out in one printing job.

It is also important to be aware of the fact that the impossibility to print in intervals, limits the amount of forms that can be printed. This because only forms that can be build up by a single continuous printing line, can be obtained by the Kamermaker.

#### 4. Printed and Laser-cut Test Specimens

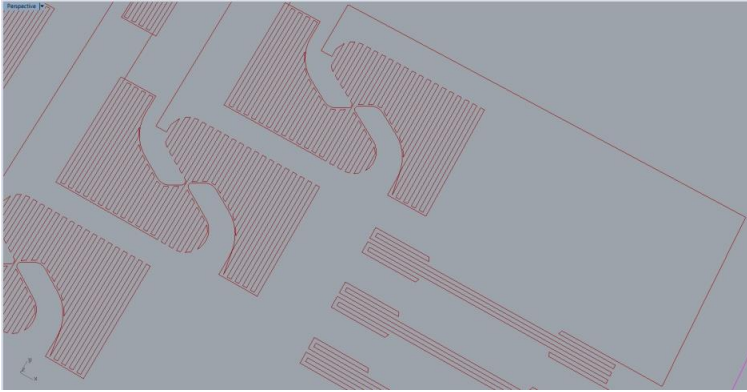


**Fig. 25** Cad-drawing of the path that need to be followed by the printer head

**Step 3:** Saving/exporting the file under the .stl-extension and open it within the software program Octoprint [Octoprint, 2014]. Within Octoprint, the printer resolution can be set by adapting the printing parameters speed, pressure and height of the printer head. For all samples a resolution of 2.1 mm is used here that is obtained by iteratively change the three printing parameters till a satisfying result was obtained. As earlier explained, this resolution is not varied but hold constantly for all the specimens. Once the file is opened in Octoprint and the parameters are set, then the printing process can be started and controlled via Octoprint.

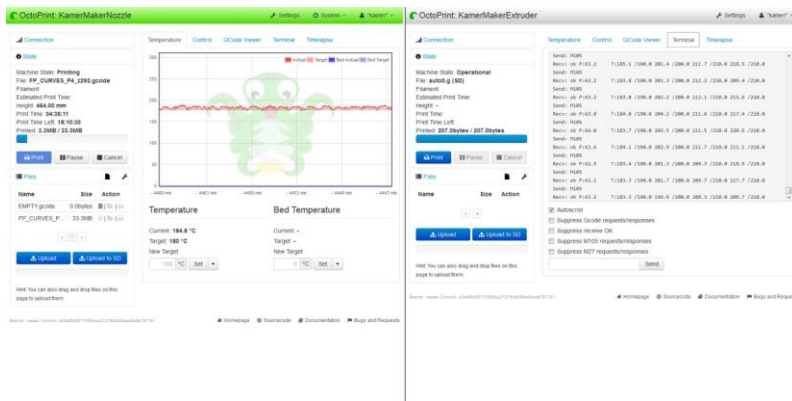


**Fig. 26** Screenshot of Octoprint, the software-program in which the printer can be controlled. The printer resolution can be set in this program by adapting the printing parameters speed, pressure and height of the printer head.

**Step 4:** Printing out the samples. Although this process goes automatically, the printing technique is not fully constant and reliable, such that undesired deviations and failed prints can always occur. For that reason it is recommended to keep a small eye on the printed output during the printing process.



**Fig. 27** Shear-specimens printed within the 'KamerMaker'

**Step 5:** Sawing the connective lines between the samples. And in the case of the shear-samples, holes need to be drilled in the sample. Now the final samples are obtained.

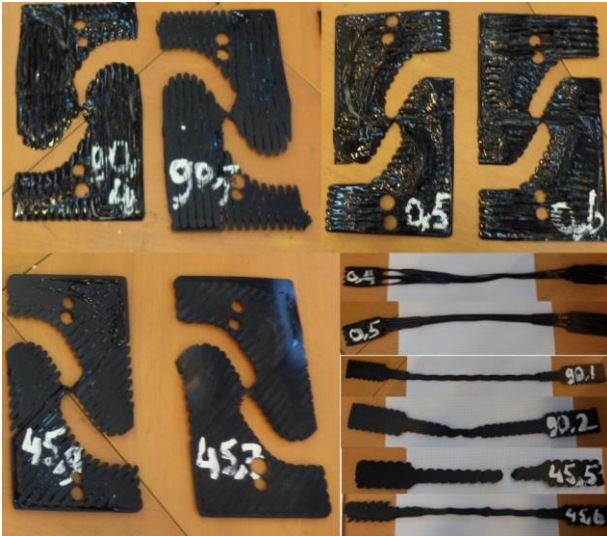


**Fig. 28** Final result of the samples that are directly printed by the 'Kamermaker' within the xy-plane

As can be seen on the pictures of the results, the quality of the created test specimens is not very accurate. This is because of the following reasons:

- The printing resolution in the xy-direction is, with a line-thickness of about 5-6 mm, quite low, which results in samples that are only build up out of a few lines. Another consequence of the low resolution is that the contour lines are non-straight.
- So far in the 3D print Canal House Project, all printed blocks are build up such that in the xy-plane only single lines are printed all the time. Therefore, before printing these samples in xy-direction, there was no experience at all to print lines in the xy-direction that connect to each other. This fact, also has contributed to a lower sample quality. Although in future, the resolution parameters can be optimized in the xy-direction, still the quality/accuracy of printed samples in this direction will stay relatively low because the printing resolution, although optimized, still will be lower than the resolution in the xz-plane.

Within the xy-direction, so far only single layers have been printed



**Fig. 29** Within the building project, so far only single lines are printed within the xy-direction. So printing connecting parallel lines in the horizontal plane, like is done for the samples in Figure 27, was a novelty

- The fact that the printer is only able to print continuously without the possibility of stopping intervals, limits the possibilities for printing line configurations. This sometimes goes at the cost of the printed quality as well, because sometimes printing line solutions have to be chosen that are not optimal from the viewpoint of accuracy, just because the printer can only print continuously.

#### 4.2.2 Production Method 2: Laser-cutting Test Specimens

As explained before, in the xz-plane it is not possible to directly print out the test samples due to the fact that no spans/cantilevers can be obtained with this 3D-printer.

Therefore, for the samples that needs to be printed in the xz-plane, a different fabrication method is conceived: By first printing out vertical plates in the xz-plane and after that cut-out the samples out of the plates with a computer-controlled laser-cutter, samples printed within the xz-plane still can be obtained.



#### 4. Printed and Laser-cut Test Specimens

This fabrication method required the following steps to be taken:

step 1: Studying the maximum dimensions of a plate that can be cut in the used laser-cutter.

Step 2: Drawing plates with the measured dimensions in a CAD-program and add all the samples that need to be obtained to this plates. The plug-in Rhinonest of the program Rhinoceros can be used to automatically place the samples within the plates as efficient as possible. In this way, the number of plates that need to be printed is determined and minimized. Next to that, this cad-file will also be used under step 6, where the laser-cut-jobs will be executed.

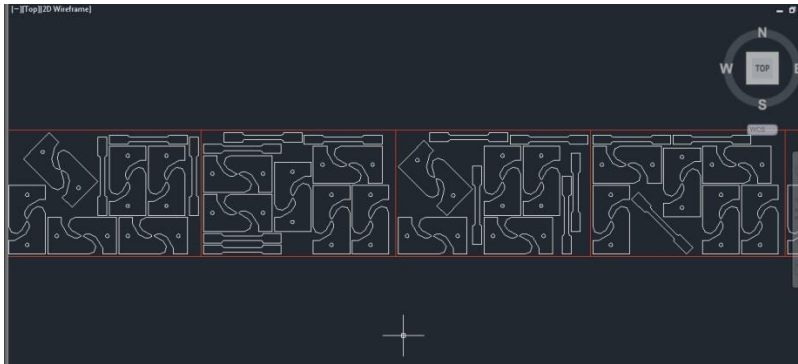


**Fig. 30** Efficient division of the specimens over the plates that will be printed within the xz-direction

Step 3: Now that the size and the number of plates are determined, a printable 3D-structure, that contains the required plates, needs to be designed using a cad-program. The reason that a 3D-structure needs to be printed, is that a single vertical plate will not be stable on its own so it will sag or fall over when printed individually. By combining the plates into a 3D structure, the plates will stabilize each other.

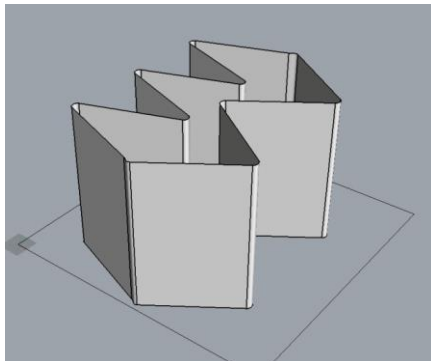


**Fig. 31** Printable structure consisting of the required plates out of which the specimens can be cut later on

Step 4: The .stl-file of the 3D-structure can now be send to the 3D-printer. Again it is important to keep an eye on the printing process, to prevent the print job from failing.

For this research, the printing process partially failed, because within the designed structure, the plates were not supported enough. As a consequence, the plates did not become completely straight in the z-direction. Instead, curvatures arose in the plates due to the fact that printed lines were sagging in the horizontal direction. This sagging was caused by a lack of support in the horizontal directions. In future this problem can be tackled by adding more supports in the horizontal direction perpendicular to the plate, such that the spans within the plane of the plate, become smaller.

Step5: When the 3D-structure is printed, the plates have to be separated from each other and from an occasionally help-structure by using a suitable saw.

Because big parts of the plates for this research had curves in it, the plates where further sawn into smaller pieces, to separate useful straight parts of the plate from curved parts of the plate.

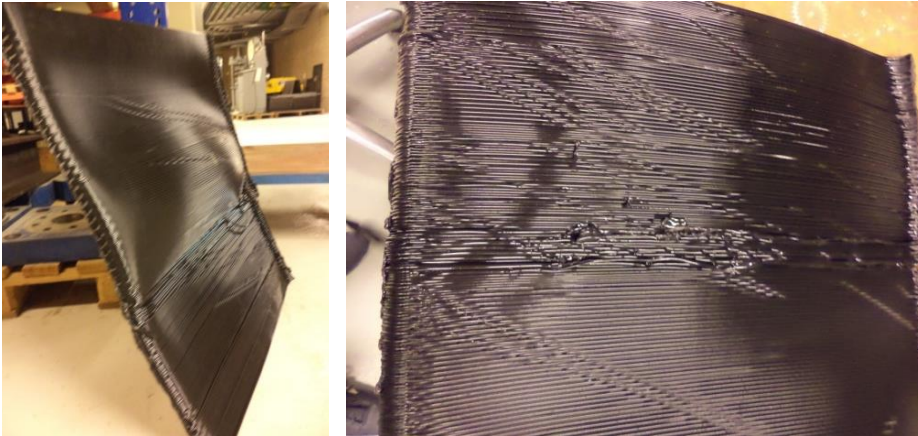


**Fig. 32** Internal curves and large inaccuracies on the plates, due to the absence of an internal structure in the printed block

Step 6: In case of perfectly straight plates, the plates can directly be put in the laser cutter without the need of any further treatment. During this research, the laser cutter at the IWS (Room G-0-230) of the faculty 3ME at the Delft University of Technology, is used.

The applied laser cutter software program, called Lasercut 5.3, is installed on the computer that is connected to the used laser-cutter and reads .dxf-files that can be created with AutoCAD. For making the files for the laser-cutter, the same AutoCAD-file as under step 2 can be used, since in that file the required samples are already divided over the plates in an optimum way. The only edition that has to be made is that the different plates from this single AutoCAD file have to be copied into a separate .dxf-file for every plate. In this way it is certain that the software program Lasercut 5.3 processes the right part of the .dxf-file.

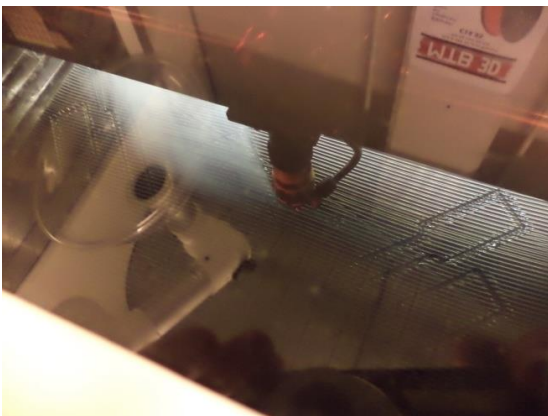


**Fig. 33** Laser cutting the specimens out of the plates that are printed within the vertical direction

Because big parts of the plates that were obtained for this research, were curved instead of straight, two extra measurements need to be taken:

- Under step 5 the plates were already divided into smaller pieces. Some of these pieces were straight enough to use, but a lot of them were too much curved. Therefore weights were placed on these plates for several days and plates were clamped and curved in the opposite direction of the original curve, to un-curve them. For some of the curved plates, this resulted into useable plates, but others were still not applicable, often because they contained multiple curves in different directions, or curves that were too big.
- Since the plates were sawn into smaller pieces, the original cad-files were not useable anymore for the division of the samples over the plates. Therefore, the dimensions of the 'new' smaller plates needed to be measured, put into AutoCAD and again the samples needed to be divided over the plates again.

#### 4. Printed and Laser-cut Test Specimens



**Fig. 34** Attempts to decrease the curvatures of the plates by placing weights on the plates and curving them in the opposite direction of the internal curve

Because big parts of the plates were not usable due to the curves, the decision is made to decrease the dimensions of the shear-samples with a factor 2, such that they had the original sample-sizes again. A disadvantage of this decision is that now the shear-samples in xy-direction, do not have the same dimensions as the shear-samples in xz-direction. Still this decision had to be made, because with the available material it else would just not be achievable to obtain a sufficient amount of samples. Fortunately the higher resolution in the xz-direction compared to the resolution in the xy-direction together with the accuracy of the laser-cutter, made it possible to still obtain samples of a good quality and utility.

Step 7: In case of perfectly straight plates, the samples are perfectly cut out from the plates in a very accurate quality. The plates were just thin enough to make direct cutting possible



**Fig. 35** Left: in case of straight plates, the samples are perfectly cut out from the plates. Right: In case of curved plates, the laser did not fully cut through the plate, such that using a fretsaw was required to obtain the sample.

Since most of the plates that were used during this research, still had some curves in it, the laser often was only able to cut out the first few millimeters of the sample thickness. Although this was not sufficient to obtain the sample directly, this partly cut line was good useable as a sawing line. By using a fretsaw, the sample still could be sawn out, although this was quite a time-consuming operation to perform for about 40 samples.

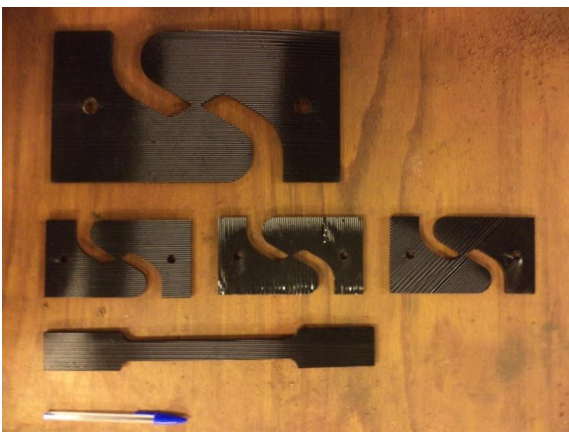


**Fig. 36** End result of the laser cut specimens

#### 4.2.3 Evaluation of the Production Methods

As can be seen on the picture above the obtained samples for the xz-direction that are made by using a laser-cutter are of a better quality than the samples in the xy-plane. This has the following reasons:

- The resolution in the xz-plane is higher, and because the previous layer is almost dried up when the next layer is printed on top of it, the composition is less untidy than within the xy-plane.
- There is far more expertise for printing in the xz-plane than printing in the xy-plane. This, because so far, all blocks in the Canal House project are printed such that in the z-direction, multiple layers are piled up on top of each other, while in the horizontal direction it has never occurred before that multiple layers were placed next to each other. Therefore the resolution properties in the z-direction are better optimized.
- The laser-cutter was able to cut out the contours of the samples with a high accuracy, such that perfectly straight sample-boundaries were obtained. This accuracy-level was defined by the accuracy of the laser-cutting process and therefore independent from the resolution of the printer, like it was the case in the xy-plane.

A disadvantage of this fabrication method however is that it is more time-consuming than printing out the test samples directly.



**Fig. 37** Left: the specimens that are directly printed within the xy-plane. Right: Specimens that are laser-cut from plates that are printed within the xz-plane.

When looking at the process and the results of both methods, it can be concluded that for this particular printer it is recommended to use the laser-cutting method in the future for both directions. This, because the laser-cutting method leads to samples of a better quality, which means that the dimensions are more accurate and the grain-direction is better noticeable. This also means for the laser cut samples, that the size fluctuations between the different copies of the same sample type are less and that these laser cut samples lead to more reliable testing results than the direct printed samples.

However, in case a more accurate 3D-printer is used that is able to print cantilevers and spans as well, then it is really considerable to use a 3D-printer to print out test specimens directly, because it is a simple and quick way to obtain complex-formed samples.

## 5. Material Tests – Elementary Level

In this chapter, an elaborate description is given of the material tests that are performed in order to define the elementary material properties of the printing material. With elementary properties, the basic properties of the material are meant that are independent of the dimensions and form of printed geometries. The elementary properties that need to be obtained within this chapter are selected and listed in paragraph 3.3.3.

In every paragraph of this chapter, a different test is described. All tests are described in such a way that first the aim of the test is specified, often in the form of material properties that need to be obtained from the particular test. After this, in the second subparagraph, a description of the test specimens is given. Then, in the third subparagraph, the test setup is shown and described. The fourth subparagraph gives an overview and description of the test results, followed by an evaluation of the test and drawn conclusions in subparagraph five.

An overview of all the numerical test results can be found under Appendix III. The characteristic values and standard deviations that can be found in most of the result-tables, are determined according to the method that is described under Appendix I. In Appendix II, a description is given of the way in which the dimensions of test specimens are measured and how is dealt with measurement inaccuracies.

### 5.1 Tensile Test

#### 5.1.1 Aim of Test

The aim of this test is to find the following properties of the building material:

Material Properties xz-direction	Symbol	Unit	Material Properties xy-direction	Symbol	Unit
Ultimate tensile strength //	$f_{t;0,xz}$	MPa	Tensile strength //	$f_{t;0,xy}$	MPa
Ultimate tensile strength $\perp$	$f_{t;90,xz}$	MPa	Tensile strength $\perp$	$f_{t;90,xy}$	MPa
Tensile breaking strength //	$f_{f;0,xz}$	MPa	Tensile breaking strength //	$f_{f;0,xy}$	MPa
Tensile breaking strength $\perp$	$f_{f;90,xz}$	MPa	Tensile breaking strength $\perp$	$f_{f;90,x}$	MPa
Yield strength $\perp$	$f_{y;0,xz}$	MPa	Yield strength $\perp$	$f_{y;0,xy}$	MPa
Yield strength //	$f_{y;90,xz}$	MPa	Yield strength //	$f_{y;90,xy}$	MPa
Elongation at tensile strength $\perp$	$\epsilon_{f;0,xz}$	%	Elongation at break $\perp$	$\epsilon_{f;0,xy}$	%
Elongation at tensile strength //	$\epsilon_{f;90,xz}$	%	Elongation at break //	$\epsilon_{f;90,xy}$	%

**Table 8** Properties to obtain within the Tensile test [Hartsuijker, 2005]

On the figure below it is shown in what way these properties can be obtained from a stress-strain diagram, which will form the output of the performed tensile tests.

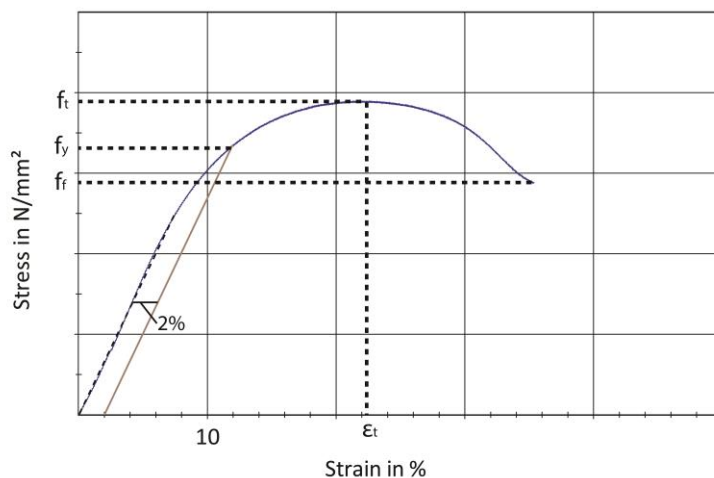


**Fig. 38** Obtaining the different tensile properties from the stress-strain curve

As can be seen in the figure on the previous page, the tensile breaking strength  $f_t$  is the stress-level of the end-point of the graph, which is the point where the material will fail under the applied load. In the tensile tests, a maximum height is set for the movement of the upper clamp of the testing machine. This maximum height leads to a maximum possible elongation. In the test cases where the material sample has not failed yet at the point of reaching this maximum set elongation, no breaking strength will be obtained.

The ultimate tensile strength is the stress level of the graph's maximum, so this property gives the maximum stress that is taken by the test specimen. The elongation at the tensile strength logically is the x-coordinate of the graph's maximum.

The yield strength is the stress level where the material starts to yield. Because of the absence of a clear horizontal yield track in the graph, the yield strength is taken at the 2% offset yield strength, which is the amount of stress that results in a plastic strain of 2%. This 2% strain is a common number for plastics. [Instron glossary, 2014]

### 5.1.2 Tested Samples

For every different sample coordination, a number of 6 samples are tested for this tensile test, such that the total number of tested samples within this test is 36:







Tested samples xz-plane	Grain Direction	Nr.	Tested samples xy-plane	Grain Direction	Nr.
	0°	6		0°	6
	90°	6		90°	6
	45°	8		45°	6

Table 9 Available test specimens for the Tensile test

All these samples have the dimensions as shown on the picture below (of course with the presence of measurement inaccuracies as described under Appendix II).

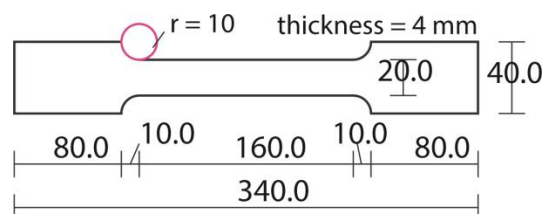


Fig. 39 Applied test specimen

### 5.1.3 Test Setup

For the tensile test a Zwick testing machine is used from the faculty of Mechanical, Maritime & Materials Engineering (3mE) that can apply tensile forces up to 100 kN. The testing machine consists of an unmovable bottom platform and a moveable upper device that is connected to a lifting system and therefore can move upwards and downwards. Both to the bottom and upper device a tool with a strong clamp is attached, which grabs the two wider ends of the dumbbell-shaped material samples. The sample is placed in such a way that the dumbbell sample is clamped over the full width of the wide ends of the dumbbell. In this way, the less wide middle part and the circular parts are unclamped and therefore the sample will deform over this middle part of the sample.

Furthermore the sample is placed as centralized as possible within the clamps such that the tensile load is applied symmetrically over the cross-section of the sample.

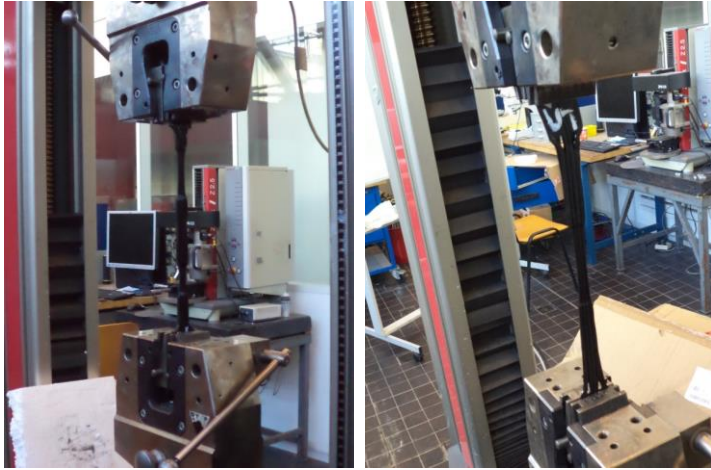


Fig. 40 Test setup of the tensile test. On the left a xz-sample is tested, on the right picture a xy-sample.

The Zwick testing machine is connected to a computer on which the measuring and analysis program called Testxpert II is installed. Within this program, it is set that a tensile test will be performed with a dumbbell shaped test sample. The following dimensions are set for the samples:

Samples xz-plane	Samples xy-plane
Parallel specimen length = 160 mm	Parallel specimen length = 200 mm
Specimen width = 20 mm	Specimen width = 23 mm
Thickness = 7.5 mm	Thickness = 6 mm

Table 10 Set dimensions for the gauge area within the control program

For the samples printed in the xz-plane, the parallel specimen length and width are set according to the designed length and width of the narrow middle part of the dumbbell. The specimen length of the samples printed in the xy-plane was picked at 200 mm, since this length was quickly estimated at the start of the testing procedure. The width of 23 mm is based on an average of the measured specimen widths. The reason that the samples printed in xy-plane don't have a width of 20 mm is because of the inaccuracy caused by the high resolution of the printer in the xy-plane. The thicknesses are again based on an average of the measured thicknesses of all the test samples. The difference in thickness between the xz- and xy-samples is caused by the resolution differences in both directions. It is important to note that after the performance of the tests, the actual widths and thicknesses of all the test specimens are entered within the testing software. In this way, the obtained stress values of a sample are corrected for the actual thickness and width of the particular sample. The test speed is set at 25 mm/minute, a preload of 10 N is taken and the max extension is set at 300 mm.

#### 5.1.4 Test Results xz plane

The specimens on which the tensile load is applied in the 'grain direction' (0°), look as follows after the test:

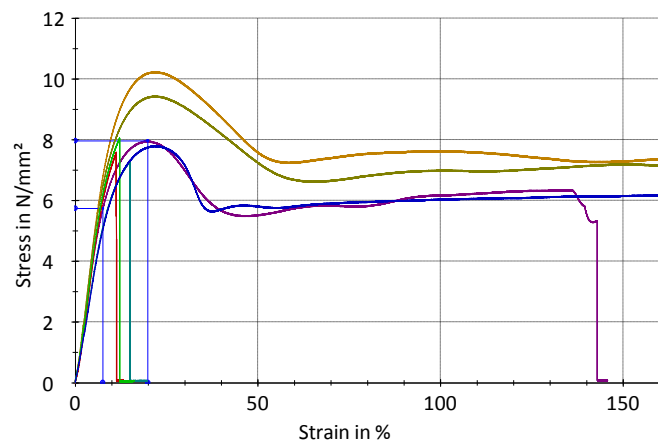


Fig. 41 Left: Specimens printed in the xz-plane and loaded in the grain direction, after they have been tested. Right: Curves of the tests specimens

As can be seen on the picture, four of the samples did not reach the elongation limit of 300 mm. For sample 0,3; 0,5 and 0,6, it seems that not even the yielding point is reached, as no permanent deformation can be observed for these three samples. This means these samples failed quite suddenly, without giving a clear warning.

Sample 0,2; 0,4 and 0,5 show a clear and large permanent elongation of the material. Which is a more favorable behavior, since in practice, failure will then obtain less sudden.

The graph in Figure 41 shows the stress-strain relation as obtained from the test, and the corresponding table 11 gives the numerical input and output values of the test.

Specimen Name	thickness [mm]	width [mm]	Cross Sectional Area [mm <sup>2</sup> ]	End of Test	Tensile strength $f_{t,0,xz;k}$ [MPa]	Tensile Strain $\epsilon_{f,0,xz}$ [%]	Yield Strength $f_{y,0,xz;k}$ [MPa]	Yield Strain $\epsilon_{y,0,xz}$ [%]	Tensile Breaking Strength $f_{f,0,xz;k}$ [MPa]	Tensile Breaking Strain $\epsilon_{f,0,xz}$ [%]
0,1	6.4	20.0	128.00	max extension reached	10.20	21.9	9.2	13	/	Max strain of 150 reached
0,2	7.5	21.0	157.50	Break	7.95	19.9	6.8	12	5.3	143
0,3	8.2	20.0	164.00	Break	7.28	15.0	6.4	11	7.28	15.0
0,4	7.2	19.5	140.40	max extension reached	9.43	22.2	7.9	11	/	Max strain of 150 reached
0,5	7.0	20.6	144.20	Break	7.58	11.3	7.4	11	7.58	11.3
0,6	7.3	20.0	146.00	Break	8.05	12.2	6.9	10	8.05	12.2
0,7	8.4	19.5	163.80	max extension reached	7.79	22.2	6.6	12	/	Max strain of 150 reached
<b>Average</b>					8.33	17.8	7.3	11	7.05	90.2
<b>Standard deviation</b>					1.07	n.a.	0.97	n.a.	1.21	n.a.
<b>Characteristic</b>					6.45	n.a.	5.6	n.a.	4.83	n.a.

Table 11 Numerical results for the xz-specimens that are tested within the grain direction

The samples that are loaded perpendicular to the grain (90°) all broke during the test, as can be seen on the picture below. For all the samples, the line of fracture was located between two printed lines, which proofs clearly that the binding parts between to printed lines are weaker than the printed lines themselves.

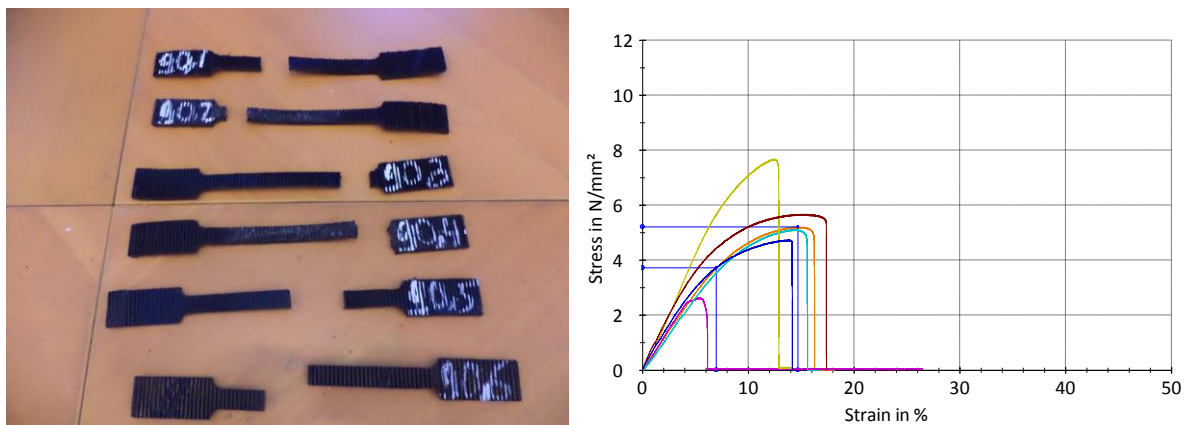


Fig. 42 Left: Tested xz-samples that have their grains perpendicular to the load direction. Right: Stress-Strain curves of these tested samples

Below the graphs and table-results for these 90°-samples are given. The graphs clearly show that for all the tests, there was a brittle failure of the test sample. This is an undesirable behavior, since the material will fail



## 5. Material Tests – Elementary Level

without giving a clear warning. This means that it becomes hard to predict the behavior of the material when it is loaded in the direction perpendicular to the grain. For that reason, the characteristic strength value in this direction will turn out to be relatively low, since this test shows that a sudden failure between two printed lines can happen already at strongly deviating stress rates.

Specimen Name	thickness [mm]	width [mm]	CS Area [mm <sup>2</sup> ]	End of Test	Tensile strength [MPa]	Tensile Strain [%]	Yield Strength [MPa]	Yield Strain [%]	Tensile Breaking Strength [MPa]	Tensile Breaking Strain [%]
90,1	6.4	19.2	122.88	Break	5.66	15.0	4.8	7.9	5.66	15.0
90,2	6.9	19.8	136.62	Break	5.20	14.7	4.9	10.9	5.20	14.7
90,3	7.0	19.5	136.50	Break	2.62	5.3	2.4	4.1	2.62	5.3
90,4	6.8	20.0	136.00	Break	5.10	14.4	4.8	11.6	5.10	14.4
90,5	5.7	19.5	111.15	Break	7.67	12.4	7.3	10.8	7.67	12.4
90,6	7.2	20.0	144.00	Break	4.73	13.9	4.8	11.6	4.73	13.9
<b>Average</b>					5.16	12.6	4.8	9.5	5.16	12.6
<b>Standard deviation</b>					1.62	n.a.	1.55	n.a.	1.62	n.a.
<b>Characteristic</b>					2.28	n.a.	2.1	n.a.	2.28	n.a.

**Table 12** Numerical results of the tested xz-samples that have their grains perpendicular to the load direction.

The test specimens that are loaded 45° to the 'grain-direction' also failed without any exception. Most of the specimens again ruptured on the line between two printed lines, such that a diagonal fracture line of 45° is visible on the picture below. Sample 45,1; 45,5 and 45,7 however, failed in a straight line. This is probably caused by the fact that this straight failure path is shorter and in case of a low quality or small dimensions of the printed lines, than this path becomes even weaker than the diagonal path between two printed lines.

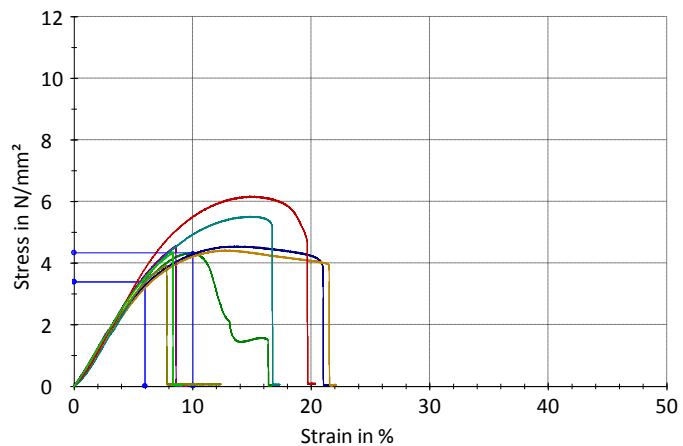


**Fig. 43** Left: Samples that are loaded 45 degrees to the grain direction and their curves

As the graph shows, this time not all the samples failed on their highest point, like was the case for the samples loaded in the 90°-direction. Surprisingly the strength of these samples, on an average, is lower than the strength of the 90°-samples, while the breaking strain is bigger.

Specimen Name	thickness [mm]	width [mm]	CS Area [mm <sup>2</sup> ]	End of Test	Tensile strength [MPa]	Tensile Strain [%]	Yield Strength [MPa]	Yield Strain [%]	Tensile Breaking Strength [MPa]	Tensile Breaking Strain [%]
45,1	7.0	19.2	150.00	Break	4.35	8.3	4.0	7.2	4.35	8.3
45,2	7.0	19.6	137.20	Break	4.33	10.0	4.3	9.9	4.33	10.0
45,3	7.0	19.6	150.00	Break	4.54	13.5	4.3	9.8	4.0	21
45,4	7.3	19.6	150.00	Break	4.41	12.9	4.1	9.7	4.0	22
45,5	7.0	20.0	140.00	Break	4.56	8.6	5.0	10.2	4.56	8.6
45,6	7.2	21.2	152.64	Break	5.51	14.8	4.9	10.0	5.51	14.8
45,7	7.8	19.2	149.76	Break	3.93	7.8	3.7	6.3	3.93	7.8
45,8	7.0	19.5	136.50	Break	6.16	14.9	5.8	11.2	6.16	14.9
<b>Average</b>					4.72	11.35	4.5	9.3	4.61	13.4
<b>Standard deviation</b>					0.73	n.a.	0.68	n.a.	0.81	n.a.
<b>Characteristic</b>					3.44	n.a.	3.3	n.a.	3.20	n.a.

Table 13 Numerical results of the samples that are loaded 45 degrees to the grain direction

By plotting the results of the xz-samples in the 0°-direction, 90°-direction and 45°-direction in one graph, the following figure is obtained:

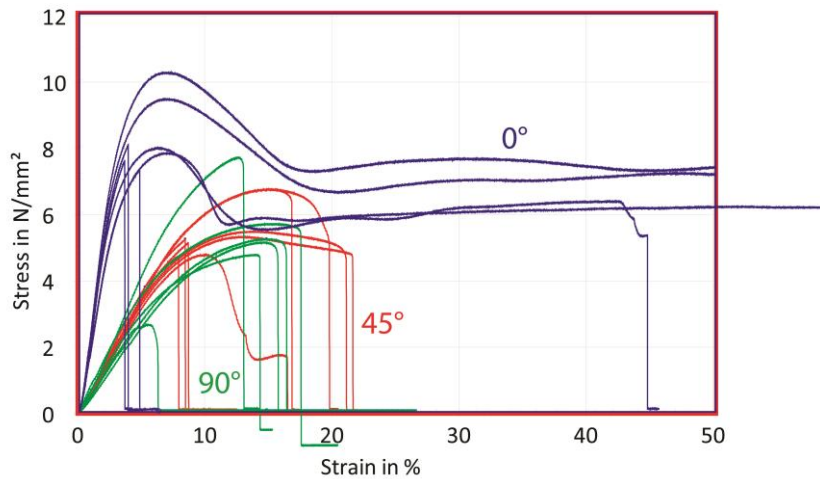


Fig. 44 Comparison between the samples loaded parallel (0°), perpendicular (90°) and 45° to the grain

And next, in the table below the tensile strengths and elongations at break are compared for the specimens that are tested parallel to, perpendicular to and 45° to the printing/grain direction.

Grain direction	Tensile strength [MPa]			Tensile strain [%]
	<i>aver</i>	<i>st. dev.</i>	<i>char.</i>	<i>aver</i>
0°	8.33	1.07	6.45	17.8
90°	5.16	1.62	2.28	12.6
45°	4.72	0.73	3.44	11.35

Table 14 Comparison between the obtained tensile strengths for the different grain directions within the xz-plane

## 5. Material Tests – Elementary Level

### 5.1.5 Test Results xy plane

As already mentioned and displayed in chapter 4, the specimens that were printed in the xy-plane-direction are of a poorer specimen-quality than the samples that are cut from plates that are printed in the xz-plane. Especially because of the low printing resolution in the xy-plane, the loaded middle area of the dumbbell has become relatively wide and the transitions between the clamped parts of the sample and the loaded middle part are not very accurate and circular.

Furthermore, the connection perpendicular to the 'grain' between the printed lines is poor, as can be clearly seen in the following picture of the deformed samples:

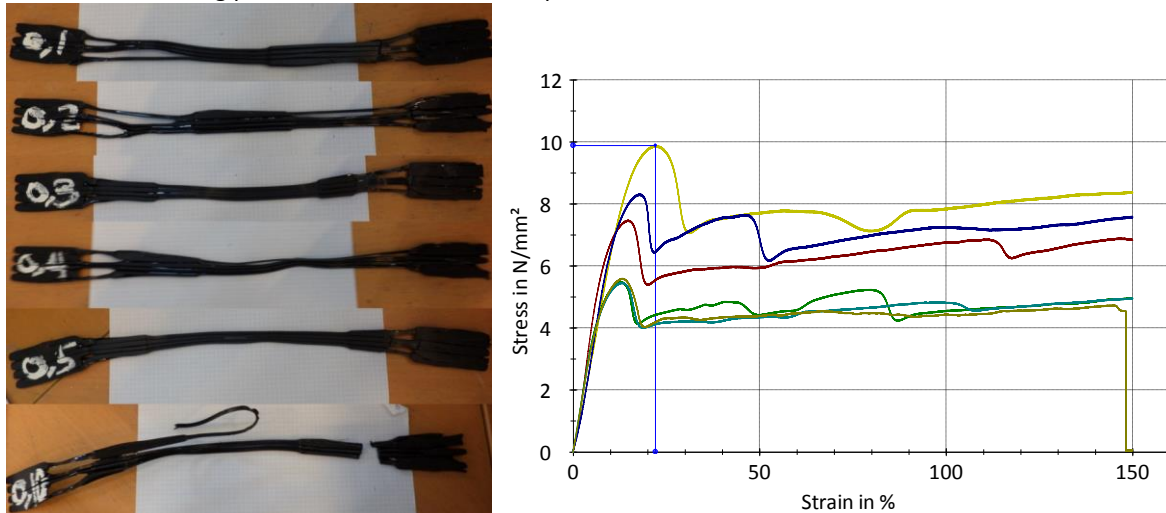


Fig. 45 Samples printed in the xy-plane after they are loaded parallel to the grain, and their stress-strain curves

Although the strength of these samples on an average is smaller than the strength of the 0°-samples that were printed in the xz-plane, still most of the samples reach the maximum deformation, without breaking. Only sample 0,10 failed just near the end of the test.

The picture above clearly shows that the printed lines/grains of most of the samples, extended individually, without supporting each other. This again clearly shows that the strength and connectivity in the printing/grain-direction is much higher than parallel to the grain.

Specimen Name	thickness [mm]	width [mm]	CS Area [mm <sup>2</sup> ]	End of Test	Tensile strength [MPa]	Tensile Strain [%]	Yield Strength [MPa]	Yield Strain [%]	Tensile Breaking Strength [MPa]	Tensile Breaking Strain [%]
0,1	6.2	22.3	138.26	max extension reached	7.46	14.7	7.2	12	/	Max strain of 150 reached
0,2	8.0	22.8	182.40	max extension reached	5.49	12.7	5.2	10	/	Max strain of 150 reached
0,3	5.3	20.4	108.12	max extension reached	8.31	17.8	7.7	13	/	Max strain of 150 reached
0,4	7.5	24.7	185.25	max extension reached	5.45	13.1	5.1	10	/	Max strain of 150 reached
0,5	4.6	20.3	93.38	max extension reached	9.87	22.1	9.3	18	/	Max strain of 150 reached
0,10	8.0	23.6	188.80	Break	5.59	13.3	5.3	10	4.6	148
<b>Average</b>					7.03	15.6	6.6	12	n.a.	150
<b>Standard deviation</b>					1.83	n.a.	1.72	n.a.	n.a.	n.a.
<b>Characteristic</b>					3.78	n.a.	3.6	n.a.	n.a.	n.a.

Table 15 Test results of the specimens that are printed within the xy-plane and tested in the grain direction

Then, for the samples printed in the 90°-direction, one would again expect that all the samples would fail on the line between to printed lines again. However, since these samples in the xy-plane are 3D-printed directly, these samples are printed in a continuous line. This means that for this samples it does not hold that they only exist of printed lines perpendicular to the grain, as was the case for the 90°-samples that were laser-cut in the xz-plane. Instead, due to the continuous printing movement, side connections between the grains are made, because the printer head needed to move from one fiber to the other.

Furthermore, due to the low resolution and the fact that the previous fiber was still liquid when printing the next one, a relatively strong wave-structure is obtained here.

This can be seen in the picture of the deformed samples: only one of them failed and all of them seemed to rely on this quite strong wave-structure.

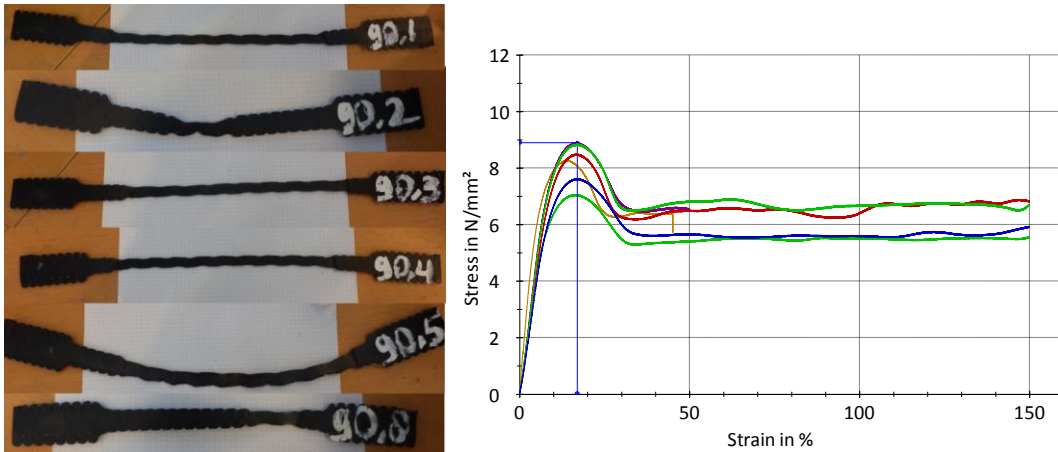


Fig. 46 Samples that are printed in the xy-plane and loaded perpendicular to the grain direction

Also the graph shows, that this sample structure lead to relatively high strengths and quite homogeneous testing results. In fact, none of the tensile tests led to results as homogeneous as this one. From this, it might be concluded that by printing parts that have printed connections in both horizontal directions, lead to stronger, more homogeneous and therefore better predictable testing results.

Specimen Name	thickness [mm]	width [mm]	CS Area [mm <sup>2</sup> ]	End of Test	Tensile strength [MPa]	Tensile Strain [%]	Yield Strength [MPa]	Yield Strain [%]	Tensile Breaking Strength [MPa]	Tensile Breaking Strain [%]
90,1	5.7	18.8	107.16	max extension reached	8.49	16.7	7.8	11	/	Max strain of 150 reached
90,2	5.4	19.3	104.22	max extension reached	8.89	17.0	8.2	11	/	Max strain of 150 reached
90,3	5.5	19.4	106.70	max extension reached	8.84	17.0	8.0	11	/	Max strain of 150 reached
90,4	6.5	18.5	120.25	max extension reached	7.61	16.9	6.9	11	/	Max strain of 150 reached
90,5	5.4	23.7	127.98	max extension reached	7.05	16.6	6.6	11	/	Max strain of 150 reached
90,8	5.5	18.2	100.10	Break	8.26	14.0	7.5	8	6.3	45
<b>Average</b>					8.19	16.4	7.5	11	6.3	132.5
<b>Standard deviation</b>					0.73	n.a.	0.63	n.a.	n.a.	n.a.
<b>Characteristic</b>					6.90	n.a.	6.4	n.a.	n.a.	n.a.

Table 16 Test results of the tensile specimens that are printed within the xy-plane and loaded perpendicular to the grain direction

## 5. Material Tests – Elementary Level

The 45°-direction samples unfortunately were from a poor and inconsistent quality. It turned out to be hard to set a proper grain distance, therefore the samples differ significantly from each other.

With the exception of sample 45,6, all the samples failed before reaching the maximum elongation.

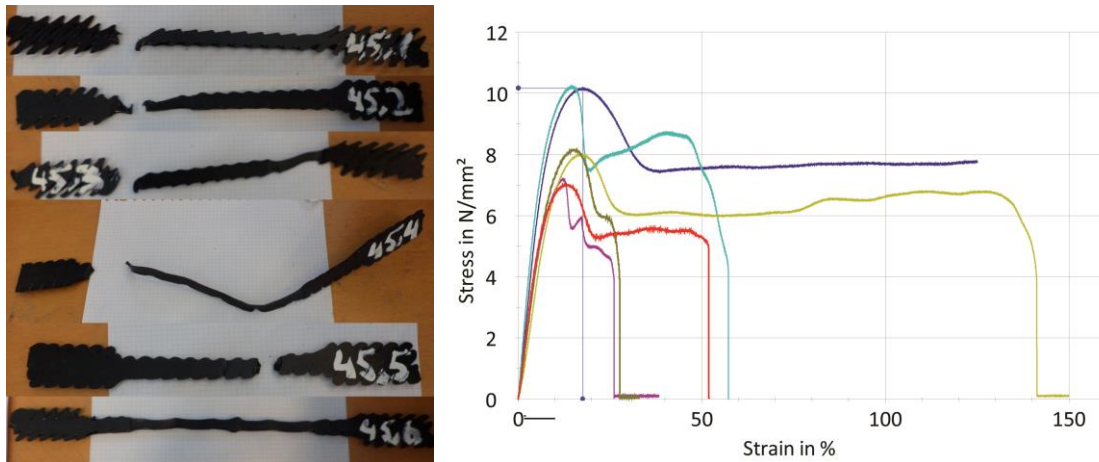


Fig. 47 Samples that are printed in the xy-plane and loaded 45 degrees to the grain direction

Still, when looking at the graph, the results are not as negative as could have been expected when observing the quality of the test specimens. Most of the specimens failed after reaching the yield point and maximum strength, which is a positive given. Furthermore the reached maximum strength-range is relatively good. Again, it seems the case that the samples have benefited from the fact that side connections between the printed fibers need to be made because the printer prints continuously. Since these side connections are in the direction of the load, they really contribute to the strength of the samples.

Specimen Name	thickness [mm]	width [mm]	CS Area [mm <sup>2</sup> ]	End of Test	Tensile strength [MPa]	Tensile Strain [%]	Yield Strength [MPa]	Yield Strain [%]	Tensile Breaking Strength [MPa]	Tensile Breaking Strain [%]
45,1	7.0	12.7	88.90	Break	7.21	12.1	6.9	10	4.2	26
45,2	5.5	18	99.00	Break	8.16	15.2	7.9	12	4.7	27
45,3	6.0	11.3	67.80	Break	10.20	14.7	9.3	10	4.5	57
45,4	6.0	24	144.00	Break	8.00	17.0	7.3	12	5.2	139
45,5	5.0	21.4	107.00	Break	7.04	13.1	6.4	9	5.0	52
45,6	7.0	16.8	117.60	Test stopped	10.2	17.6	9.3	10.2	/	/
<b>Average</b>					8.47	14.95	7.9	11	4.7	60.2
<b>Standard deviation</b>					1.41	n.a.	1.23	n.a.	0.40	n.a.
<b>Characteristic</b>					5.97	n.a.	5.7	n.a.	4.0	n.a.

Table 17 Test results for the specimens that are printed within the xy-plane and loaded in tensile, 45 degrees to the grain

If the results of the tested specimens printed in the xy- and xz-planes are now added together in a table, a clear comparison between the two printing planes can be made, together with a comparison between the different grain directions within the two printing planes. This table can be found on the next page.

	Grain direction	Tensile strength [MPa]			Tensile strain [%]
		<i>aver</i>	<i>st. dev.</i>	<i>char.</i>	<i>aver</i>
xz-plane	0°	8,33	1,07	6,45	17.8
	90°	5.16	1.62	2.28	12.6
	45°	4.72	0.73	3.44	11.35
xy-plane	0°	7.03	1.83	3.78	15.6
	90°	8.19	0.73	6.90	16.4
	45°	8.47	1.41	5.97	14.95

**Table 18 Comparison between the obtained tensile strengths for the all the different orientations**

### 5.1.6 Test Evaluation and Conclusions

The most important conclusion that can be drawn from the xz-plane part of this tensile test, is that the printing material shows clear directional behavior in the way that the tensile strength parallel to the grain is significantly higher than perpendicular to the grain. Furthermore on an average, the achieved elongation for specimens that are loaded in the direction of the printed lines, is much higher than for specimens loaded perpendicular to or 45 degrees to the printed lines. This is due to the fact that when the material is loaded in the grain direction, the material first elongates before it breaks. This is desirable behavior, because this means the material fails after giving a warning in the form of a deformation. When the material however is loaded in another direction than the direction of the printed lines, the material fails in a brittle manner, which means it fails suddenly without giving a warning.

From this obtained testing results, the recommendation can be given that one should always try as much as possible to load the material within the direction of the printed lines, especially when the material is loaded in tension.

A danger is still that although on an average the samples loaded in the grain direction reached a high elongation, big deviating results in the form of quick failures without much elongation still occurred. This means that sudden brittle failures of the material cannot be excluded, even when the material is fully loaded in the direction of the printed lines. This is probably caused by the fact that the material is very sensitive to local inaccuracies, that are often present due to the fact that the printing process is not a completely constant process. This inconsistency of the printing process can lead to inaccurate printing results.

For the specimens that were printed within the xy-plane, the intension was to obtain material specimens within a certain grain direction as well. However, the material actually performed quite isotropic, which lead to quite even results for the three different loading directions. This is caused by the effects explained in 3.1.3 and shown on the two left pictures of Figure 7. Because, in the xy-direction, the previous printed line often is not dry yet on the moment subsequent line is printed, and due to the end connections when the continuous printing printer head goes around the corner, the material starts to make a lot of connections perpendicular to the printing direction. Therefore the material behavior becomes more isotropic, resulting in the equal results as obtained.

The fact that the material in the xy-plane behaves isotropic also has to do with the way the material specimens in this direction are obtained compared to the fabrication of the specimens in the xz-plane. When the specimens in the xy-plane would also been cut out from plates, then the end connections (around-the-corner-connections) would not have been present. This probably would have led to more anisotropic behavior for these samples as well. For that reason, it might be true that a fairer comparison between the xy- and xz-plane will be obtained on the moment the specimens are fabricated in the same way, so laser cut from plates for both planes.

Still, also this test in the xy-direction led to some interesting insights. At first, it was the first time ever that multiple lines where printed directly next to each other in the xy-plane. So far the building blocks are all composed out of vertical 2d-plates in the z-direction that are all only one line thick in the horizontal xy-plane. By this test, an interesting alternative is studied and presented by actually printing multiple lines connected to each other in the xy-direction as well, instead of only in the z-direction. Of course this will lead to stronger building blocks. But an even bigger advantage may lie in the fact that by printing in the xy-direction, stronger and more isotropic material behavior will be obtained, as can be concluded from the testing results. This isotropic behavior will lead to a more constant and therefore better predictable mechanical behavior of the building blocks.

So from this, it can be recommended to experiment more in creating building blocks that exist of multiple

## 5. Material Tests – Elementary Level

layers connected to each other in the xy-direction.

When the obtained values within this test are compared to the values on the datasheet of Henkel (see paragraph 3.3.2), it can be noticed that the tensile strength value of 12 MPa, that is mentioned on the datasheet, is not reached within this test, as the maximum obtained value over all of the different grain- and plane-directions was 10.2 MPa. Also, the elongation of 600%, is by far not reached for any grain-direction, since most of the samples failed at significant lower elongations. Only for the samples that did not fail and reached the maximum strain of 150%, it is hard to say what percentage they would have reached on the moment that an unlimited deformation would have been possible with the used testing device.

The values that are obtained within the research of Henkel are probably higher, because Henkel used specimens for their tensile test that were perfectly isotropic and homogeneous. This, while the samples that are obtained by the printing process, show clear anisotropic behavior.

Furthermore the specimens that are used by Henkel are produced by pressing the granular material 20 degrees above the softening temperature, between two steel plates. In this way, it is possible that the material is more compressed and therefore of a higher density and strength than the samples that are produced by the 3D-printer. Therefore, the value on the factsheet of Henkel can be seen as an upper limit for the strength performance of the material, which is also valuable information for materials that will be applied in the future.

## 5.2 Shear Test

### 5.2.1 Aim of Test

The aim of this test is to find the ultimate shear strength in both the direction parallel to the grain as perpendicular to the grain. Also these different strengths need to be researched for both the xz- and the xy-printing-plane again:

Material Properties xz-direction	Symbol	Unit	Material Properties xy-direction	Symbol	Unit
Shear strength //	$f_{s;0,xz}$	MPa	Shear strength //	$f_{s;0,xy}$	MPa
Shear strength $\perp$	$f_{s;90,xz}$	MPa	Shear strength $\perp$	$f_{s;90,xy}$	MPa

Table 19 Properties that need to be obtained within the Shear test

### 5.2.2 Tested Samples

As already described under paragraph 4.2, due to the inaccuracy/low resolution of the printing method, all the dimensions of the samples in the xy-plane had to become twice bigger than originally intended.

For the samples in the xz-plane that are cut from printed plates, there was not enough material available to produce these samples in the same big dimensions as used for the xy-samples. Therefore, the samples in xz-direction have the original sample-size.







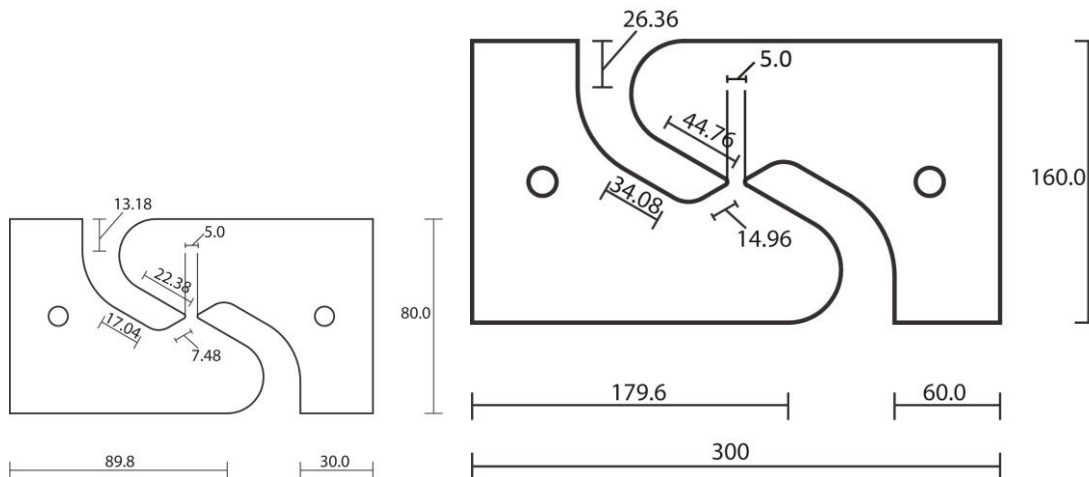
Tested samples xz-plane	Grain Direction	Nr.	Tested samples xy-plane	Grain Direction	Nr.
	0°	8		0°	6
	90°	9		90°	5
	45°	9		45°	6

Table 20 Test specimens that are available for the shear test

The samples printed in the xz-plane, that are shown in column 1, have the size as indicated on figure 48 on the left. The specimens that are printed in the xy-plane have double the dimensions of this xz-samples as indicated on the right picture of figure 48. Only the middle part, the part that will fail on shear, has the same size (5 mm) for both specimen sizes. This because during the testing process it was found that if this part becomes too big, the sample does not always fail in this part, but can fail in other parts of the sample as well.





**Fig. 48** Left: Specimen dimensions of the xz-samples. Right: Specimen dimension of the xy-samples.

Because of the size-differences between the samples in the xz- and xy-plane, different test setups had to be used for both different specimen-sizes. This will be described in the following subparagraphs.

### 5.2.3 Test Setup – samples xz plane

For the shear tests, the same Zwick testing machine as for the tensile test is used. The big advantage of the chosen sample form of the shear test specimen, is that the same standard accessories (the clamps) could be used here as well, while normally complicated attachments and tools that require real accurate samples, are needed to perform a shear test.

So because of the chosen sample form, the testing process is easier and quicker and the inaccuracies in the dimensions of the produced samples do not form a crucial problem for the performance of the test.

The test specimen is clamped in the test device as shown in the pictures below.

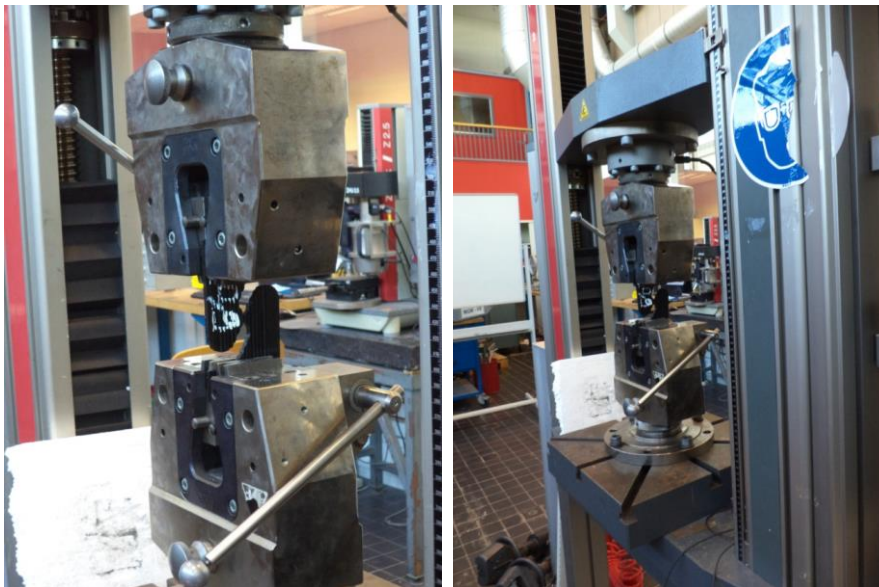


**Fig. 49** Test setup for shear specimens that are printed in the xz-direction. These samples can be simply clamped within the same tools as used for the tensile test

In this test, it is really important that the middle part of the test specimen, that fails on shear, is centralized and therefore falls in the same line as the central resultant load that is applied by the testing machine. This is obtained by using a straight metal block, to control that the middle part of the specimen falls on the same line as the central line that is indicated on the clamp tools. To make sure that the specimen is placed fully straight in the two clamps, a caliper is used to check that the sample equally protrudes from the bottom and top clamp.

These two processes are shown on the pictures below:

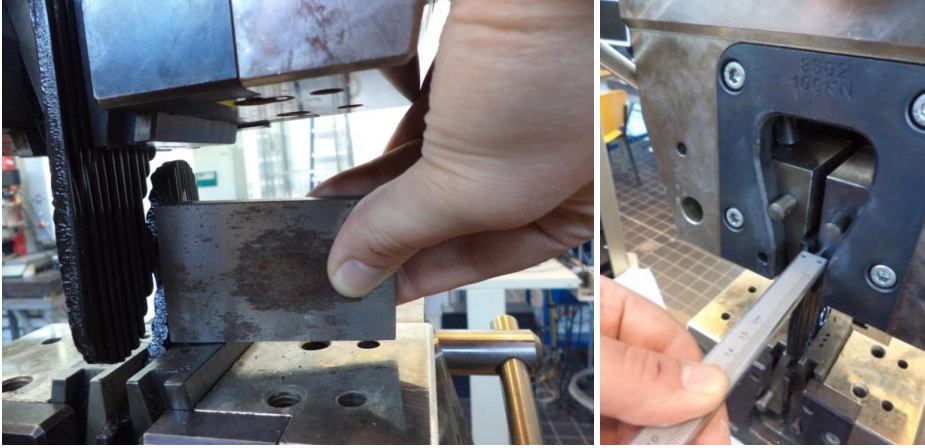


**Fig. 50** Left: A steel block is used to ensure that the shear area of the specimen falls in the same line as the middle point of the clamps. Right: A caliper is used to check that the specimen is placed fully straight in the two clamps.

Because the used sample is not standard available in the Zwick Testxpert II test program, a dumbbell formed sample is chosen again from the list of available sample types. This, because the same testing tools are used as in case of the tension test. This time, the following dimensions are set for the samples:

Samples xz-plane
Parallel specimen length = 5.0 mm
Specimen width = 5.0 mm
Thickness = 6.5 mm

**Table 21** Set dimensions of the loaded shear area within the control program

The specimen length in this case is the length of the narrow central part of the specimen, because this is the part on which the sample will deform and fail. This length is 5.0 mm.

Although the exact middle part of the test sample has an infinitely small width because it is formed between two circular inlets, it is quite plausible that the specimen will not break at this exact middle line of the sample, but nearby this line. Based on the resolution of 2.1 mm at both sides of the middle line, a specimen width of about two lines is chosen by setting the specimen width as 5.0 mm.

For the thickness, again an average thickness of all the samples is initially set, which for these samples is about 6.5 mm. Later on, during the exact calculation of the strengths of individual samples, the actual measured widths and thicknesses of the individual samples will be used. The test speed is set at 10 mm/minute, a preload of 10 N is taken and the max extension is set at 300 mm.

#### 5.2.4 Test Results – samples xz plane

The result of the tested shear-samples that were loaded in such a way that the applied shear force was working perpendicular to the grain, looks as follows:

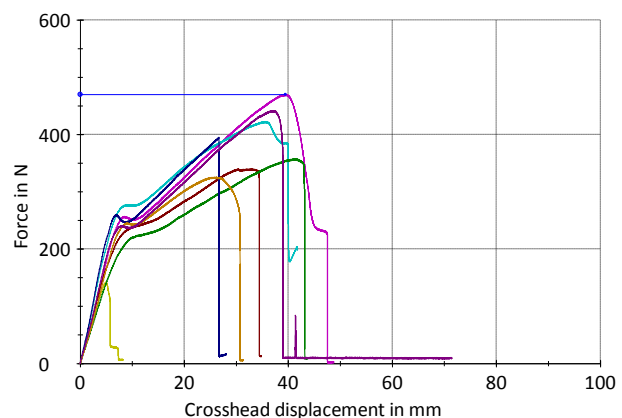


**Fig. 51** Shear samples printed in the xz-plane and loaded in shear perpendicular to the grain direction

## 5. Material Tests – Elementary Level

As can be seen on the picture, apart from sample 0,3, all the samples failed in the intended area that was loaded in shear. A small extension of the shear-part can be observed, which is caused by the situation that these fibers were loaded in tension after the initial failure on shear occurred. The shear area actually failed in such a way that first only a part of the shear area broke, due to the applied shear force. Due to this partial failure in the form of a crack, the resulting material, often only one fiber, was able to rotate, such that it was loaded in the direction of the applied tensile load.

This process can also be observed in the graphs. Cracking/Failure on shear occurs at the initial peak. Then the second increasing part of the curve-lines shows the described loading of the resulting part in tension. Because the initial peak of the curve is the point where the specimen actually fails on shear, this point represents the shear strength of the material. Therefore the value in this point is chosen as the maximum shear force that is given in the table below. The stress value that can be derived from this force, forms the shear strength of the specimen.

The second stage of the graph in which the remaining fibers are loaded in tension, are of no further significance.

Specimen Name	thickness [mm]	width [mm]	CS Area [mm <sup>2</sup> ]	Max Shear Force* [N]	Shear strength [MPa]
0,1	6.0	5.0	30.0	255	8.5
0,2	7.4	5.0	37.0	275	7.4
0,3	6.8	7.0	47.6	140	2.9
0,4	6.3	5.5	34.7	240	6.9
0,5	6.7	4.7	31.5	220	7.0
0,6	6.4	5.3	33.9	260	7.7
0,7	6.6	5.2	34.3	245	7.1
0,8	6.4	5.0	32.0	240	7.5
<b>Average</b>					6.9
<b>Standard deviation</b>					1.68
<b>Characteristic</b>					4.0

**Table 22 Test results of shear samples printed in xz-plane and tested in shear perpendicular to the grain direction**

\* Accuracy of the measured Max Shear Force is 5 N, due to the fact that this value needed to be read from the graph.

As can be seen in the graph, the strength value of sample 0,3 is significantly lower than the other values. This is due to the circumstance that this sample did not fail over the intended shear-area, but between to fibers within the sample itself. When the result of this failed test would be left out this analysis, the average shear value becomes 7.4, which is a value that is more in line with the results of the successful tests.

Still, the failure over the alternative area of sample 0,3, shows that unpredicted and brittle failures can always occur between two printed lines that are loaded perpendicular to the connection between the lines, so one should always account for these kind of failures.

For the samples that are loaded such that the shear force works parallel to the grain direction, the tested samples are shown on the picture below.

As can be seen, all samples failed in the intended shear area, and this time no, or only a very small extension can be observed. This more brittle failure, is caused by the situation that the samples all failed in a weak line between two printed lines this time, since the plane of rupture is between two printed lines that slide relative to each other.

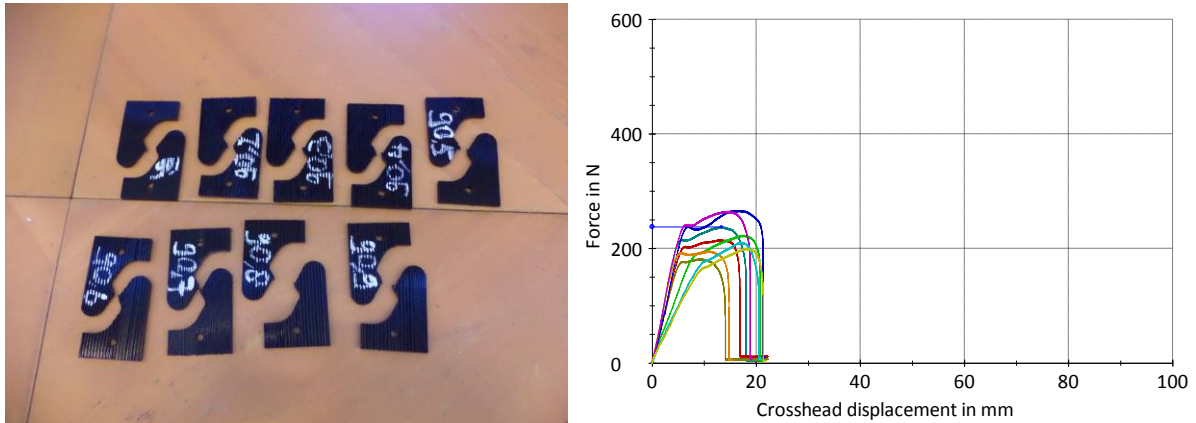


**Fig. 52** Samples printed in the  $xz$ -plane and loaded in shear parallel to the grain.

In some cases, again a small initial peak can be observed which again is caused by an initial partial crack. Since the remaining material will this time not be loaded in the direction of the fibers but perpendicular to them, the second crack and completion of the failure now occurs quicker after the first crack.

Again the first peaks of the curve are taken for the determination of the maximum shear force and the shear strength, because at this point, the sample actually fails on shear already.

As expected, the obtained shear strengths in this direction are lower than for the samples that were loaded in shear perpendicular to the grain direction. This, because the plane of rupture in this case falls in the weak connection part between two printed lines. While in the case of loading perpendicular to the grain, the fibers itself are loaded in shear over their cross sectional area and therefore the fibers itself need to fail. As one can imagine, this failure mechanism requires a higher force than a failure in the plane between two printed lines.

Specimen Name	thickness [mm]	width [mm]	CS Area [mm <sup>2</sup> ]	Max Shear Force [N]	Shear strength [MPa]
90,1	6.5	5.0	32.5	215	6.6
90,2	7.3	5.2	38.0	175	4.6
90,3	7.0	5.5	38.5	205	5.3
90,4	6.0	5.4	32.4	190	5.9
90,5	6.7	5.0	33.5	240	7.2
90,6	7.3	5.8	42.3	190	4.5
90,7	6.4	5.0	32.0	245	7.7
90,8	6.0	5.0	30.0	175	5.8
90,9	7.3	5.0	36.5	165	4.5
Average					5.8
Standard deviation					1.19
Characteristic					3.7

**Table 23** Results of  $xz$ -specimens tested in shear parallel to the grain direction

Then, for the tested samples in the  $45^\circ$ -direction, an elongation of the area loaded in shear can be observed again. This means the samples failed in two phases again, of which only the first phase is relevant for obtaining the shear strength.

5. Material Tests – Elementary Level

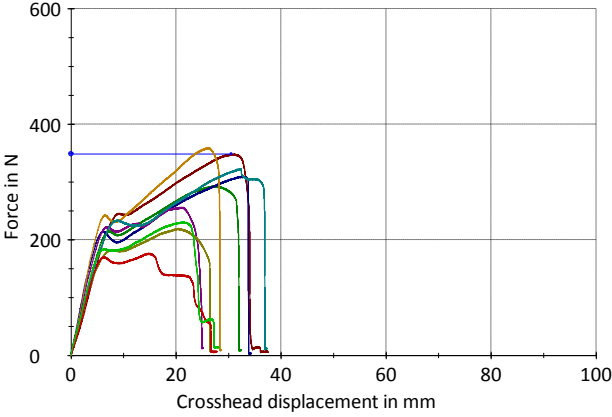


Fig. 53 Specimens printed within the xz-plane and loaded 45 degrees to the grain

The obtained values for the 45°-samples are about the same as for the 90°-samples, as can be seen in the below table. This, while the weak surface between two printed lines makes an angle of 45° with the shear load this time, instead of a rupture surface and a shear load that are falling in the same line. Therefore one would expect a bit higher results for these 45°-samples. This is probably not obtained due to the situation that the initial crack still occurs quickly, because the weak plane between two printed lines, appears on the surface in these samples as well. Therefore, the weak plane quickly will be loaded and cracked again.

Specimen Name	thickness [mm]	width [mm]	CS Area [mm <sup>2</sup> ]	Max Shear Force [N]	Shear strength [MPa]
45,1	7.0	6.0	42.0	245	5.8
45,2	6.0	6.0	36.0	215	6.0
45,3	7.0	6.0	42.0	215	5.1
45,4	6.4	4.8	30.7	240	7.8
45,5	7.0	6.8	47.6	220	4.6
45,6	7.0	6.0	42.0	235	5.6
45,7	6.7	5.0	33.5	180	5.4
45,8	6.8	6.9	46.9	165	3.5
45,9	7.3	5.2	38.0	180	4.7
Average					5.4
Standard deviation					1.18
Characteristic					3.3

Table 24 Test results of xz-specimens, loaded 45 degrees to the grain, in shear

Combining the obtained shear curves all in one graph, leads to the following figure:

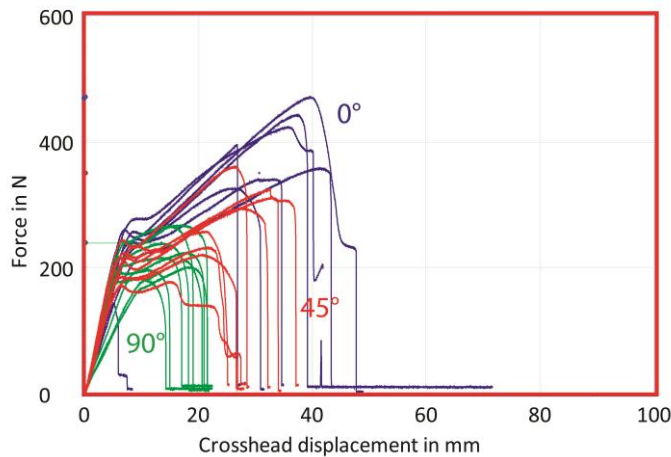


**Fig. 54** Comparison between the shear specimens that are loaded such that the shear forces work perpendicular to the grain (0°), parallel to the grain (90°) and 45 degrees to the grain.

The first peaks in the graph show that the obtained strengths for the zero degree direction, on an average, are a little higher than for the 45 degrees direction. The 45 degrees direction on its turn is again a little higher than the 90 degrees direction. Still, the obtained shear strength values are relatively even, as the first peaks lie quite close to each other.

The real difference between the different loaded orientations can be observed in the second stages of the curves. Where the zero degree samples are loaded and extended further till a significantly higher value, the 90 degrees samples fail at or quick after reaching the maximum strength value. The behavior of the 45 degree samples is a little bit in between the behavior of the samples that are loaded parallel and perpendicular to the grain direction.

When listing the results from the samples loaded in shear, parallel, perpendicular and under an angle of 45 degrees to the grain, the following table is obtained:

Grain direction	Shear Strength [MPa]		
	<i>aver</i>	<i>st. dev.</i>	<i>char.</i>
0°	6.9	1.68	4.0
90°	5.8	1.19	3.7
45°	5.4	1.18	3.3

**Table 25** Comparison between the obtained test results of xz-specimens that are loaded in shear perpendicular to the grain (0°), parallel to the grain (90°) and under an angle of 45° to the grain

If sample 0,3, that failed in another than the intended section, is not taken into account, the shear strength in the direction of the printed lines turns out to be a little higher than when the material is loaded in shear under an angle or perpendicular to the grain. This result is in line with what could have been expected, since if a shear load is applied parallel to the grain (so the actual forces work perpendicular to the grain), than the material has to fail on a printed line. This while, if the material is loaded under an angle with respect to the grain direction, then the material can fail over the surface between to printed lines. Since the material is weaker between the printed lines than in the printed lines itself, the obtained results can be declared.

### 5.2.5 Test Setup – samples xy plane

Because the samples that are printed in the xy-direction, are twice as big as most of the samples that are printed in the xz-direction, these xy-samples do not fit in the clamped tools that were used for the samples in xz-direction. A solution for this problem was found by putting bolts through the holes of the sample and clamp these bolts between the clamping tools, instead of clamping the sample itself.

When using this testing method, another problem was faced: the sample, as it happens, was turning around during the test, such that the sample no longer was loaded in shear, but on a combination of shear and normal tensile forces. This issue was solved by drilling a second hole at both sides of the sample and put in another bolt, such that rotation of the sample over the bolts, was not an option anymore.

By these measures, the initial problems regarding a working testing method were solved and the right testing

## 5. Material Tests – Elementary Level

method was found. This applied testing method, is shown on the below pictures:



**Fig. 55 Test setup for shear specimens that are printed within the xy-plane.**

Like is done for the shear test with samples printed in xz-direction, again a dumbbell formed sample is chosen from the list of available sample types in the Zwick Testxpert II program. This time, the following dimensions are set for the samples:

Samples xz-plane
Parallel specimen length = 6.0 mm
Specimen width = 15 mm
Thickness = 6.0 mm

Because these samples were printed and the resolution of the printer is quite high, the middle part of the sample that is loaded on shear originally had a parallel specimen length of about 20 mm. Because this length turned out to be too big to let the sample fail on shear in this middle part, this length was sawn and cut such that it became 6.0 mm on an average. Again due to the fact of the high printing resolution, the region in which the sample can fail will be larger than in case of the samples in xz-direction, which were laser-cut. Therefore quite a big region of 15 mm on which the specimen can fail, is chosen as the specimen width.

For the thickness an average thickness of all the samples is set again, which for this samples is about 6.0 mm.

The test speed is set at 25 mm/minute, a preload of 10 N is taken and the max extension is set at 300 mm.

### 5.2.6 Test Results – samples xy plane

The samples that were loaded by a shear force working perpendicular to the direction of the printing lines, are shown on the picture below. Like was the case for the samples printed in the xz-plane, but loaded in the same direction (see paragraph 5.2.5), again an elongation of the material can be observed around the area loaded and failed on shear.



Fig. 56 Test specimens printed within the xy-plane and loaded in shear perpendicular to the grain direction

This effect also can be observed in the curves, because again, two peaks are visible. Like was done in paragraph 5.2.5 the first peak is picked as the stress level for the actual shear strength, since at this peak, the sample actually failed on shear already.

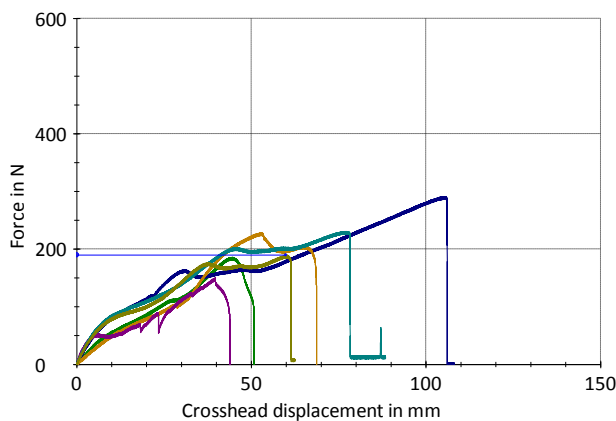


Fig. 57 Shear curves of the specimens loaded in shear perpendicular to the grain

Specimen Name	thickness [mm]	width [mm]	CS Area [mm <sup>2</sup> ]	Max Shear Force [N]	Shear strength [MPa]
0,2	5.4	5.0	27.0	165	6.1
0,4	7.7	6.4	49.3	225	4.6
0,5	8.1	5.4	43.7	125	2.9
0,6	5.4	6.7	36.2	200	5.5
0,7	6.1	4.6	28.1	160	5.7
Average					5.0
Standard deviation					1.28
Characteristic					2.7

Table 26 Results of test specimens printed within the xy plane and loaded in shear perpendicular to the grain

The samples that are loaded by shear forces that fall in the same line as the 'grain', this time do not show the same brittle failure as was the case for samples that were loaded in the same direction, but produced within the xz-print-direction (see paragraph 5.2.5). Instead, an extension of the material can be observed here as well. This is simply caused by the fact that it hardly was possible to obtain a shear area within this grain direction. These samples in the xy-plane are printed directly and because the printer prints continuously, the shear area needs to be printed in a wave pattern. Due to the low resolution and the consequential thick lines, this small shear loaded area, became one coherent and almost isotropic piece of material. Therefore these samples did



## 5. Material Tests – Elementary Level

not have the intended orientation over the part that is loaded in shear, and the behavior thereby is about the same as for the previous samples.



**Fig. 58** Tested specimens that are printed within the xy-plane and loaded in shear parallel to the grain

The fact that the loaded area of these samples acts the same as for the previous sample batch, can also be observed in the graphs and table results, that show about the same results as were obtained for the samples that were loaded in shear perpendicular to the grain.

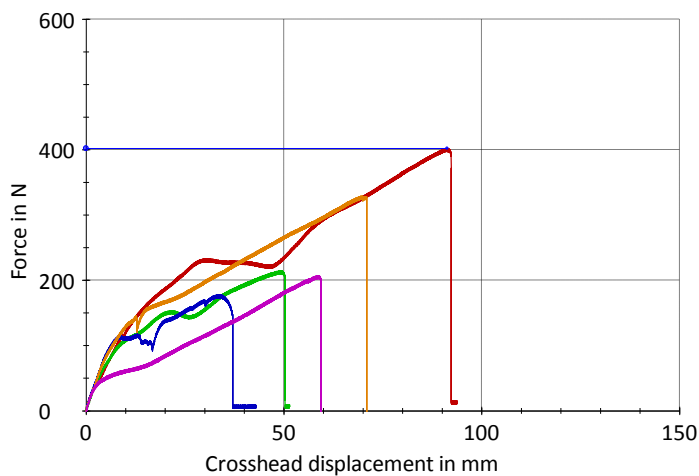


**Fig. 59** Force-displacement curves of the specimens loaded in shear parallel to the grain

Specimen Name	thickness [mm]	width [mm]	CS Area [mm <sup>2</sup> ]	Max Shear Force [N]	Shear strength [MPa]
90,1	5.7	5.0	28.5	230	8.1
90,3	5.4	5.0	27.0	150	5.6
90,4	4.3	5.4	23.2	115	5.0
90,7	5.6	6.0	33.6	155	4.6
90,8	5.4	6.5	35.1	60	1.7
Average					5.0
Standard deviation					2.29
Characteristic					0.9

**Table 27** Test results of xy-specimens that are loaded in shear parallel to the grain direction

The 45 degree samples finally, fail after elongation in the 45°-direction of the grain. Again, these samples cannot fail over the weak surface between two printed lines, like their 45°-direction brothers that were produced in the xz-printing-plane. Because the resolution in the xy-printing-plane actually is smaller than in the xz-plane, the loaded shear area this time actually only consists of one printed line, such that no weak surface between multiple printed lines is present. Instead, only the one line present is loaded, partly in shear and partly

in the normal force direction, which leads to about the same results as obtained in the previous two sample batches.



Fig. 60 Tested samples printed in the xy-plane and loaded in shear 45 degrees to the grain

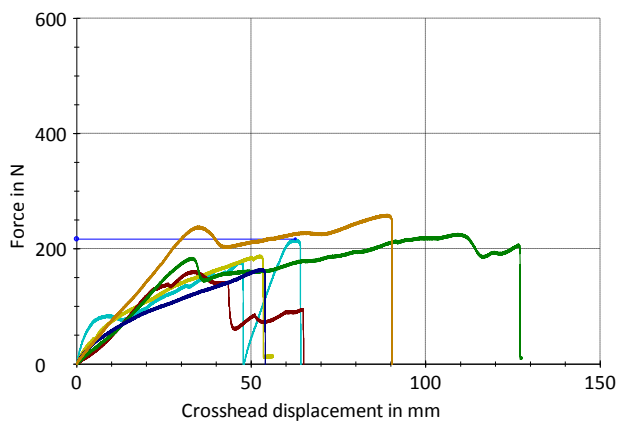


Fig. 61 Shear curves of the tested samples that are shown on Figure 60.

Specimen Name	thickness [mm]	width [mm]	CS Area [mm <sup>2</sup> ]	Max Shear Force [N]	Shear strength [MPa]
45,1	6.2	5.8	36.0	170	4.7
45,2	5.0	5.9	29.5	190	6.4
45,3	5.0	6.8	34.0	155	4.6
45,4	7.1	6.0	42.6	185	4.3
45,7	4.0	5.6	22.4	165	7.4
45,9	7.1	7.0	49.7	240	4.8
Average					5.4
Standard deviation					1.24
Characteristic					3.2

Table 28 Test results of specimens that are printed within the xy-plane and loaded 45 degrees to the grain

## 5. Material Tests – Elementary Level

Below the obtained results from the shear test are listed, both for the samples that were printed in the xz-plane as the samples printed in the xy-plane:

	Grain direction	Shear Strength [MPa]		
		<i>aver</i>	<i>st. dev.</i>	<i>char.</i>
xz-plane	0°	6.9	1.68	4.0
	90°	5.8	1.19	3.7
	45°	5.4	1.18	3.3
xy-plane	0°	5.0	1.28	2.7
	90°	5.0	2.29	0.9
	45°	5.4	1.24	3.2

**Table 29** Comparison of the shear strengths for all the different orientations

### 5.2.7 Test Evaluation and Conclusions

As table 29 shows, for the samples printed in the xz-plane, a difference can be noticed between the specimens that are loaded in the 0°-direction (so shear force works perpendicular to the grain) and the specimens that are loaded under an angle to the grain. Especially when test sample 0,3, which did not fail in the shear area, is not taken into account, this difference is good noticeable.

This same difference however, cannot be noticed between the different directions within the xy-plane. As already explained throughout the paragraph, this is due to the fact that the loaded shear area for these samples simply does not have the intended orientation. This, because the low printing resolution within the xy-plane is not sufficient for obtaining multiple lines in a certain direction on such a small scale. Instead, the material behavior within the loaded shear area is close to isotropic, which leads to homogeneous results for the three different orientations.

## 5.3 Compressive Test

### 5.3.1 Aim of Test

The aim of this test is to find the following compressive properties of the building material:

Material Properties	Symbol	Unit
Compressive strength in 3 directions (taken at 10% strain)	$f_{c,1}; f_{c,2}; f_{c,3}$	MPa
Compressive Yield strength in 3 directions (taken at 2%)	$f_{y,1}; f_{y,2}; f_{y,2}$	MPa
Compressive Strain (at compressive strength and at yield) in 3 directions	$\epsilon_1, \epsilon_2, \epsilon_3$	MPa
Compressive Modulus $E_c$ in 3 directions	$E_{c,1}, E_{c,2}, E_{c,3}$	MPa

**Table 30** Compressive properties that need to be found by means of the Compressive Test

The following graph shows how these different properties are obtained from the stress-strain curve that forms the output of the compressive test:

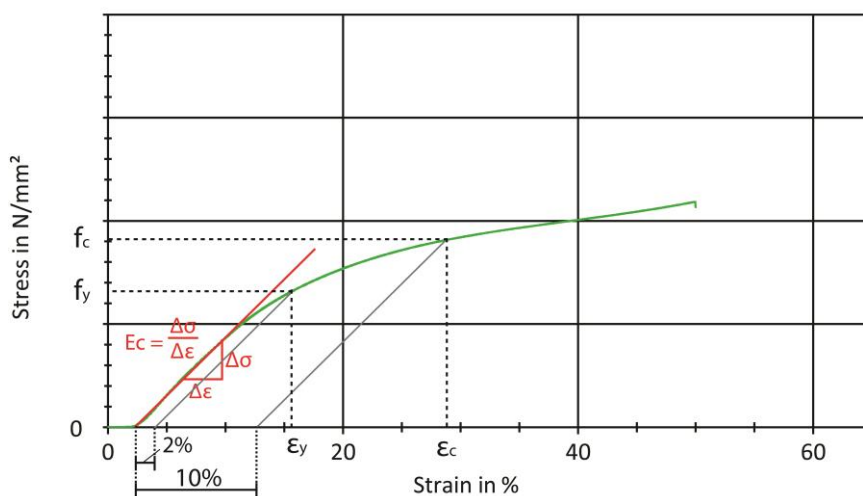


**Fig. 62** Determination methods of the different compressive properties out of the stress-strain curve

Because this material does not break, like for example concrete does, there is no presence of a clear point in which the compressive strength can be determined. Therefore, for plastics it is common to pick the compressive strength at a point that can be determined in the following way: first a diagonal line is drawn along the linear-elastically beginning part of the curve. Then on the x-axis, on 10% from the starting point of this linear line, a diagonal line is drawn under the same angle, until it touches the compression curve. In the point where this line touches the curve, the compressive strength  $f_c$  and the compressive strain  $\epsilon_c$  are determined. In the same way, but then on a distance of 2% from the linear-elastic part of the curve, the yield strength and yield strain are determined.

The Compressive Modulus is determined by calculating the slope of the linear-elastic part of the curve, by dividing the stress over this linear elastic part by the strain over this part.

For less elastic materials it is common to take smaller strain-percentages for the distance on which the yield strength and ultimate strength are determined. For plastic however, this 2% and 10% are common values. [Rosato, 2003].

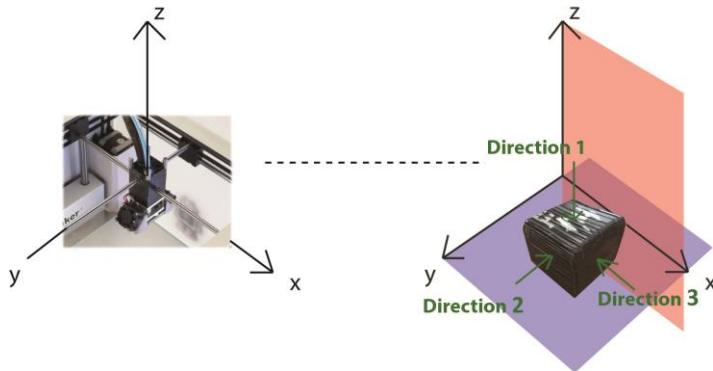
### 5.3.2 Tested Samples

Since the produced samples for the pressure test have the form of a cube, the samples are printed in a 3D-orientation. Therefore, this time no distinction is made between a xz-plane and xy-plane or a 0,90 or 45 grain-direction. Instead, the cubical samples are all the same and can be loaded in three different directions, which can be simply called loading direction 1, loading direction 2 and loading direction 3.

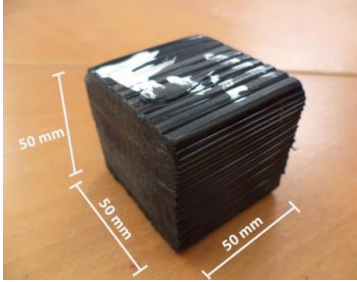
Loading direction 1 loads the cube sample in the direction of the z-axis, so it loads the sample in the direction in which the line thickness of the printed lines is 2.1 mm. Loading direction 2 loads the sample within the horizontal plane, so in the direction where the line thickness of the printed lines is about 5-6 mm. Finally, loading direction 3 is the load in the horizontal plane directed perpendicular to loading direction 2. Loading direction 3 loads the cube in the same direction as the direction in which the lines are printed, so in the grain-

## 5. Material Tests – Elementary Level

direction. This probably means that a higher compressive strength can be expected in this direction. On the picture below, these three different directions are shown in relation to the composition of the printed cubical test samples.



**Fig. 63** Different loading directions for the cubical compressive specimens

Tested samples	Load direction	Nr. of samples
	1	7
	2	7
	3	7

**Table 31** Available test specimens for the compressive tests

As can be seen on the above picture of sample, the surface on the left (which is the surface, on which the load will be applied when loading in direction 3), looks almost homogeneous, as no fibers are noticeable anymore on this surface. This means that when obtaining these kind of 3D-oriented-samples, orientation effects seems to disappear within the cross-section of the material, as printed lines will glue together in the direction perpendicular to the line orientation. Only at the surfaces of the samples, the printed lines are still noticeable.

### 5.3.3 Test Setup

The same Zwick testing machine is used as in the tension and shear tests. This machine can apply compressive forces up to 100 kN. Instead of using the clamp-devices that are used in the previous experiments, this time a pressure-accessory is connected to the lifting system of the machine. Logically, in this experiment the upper-device moves downwards instead of upwards, such that a compression load is applied on the top surface of the cube. The test setup is shown on the picture below:



**Fig. 64** Test setup compressive test

In the Zwick Testxpert II software program, it is indicated that a compression test will be performed on a block formed sample with a height, length and width of 50 mm.

The testing speed is set at 25 mm/min and a preload of 10 N is chosen. The set maximum contraction differs per sample, because on one hand it was intended to increase the force and strain as much as possible to gain more information, but on the other hand the testing machine did not allow too much contraction to prevent the machine from breaking down when the upper and lower platform would touch each other.

### 5.3.4 Test Results

The test specimens that are loaded in direction 1 look as follows after performing the test:



Fig. 65 Test specimens that are loaded in direction 1

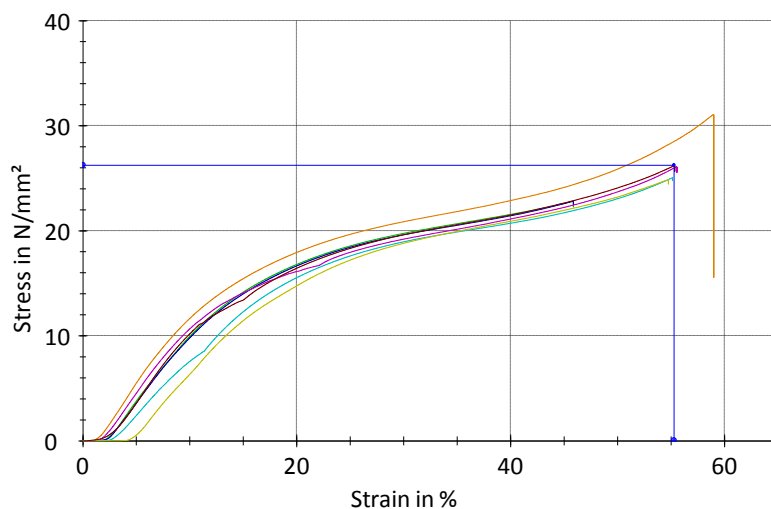


Fig. 66 Stress-strain curves of the specimens that are loaded in direction 1

As can be seen in figure 65, a permanent deformation is obtained. For all the samples it holds that the maximum set displacement of 30 mm and in some cases 40 mm was reached, which means that the sample height decreased with about 60% till a height of 20 mm. However, after that the compressive load was released, the samples folded back again to a height lower than, but quite close to the original height. At the outer surfaces of the sample, there was room for the fibers to move over each other, which led to irregular compositions at the side, while the middle of the sample stayed quite homogenous.

If we look at the graphs in figure 66, the first thing that stands out is the homogeneity of the obtained result, especially when compared to the results obtained in the previous tests. This is probably caused by the fact that the creation of a 3D-material sample, leads to a sample in which a lot of adhesion takes place in all directions, leading to a specimen that is quite cohesive. Due to the large amount of molecular connections in all three directions, a specimen of constant and predictable quality is obtained, because the influence of local inaccuracies is eliminated by the big amount of connections.

## 5. Material Tests – Elementary Level

The accuracy of the measured strengths is 0.1 MPa and the accuracy of the strains is 0.5%

Specimen Name	length [mm]	width [mm]	height [mm]	CS Area [mm <sup>2</sup> ]	Compressive Strength* [MPa]	Compressive Strain [%]*	Compressive Yield Strength [MPa]	Compressive Yield Strain [%]	Compressive Modulus [MPa] or MPa
F1,1	51.5	46.5	54.5	2394.8	18.8	25.5	13.6	14.0	140
F1,2	51.6	46.7	54.5	2409.7	18.6	25.7	13.4	14.2	139
F1,3	51.4	48	54.0	2467.2	17.7	24.0	13.1	13.0	144
F1,4	52.0	46.9	54.4	2438.8	18.9	30.5	14.5	18.0	107
F1,5	51.0	47.1	54.8	2402.1	19.5	32.5	15.1	20.5	118
F1,6	50.5	48.3	54.2	2439.2	18.2	25.0	12.3	13.0	143
F1,7	50.6	48.0	54.4	2428.8	19.5	24.5	13.8	12.5	156
<b>Average</b>					18.7	26.8	13.7	15	135
<b>Standard deviation</b>					0.66	n.a.	0.92	n.a.	8.66
<b>Characteristic</b>					17.5	n.a.	12.1	n.a.	120

**Table 32** Test results for specimens that are loaded in direction 1

As could have been expected, the compressive strength of the material is considerably higher than the tensile and shear strength. Although the sample is loaded perpendicular to the grain direction, the fibers now are pressed towards each other instead of pulled apart, like was the case in the previous tests. The high elasticity of the material furthermore has the effect that there always seems room for further deformation without breaking.

The samples loaded in direction 2 are shown on the following picture:



**Fig. 67** Test specimens loaded in direction 2

Again all samples reached the maximum set displacement of 30 mm and folded back partly after the removal of the load. This time however the permanent deformation is a little higher than was the case when loading the samples within direction 1. This probably is due to the fact that the resolution is smaller in direction 2, resulting in higher line-thicknesses and bigger distances between the successive lines. When now two lines move over each other, this leads to a bigger deformation than was the case for lines rolling over each other in direction 1. The bigger permanent deformation in direction 2 can be explained by this.

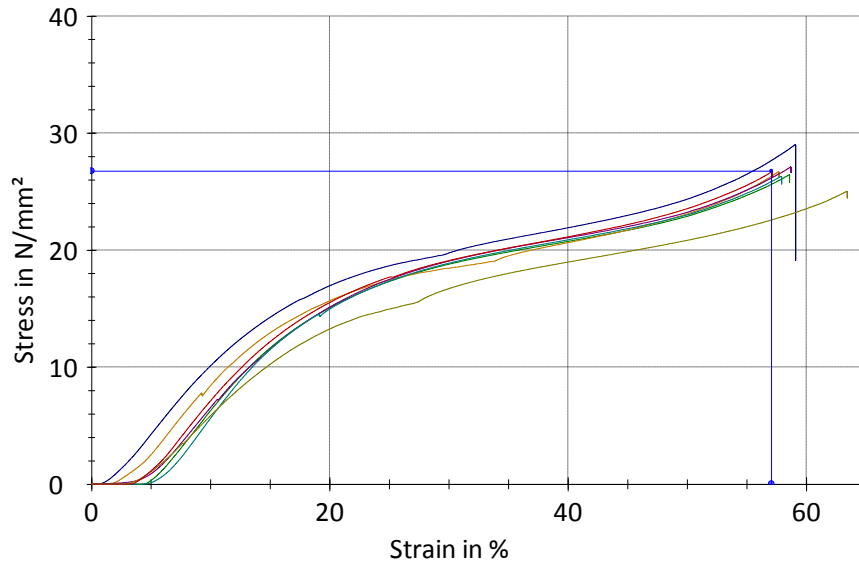


**Fig. 68 Stress-strain curves of the specimens tested in direction 2**

The obtained values for the strength are of the same order of magnitude as was the case for loading in direction 1. This probably is due to the fact that the cross section of the material becomes quite homogenous as line orientations disappear due to gluing together of the printed lines in the directions perpendicular to the print directions. This leads to a coherent and homogeneous composition, as already explained in paragraph 5.3.2.

Specimen Name	length [mm]	width [mm]	height [mm]	CS Area [mm <sup>2</sup> ]	Compressive strength [MPa]	Compressive Strain [%]	Compressive Yield Strength [MPa]	Compressive Yield Strain [%]	Compressive Modulus [MPa] or MPa
F2,1	54.1	48	51.2	2596.8	18.7	30.0	14.0	18.0	128
F2,2	53.9	48.2	50.7	2598.0	19.3	27.0	14.6	15.5	123
F2,3	54.0	46.5	52	2511.0	18.0	27.0	13.8	16.0	124
F2,4	54.3	48.3	51.1	2622.7	19.1	30.0	13.7	17.5	118
F2,5	54.5	48	51.8	2616.0	18.8	30	14.1	18.5	134
F2,6	54.4	47.7	47.3	2594.9	17.3	31.5	12.6	19	100
F2,7	54.3	48.6	52.5	2639.0	18.8	29.0	13.8	14.5	128
<b>Average</b>					18.6	29.2	13.8	17	122
<b>Standard deviation</b>					0.69	n.a.	0.61	n.a.	10.27
<b>Characteristic</b>					17.4	n.a.	12.7	n.a.	104

**Table 33 Test results for specimens that are loaded in direction 2**

The samples that are loaded in direction 3 look as follows after the obtained compressive test:





Fig. 69 Tested specimens that were loaded in direction 3

For these samples, the permanent deformation is best noticeable in the form of the fibers at the surface which are bended and which were standing further apart from each other resulting in gaps in between the lines. In fact, the fibers buckled out, since they are loaded in compression in the longitudinal direction of the fibers. The obtained permanent deformation is bigger than in case of loading in direction 1 and 2. This is probably caused by the fact that the deformation when loading perpendicular to the grain happens, for the most part, elastically, while the buckling of the grains is a permanent deformation.

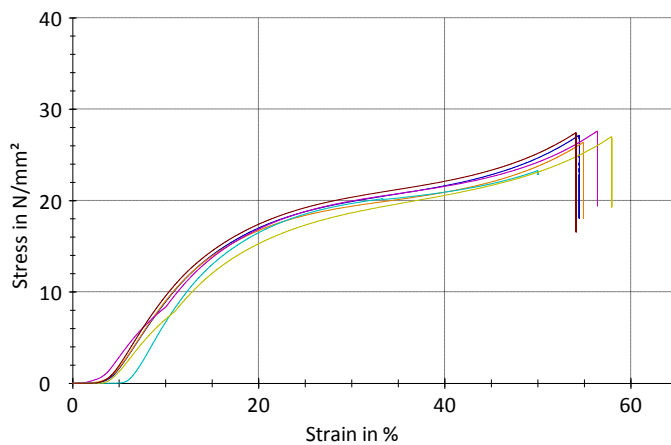


Fig. 70 Stress-strain curves of the specimens that were tested in direction 3, which is the direction parallel to the grain

Specimen Name	length [mm]	width [mm]	height [mm]	CS Area [mm <sup>2</sup> ]	Compressive strength [MPa]	Compressive Strain [%]	Compressive Yield Strength [MPa]	Compressive Yield Strain [%]	Compressive Modulus [MPa] or MPa
F3.1	54.3	50.9	47.8	2763.9	19.4	26.5	14.3	15.5	152
F3.2	54.5	51.0	47.5	2779.5	18.4	29.5	14.1	18.0	118
F3.3	54.3	52.7	47.5	2861.6	18.6	26.5	14.3	15.5	146
F3.4	54.0	50.6	48.3	2732.4	19.3	28	14.4	16.0	131
F3.5	54.1	51.3	50.0	2775.3	19.3	27.5	14.5	17.0	165
F3.7	54.2	50.8	45.0	2753.4	19.8	26.5	14.6	15.5	155
<b>Average</b>					19.1	27.4	14.4	16.3	145
<b>Standard deviation</b>					0.53	n.a.	0.18	n.a.	17.17
<b>Characteristic</b>					18.2	n.a.	14.1	n.a.	114

Table 34 Test results for specimens that are loaded in direction 3

The compressive load in direction 3 (direction of the grain) led, on an average, to a strength that is approximately 4 to 5 percent higher than in case of loading in the directions 1 and 2. This probably can be explained easily by the fact that loading in the direction of the fibers/printed lines leads to the highest strength, since the fiber-direction simply is the strongest direction. Still, these orientation effects are for the compressive test significantly smaller than for the tensile and shear test. This, because the production of a 3D-sample leads to samples that are almost homogeneous and un-oriented, especially at the middle part of the sample. It seems to be that only at the surfaces/sides of the sample, the printed orientations are still present, for they are only noticeable there. For that reason still some differences are obtained between the loading direction parallel to the grain (direction 3) on one hand, and the two other loading directions (direction 1 and 2) on the other. But since the surfaces only form a small part of the total sample and the middle part seems to be homogenous and without a certain orientation, the strength differences in the compressive test between the different directions/orientations are relatively small.

### 5.3.5 Test Evaluation and Conclusions

Although the results of this test showed a compressive strength which is about 2-2.5 times larger than the tensile strength, it might be the case that the used test samples are not fully representative for the printed house-blocks as they are designed by DUS Architects so far. The reason for this doubt lies in the fact that the use of a solid 3D sample lead to an almost homogeneous material composition and behavior, due to gluing/attaching together of the material in directions perpendicular to the grain direction. This, while in practice, so far it never occurred that DUS printed building blocks in such a way that multiple layers are attached to each other in multiple directions. In fact, all blocks are composed from 2d-surfaces of one layer thick.

Therefore, there is no full certainty if the strength results of this compressive test can be extrapolated towards these kind of 'DUS'-geometries. For that reason, it might be valuable to perform a compressive test on a hollow section as well, to compare the solid and closed geometries of this test, with open ones.

On the other hand, the results of this test also might form a trigger for the involved parties DUS and Tentech, to consider a different way of block-designing. Since this test has proven that stacking printed layers in two directions instead of only one, leads to a more homogeneous, consistent and therefore better predictable material behavior, it might be worth to consider the option to build up blocks (partly) by solid elements as well instead of composing the whole block out of 2d-plates.

From the tensile- and shear-test, it is learned that a local inaccuracy can lead to a significant lower mechanical performance, and therefore the mechanical behavior becomes quite unpredictable, leading to relative low allowable strength capacities. This problem seems to be solved by building up the house blocks out of 3D-elements that are much more consistent, better predictable and therefore have a higher strength capacity.

So, to summarize, the following conclusions can be drawn:

- The compressive strength, on an average is about 2-2.5 times bigger than the tensile strength
- There is not much difference in strength between the three different orientations. The strength in the grain-direction is only a little higher than in the other two directions.
- It might be the case that the results cannot be completely extrapolated towards designs that are fully built up by 2d-plate-elements. Therefore it might be useful to test a hollow sample as well.
- The designing parties DUS and Tentech could consider to (partly) compose the building-blocks out of 3D-elements instead of only 2d-plate elements.

## 5.4 Determination of the Young's moduli

### 5.4.1 Aim of Test

The aim of this test is to find the Young's moduli for the different grain directions and for the different printing planes in which the building material can be printed:

Material Properties xz-direction	Symbol	Unit	Material Properties xy-direction	Symbol	Unit
E-modulus 0°-direction	$E_{0,xz}$	MPa	E-modulus 0°-direction	$E_{0,xy}$	MPa
E-modulus 90°-direction	$E_{90,xz}$	MPa	E-modulus 90°-direction	$E_{90,xy}$	MPa
E-modulus 45°-direction	$E_{45,xz}$	MPa	E-modulus 45°-direction	$E_{45,xy}$	MPa





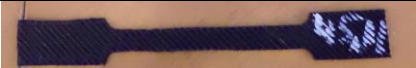

**Table 35** Different Young's Moduli to obtain within this test

The Young's moduli are determined by calculating the slope over the initial, linear-elastic part of the obtained stress-strain curves. This can be represented by the following formula that can be derived from Hooke's law:

$$E = \frac{\Delta\sigma}{\Delta\epsilon} \quad (5.1)$$

### 5.4.2 Tested Samples

For every different sample coordination, a number of 2 samples are tested for this tensile extensometer test, such that the total number of tested samples within this test is 12:

Tested samples xz-plane	Grain Direction	Nr.	Tested samples xy-plane	Grain Direction	Nr.
	0°	2		0°	2
	90°	2		90°	2
	45°	2		45°	2

**Table 36** Test specimens that are available for this test

Unfortunately, due to lack of availability of the 3D-printer, no more specimens were available for performing this test.

All these samples have the dimensions as shown on the picture below:

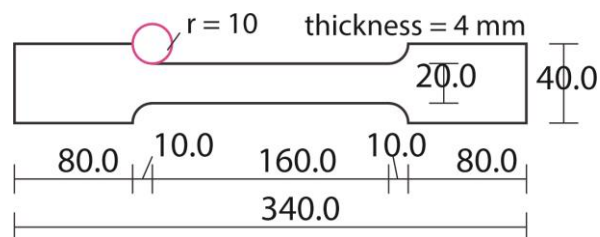


**Fig. 71** Specimen dimensions

### 5.4.3 Test Setup

The test setup is the same as for the normal tensile test, which is described under paragraph 5.1.3, with the addition that an extensometer is placed around the width of the middle part of the dumbbell sample.



**Fig. 72** Test setup for the determination of the Young's moduli

A dumbbell formed sample is chosen from the list of available sample types in the Zwick Testxpert II program for which the following dimensions are set:

Samples xz-plane	Samples xy-plane
Parallel specimen length = 160 mm	Parallel specimen length = 160 mm
Grip to grip distance = 185 mm	Grip to grip distance = 185 mm
Specimen width = 20 mm	Specimen width = 20 mm
Thickness = 6.0 mm	Thickness = 5.0 mm
Gauge length = 20 mm	Gauge length = 20 mm

**Table 37** Dimensions that are set in the control program for the gauge area

The parallel specimen length is the length of the straight narrow middle part of the dumbbell formed sample. The grip to grip distance is the average distance between the two clamps that hold the sample. The specimen width is the width of the narrow middle part of the sample, the thickness is based on the average of all the measured samples and the gauge length in this case is the distance between the two ends/clamps of the extensometer.

The test speed is set at 25 mm/minute and a preload of 10 N is taken. The set maximum applied stress level differs per sample, because the intension was to find a balance between a maximum applied stress and consequently strain on one hand, but no material failure on the other hand because this could break down the extensometer.

#### 5.4.4 Test Results

The figure below shows the obtained extensometer-curves from the loaded specimens that are printed within the xz-plane. It is not surprisingly that the specimens that have their grain-direction in the direction of the applied tensile load, show the steepest slope and therefore have the highest value of the Young's Modulus.

## 5. Material Tests – Elementary Level

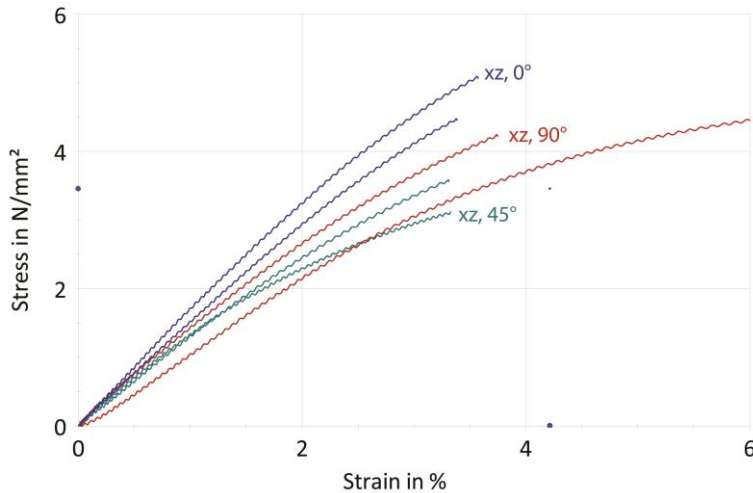


**Fig. 73** Stress strain curves of the specimens that are printed within the xz-plane. Specimens that are loaded parallel to the grain, perpendicular to the grain and 45 degrees to the grain, all can be found in this figure

The stress-strain curves of the specimens that are printed within the xy-plane, are shown in figure 74. For two of these samples it holds that it is a little harder to determine the Young's modulus, since no clear linear course is present from the Origin. These curved courses are probably caused by the inconsistent form and quality of these specimens, which leads to a non-linear extension. The Young's Modulus is obtained in these cases by drawing a diagonal linear line from the origin that starts above the particular curve and ends underneath the curve or vice versa. By ensuring that the area between this diagonal line and the curved line, above the diagonal line, is about the same as the in between area under the diagonal, this drawn diagonal line provides a reasonable reflection of the original curve. Then, the slope of this diagonal is determined such that the Young's Modulus is obtained.

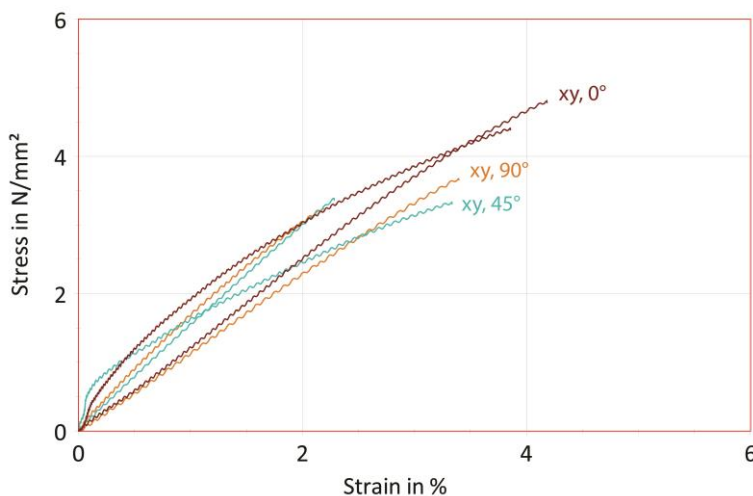


**Fig. 74** Stress-strain curves of the specimens that were printed within the xy-plane

Like in the performed tensile and shear test, that are described under paragraph 5.1 and 5.2, it again is the case that the samples that are printed within the xy-plane, do not show an obvious slope-difference between the different grain directions. This again can be explained by the isotropic behavior of the material samples in the xy-plane, which is caused by the effects as explained under paragraph 3.1.3.

The table below clearly shows that, as expected, the Young's moduli are the biggest for samples that are printed within the xz-plane and loaded within the direction of the printed lines/grains.

For the other results, it is hard to draw too much conclusions based on only the two tested samples. Especially the values of the samples that are printed within the xy-plane, lie too far apart to make a proper statement about them. This large variation in values, probably is partly caused due to the situation that curved lines were

obtained instead of linear lines for these samples, which presumably makes some of the determined values more inaccurate.

Specimen Name	thickness [mm]	width [mm]	CS Area [mm <sup>2</sup> ]	Young's Modulus [MPa]	Aver. value [MPa]	St. dev. [MPa] [Domone, 2010]	Char. value [MPa] [Domone, 2010]
xz,0,9	19.6	8.2	160.7	150.2	160.2	14.14	131.8
xz,0,10	19.6	7.2	141.1	170.2			
xz,90,7	20.0	7.1	142.0	120.7	129.6	12.59	104.3
xz,90,8	19.1	7.0	133.7	138.5			
xz,45,9	19.6	7.2	141.1	131.1	121.4	13.72	93.8
xz,45,12	19.4	7.0	135.8	111.7			
xy,0,7	20	6.8	136.0	113.1*	121.25	11.53	98.1
xy,0,8	22.7	5.5	124.9	129.4			
xy,90,7	21.4	5.1	109.1	112.2	129.6	24.54	80.2
xy,90,9	22.9	5.4	123.7	146.9			
xy,45,7	21	7.0	147.0	153.1	119.4	47.66	23.6
xy,45,8	20	6.0	120.0	85.7*			

**Table 38 Test results Extensometer-tests**

\*Inaccurate measurement, due to curved line.

#### 5.4.5 Test Evaluation and Conclusions

As mentioned in the previous paragraph, the amount of results obtained in this test is not sufficient for drawing up well-founded conclusions. However, the test results from this test, can be used for validation of earlier obtained results and for some new insights.

The obtained value for the Young's modulus in the grain direction of the xz-plane is a bit higher than the average value of the compressive moduli as found under the compressive test. Still, as the compressive moduli gained from the compressive test on an average have a magnitude of 145 MPa with a maximum value up to 165 MPa, the obtained values (150 and 170 MPa) from this test are of the same order of magnitude as the values that are obtained during the compressive test. This is in line with what could have been expected, as within the elastic range, these Moduli often are close or equal to each other.

The same thing holds for the obtained results for the xz-plane samples that are loaded 90-degrees and 45-degrees to the grain. With an average value of 120-30 N/mm, also these results have the same order of magnitude as the obtained results during the compressive test.

Like in the previous tests, this test again confirmed that for samples that are printed within the xy-plane, the results do not show a clear different behavior for the different grain directions.

What also can be observed for both the xy-plane as the xz-plane is that the deviations between the different results, are quite large. This also could be observed in the compressive test where large value-ranges were obtained as well. This means on one hand that the material behavior is quite unpredictable since different values are obtained for the same test within a large range. On the other hand will the material become better predictable on the moment that a higher number of samples are tested, because deviations and averages could be better mapped in that case.

## 5. Material Tests – Elementary Level

### 5.5 Determination Density

#### 5.5.1 Aim of Test

Although on the factsheet of Henkel the density is already given, it can be the case that the density of the material, when it has left the 3D-printer, differs from the density of the material in granular form. This, because the extrusion process might change for example the molecular distance or the amount of air within the composition. Therefore, in this test, the density of the printed material will be determined and compared to the value on the factsheet.

#### 5.5.2 Tested Samples

The three tested sample types are displayed on the below picture. There is chosen to test specimen-parts that are printed in different orientations, because it might be the case that densities differ for samples that are printed in a different direction.

Therefore, 50x50x50 cubes are tested, which are printed in three directions and therefore form 3D-objects. Furthermore pieces of flat specimens which are printed within the xy-plane are tested, next to flat specimens which are printed within the xz-plane.

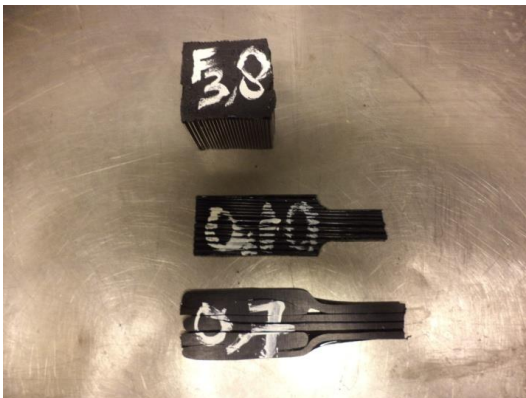


Fig. 75 Tested specimen types for the density test

#### 5.5.3 Test Setup

At first, the dry weight of the test specimens is measured.

The required equipment for performing this test is shown on the picture below. The cup on the right is filled with water up to the brim. When a specimen is placed in this cylinder, an amount of water equal to the volume of the specimen will flow over the edge and fall within the white bucket. By pouring the water in the measurement cup in steps via the measuring cylinder, the volume of the specimen can be defined.

There is chosen for this method instead of using just one cup and reading the rise of the water level within this cup, because the use of the small measuring cylinder with a smaller scale enables a more accurate reading.



Fig. 76 Test setup density test

Because the material floats in the water (the density of the printing material is smaller than the water density), a sharp object is used to immerse the sample, just under the water level.



Fig. 77 By immersing the test sample and collecting the water that flows over the edge, the volume of the test specimen is determined

#### 5.5.4 Test Results

Specimen	Henkel-Sheet	Cube-formed samples			xy-printed samples			xz-printed samples		
		Sample 1	Sample 2	Sample 3	Sample 1	Sample 2	Sample 3	Sample 1	Sample 2	Sample 3
Mass [g]		131.5	122.66	121.6	17.1	11.7	14.9	22.4	18.2	28.5
Volume [ml]		145	127	128	21	13.0	16.0	31	20.4	30.3
Density [ $\text{g}/\text{cm}^3$ ]	0.98	0.91	0.97	0.95	0.81	0.90	0.93	0.72	0.89	0.94
Average density [ $\text{g}/\text{cm}^3$ ]	0.98	0.94			0.88			0.85		

Table 39 Test results density test

#### 5.5.5 Test Evaluation and Conclusions

The obtained values for the density are all lower than the density that is given on the Henkel sheet. This result can have two causes: Either the density value on the Henkel sheet is higher, because the density of the printing material, once compressed, indeed is higher than the density of the material when it is printed. Or the measured density values are just lower because the measuring method was insufficient.

Both causes actually can be valid. The mechanical tests already have proven that the values on the Henkel sheet are on the high side and form upper boundaries for the strength values of the material once it is printed. For the density value, the same situation can hold. On the other hand, it is plausible as well that the applied measurement method is not sufficient, because only the water that actually flows over the edge of the measuring cylinder, is measured. This, while it is likely that not all the water that is taken in and pushed upward by the sample, will actually flow over the edge. Because the cylinder was fully filled, the first part of the water that is pushed away by the sample, indeed will flow over the edge. However, after the moment that this first amount of water has left the cylinder, the remaining part of the water that is pushed upward by further immersing the sample, probably will stay in the cylinder as the cylinder is not filled to the edge anymore by then.

To be on the safe side, it is recommended to always apply the density of  $0.98 \text{ g}/\text{cm}^3$ , that is mentioned on the Henkel-sheet, in practice. This, because it cannot be excluded that the lower obtained density values are caused by an insufficient measuring method. When one actually wants to find out if the density of the material, once printed, differs from the density of the raw material, it is recommended to perform a more accurate testing method.



## 5. Material Tests – Elementary Level

### 5.6 Absorption and Drying Test

#### 5.6.1 Aim of Test

Apart from the behavior of the material under its loads, that is expressed by the mechanical properties, the material will also be exposed to weather and environmental conditions. The printing material actually is applied both structurally as for the façade, at least in the early phases of the project. Therefore the material must be able to deal with the weather and environmental circumstances as well.

An important condition is of course the exposure of the printing material to water. In most cases this will go on to rainwater, but since the house will be situated alongside a river, it can also be that the water from the river spurts against the house in case of many wind or, in worst case scenarios, the water from the river can even flood.

Aim of this test is to study the way in which the printing material reacts on water. This is done by performing both an absorption test as a drying test. In the absorption test, the amount of water that is absorbed by the material is plotted against the elapsed time and in the drying test there will be researched how quick the material will dry after being fully saturated.

#### 5.6.2 Tested Samples

For both the absorption and the drying test, a cube sample of 50x50x50 mm, like on the picture below, is used.

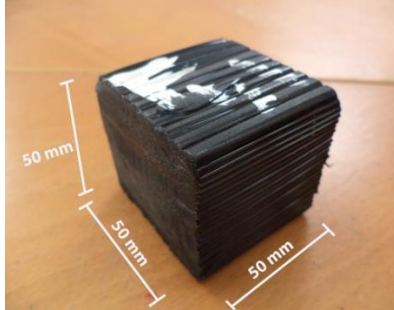


Fig. 78 Used test samples for the Absorption and Drying tests

#### 5.6.3 Test Setup

First of all, the dry mass of the specimen that is used for the absorption test and the dry mass of the specimen used for the drying test, are measured.

For the absorption test, the test specimen is placed in a small bucket. After that, the bucket is filled with water until the water level reaches half the height of the specimen. Then the test can actually start by measuring the weight of the sample after every 24 hours, till a weight is reached that is about constant.

By calculating for every measurement the  $(\text{absorption mass-dry mass})/\text{dry mass}$ , the water absorption can be expressed in a percentage of weight increase. Since the weight increase after every 24 hours can be calculated this way, the weight increase subsequently can be plotted against time in a graph.

The cube is placed in the bucket, such that the side of the cube with the printing-line-structure printed in the xz-direction is facing the bottom. This means the sides of the cube with the printing-line-structure printed in the xy-direction and the end faces will be exposed to the water the most. This is done because it is expected that the xy-direction surfaces will be the most permeable sides of the cube and therefore especially these sides should be tested by exposing them to the water the most.



**Fig. 79 Test setup absorption test**

For the drying test, the test specimen first is completely immersed during a week. Because the material floats, a mass was placed on top of the sample to be able to place the sample fully under the water level.



**Fig. 80 Test setup submersion/drying test**

After a week, the mass of the fully saturated sample is measured. After that, the sample is laid down in a tray filled with gravel, such that the sample can dry. When measuring the mass of the sample then after every 24 hours and again calculating  $(\text{wet mass}-\text{dry mass})/\text{dry mass}$ , the dry-curve can be obtained by plotting these mass-percentages against time.

#### 5.6.4 Test Results

##### Absorption Test

	Dry	Wet	Wet	Wet
Date	8-May	9-May	10-May	11-May
Time	15.20	15.20	15.45	15.45
Mass [g]	123.2	123.3	123.3	123.3
Mass increase [%]	/	0.081	0.081	0.081

**Table 40 Test results absorption test**

As can be seen in table above, there barely was measured an increase of the mass. After every day, the balance signaled a rise in the mass of only 0.1 g. This rise does not even have to be caused by absorption, because although the surfaces of the specimen were dried before every measurement, it is quite plausible that this 0.1

## 5. Material Tests – Elementary Level

g still, is caused by some water that was left over at the surface.

Because normally the absorption curve shows a declining growth, not much increase was expected to happen after the third measurement. Therefore the test was stopped after the third measurement, concluding that the material absorbs a negligible amount of water.

Also from the dry test, this same conclusion can be drawn. After completely immersing the sample during a week, the sample mass was only increased by 0.1 g again. This small increase again probably is, for the most part, caused by water. Therefore it was unnecessary to further perform a drying test, for one could hardly speak about a saturated specimen with mass increases of this order of magnitude.

### Dry Test

	Dry	Immersion during a week	Wet
Date	8-May		16-May
Time	15.20		15.50
Mass [g]	123.0		123.1
Mass increase [%]	/		0.081

**Table 41** Test results Dry test

### 5.6.5 Test Evaluation and Conclusions

From the results that are obtained during both the absorption test as during the dry test, it can be simply concluded that the amount of water that is absorbed by the material is negligible. This means that not much problems are expected for the material being exposed towards rain and/or frost, as the material blocks almost all the water.

However, one should be aware of the fact that the material, in the form as it is applied within the printed blocks so far, is permeable. This, because all the blocks that are printed so far, are build up by 2d-plates of one layer. Due to local inaccuracies that are often present within these plates between printed layers that don't connect properly, the building blocks will not always be waterproof. In case multiple layers are printed next to each-other in the xy-direction, the permeability will be reduced for every extra layer that is added, as the layers will melt together and holes will be filled.

So apart from using multiple layers in the xy-direction for obtaining a more isotropic, better predictable and stronger behavior as was concluded from the mechanical tests, another good reason to apply multiple layers, is that the building blocks become waterproof.

## 5.7 Temperature – Strength Test

### 5.7.1 Aim of Test

As is mentioned in chapter three, the properties that make the printing material suitable for use in a 3D-printer (low melting point, thermoplastic behavior etc.), may cause problems for applying this material in a building construction. For an extreme occasion, like fire, one can predict with almost certainty that this material alone cannot withstand the heating load. But it can also be the case that a normal heating load, produced by the sun on a summer day, might lead to degradation of the structural behavior already. Although structural failure in case of fire of course is undesirable, failure under normal circumstances is impermissible for it will prevent the building construction from normal functioning.

The aim of this test therefore is, to find out if temperature differences to which the material can be exposed to in The Netherlands under normal circumstances, have an influence on the mechanical properties of the material. Fire resistance, in its turn, is something which is recommended to research in future studies.

Since this test focuses on temperature dependencies of the material under normal circumstances, first the temperature reach for the Netherlands should be determined, by defining the extreme boundaries to which a material that is exposed to the sun, can be heated up to.

According to the figure below, the maximum temperature of the surface of a roof in the Netherlands is about 80 degrees Celsius and the minimum temperature about -30 degrees Celsius.

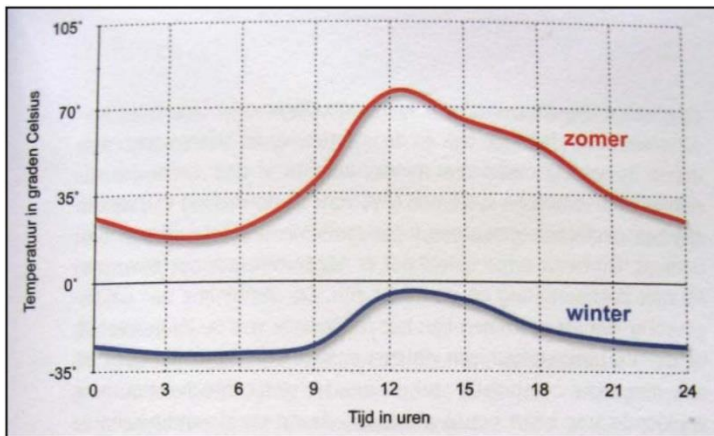


Fig. 81 Maximum and minimum surface temperature curves in the summer respectively winter [Source: Krusche et al., 1982]

Because the roof is the surface of a building that is loaded the heaviest by the sun, these temperatures of 80 degrees and -30 degrees are normative for the extreme temperatures the material can be heated up to or cooled down to, when applied in the building and exposed in open air.

The temperature range to which the material has to be exposed to in this research, is herewith defined. Although different strength properties that are mentioned under paragraph 3.3.3 may be influenced by the temperature, in this test only the influence of temperature on the tensile strength will be studied, to prevent the material study to become unnecessarily elaborate. Based on the results of this tensile test, it actually will be possible already to make a more general statement about the influence of the temperature on the general mechanical behavior of the material and to come to a conclusion whether or not measurements should be taken to prevent the structure from failing.

Therefore, the following material properties need to be obtained during this test:

Material Properties xz-direction	Symbol	Unit
Ultimate tensile strength // for temperatures between -30° C and 80° C	$f_{t;0,xz,temp}$	MPa
Elongation at ultimate tensile strength // for temperatures between -30° C and 80° C	$\epsilon_{t;0,xz,temp}$	%

Table 42 Properties that need to be obtained within the temperature-strength test

## 5. Material Tests – Elementary Level




### 5.7.2 Tested Samples

The intention is to increase the temperature from -30 degrees towards 80 degrees by 10 steps of 11 degrees, such that 11 samples are needed that have the exact same properties.

Since a tensile test under different temperatures is performed here, the use of dumbbell-shaped specimens, as used under the 'normal' tensile test, would be ideal here. Unfortunately, due to a lack of availability of the 3D printer and the laser cutter, not enough of these specimens with the same properties were produced.

Therefore, instead of dumbbell-shaped specimens, 11 straight rectangular samples are used, having the same length as the dumbbell-samples and the same width as the center part of the dumbbell. The grains of these samples are in the direction of the tensile load, such that useful test results are obtained.

During the heating up process of the oven-area to the required temperature, some of the rectangular samples already started to soften, such that performing a proper tensile test was not possible anymore. To still obtain enough useful test results, it was necessary to test 4 dumbbell-samples instead, that were left over from the tensile test. The use of these dumbbell samples of course is not ideal, since they are wider around the wedged area and two of these samples are printed in a different plane. Still, the results of these tested samples probably can be fit in within the other test results, since the loaded middle area is the same and the influence of the temperature is of such a magnitude, that the influence of the difference in sample form will probably be subordinate to this temperature influence.

Tested samples xz-plane	Grain Direction	Plane	Nr.
	0°	xz-plane	11
	0°	xz-plane	2
	0°	xy-plane	2

**Table 43** Specimens that are tested in the Temperature-Strength test

### 5.7.3 Test Setup

For this test, a 250 KN Zwick tensile testing machine with oven is used which is located in the 'Vliegtuighal' of the faculty of LR. The testing machine works in the same way as the testing machine which is used for the tensile, shear and compressive test, with the addition that the tensile clamps are surrounded by an oven this time. At the right side of the left picture of figure 82, a tank containing liquid nitrogen is just visible. This tank can provide the oven with nitrogen in case temperatures below room temperature need to be set.

The machine enables a temperature range between -60 and 300 degrees Celsius, which means the desired range for this test (-30 and 80 degrees) easily can be reached.

Like was the case with the Zwick testing machine that was used during the previous tests, this machine is controlled by the software program Testxpert II as well. This program also enables to set the oven temperature.

The temperature that is set, is the temperature of the air in the oven, which was expected to be different from the temperature of the specimen. Therefore, an electric thermometer with a wire sensor was used, to be able to register the specimen-temperature as well. Unfortunately this wire sensor was not used yet during the first five test, so from these tests, only the air temperature is known. The wire sensor was clamped between the steel clamp and the test specimen during test 6,7 and 8 as can be seen on the right picture, but was taped to the specimen to obtain more accurate surface temperatures from the ninth test.

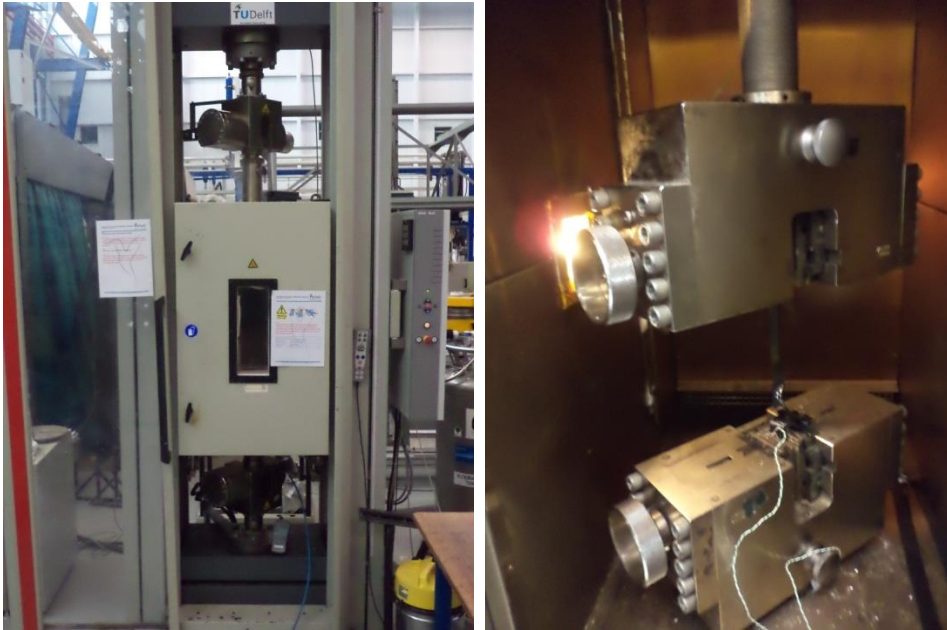


**Fig. 82** Test setup Temperature-Strength test

A 'Flat specimen' is chosen from the list of available sample types in the Testxpert II program for which the following dimensions are set:

Samples xz-plane
Grip to grip distance = 185 mm
Specimen width = 20 mm
Thickness = 6.0 mm

**Table 44** Dimensions that are set for the gauge area

The grip to grip distance is the average distance between the two clamps that hold the sample. The specimen width is the width of the narrow middle part of the sample and the thickness is picked as an average of all the samples. Later on, the measured widths and thicknesses of the different specimens will be added to the program, such that the obtained strength values are corrected for the actual dimensions of the individual samples.

The test speed is set at 5 mm/minute and a preload of 10 N is taken. The possible displacement is limited by the maximum testing height of  $l=244.377$  mm. This maximum height is lower than in the previous tests, because the movement of the upper device this time is limited by the height of the oven.

The intension is to obtain the Force-displacement curve or stress-strain curve for the following different temperatures:

-30 °C	36 °C
-19 °C	47 °C
-8 °C	58 °C
3 °C	69 °C
14 °C	80 °C
25 °C	

**Table 45** Intended surface temperatures of the tested samples

From the 11 stress-strain curves that are obtained in this way, the stress-temperature curve can be determined.

### 5.7.4 Test Results

On figure 83, all the tested specimens are shown. As explained in paragraph 5.8.2, the intension was to only use the rectangular samples that are numbered 1 to 11, for this test. The samples 9, 10 and 11 softened and deformed too much, because after testing the eight sample, there was experimented with heating up the oven to temperatures above 100 degrees. This was done because it was experienced as a relative hard task to give the sample surfaces the same temperature as the air temperature in the oven. By heating up the over to above 100 degrees, the intension was to heat up the sample surfaces quickly to the required heat, but as can be seen on the picture, this failed due to softening and permanent deformation of the material.

As explained in paragraph 5.8.3, during the first five tests only the air temperature is measured. The assumption is made here that the surface temperature of these specimens, is the same as the air temperature that is set. This is quite plausible, because the nitrogen was added to the oven under high air circulations, and therefore the specimens probably were cooled down quickly.

For the samples 6, 7 and 8, a relative large difference was measured between the air temperature and the specimen temperature. This probably is partially caused by the fact that the wire sensor was clamped between the specimen and the steel clamp. In this way, the sensor probably registered a lower temperature than the actual temperature that the middle part of the test specimen had. For the other part, the difference between the air temperature and measured specimen temperature can be explained by the fact that the specimen just does not heat up as quick as the air temperature does. For these reasons, a temperature range is estimated here between the measured surface temperature and the air temperature, because it is most likely that the actual specimen temperature was somewhere in between for these three samples.

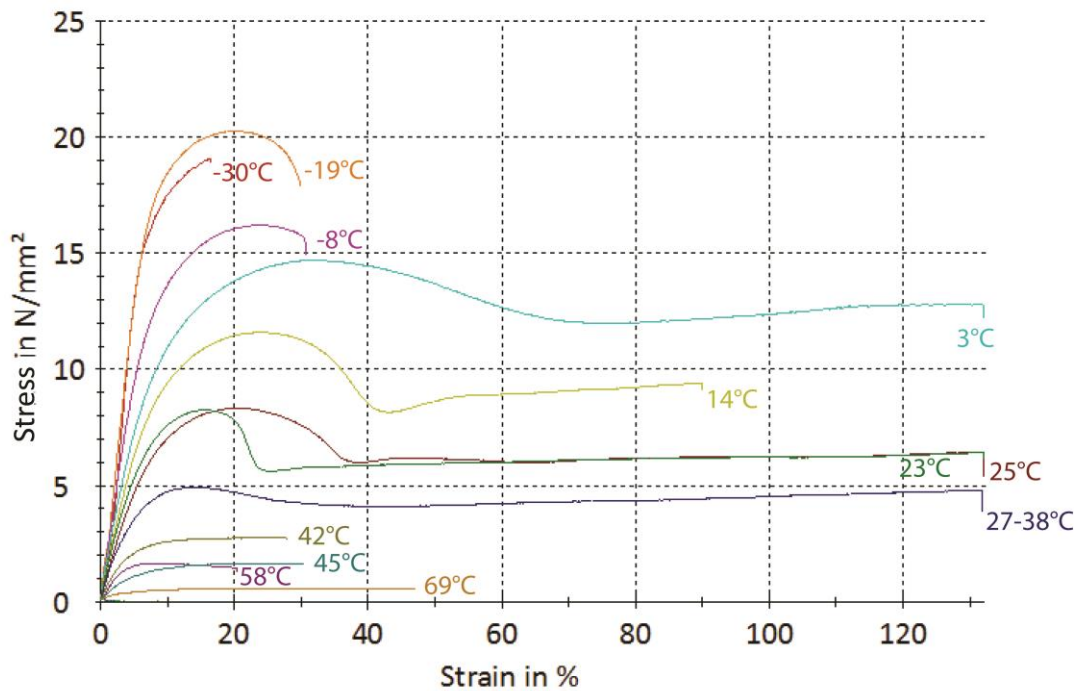
To improve the accuracy of the measurement of the sample temperature, for the four dumbbell-samples there was chosen to tape the wire sensor to the material. This seemed to work, since more realistic temperatures were displayed by the thermometer this time. Therefore the measured surface temperatures for these last four test are assumed as being reliable, and therefore no estimations needed to be made here.



Fig. 83 Tested specimens and their surface-temperatures during the test

For the first 8 samples, it can be clearly noticed that the permanent deformation grows a bit with every sample. Although it would have been logical if this effect continued by further increasing the temperature, no big elongation can be noticed for the dumbbell-samples. This is due to the fact that Testxpert noticed and recorded a break for these specimens quite soon and therefore stopped the test before further elongation was possible. The reason Testxpert stopped so quickly, was probably because the softening temperature was reached already and therefore no material strength was measured anymore.

The graph below shows the stress-strain curves for test samples 1 to 8 and for the four dumbbell samples, all in one figure. The decrease in strength for increasing temperatures already can be noticed here clearly.



**Fig. 84** Stress-strain curves of all the tested specimens. The surface temperatures of the specimens during the test are indicated at the end of each curve

In the graph below the ultimate strengths of the different curves from the figure above, are plotted against the temperature. In this way, the strength-temperature relationship becomes better visible:

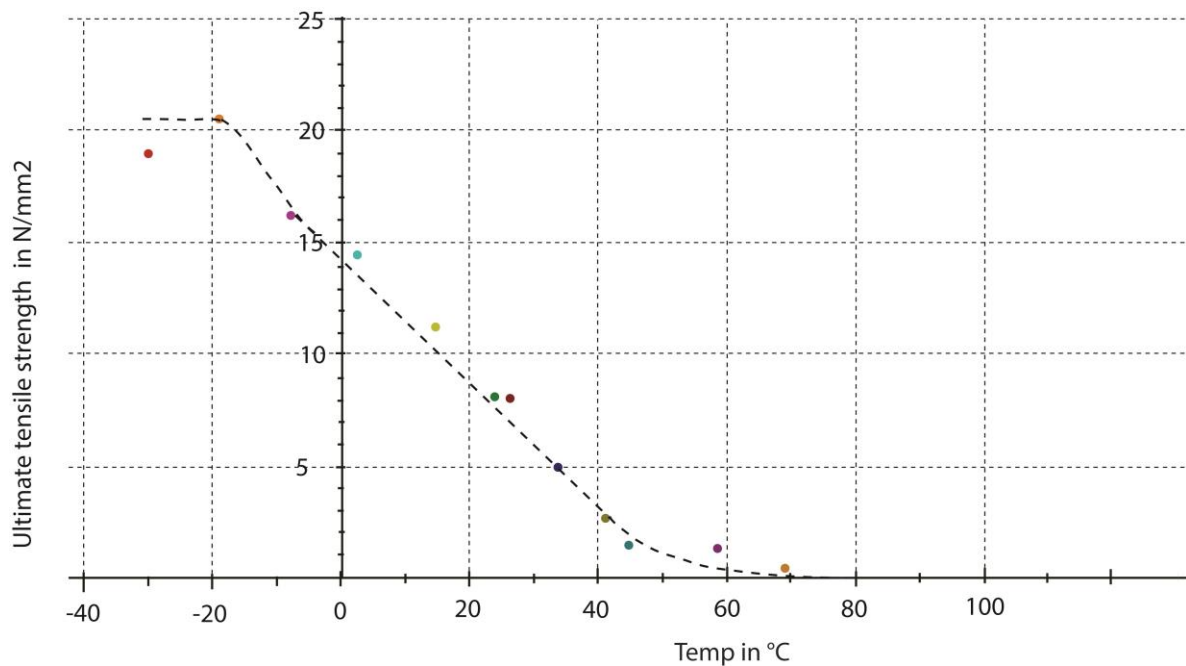


**Fig. 85** Strength-temperature curve obtained from the curves of Figure 84

The table on the next page displays the measured values of all the test:



## 5. Material Tests – Elementary Level

Specimen Name	Set oven temperature [°C]	Measured surface temp. material [°C]	Estimated actual surface temp. [°C]	thickness [mm]	width [m]	Cross Sectional Area [mm <sup>2</sup> ]	End of Test	Tensile strength $f_{t;0,xz,temp}$ [MPa]	Tensile Strain $\epsilon_{f;0,xz,temp}$ [%]
1	-30	/	-30	5.6	21	117.6	Testxpert mentions a break	19.07	16.3
2	-19	/	-19	6.6	18.7	123.4	Testxpert mentions a break	20,27	20.3
3	-8	/	-8	5.5	22.05	121.3	Testxpert mentions a break	16.21	24.4
4	3	/	3	5.7	19.35	110.3	max extension reached	14.69	33.0
5	14	/	14	5.7	17.75	101.2	max extension reached	11.59	23.3
6	25	11.4	15-22	5.5	16.95	93.2	max extension reached	8.33	20.2
7	36	23.0	23-30	5.5	20.2	111.1	max extension reached	8.25	15.5
8	47	27.0	27-38	6.6	21	138.6	max extension reached	4.93	13.9
9	/	/	/	5.7	19.0	108.3	/	/	
10	/	/	/	5.8	20.0	116.0	/	/	
11	/	/	/	5.5	19.5	107.3	/	/	
0,9 (xz)	80	69	69	8.2	19.2	157.4	Testxpert mentions a break (material softens)	0.57	23.9
0,8 (xz)	78	58	58	8.2	19.7	161.5	Testxpert mentions a break softens)	1.65	9.1
0,6 (xy)	60	45	45	4.6	20	92.0	Testxpert mentions a break (material softens)	1.64	28.0
0,9 (xy)	57.0	42.0	42.0	6.9	22.3	153.0	Testxpert mentions a break (material softens'	2.77	26.8

Table 46 Test results Temperature-Strength test

## 5.7.5 Test Evaluation and Conclusions

At first, it should be noticed again that the test results of this test have an accuracy of about 10 degrees, mainly because during test 6, 7 and 8, an estimation of the surface temperature needed to be made due to the use of an insufficient measuring method of the surface temperature. During the last tests, the measurement methods were improved, but for these tests, different sample forms are used then for the earlier tests.

For these reasons it is recommended to repeat this test a few times, such that the results can be validated, especially around the critical area between 30 and 80 degrees. Unfortunately due to the lack of availability of the testing equipment and funding, there was no option to repeat this test within this research.

Although the execution of this test might not have been optimal and therefore the results might have a relatively low accuracy, the obtained strength-temperature curves from this test still give quite a good insight in the reduction of the strength under an increasing temperature, as the inaccuracy-range of about 10 degrees is small enough to obtain a good idea of the material behavior.

The obtained results from this test demonstrate where probably the biggest problem concerning the applied printing material lies and where a lot of attention should be paid on: improving the temperature-behavior of the material.

It could have been expected that a material which is well suitable for 3D-printing according to the FDM-

technology does not show the perfect temperature behavior for the application within a building. This, because the FDM-technology implies that the softening and melting temperature should not be too high, while for a building material it holds that it should be able to resist high temperatures as much as possible. However, the results from this test show that the behavior of the current applied material under high temperatures is relatively poor: Already at a surface temperature of 40 degrees, the material has lost about 70% of its material strength at room temperature and at about 70 degrees the material will have lost almost all its strength. This, while surfaces exposed to the sun in The Netherlands, can be heated up to temperatures of about 80 degrees. So without taking measurements, like for example adding a heat-resistant layer at the surface, the material is not suitable at all for making a house or even for making initial building blocks, as these can already deform permanently or break down under normal temperature circumstances.

Apart from taking measurements around the current applied material, it is expected that the properties of the currently applied material are not optimized for its purpose. So further research on the improvement of the building material itself should be performed as well.

As explained, an optimization should be found between temperature resistance on one hand for applicability within a building, and suitability for the FDM-printing-technology on the other. Although these are quite conflicting applications, it probably is the case that the material properties can be improved to suit both applications better.

For the temperature behavior within the building, the minimum performance should actually be such that it retains much of its strength under normal thermal circumstances. Later on, the material perhaps can be improved such that it also behaves well under special (fire) conditions. Since the material currently does not fulfill the minimum performance under normal temperature conditions, it seems obvious that within the Canal House project, further improvement of the applied printing/building material is essential.

## 5. Material Tests – Elementary Level

### 5.8 Differential Scanning Calorimetry Test

#### 5.8.1 Aim of Test

The purpose of the Differential Scanning Calorimetry test is to find the thermal properties of the printing polymer. The following properties can be obtained from this test:

Material Properties	Symbol	Unit
Specific Heat Capacity	c	J/kg°C
Softening point/temperature	T <sub>soft</sub>	°C
Melting point/temperature	T <sub>melt</sub>	°C
Solidification temperature	T <sub>solid</sub>	°C

**Table 47 Properties to obtain within DSC Test**

Since these properties form elementary aspects of the material, these properties are independent from the orientation in which the material is printed. Therefore, no distinction needs to be made for different grain directions or for different printing planes.

The Specific heat capacity is the amount of heat that is required to increase the temperature of 1 gram of the material with 1 °C. Within a formula this is expressed in the following way:

$$c = \frac{\Delta Q}{m \cdot \Delta T}$$

The specific heat capacity can be obtained from the DSC-curve by calculating the slope of the heat-temperature curve (Q/T-curve). The three temperatures that need to be obtained, the softening temperature, melting temperature and solidification temperature can be derived from the heat-temperature curve as well. This is done by looking at notable peaks in the curve and comparing the curve to reference DSC-tests, such that the cause of the peaks can be interpreted in a proper manner.

#### 5.8.2 Tested Samples

As mentioned in the previous paragraph, the material properties that are obtained with the DSC-test, are elementary properties of the material, which means that these properties are independent from the orientation in which the material is printed. Therefore, for the test samples of the DSC-test it holds that a random piece can be used as long as it fits within the used aluminum cups that have a diameter of circa 5 mm and an inner height of circa 2 mm. These samples could be easily obtained by cutting or sawing a small piece from a bigger part that comes out of the 3D-printer.



**Fig. 86 Tested sample within aluminum cup**

### 5.8.3 Test Setup

For the DSC-test a differential scanning calorimeter at the Faculty of Chemical Engineering of the TU Delft has been used. The brand of the machine is Perkin-Elmer and the model-name is DSC-7. The temperature of this DSC device can range between 25 to 400 degrees Celsius.

The used DSC testing device is shown on the picture below. The cylinder in the middle part of the device can be removed such as is visible on the picture on the right. Inside there are two separate little ovens/cells. In one of the cells the aluminum cup containing the sample of the printing material is placed, the other cell stays empty.

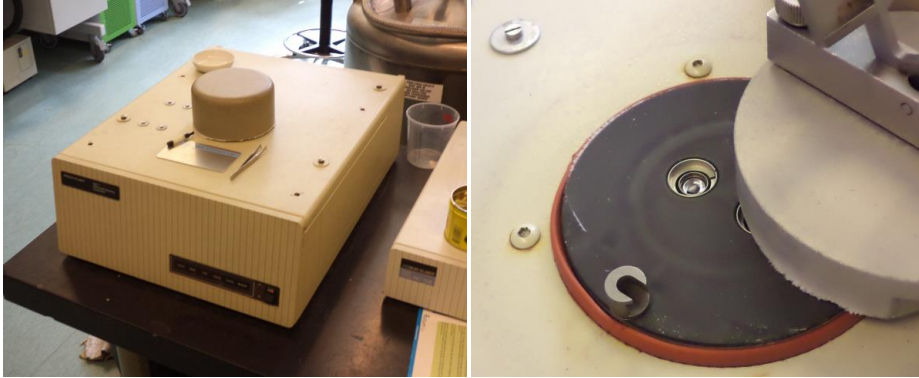


Fig. 87 Used DSC-7 device (left) and tested sample placed within device (right)

The temperature of both cells is increased by 10°C per minute, starting at a temperature of 25°C and ending at 150 °C. The minimum temperature of 25°C was just the minimum temperature of the temperature range of the applied DSC-device and the maximum temperature of 150 °C is chosen because according to [Henkel, 2014], the Macromelts are applicable at temperatures between -40 °C and 140 °C. Therefore, there is no reason to take measurements above 150 °C. During this process, for both the cells the required amount of energy to heat up a cell is measured as a function of the temperature. On the moment that the material sample in the filled cell undergoes a phase transition, extra energy is required or is released, dependent on whether the reaction is endothermic or exothermic. As a consequence, a higher respectively lower amount of energy is needed for keeping the cell with the material sample on the same temperature as the cell without the material sample. By subtracting the obtained heat-temperature curve of the empty cell from the heat temperature curve of the cell containing the material sample, the obtained data is corrected and the heat-temperature curve of the printing material itself (so without the energy required to heat up the cell environment) is obtained. This correction process is performed within Pyris, the software package that is installed on the computer which is connected to the DSC-device. The corrected heat-temperature curve of the printing material now can be used to obtain the required material properties.

After the process of heating up the two cells, the cells are cooled down from 150 °C back to 25°C with the same speed of 10°C per minute. For this cooling process, the corrected heat-temperature curve is obtained in the same way as for the heating process.

The DSC-test is performed in twofold and a different sample is used for the two separated tests. The mass of the samples is measured before the performance of the test and entered within the software program Pyris. In the table below the input data for the two performed DSC-tests are listed:

Test 1	Test 2
Sample mass = 15,12 mg	Sample mass = 9.04 mg
Starting temperature = 25°C	
Final temperature = 150 °C	
Heating speed = 10°C/minute	
Both at the starting point of 25°C and maximum temperature of 150 °C, the temperature is kept constant for 2 minutes.	

Table 48 Test setting DSC test

## 5. Material Tests – Elementary Level

### 5.8.4 Test Results

The figure below shows the DSC-curves for the heating process of both the tested samples 1 and 2. Since the graph starts at 25°C, the glass transition temperature, which is the temperature at which the material goes from a brittle state to a more flexible/rubber-like state, is already passed. This can be concluded based on the observation that the material is bendable and flexible at room temperature instead of being hard and brittle and is also endorsed by the Macromelt Factsheet of Henkel [Henkel, 2014] on which a glass transition temperature of 5°C is given.

For both the samples 1 and 2, two peaks are observed at temperatures of 64 and 87 respectively 62 and 84 degrees Celsius. This probably means that the material first softens at a temperature of about 62-64 degrees and fully melts at 84-87 degrees. The melting process is an endothermic reaction which explains the upward peak, as the amount of heat that is required to heat up the material increases during this reaction. It is not uncommon for polymers that the melting process shows multiple peaks. [Södergard et al, 2002, Middleton et al, 2000] This multiple peaks are probably caused by the situation that the chains of the crystalline structure of this semi crystalline polymer [Södergard et al, 2002; Middleton et al, 2000; Biostructproject, 2014] are breaking in multiple stages. As mentioned before, in practice this probably means that the material is already acting soft and viscous around 62-64 degrees and molten at 84-87 degrees.

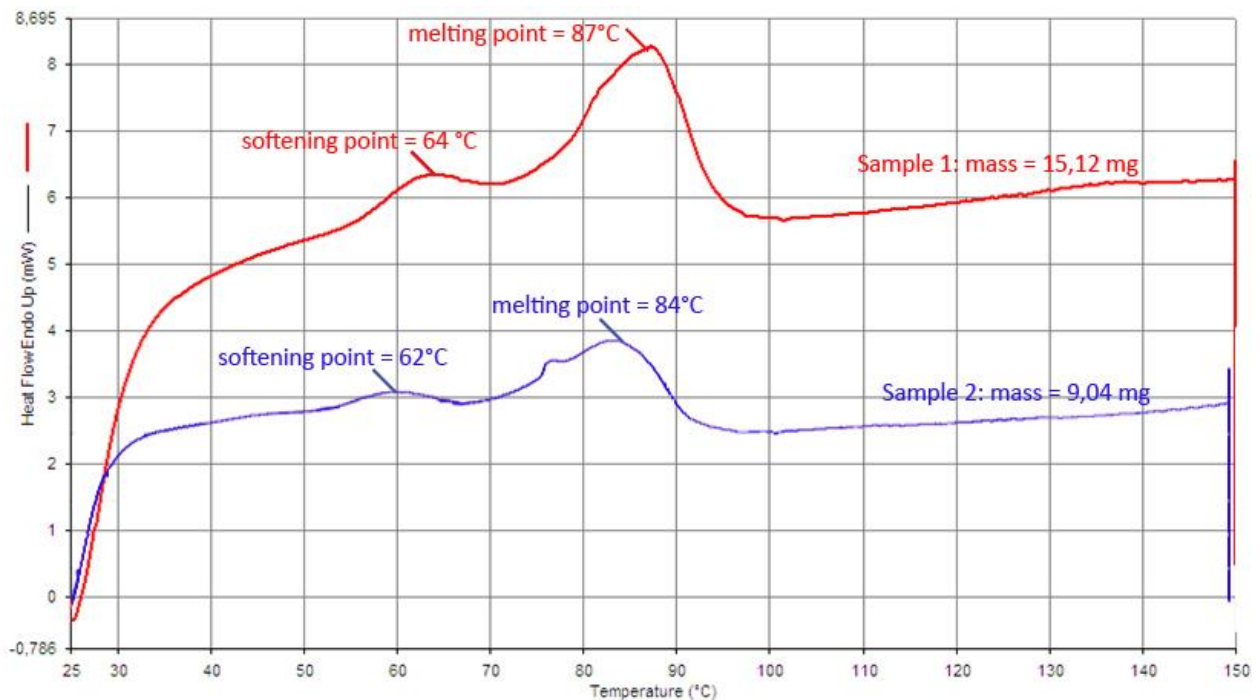


**Fig. 88** DSC curves of two tested samples – heating process

The following two curves show the process of cooling down the sample of test 1 respectively test 2 from 150 degrees back to 25 degrees Celsius again. In this cooling down process, one peak in the downward direction can be observed at 42 respectively 45 degrees which probably is the point in which the material goes back from a liquid into a solid state in the form of an exothermic reaction. The reason that the temperature of solidification is lower than the softening temperature lies in the fact that for crystalline structures a high activation energy is required to enable homogeneous nucleation, which is an important part of the crystallization process. It is common for crystalline structures that this required energy is reached at a lower temperature point than the melting temperature. [Franks, 2003]

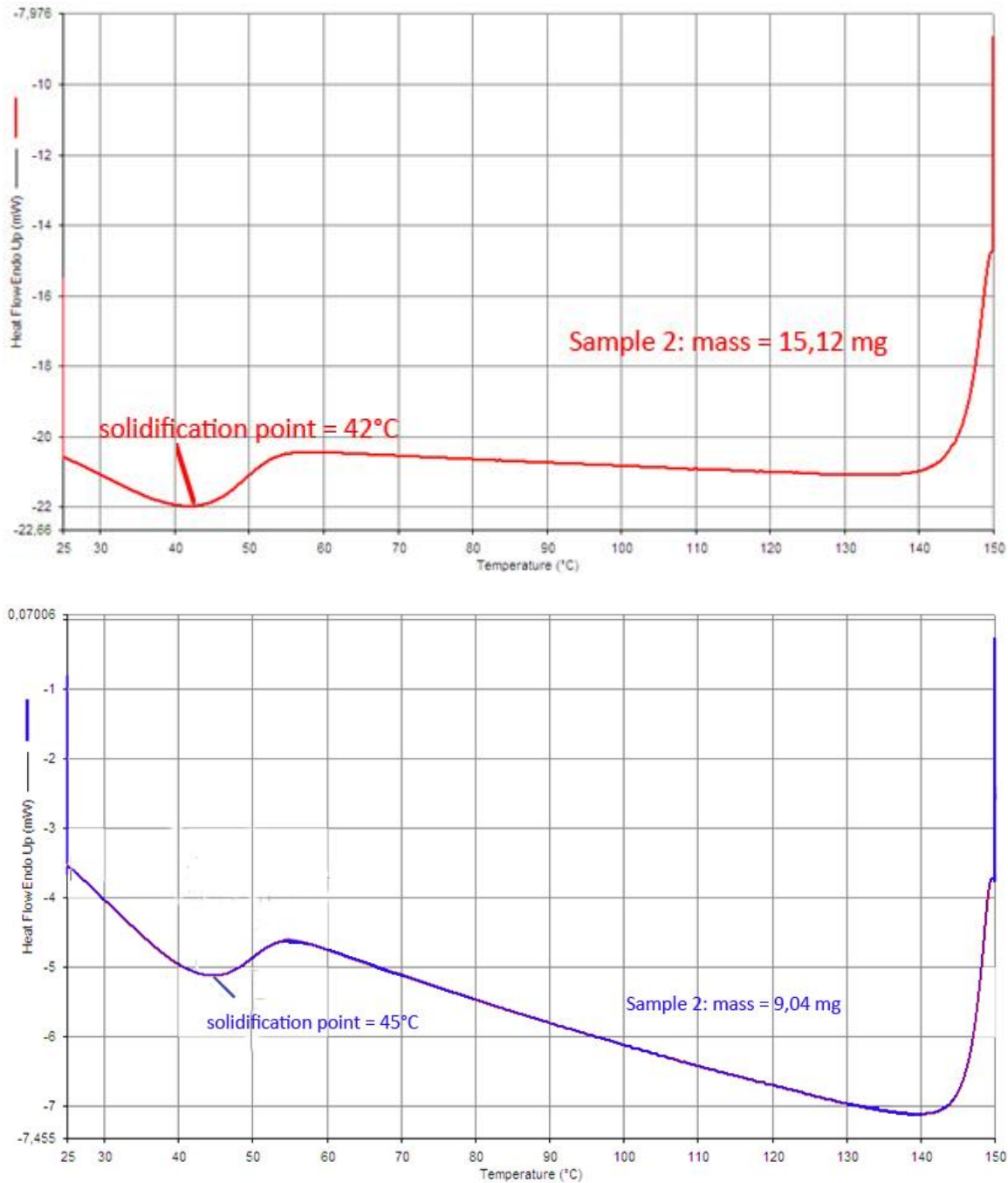


**Fig. 89** DSC curves of two tested samples – process of cooling down

In the graph below the specific heat capacity ( $Jg^{-1}K^{-1}$ ) is plotted against the temperature range for both test 1 and 2. The reason that the specific heat capacity is fluctuating and not constant lies in the fact that endothermic reactions take place during the phase transition from solid to liquid, as we have seen in the Heat-temperature curve. Therefore the amount of heat that is required to heat up one gram with one degree, fluctuates. This can also be logically derived from the fact that the slope of the Heat-temperature curve (which is equal to the heat capacity) fluctuates.

The value of the specific heat capacity at the minimum measured temperature of 25 degrees, which is about room temperature, is  $2.2 J/g^{\circ}C$  for specimen 1 and  $2.0 J/g^{\circ}C$  for specimen 2. The maximum measured specific heat capacity is  $2.72$  at a temperature of  $42^{\circ}C$  for specimen 1 and  $2.71$  at  $43^{\circ}C$  for specimen 2. The average specific heat capacity within the range of 25 degrees to 150 degrees is  $2.33$  respectively  $2.34 J/g^{\circ}C$

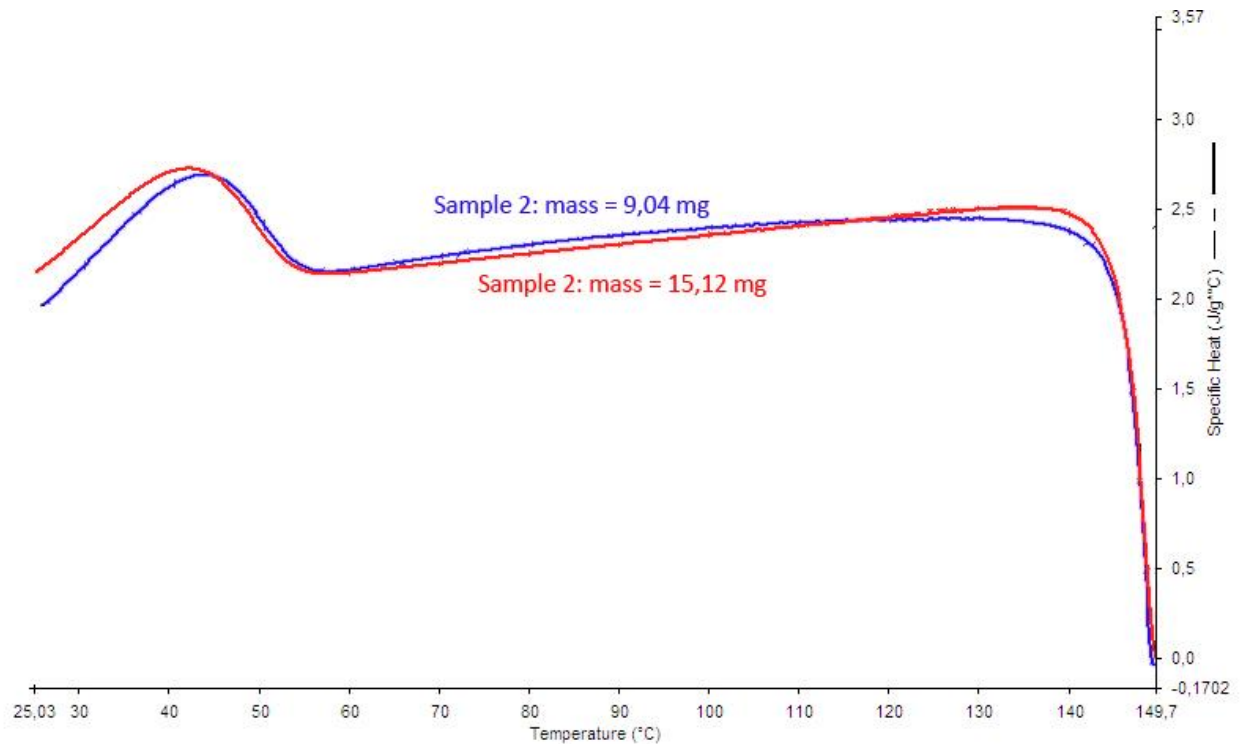


Fig. 90 Specific heat capacity curves for the two tested samples

Table 49 gives an overview of the obtained results from the DSC-test:

Material Properties	Symbol	Unit	Test sample 1			Test sample 2			Average Value
			average	maximum	Room temperature	average	maximum	Room temperature	
mass	m	mg	15.12			9.04			
Specific Heat Capacity	c	J/g°C	2.33	2.72	2.2	2.34	2.71	2.0	
Softening point/temperature	T <sub>soft</sub>	°C	64			62			63.0
Melting point/temperature	T <sub>melt</sub>	°C	87			84			85.5
Solidification temperature	T <sub>solid</sub>	°C	42			45			43.5

Table 49 Test results DSC test

### 5.8.5 Test Evaluation and Conclusions

During the strength-temperature test (paragraph 5.7) it was found that the material has almost lost all its strength at a temperature of about 70 degrees Celsius. This is in accordance to the results that are obtained in this DSC-test, as the found softening point is 63 degrees Celsius on an average. On the point of softening, the material already becomes unusable for the application as a building material. Therefore it can be concluded from this test that 63 degrees Celsius or, to be on the safe side, 60 degrees Celsius, should be seen as the upper boundary and maximum temperature to which the material can be heated up. However, one should be aware of the fact that on this point, more than 80% of the material strength is lost and at 40 degrees already 70%. This means that especially when using the printing material for structural purposes, the maximum temperature to which the material can be heated up, lies way lower than the softening point of 60 degrees.

The obtained result that the melting temperature lies around 85 degrees is less important, as the material already loses its function at the softening point. Still, the melting temperature lies alarmingly low. Fortunately just high enough to prevent melting under 'regular' conditions, as the maximum surface temperature in the Netherlands is 80 degrees [Krusche et al., 1982]. But in case of a fire, the material will quickly melt away or even vaporize. The last can unfortunately not be concluded based on the DSC-test, because at the maximum measuring temperature of 150 degrees, the material was still liquid. However, a quick experiment with a

butane burner learned that the material, when exposed to fire, inflames and vaporizes.

When comparing the obtained temperature values with the values as given on the factsheet of Henkel (see paragraph 3.3.2), a striking difference can be noticed between the obtained value of the softening temperature and the value as mentioned on the Henkel sheet. The Henkel sheet mentions a softening point of 135-145 degrees Celsius, while this DSC-test gave a value of 63 degrees for the softening point. Although this is quite odd, the strength-temperature test endorses the result as obtained during this DSC-test, as the material obviously was softened and viscous at a measured temperature around 70 degrees.

The difference between the softening temperature values may partly be caused by the difference in determination methods. Henkel used the Ring & Ball test [Marchese, 2014] to determine the softening point. Still, this does not entirely explain the difference, as the material already is molten at 84 degrees. So the maximum obtained temperature for the softening point can never be higher than 84 degrees, regardless of the determination method that is chosen.

The average specific heat capacity of 2.33 and the specific heat capacity of 2.1 at room temperature are quite high compared to more general construction materials. Concrete for example, has a specific heat capacity of 0.92 and steel of 0.48-0.53 [Granta, 2014]. Wood comes closer to this material with a specific heat capacity of 1.88. The specific heat capacities for other plastics vary quite much for different polymer types. But the obtained specific heat capacities for this particular plastic are not unusual for polymers.

The relatively high heat capacity means that quite some heat is required in order to heat up the material, but also that the material retains the heat relatively good. As a consequence, the printing material has a high insulating value. On one hand this is positive, as the climate inside and outside can be separated well with this material. On the other hand, this means that once the inner side of a building is heated up, it will be difficult to cool it down again. Especially during the summer this might lead to undesirable warm rooms.



## 5. Material Tests – Elementary Level

### 5.9 Creep Test

#### 5.9.1 Aim of Test

The aim of this test is to study the creep behavior of the applied printing material. Because the material, when applied in the building, will be exposed to long-term loads, it is important to find out how much the material will deform under this long-term loads.

The creep behavior can be studied for the situation of an applied constant tensile load and for a compressive load. The form and dimensions of the test specimens for a creep test are really dependent of the testing devices that are available for the performance of the creep test. Because a creep test takes quite a lot of time, there often is a lack of availability for creep testing devices. Unfortunately for the compressive creep testing machine that was available, the required test specimen could not be obtained from the printing materials/specimens that were made available.

For that reason, only a tensile creep test is performed, because for this test, it actually was possible to make the required sample out of the available material. Positive thing is that it is more important to look at the tensile creep behavior than to the compressive behavior, because a long-term tensile load probably can lead to bigger structural problems than a long-term compressive load. This, because during the tensile and compressive tests could be seen that a tensile test often leads to failure of the material, while a compressive test doesn't.

The creep can be expressed by a creep-curve in which the elongation/strain of the material is plotted against a (logarithmic) time scale.

#### 5.9.2 Tested Samples

Due to the lack of availability of testing devices, it was unfeasible to perform a creep test in twofold both in the direction parallel to the grain as perpendicular to the grain. Therefore, the choice is made to only perform the creep test in the direction parallel to the printed lines, because it is expected that the results from a creep test in the parallel direction are more suitable for describing the basic creep behavior of the printing material. This, because the material is more homogeneous in the parallel direction.

As is mentioned in the previous paragraph, the form and dimensions of a test specimen for a creep test are dependent of the testing machine that is available. For the tensile creep test, a particular creep-set-up was available that required a sample with the following form and dimensions:

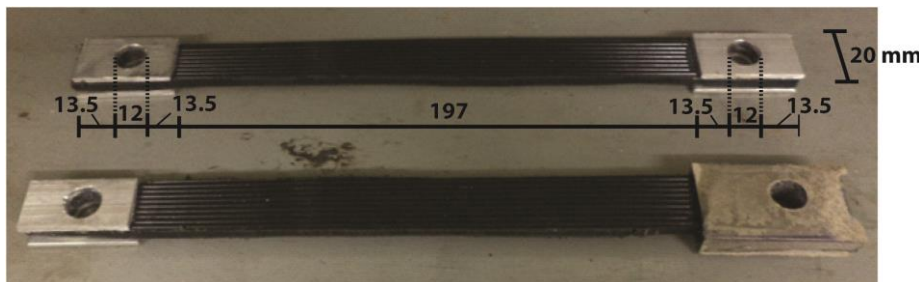


**Fig. 91 Tested samples Creep test and their dimensions**

The function of the steel plates, that are glued to the printing material, is to prevent the material from failing at the points of connection and to make the connection area wider than the middle area, which is important to enable the material for deforming and failing at the middle part and not areas around the connection.

Because the steel plates at the right side of the lowest sample released from the printing material and broke down during the drilling of the holes, a new connection of epoxy resin was made here.

### 5.9.3 Test Setup

Below the two used creep test-setups are shown. These setups were available at the basement of FAM lab at the faculty of Aerospace Engineering at the TU Delft.



Fig. 92 Test setup creep test

On the picture below the working-principle of this test setup is shown. A desired amount of weights can be added to the vertical bar. The vertical movement that is caused by adding this weight is transformed into a horizontal inward movement on top by a mechanism. This inward movement leads to a movement to the outside at the bottom part of the mechanism. This movement to the outside, draws the test sample along to the outside, and therefore applies a tensile load on the test sample. Because this set-up works as a lever, the big vertical movement to which a small weight is applied, leads to a big horizontal tensile load applied to the sample.

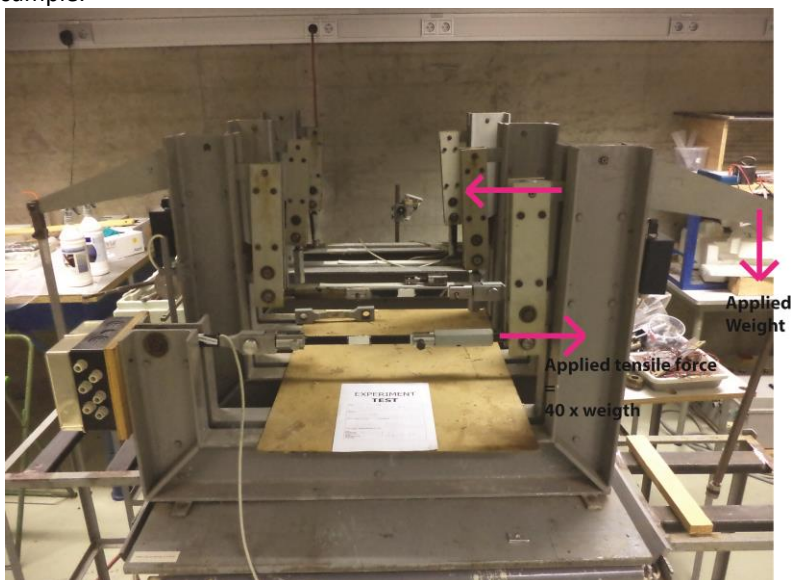
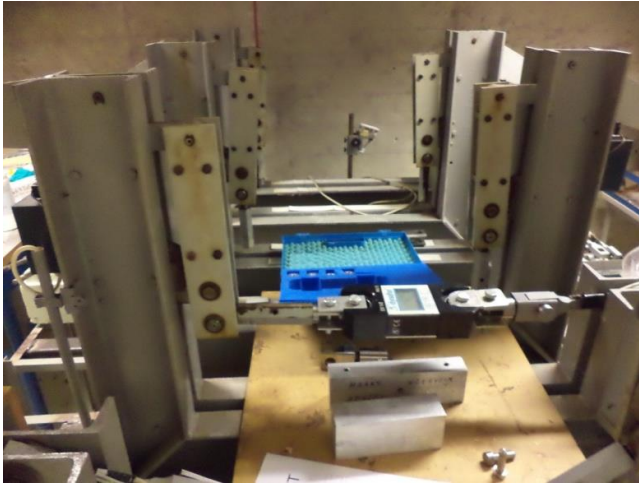


Fig. 93 Working principle of the creep test setup. The arrows show the way in which the weight and loads are applied

There was chosen to apply a load leading to a stress level equal to 50% of the average tensile strength, to one of the samples and a stress level equal to 80% of the average tensile strength to the other tested sample. This means a stress level of  $50\% \times 8.33 \text{ MPa} = 4.165 \text{ MPa}$  to one of the samples and  $80\% \times 8.33 \text{ MPa} = 6.66 \text{ MPa}$  to the other. With a cross-section of  $6 \times 20 \text{ mm}^2$ , this leads to applied forces of  $4.165 \times 120 \approx 500 \text{ N}$  respectively  $6.66 \times 120 \approx 800 \text{ N}$ . This means that the applied load in kg, should be 50 respectively 80 kg. By spanning an electrical Force meter (Also called a Newton meter) between the connections, the test devices

## 5. Material Tests – Elementary Level

could be set at the right load by adding enough weights to the vertical bar till the required loads of 50 and 80 kg were measured. The multiplication turned out to be about the forty-fold of the applied weight, which means that applying a weight of about 1.2 respectively 2.0 kg was enough.



**Fig. 94** Calibration of the test setup, such that the desired tensile load is added to the sample

Once both test devices were set at the right load, the test specimens could be spanned between the two connections and the vertical weight could be released such that the samples were loaded under the required tensile force.

A gauge area of 40 mm was drawn on both test samples, such that the elongation could be measured by using a caliper. Since it is conventional to plot the elongation against a logarithmic time scale, the intension was to measure the elongation after 1 minute, 10 minutes, 100 minutes, 1000 minutes and 10.000 minutes.

### 5.9.4 Test Results

As can be seen on the picture below, although measurements at the connection points were taken, both specimens still failed at the connection holes. This was possible because the glue between the aluminum plates and the printing material turned out not to be sufficient for making a proper fusion between the two materials. Although the material deformed and failed at the connections, there still was measured some extension in the middle gauge area over the time. However, if the connections would have been sufficient and deformation would have fully appeared in the middle part and not at the connection parts, then the extension of the gauge area probably would have been bigger than what is measured now.



**Fig. 95** Failed test specimens. As can be seen the specimens failed at the connection points

So we may assume that the measured results, that are given in the tables below, are lower than what would have been the case when deformation and failure would not have been occurred at the connections. Furthermore, the creep proof probably would have last longer and therefore would have led to more complete

results, in case of proper connections.

The initial gauge length before loading is 40.0 mm.

**50 kg:**

Time [minutes)	1 minute	10 minutes	100 minutes	1760 minutes	10.000 minutes
Gauge Length (mm)	40.1	40.5	40.5	40.0 (Specimen broken at connection point)	/
Strain [%]	0.25	1.25	1.25	0	
Creep coefficient = $\epsilon_{creep} / \epsilon_{initial}$ [-]	1.0	5.0	5.0	0	/

**Table 50 Test results 50kg creep test**

**80 kg:**

Time [minutes)	1 minute	10 minutes	100 minutes	1760 minutes	10.000 minutes
Gauge Length (mm)	41.4	42.2	43.2	40.5 (Specimen broken at connection point)	/
Strain [%]	3.5	5.5	8.0	1.25	
Creep coefficient = $\epsilon_{creep} / \epsilon_{initial}$ [-]	1	1.6	2.3	0.36	/

**Table 51 Test results 80 kg creep test**

In the graph below the strain for both samples is set against time. As can be seen the values for the strain at 1000 minutes are with 8% still quite low, since during the tensile test, an average strain of 90.2% was obtained. For an important part this is caused by the situation that the sample deformed for the most part around the connection point and not in the middle part. On the other hand, the small measured elongation probably means that the material still was able to elongate quite much after the moment of failure.

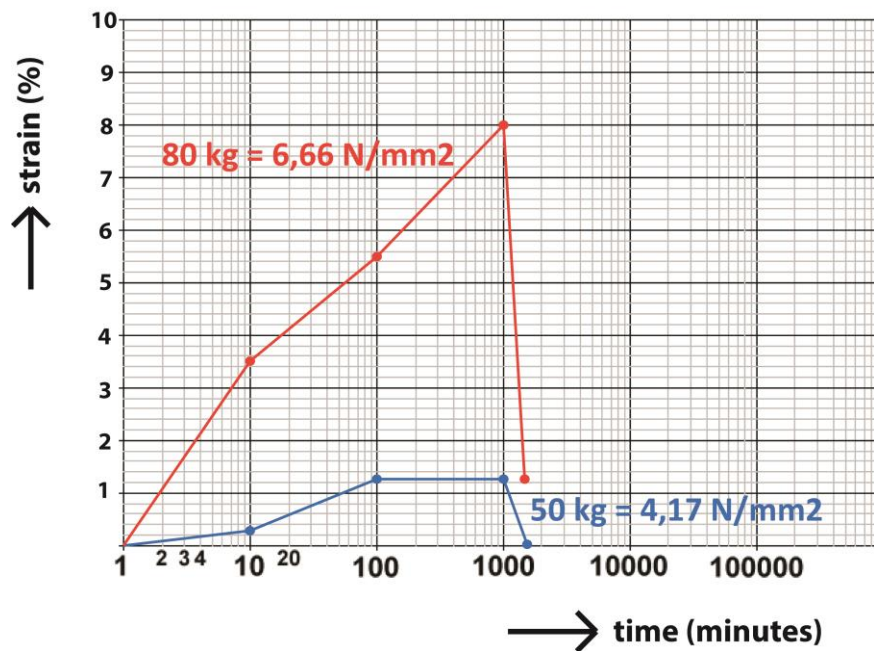


**Fig. 96 Obtained creep curves**

## 5. Material Tests – Elementary Level

Since the quantitative results of this test are not reliable and incomplete due to failure at the connections, a second attempt was made to perform this tensile creep test, by making two new test specimens. This time, epoxy resin was used for all the connections instead of a glued connection between aluminum and plastic. The expectation was that this would lead to stronger connections because the fusion between the epoxy resin and printing material would probably be better. Furthermore, the sample was made in a dumbbell-shape this time, with a specimen width of 40 mm at the sides and 20 mm in the middle. By this, the area around the holes would be both thicker and wider than the area in the middle. The only disadvantage that still was present was the small end distance between the connection hole and side of the specimen. This was limited to a maximum width of 13.5 mm because else the specimen would not fit within the clamp.



**Fig. 97** Second attempt to create suitable test specimens for this test

Unfortunately when trying again to test one of the specimens in the 50 kg device and the other in the 80 kg device, the specimens immediately started to fail at the connection hole. While in the previous tests, the specimen deformed slowly and unobvious at the connections, parallel to an elongation in the middle part, this time the specimens directly started to deform at the connection, such that the results would not be sufficient at all.

So the connection this time was even weaker than in the previous test.

Because the 13.5 mm end distance always would stay the weakest part of the sample, there was no other option to improve the test specimens. Therefore, it was concluded that this test setup was not appropriate for performing a tensile creep test with the printing material.

### 5.9.5 Test Evaluation

Because this test failed at both the performed attempts, it can be concluded that the applied test setup is not suitable for performing a tensile creep test on this material. This is due to the fact that the printing material is very sensitive to locally applied forces and therefore failed at the connection points instead of at the middle part of the specimen, which was the intention.

Based on the obtained test result here and during the general tensile test, the hypothesis can be made that this material will display strong creep behavior, as the strain percentages are of an extreme high order compared to general applied building materials like steel and timber.

Although the obtained results are not very useable to come to proper statements about the creep behavior of the material, the outcome of this test can be used to come to another conclusion that might be important for the building project as well: The failure at the connections during this test actually showed that this material is very sensitive for locally applied forces. For that reason loads should be divided over large parts of the structure instead of locally. Especially for the case of making connections between the different building blocks, this means special attention should be paid to the design of these connections, to prevent the structure from failing at the connections. Drilling holes should be prevented as much as possible, and in case there is still chosen for a bolted connection, sufficient supporting materials should be used to strengthen the connection. An early prognosis however is that connecting the building blocks by melting them together, might lead to a stronger connection.

### 5.9.6 A Second Creep Test

Although an important lesson has been learned from the performed creep test, namely that the material is very sensitive to locally applied forces, the performed test that is described in the previous paragraphs, did not lead to the desired knowledge about the creep behavior of the printing material. For this reason, a second creep test is performed, but this time with another test setup.

#### Test setup

A Zwick testing machine is used for the creep test this time, like was the case for most of the other strength tests. This time however, not the 100 KN-machine is used, but a smaller type, namely the Zwick Z010. This machine is capable to apply forces up to 10 KN, which is sufficient for the performance of this test.

The advantage of this testing method compared to the one that is previously applied for the creep test, is that the applied tensile force is distributed more equally over the material sample this time, which prevents the sample from failing locally. An extensometer is attached to the sample, as the elongation needs to be measured accurately for a creep test.



Fig. 98 Test setup creep test

In the Zwick Testxpert II software program, it is indicated that a creep test will be performed. At first, a sample is tested under a constant load of 800N ( $\approx 80\%$  of the average tensile strength), as was the case for the previous performed creep test. This Load will be build up with a speed of 5 mm/min. A maximum testing time of 10.000 minutes is set, first because this is a commonly used testing time for creep tests on polymers [Harrington, 1997] and secondly because the availability of the testing device was limited, such that an ending time needed to be set. A measurement is automatically taken at every 30 seconds.

The second sample is tested under a constant load of 500N ( $\approx 50\%$  of the average tensile strength). This load is build up quicker, with a speed of 25 mm/min, because it turned out that the build-up time for the 800 N sample was unnecessarily long. Again a maximum testing time of 10.000 minutes is set and a measurement is taken every 30 seconds.

#### Tested Samples

Two dumbbell-formed specimens are tested this time, with the same dimensions as was the case for the tensile test in paragraph 5.1. Because these samples were not obtained from a printed plate by laser-cutting, but with a fret-saw, the accuracy of the sample edges is not as high as was the case for the tensile samples. Both samples are tested in the direction parallel to the grain. Due to lack of availability of the testing device, it unfortunately was not possible to perform a creep test in the direction perpendicular to the grain as well.

## 5. Material Tests – Elementary Level

The lower sample on figure 99 is used for the 800N-test and the upper sample for the 500N-test.



**Fig. 99** Test samples - creep test 2

The dimensions of the tested samples are as given in the table:

Sample 800 N	Sample 500 N
Parallel specimen length = 160 mm	Parallel specimen length = 160 mm
Specimen width = 18.2 mm	Specimen width = 18.2 mm
Thickness = 5.5 mm	Thickness = 5.5 mm

**Table 52** Dimensions tested creep specimens

### Test Results

The picture below shows that the sample to which 800 N was applied, shows a local constriction. This means the specimen started to deform plastically. This was not a desirable results, because with a creep test it is the intention to stay within the elastic phase, as this is the phase in which the material will be applied in practice. Although a load of 800 N formed 80% of the average tensile strength, the tested sample unfortunately was weaker, such that the plastic phase was reached earlier. This was probably caused by the fact that 80% of the average tensile strength (8.33 MPa) was taken instead of 80% of the characteristic tensile strength (6.45 MPa). Furthermore, the actual cross-sectional area of the sample was smaller than the usual 120 mm<sup>2</sup> of these samples. These two causes explain the quick reach of the plastic deformation phase.

Another thing that went wrong in this test, is that the moving upper head reached the protection slot, because the elongation turned out to be bigger than expected due to the plastic deforming. However, as the sample was already deformed plastically, this did not matter much.

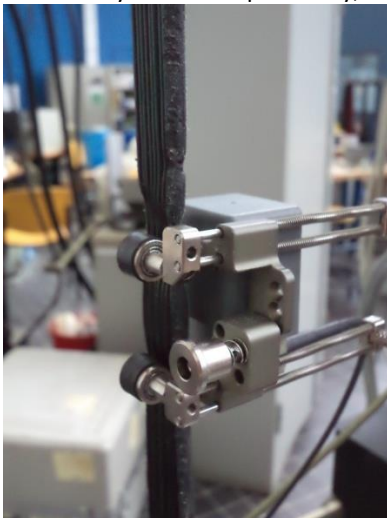


**Fig. 100** Local constriction due to plastic deformation

The graphs of the tested 800N-sample show that after about half an hour (about 2000 s), the plastic deformation process started. This process started after a strain of about 2.5% had taken place. After the plastic deformation, the strain value was around 7.5% of the parallel specimen length. The sudden plastic deformation is recognizable as the vertical line of the graph. After the plastic deformation, only a small further elongation is measured during the remaining two hours of the test. This probably means that the sample was arrived at the tertiary creep phase already.

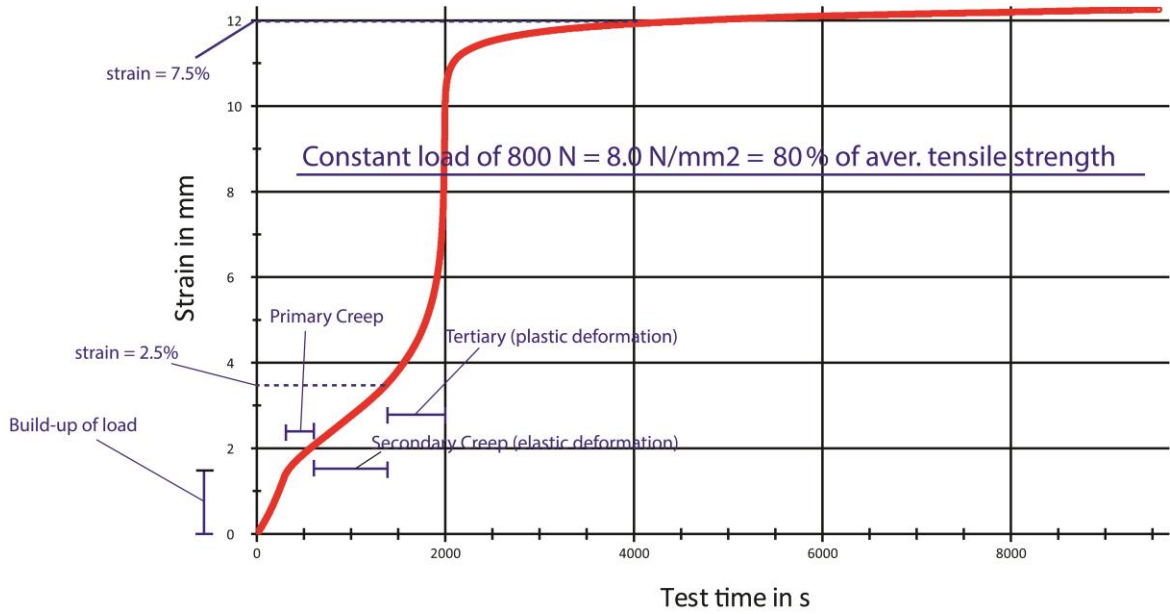


Fig. 101 Creep curve 800N-test

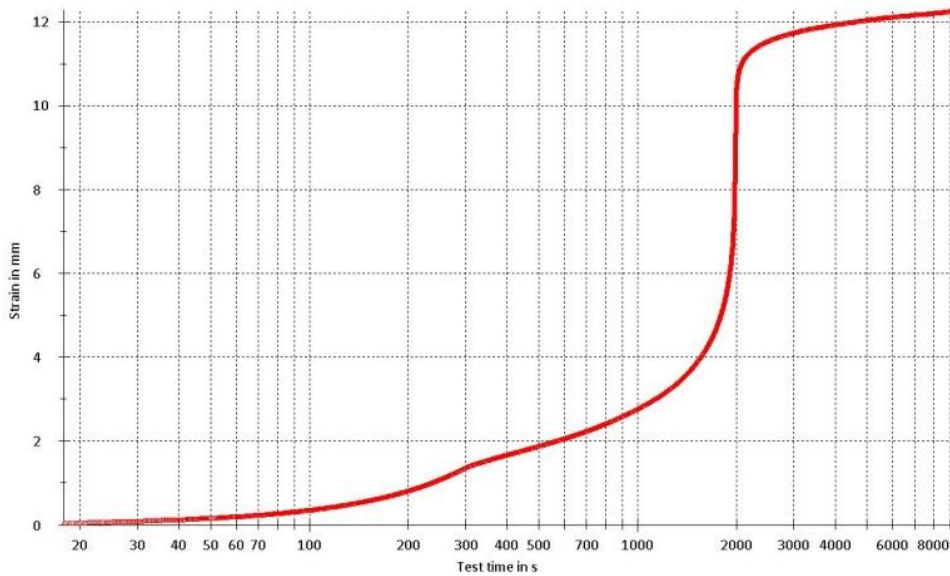


Fig. 102 Logarithmic creep curve 800N-test



The 500N-test ran successfully in the sense that no quick plastic deformation took place. In fact, no plastic deformation took place at all during the full duration of the test as the photos below, that are made after the full run of the test, show. This means that the sample was in the elastic phase during the whole test.



**Fig. 103** Sample 500N-test after test performance: no constriction is visible this time

Because the applied load of 500N formed 50% of the average tensile strength, it is possible that the 500 N actually formed up to a maximum of 78% percent of the strength of the tested sample. This again is caused by the fact that 50% of the average strength is taken, while the characteristic strength and thus the actual strength of the tested sample could have been lower. Still, 78% of the characteristic strength means that the applied load is well within the possible allowable stress range of the material when it is applied in practice. This means this second test forms a proper representation of the creep behavior of the material in practical applications.

The creep-curves below have a form which is general for creep tests in which the plastic deformation stage (tertiary creep stage) has not been reached yet. After a quick initial strain at the beginning of the test, the curve slope decreases over time, becoming almost zero at the end of the test at 600.000 seconds (= 10.000 minutes). The reached strain after 10.000 minutes is about 1.5%, which is below 2.0% and thus tolerable for structural applications. [Hosein, 2009]

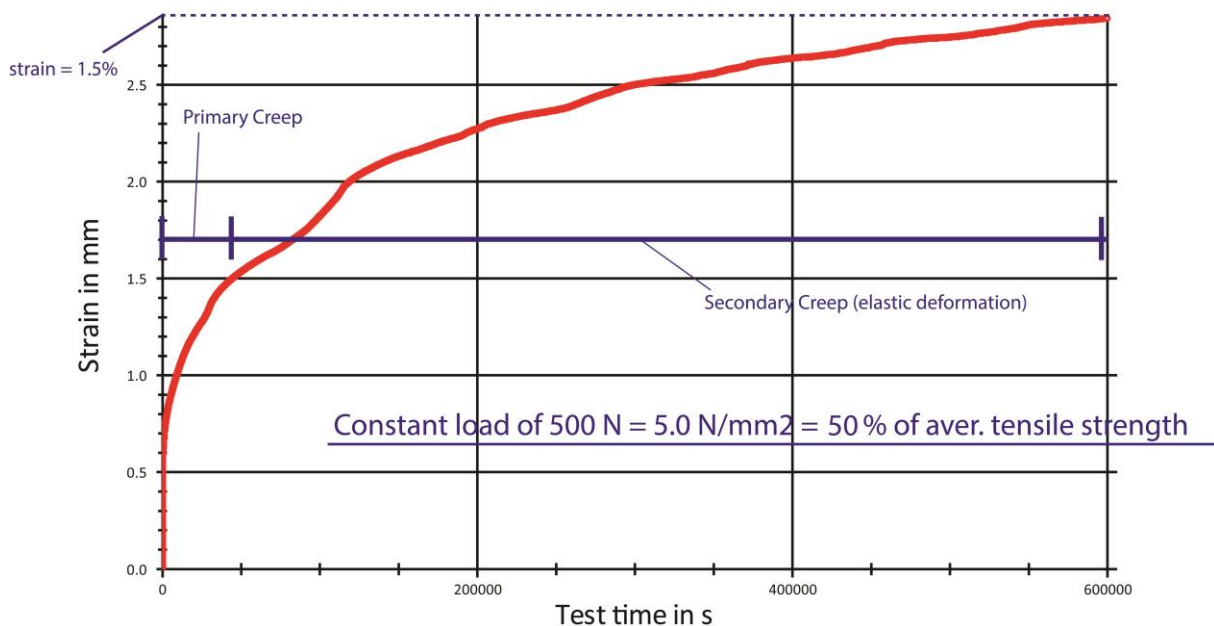


**Fig. 104** Creep curve 500N-test

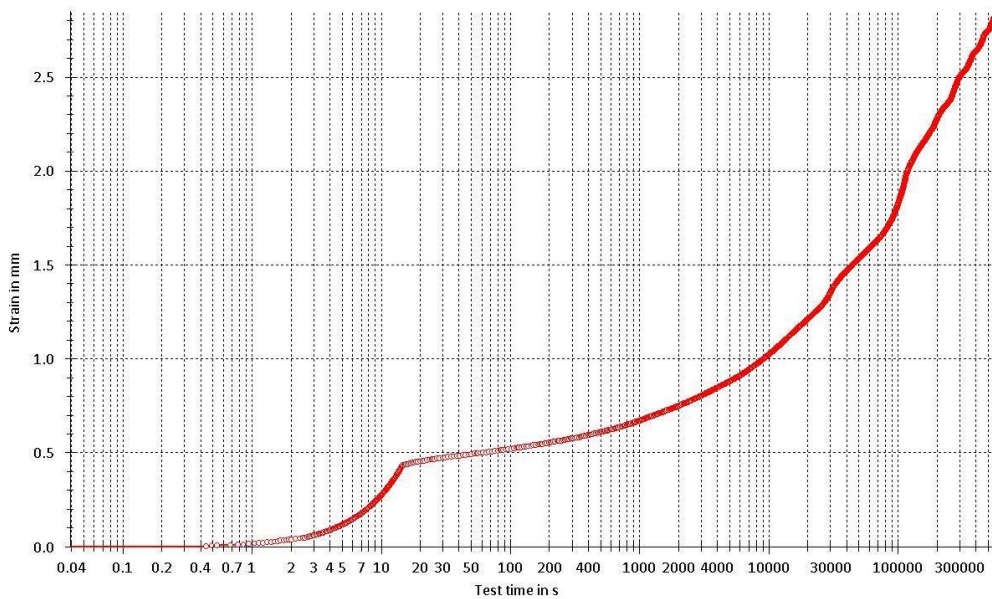


Fig. 105 Logarithmic creep curve 500N-test

### Test Conclusions and Evaluation

Because a load of 800 N meant that the sample was not loaded on 80% of the characteristic strength, but on 120% of this strength, the 800 N-test led to a quick plastic deformation. Although a quick plastic deformation might not be the result one wants to obtain with a creep test, this test result still led to an important conclusion. Namely that the strength boundaries that are set by the tensile test (paragraph 5.1), are narrow. Initially the sample deformed elastically, which means that the tested sample initially was able to resist the applied load of 800 N in case it was applied on a very short term. However, already after a short time (about 30 minutes) the sample started to deform plastically due to the constant load of 800 N. This shows that already a short overload of the characteristic strength, that could be resisted initially, leads to a failure due to creep. Therefore, one should never conclude for a geometry which initially can resist a load, that this geometry therewith is capable of actually resisting that load on a longer-term.

The 500N-test did not reach the plastic deformation phase (tertiary creep phase) during the time span of the test (60.000 seconds = 10.000 minutes). Furthermore, the maximum reached elongation during the test was of an acceptable magnitude. This at least is a positive given, because it shows that once the material is loaded up to about 50% of the average strength (which forms 78% of the characteristic strength), no quick (< 1 week) failure due to creep is expected. However, since a creep test cannot last forever and is bound to an end, it still is hard to say if and when a plastic deformation stage would have been reached. Therefore, although the performed 800N- and 500N-test enabled some initial valuable insights in the creep behavior of the material, more extensive research on the creep behavior of the material is required before it can be applied structurally with full safety.

This test proved that loading the material up to 78% of the characteristic strength, leads to an allowable creep deformation. Due to the low number of tested samples and the relative short duration of the performed creep test, it is advised to add an extra safety margin for creep behavior in practice. Therefore, it is recommended for loads that are applied on a long-term, to keep these loads below 50% of the characteristic strength, to be on the safe side. Furthermore, for geometries to which long-term loads are applied, it is recommended to create multicarrier roads within these geometries and also between different geometries. This, because the creep behavior of this material still is insecure as only two initial tests are performed and the duration of the creep test was limited. Because it is improbable that multiple geometry parts and multiple geometries fail on creep at the exact same time, creating multicarrier roads will prevent a structure from collapsing, once a sole part fails on creep. This of course means that inspection needs to be performed on a regular base to check if failure of individual parts has taken place.

## 6. Material Tests – Block/Geometry level

In chapter 5, the most important elementary material properties are determined by material tests. The mechanical properties form an important part of these obtained properties, as mechanical properties of a material are essential to be known, especially when using the material for structural applications, which is the intention of the 3D Print Canal House project. In chapter 5 it is already observed that the mechanical properties are influenced by outer circumstances and therefore dependent of variable quantities like time (creep) and temperature. Besides that the elementary mechanical properties can be influenced by the conditions to which the material is exposed, the mechanical properties of the material can also be dependent of the size, form and dimensions of the geometry in which the material is applied. For this reason, in this chapter large blocks/geometries composed of the printing material are tested. In this way it can be studied whether the elementary compressive, shear and tensile strength as determined under chapter 5, are in line with the test results that are obtained for tests of large geometries. This comparison between elementary strength properties and strength performance of larger blocks is important to be known, because it defines the predictability of the mechanical behavior of designed printing geometries.

The 3D printed house will basically be composed of printed horizontal and vertical plate-elements and/or line-elements, as a house normally consists of walls and floors. Therefore it is likely that most of the applied elements will be loaded in compression and bending. For this reason the tests that are performed in this chapter are compressive/buckling tests and bending tests. Apart from using the obtained test results in this chapter for a comparison with the elementary test results, the test results of the compressive, buckling and bending tests also provide general material data like the compressive strength and bending strength. These obtained material properties can be used for the further general description of the printing material behavior.

### 6.1 Compressive/Buckling Tests

#### 6.1.1 Aim of Test

In paragraph 5.3, as part of the research to the elementary properties of the material, a compressive test has been performed on solid cubes of 50x50x50 mm. This is done for the three different directions/orientations of the cube. As the tested blocks had a standard form and dimensions, the test offered a proper insight in the general compressive strength of the material. In practice however, so far no solid/closed geometries have been designed and fabricated within the 3D Print Canal House Project. The reason for this is that a closed geometry somewhat conflicts with the applied technique of 3D-printing. Actually, for closed geometries (think for example of solid concrete slabs) it often is the case that an inefficient amount of material is applied when purely looking at the material that is required for the structural performance. When closed geometries are applied in the building practice, this often is for physical/insulation matters or for the reason that a solid geometry can be more cost efficient to build in comparison to forms that have a higher material efficiency. Also, a solid block sometimes can be connected more easily to other blocks.

An important advantage of 3D-printing however, is that the technique enables to easily obtain complex formed geometries that are both material-efficient and cost-efficient. This benefit of 3D-printing will not be utilized when creating solid geometries, as these are material-inefficient (taking into account the structural use) and cost-inefficient. Furthermore 3D-printers often lay down the material in small portions, while in case of solid structures it is quicker and therefore more cost-efficient to build up the solid blocks by adding the raw materials in large portions.

For these reasons the fabrication method of 3D-printing is quite contrary to the application of solid bodies. Therefore, the obtained results of the tested solid cubes might not be representative for and thereby convertible to the geometries that are fabricated so far within the Canal House Project.

It is for this reason that within this paragraph open geometries will be loaded under compression, as these are more representative for the geometries as designed within the Canal House Project and therefore probably are better convertible to the designed geometries.

The obtained results within this test will be compared to the relevant elementary mechanical properties as obtained in chapter 5. In this way it can be studied whether the tested geometries of this paragraph behave like as would have been expected when extrapolating the elementary material properties to the block forms. Within this test both a hollow cube that is open at two of its four sides and a hollow column are loaded in compression. Testing of the hollow cube can somewhat be seen as a repetition of the compressive test of paragraph 5.3, but this time with a hollow cube, which might be more representative for the printed

geometries within the Canal House Project.

For loading the hollow column under compression it is expected that buckling effects will start playing a role in the behavior and deformation of the tested block. An important goal of testing the hollow columns therefore is to gain more insight in the buckling behavior of geometries that are composed of the printing material.

### 6.1.2 Tested Blocks

#### Compressive test – hollow cubes

The hollow cubes are obtained from one of the three square hollow sections of 100x100x 500 mm that are shown on Figure 106. These three square hollow sections are connected to each other, purely to save time within the printing process. Preparing the software and printer for a new printing job actually is quite a time-consuming part of the printing process and therefore blocks are connected to each other as much as possible, such that the amount of printing jobs is reduced. The three square hollow tubes on the picture are printed with their long side in the vertical direction (z-direction). Since the printer is not capable for printing spans, this was the only option to obtain these geometries.

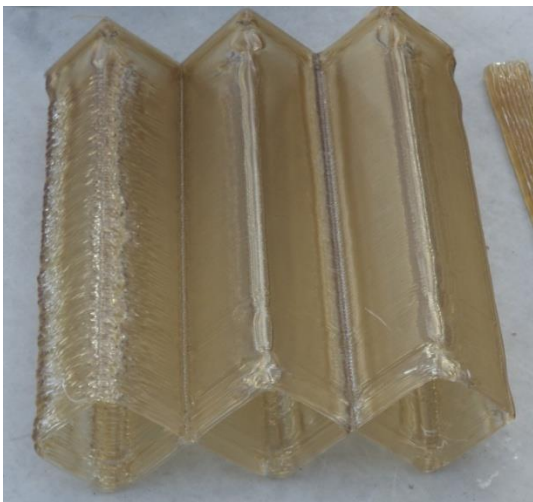


Fig. 106 Compressive and buckling test specimen as they came out of the printer

As is mentioned in the previous paragraph, the compressive test described in this paragraph somewhat is a repetition of the compressive test as performed during the elementary material research and described in paragraph 5.3, with the difference that this time a hollow cube is tested instead of a solid one.

For making a proper comparison, it was desired to test cubes with the same outer dimensions as the tested solid cubes, so cubes with dimensions of 50x50x50 mm. However when printing the hollow tubes with these small width and depth, there is a large risk of instability and therefore a poor printing result with printed lines that are not printed straight above each other. To decrease this risk, it was decided to choose for a cube with outer dimensions of 100x100x100 mm.

As explained earlier, all the blocks that are designed and printed on the building site of DUS so far, consist of one printed layer in the horizontal plane. Therefore, a single layer is chosen as the wall thickness of the cubes, as this is consistent with the way so far geometries have been printed by DUS Architects. This means the wall thickness is equal to the line thickness in the horizontal plane, which ranges between 4-6 mm.

The picture below shows the dimensions of the tested hollow cubes for the compressive test. The red lines represent the direction of the printing lines and, together with the coordinate system, they clarify the print orientation of the cubes.

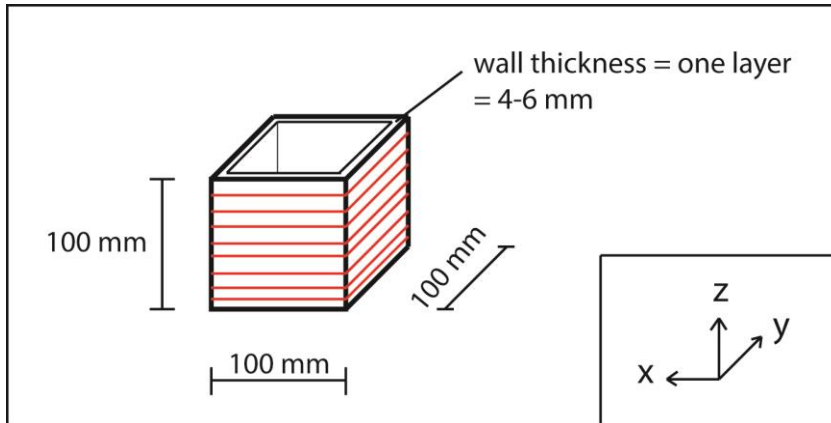


**Fig. 107 Dimensions and print orientation of tested hollow cubes**

Sawing one of the hollow tubes of 100x100x500 mm, into five equal pieces of 100x100x100 mm lead to the five test samples G1 to G5 that are shown on the picture below:

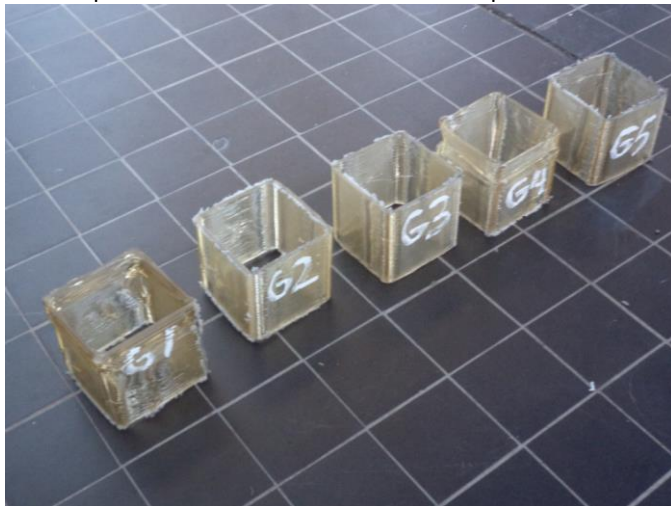


**Fig. 108 Compressive samples before testing**

The five specimens all are compressed in the direction of the four closed sides, so in the z-direction when looking at the coordinate system in Figure 107. This, because within this orientation, the specimen walls are loaded within compression, such that the compressive strength can be obtained. When putting a compressive force on the other possible direction (so x- or y-direction), a compressive force is applied on a spanning wall that is supported by two standing walls. In this way the walls are loaded in tension and bending, which is not the intention of this test.

#### **Compressive test – square hollow column**

Next to the cube-formed hollow sections that are sawn from a column of 100x100x500 mm, it is decided to test the other two produced columns in their full length. Comparing the test-results of these tested columns with the test-results of the hollow cubes, leads to insights in the effect of increasing the specimen length on the strength and therefore possibly says something about the buckling behavior of the printing material.

As the square hollow cubes are obtained from a square hollow column as well, the square hollow columns have the same width and wall thickness. Only the height is five times bigger than the height of the tested hollow cubes:

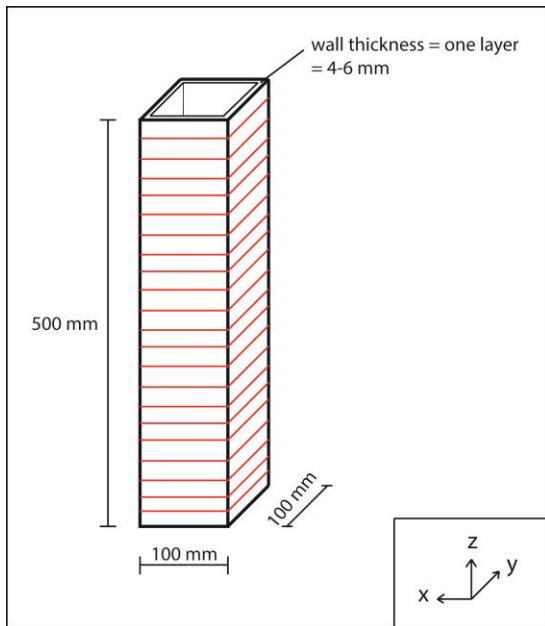


Fig. 109 Dimensions and print orientation of buckling specimen

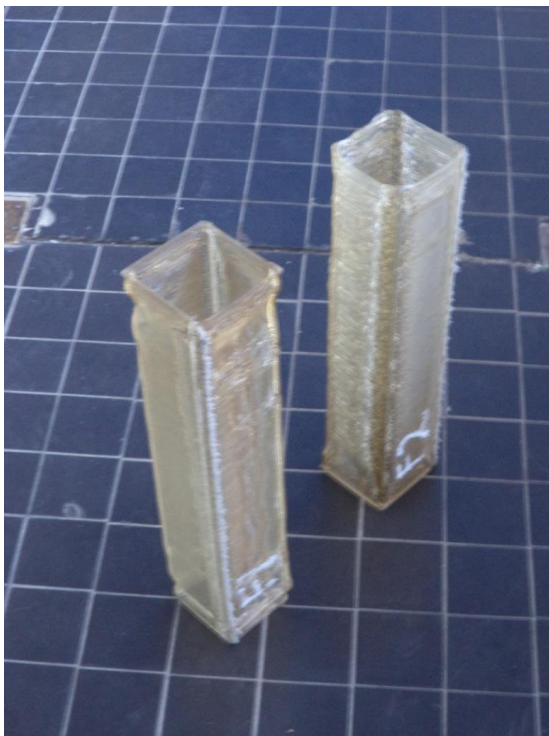


Fig. 110 Buckling specimens before testing

### 6.1.3 Test Setup

#### Compressive test – hollow cubes

For this compressive test, the same test setup is used as for the compressive test of the solid cube samples. This means the Zwick testing machine at the faculty of 3ME is used again. This machine can apply compressive forces up to 100 kN. Unfortunately, no picture is made of the test setup including a hollow cube specimen. However, since the setup of this test is the same as for the previous compressive test, it is sufficient to show a picture of the solid cube compressive test (fig. 111- left) in combination with the load direction for the hollow cube (fig. 111 - right) to clarify the test setup of this test.

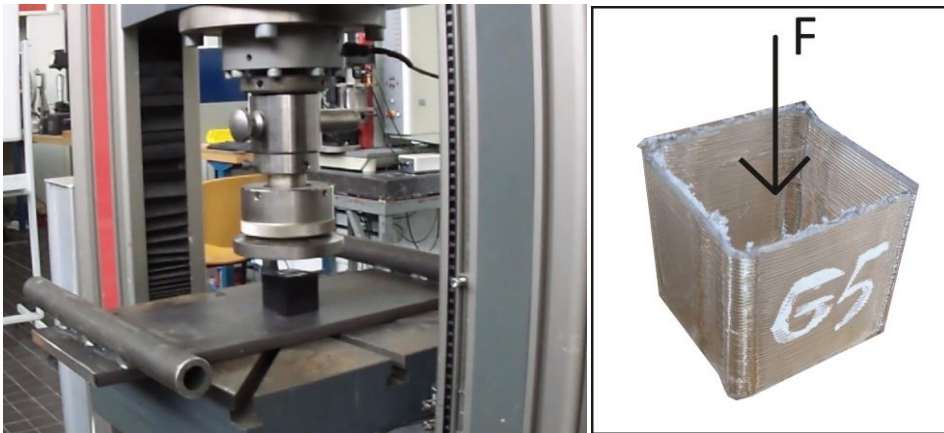


Fig. 111 Left: Test setup. Right: direction of the applied load

In the Zwick Testxpert II software program, it is set that a compression test will be performed on a circular tube with an outer diameter of 100 mm and an inner diameter of 95 mm. A circular tube was chosen here as a reference sample, since this was the only hollow section that could be chosen within the software program. Of course afterwards, the stress-results are corrected such that they are in compliance with the actual loaded cross-sectional dimensions of the tested square hollow section.

The testing speed is set at 10 mm/min and a preload of 5 N is chosen. The set maximum displacement of the compressive top head is 80 mm, which means with a sample height of 100 mm, that the maximum contraction is 80%.

#### Compressive test – square hollow column

The test setup of the buckling test is about the same as for the compressive test, as the same testing device and compressive attachments are used. The only difference this time is that a steel plate is placed on top of the specimen. This is done because in case that the specimen slides a little at the top, the test specimen would not be loaded over its full effective area anymore, as the circular compression tool is just big enough to cover the full 100x100 mm top-surface of the specimen. By placing a steel plate with an area larger than 100 x 100 mm in between, the compressive force is still applied over the full effective area of the hollow cube sample, in case of sliding of the test specimen at the top.



Fig. 112 Test setup – buckling test

The maximum displacement of the compression head is set at 400 mm (sample height = 500 mm). The testing speed is 10 mm/min and a preload of 5N is chosen.

For this test, again a compressive test on a circular hollow section is set within the Zwick Testxpert II software program as a reference. For this test, an outer diameter of 100 mm is picked and an inner diameter of 90 mm. Again, the loaded area is corrected afterwards.

#### 6.1.4 Test Results

##### Compressive test – hollow cubes

The hollow cube test specimens look as follows after performing the test:



Fig. 113 Tested compressive samples

As can be seen on the picture above, all of the test samples failed at one particular corner, which fully ruptured. This corner in which the samples fail, is the corner with which the hollow square column originally was connected to the other columns for the purpose of the printing process (see fig. 106). On Figure 114, it can be observed that separating the square hollow column from the two other columns by sawing, led to a corner with a thinner wall thickness than the rest of the sample (1.5 mm instead of 4.5 mm). The local thinner wall thickness led to a weak spot in the samples which explains the failure of the samples in this corner.



Fig. 114 Weak corner of hollow cube samples at which the samples failed.

The obtained Force-displacement curves of this test, which are shown in Figure 115, clearly show a maximum for all the tested samples. At this maximum point, the sample ruptured at the weak corner-point. After the corner failure, the rest of the material was still able to resist some load. Due to further shrinking of the flexible material, the sample became stiffer again, which explains the rise of the curve at the end. However, only the early reached maximum of the curve is relevant, because this defines the strength of the tested sample.



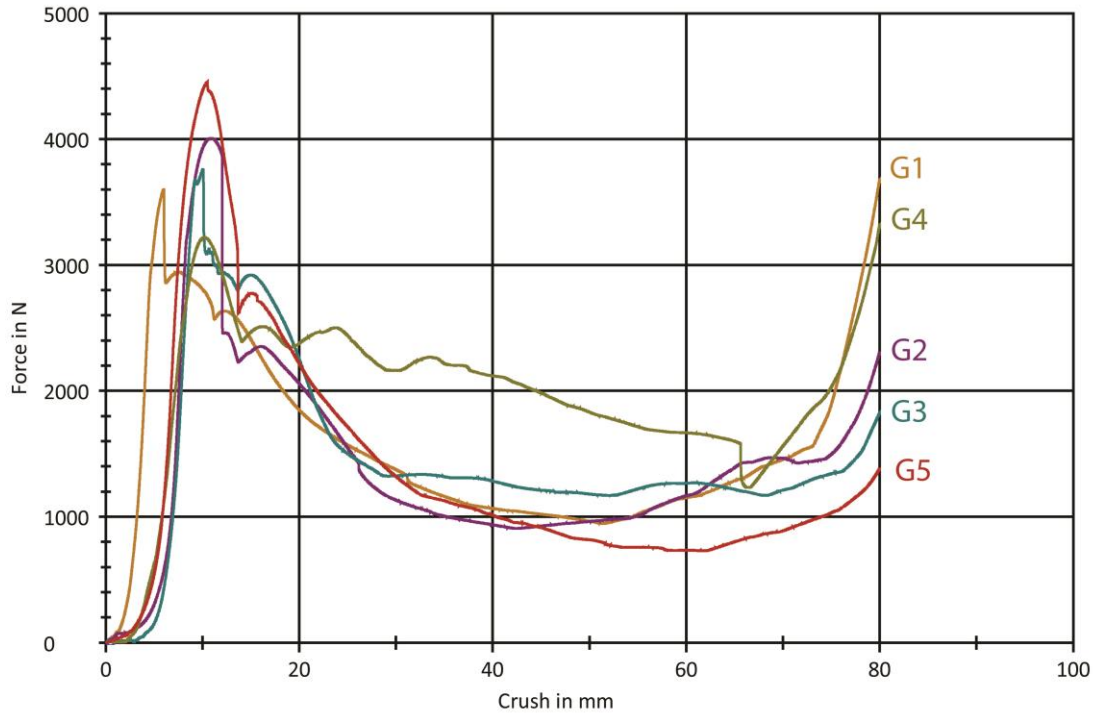


Fig. 115 Obtained Force-displacement curves of the compressive tests

The table below shows the dimensional properties of the tested samples, the maximum resisted load and the stress and strain at the point of maximum load:

Specimen Name	length [mm]	width [mm]	height [mm]	wall thickness [mm]	CS Area [mm <sup>2</sup> ]	Max Load [N]	Compressive Strength [MPa]	Crush at Max load [mm]	Compressive Strain [%]
G1	102.5	103	101	4.5	1768.5	3680	2.08	5.98	5.92
G2	105	103.7	96.8	4.5	1797.3	4010	2.23	10.8	11.16
G3	105	103	98.9	4.8	1904.64	3760	1.97	10.0	10.11
G4	104	103	99.5	4.5	1782	3330	1.87	10.3	10.35
G5	105	104	97.5	4.5	1800	4460	2.48	10.5	10.77
<b>Average</b>						3848.00	2.13	9.52	9.66
<b>Standard deviation</b>						419.8	0.24	n.a.	n.a.
<b>Characteristic</b>						3092.28	1.70	n.a.	n.a.

Table 53 Compressive strengths of the tested hollow cubes

### Compressive test – square hollow column

The deformation of the first hollow square column F1, during and after the test, can be observed on the pictures below. The large, overall deflection of the column, which can be observed in the middle picture, mostly folded back after releasing the load. This can be seen on the right picture. The local deformations at the top part of the column (middle picture) however, did not fold back entirely and therefore resulted in a permanent deformation of the shape (picture right).



Fig. 116 Test-Column F1, during the test and directly after the test

For the tested column F2, things went different than for column F1. While for column F1, deformation especially was observed at the top of the column in the neighborhood of the applied load, column F2 in particular deformed at a lower spot in the column. Because the top of the column skewed earlier for sample F2 than for F1, test F2 had to be stopped earlier to prevent the steel plate from falling of the column top. After the release of the load, the column F2 managed to fold back to its original form. No clear permanent deformations could be observed anymore. This led to the opportunity to test the square hollow column for a second time, to see what the effect would be.



Fig. 117 Column F2 during and after the test. The sample seems to fold back completely.

When testing the column F2 for a second time, about the same deformation was observed as the first time, with the only difference that this time the noticeable deformation around the top of the column was slightly bigger. After releasing the load again, this time a small permanent deformation was noticeable in the column. So the column did not completely fold back to its original shape this time.



Fig. 118 Testing the column F2 for a second time. This time a small permanent deformation at the side is visible after the test (picture right).

The Force-displacement curves of the tested columns are displayed in the graph below. The tests were stopped on the moment that the top of the column was skewed so much that the steel plate between the column head and the test compressive head was about to fall off. At this same moment, the compressive force would not be applied over the full section of the column anymore, so continuing the test after this moment would not be useful. As the deformation of the column top differed for the different columns, the end points of the curves differ as well.

The curve of the tested column F1 shows a varying, incalculable pattern, after reaching the initial maximum point. This can be explained by the observation that column F1 particularly was deforming around the top of the column, where local indentation of the column top lead to an irregular deformation pattern.

The two curves of the tested column F2 show a constant decline after reaching the maximum, which is a usual course for a curve of a geometry that fails due to buckling. The hypothesis that the column F2 failed on buckling is further confirmed by the fact that during the test a deformation around the middle part of the column was noticed that is reminiscent of a buckling deformation. For this reason it is likely that column F2 failed on buckling.

Since no cracks were observed for column F1 either, it is plausible that column F1 failed on buckling as well. However, because column F1 deformed in the neighborhood of the applied load, it seems that buckling of the walls for this sample is more a local effect than a global one, because it seems that the compressive load is not equally distributed over the whole length of the column as it was the case for column F2.

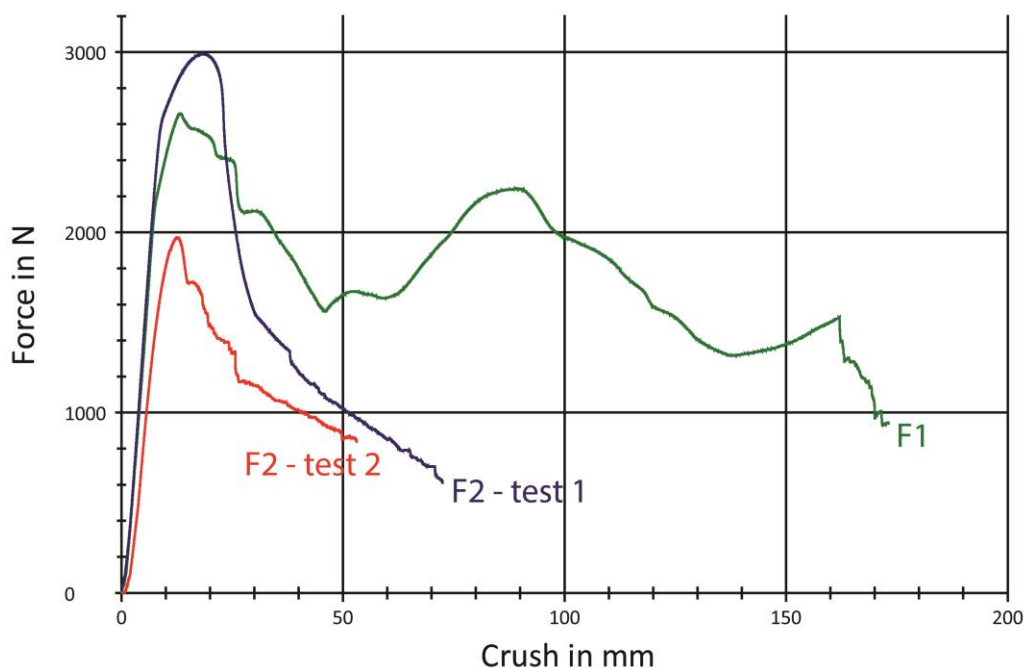


Fig. 119 Buckling curves for F1 and F2, of which the latter that is tested twice. Although sample F2 moved back to about its original form after the test, it is obvious that the strength performance has been decreased after the first test.

Although the column F2 by observation seemed to fully fold back to its original form after unloading, the curve of F2 – test 2 clearly shows that the strength of the column was reduced significantly (about one-third) after the first test. This probably means that local permanent deformations did take place in the column, which could not be noticed with one's bare eyes. For this reason, it is not advisable to judge the performance of a geometry by the observable reformation, as permanent deformations turn out not to be always noticeable.

Specimen Name	length [mm]	width [mm]	height [mm]	wall thickness [mm]	CS Area [mm <sup>2</sup> ]	Max Load [N]	Compressive Strength* [MPa]	Crush at Max load [mm]	Compressive Strain [%]*
F1	101.4	103.0	500	4.5	1758.6	2660	1.51	13.2	2.64
F2 – test 1	105.0	107.0	500	4.5	1827.0	2990	1.64	18.4	3.68
F2 – test 2	105.0	107.0	500	4.5	1827.0	1970	1.08	12.7	2.54

Table 54 Test results – Buckling Test

### 6.1.5 Conformity with results elementary tests

#### Compressive test – hollow cubes

The compressive strength properties are determined both for a cube that is completely solid (paragraph 5.3) as for a hollow cube in this paragraph. This means the results can be compared with each other now.

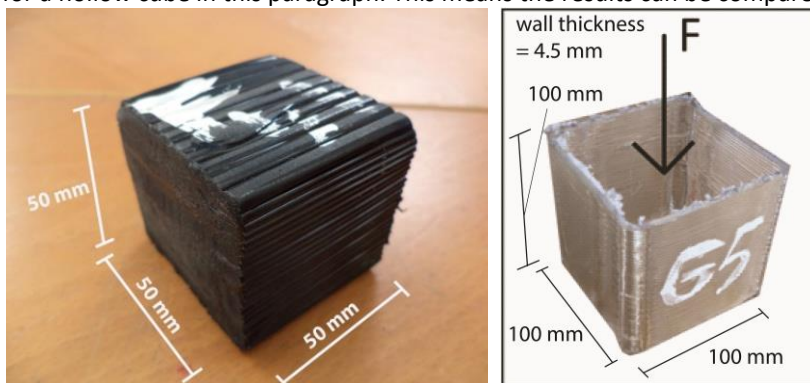


Fig. 120 Left the tested solid cube (paragraph 5.3) and right the tested hollow cube of this paragraph

When looking at the results of both the tested solid cubes (table 55) and the tested hollow cubes (table 56) it can be observed that on an average, the obtained strength values for the solid cube are about 8-9 times higher than for the hollow sections. This significant difference can be explained by the following three possible causes:

- 1) As already concluded in chapter 5, printing multiple layers in both the horizontal as the vertical plane, leads to a material performance which is stronger, more isotropic and more homogeneous than for geometries that consists of a single printed layer in the horizontal direction. Therefore the solid cubes have a higher strength than the hollow cubes that are only one layer thick.
- 2) The hollow cubes can fail on local buckling of the walls, while buckling is not a possible failure mechanism for solid cubes.
- 3) Local inaccuracies are more often present in a hollow thin-walled section than in a solid section and the impact of an inaccuracy will also be bigger for hollow sections. In the case of the tested hollow cubes, the inexact sawing of the samples lead to a locally thinner corner and therefore to a crucial weak point in which all samples failed. Inaccurate sawing of solid samples would not have had such an impact on the strength as was the case for the hollow cube samples.

The significant compressive strength difference between hollow sections and solid sections again confirms the earlier recommendation that geometries should be build up by multiple layers in the horizontal direction, as this increases the strength properties significantly.

Specimen Name	length [mm]	width [mm]	height [mm]	CS Area [mm <sup>2</sup> ]	Compressive Strength* [MPa]	Compressive Strain [%]*	Compressive Yield Strength [MPa]	Compressive Yield Strain [%]	Compressive Modulus [MPa] or MPa
F1,1	51.5	46.5	54.5	2394.8	18.8	25.5	13.6	14.0	140
F1,2	51.6	46.7	54.5	2409.7	18.6	25.7	13.4	14.2	139
F1,3	51.4	48	54.0	2467.2	17.7	24.0	13.1	13.0	144
F1,4	52.0	46.9	54.4	2438.8	18.9	30.5	14.5	18.0	107
F1,5	51.0	47.1	54.8	2402.1	19.5	32.5	15.1	20.5	118
F1,6	50.5	48.3	54.2	2439.2	18.2	25.0	12.3	13.0	143
F1,7	50.6	48.0	54.4	2428.8	19.5	24.5	13.8	12.5	156
<b>Average</b>					18.7	26.8	13.7	15	135
<b>Standard deviation</b>					0.66	n.a.	0.92	n.a.	8.66
<b>Characteristic</b>					17.5	n.a.	12.1	n.a.	120

Table 55 Test results – compressive tests performed on solid cubes (paragraph 5.3)

Specimen Name	length [mm]	width [mm]	height [mm]	wall thickness [mm]	CS Area [mm <sup>2</sup> ]	Max Load [N]	Compressive Strength [MPa]	Crush at Max load [mm]	Compressive Strain [%]
G1	102.5	103	101	4.5	1768.5	3680	2.08	5.98	5.92
G2	105	103.7	96.8	4.5	1797.3	4010	2.23	10.8	11.16
G3	105	103	98.9	4.8	1904.64	3760	1.97	10.0	10.11
G4	104	103	99.5	4.5	1782	3330	1.87	10.3	10.35
G5	105	104	97.5	4.5	1800	4460	2.48	10.5	10.77
<b>Average</b>						3848.00	2.13	9.52	9.66
<b>Standard deviation</b>						419.8	0.24	n.a.	n.a.
<b>Characteristic</b>						3092.28	1.70	n.a.	n.a.

Table 56 Test results – compressive tests performed on hollow cubes. As can be read, the strength differences with the compressive tests performed on solid cubes (table 55) are significant.

### Compressive test – square hollow column

As mentioned earlier, the tested square hollow columns actually are the same geometries as the tested hollow cubes but than five times higher. An important difference between the tested columns and the tested cubes however is that the tested columns are better sawn and therefore do not have a weak corner at the sawing point like was the case for the square cubes. This absence of a weak corner in the columns probably has led to a higher axial cross-sectional strength for the columns than for the cubes. However, if we look at the results of the tested columns (table 57) it can be observed that the obtained strength, on an average, still is about one-fourth lower than for the tested cubes (see table 56). This difference probably can be attributed to buckling effects that start to play a bigger role as the height/width ratio is increased compared to the hollow cubes.

Specimen Name	length [mm]	width [mm]	height [mm]	wall thickness [mm]	CS Area [mm <sup>2</sup> ]	Max Load [N]	Compressive Strength* [MPa]	Crush at Max load [mm]	Compressive Strain [%]*
F1	101.4	103.0	500	4.5	1758.6	2660	1.51	13.2	2.64
F2 – test 1	105.0	107.0	500	4.5	1827.0	2990	1.64	18.4	3.68
F2 – test 2	105.0	107.0	500	4.5	1827.0	1970	1.08	12.7	2.54

Table 57 Test results of tested square hollow columns

In the reflection below, a closer look will be taken on the buckling effects:

First the situation of buckling of the overall column is considered:

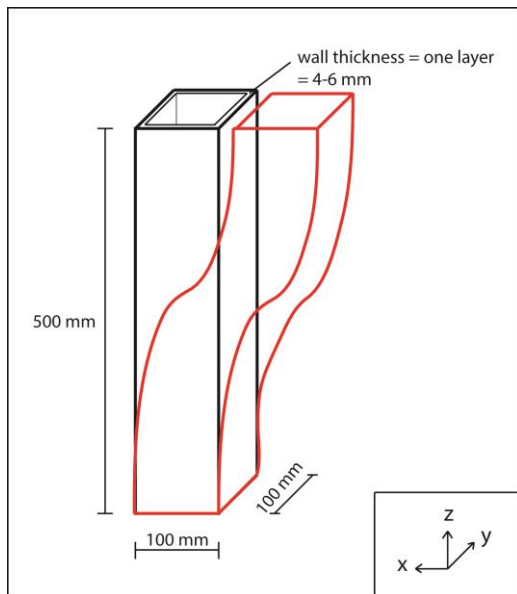


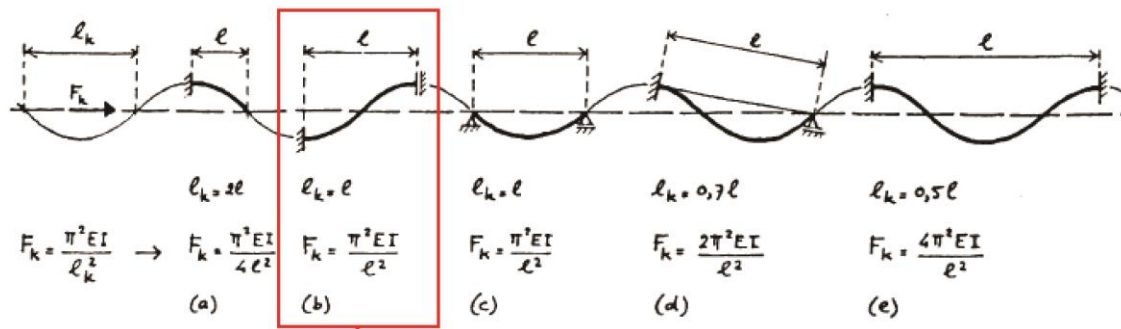
Fig. 121 Buckling mechanism of the overall column

The general formula for the Euler Buckling Force is:

$$F_k = \frac{\pi^2 \cdot EI}{l_k^2} \quad (6.1)$$

## 6. Material Tests – Block/Geometry level

As the load situation can be best compared with the general buckling case that is indicated in the picture below, the column length of  $l$  can be taken for the buckling length.



General buckling case that comes the closest to the test situation

**Fig. 122** General buckling case that is best applicable to the test situation [Hartsuijker et al, 2007]

For the Young's Modulus 'E', a value of 135 MPa is chosen as this is the average compressive modulus that was found for compressing the material in the direction perpendicular to the printed lines (see table 55).

For the moment of Inertia 'I', that is build up by four own moment of inertias for the four walls and a Steiner moment for two of the walls, a value of 12273466.5 mm<sup>4</sup> is found for column F1 and a value of 13749349.5 mm<sup>4</sup> for F2.

Filling in the obtained values in formula 6.1, the following value is found for the Euler buckling force of F1:

$$F_k = \frac{\pi^2 \cdot 135 \cdot 12273466.5}{500^2} = 65.4 \text{ KN}$$

which gives for the Euler buckling stress:

$$\sigma_k = \frac{F_k}{A} = \frac{65412.5}{1758.6} = 37.2 \text{ MPa} \quad (6.2)$$

In the same way, for test 1 of column F2 a buckling force  $F_k$  of 73.3 KN can be found and a buckling stress of 40.1 MPa.

It seems, that global buckling of the overall column is not the normative failure mechanism, as the maximum stress that was reached during the test, is significantly lower than the calculated Euler buckling stress. It can however be the case that buckling of individual walls did cause the column failure. This is quite plausible, because on the pictures that are made during the test (Figure 116-118), it indeed can be observed that the walls also deform individually and independent from each other, apart from deformation of the column as a whole.

This described local buckling effect is displayed on figure 123.

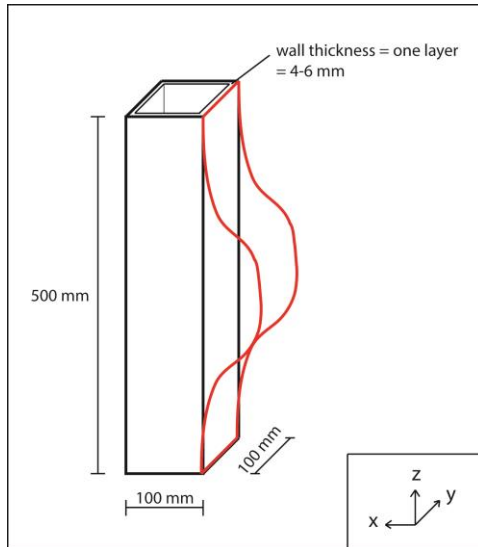


**Fig. 123 Buckling mechanism of individual walls**

When calculating the Euler buckling stress of an individual wall, the Euler buckling force now becomes:

$$F_k = \frac{\pi^2 \cdot 135 \cdot 390971.5}{500^2} = 2083.7 \text{ N}$$

and the buckling stress becomes:

$$\sigma_k = \frac{F_k}{A} = \frac{2083.7}{1758.6} = 1.18 \text{ MPa}$$

For test 2 the buckling force becomes 2313.6 kN and the buckling stress 1.26 MPa.

These obtained values for the buckling force and buckling stress are slightly lower than the obtained maximum values during the test (table 57), which means that it is likely that local buckling of individual walls indeed is the normative failure mechanism for these tested columns. The small difference between the calculated values and the measured values can be explained by understanding that in the above calculation an individual wall is considered that is standing on its own, while in the tested situation, an individual wall is partly supported by the three other walls to which the individual wall is connected.

Nevertheless the outcome of this Euler buckling calculation of individual walls, confirms that the difference in strength performance between the hollow cube samples (table 56) and the tested square hollow columns (table 57) can be explained by the effect of a higher buckling length of the column and the consequently lower buckling strength performance.

### 6.1.6 Test Evaluation and Conclusions

The obtained compressive strength performance of thin-walled hollow cubes is significantly (about 8-9 times) lower than the compressive strength of solid cubes. Of course it is unfortunate that the tested hollow cube samples did not have a uniform wall thickness, but possessed a thin weak corner on which all the samples failed. The compressive strength of the thin-walled cubes probably would have turned out higher if this corner would not have been present. On the other hand this also confirms the earlier conclusion that thin-walled geometries are sensitive to local inaccuracies. As the current printing process cannot guarantee a constant and uniform printing quality, there always is a chance of presence of these kind of local inaccuracies. The impact of local inaccuracies reduces with the increase in amount of mutual connections within the material. Therefore again the recommendation is confirmed that one should print geometries with multiple layers instead of single ones, as this reduces the impact of local inaccuracies.



## 6. Material Tests – Block/Geometry level

Printing multiple layers will also increase the buckling stiffness and the cross-sectional strength of geometries and their individual walls. So by printing multiple layers, the overall structural performance increases for multiple reasons.

A first conclusion that can be drawn based on testing the hollow square columns is that once a geometry is tested to its full capacity, one can assume that the strength capacity is decreased. Although the material sometimes seems to completely reform back to its original shape, it probably still is the case then that the inner structure of the material has been changed, which leads to a lower strength. It therefore is advised not to judge the structural performance of geometries with one's bare eyes, as structural degradation is not always visible in the form of permanent deformations.

For the tested hollow square columns the ratio between the column height and overall column width turned out to be too small for a failure of the column on overall column buckling. This test however still was useful for studying the local buckling effect of individual walls. As the wall height was five times bigger now than in the case of the tested hollow cubes, the effect of this increased wall on the strength could be observed.

The outcome of the tested hollow columns indeed was that the maximum applied stress was about one-fourth lower than was the case for the hollow cubes. This, while the hollow columns did not even contain a weak corner like the hollow cube samples had. From this it can be concluded that buckling of individual walls is a normative failure mechanism for axial loaded walls. Therefore, the structural performance of printed geometries can be improved by applying more supporting points for individual walls, as this decreases the buckling length. The structural performance can also be improved again by printing multiple layers as this increases the stiffness and therefore the buckling strength.

The first measure, applying more supporting points for individual walls, can increase the material efficiency as the influence of a reduced buckling length is quadratic in the buckling formula (formula 6.1). Therefore, in case of smart design choices for supportive members within geometries, the strength of a geometry can increase with a higher factor than the increase in printing material that is necessary for adding the supportive members. The second measure, printing in multiple layers, does not increase the material efficiency when only taking into account the buckling strength. This because the stiffness  $EI$  increases with the same factor as the increase in material use. However, since printing in multiple layers also lead to more mutual connections in the material, the axial strength increases as well and the influence of local inaccuracies decreases which also leads to an improved strength performance. Therefore, increasing the thickness of walls by printing in multiple layers still is an effective measure as this does increase the material efficiency when taking into account all the possible failure mechanisms.

### 6.2 Bending Tests

#### 6.2.1 Aim of Test

The goal of this paragraph is to study the bending behavior of different geometries, such that the following properties can be obtained:

Material Properties	Symbol	Unit
Flexural strength //	$f_{t,0}$	MPa
Flexural strength $\perp$	$f_{t,90}$	MPa
Flexural Modulus //	$E_{f,0}$	MPa
Flexural Modulus $\perp$	$E_{f,90}$	MPa
Flexural strain //	$\epsilon_{f,0}$	%
Flexural strain $\perp$	$\epsilon_{f,90}$	%

**Table 58 Flexural properties to obtain**

Another important goal of this test is to research whether the elementary compressive, shear and tensile strength as determined under chapter 5, are in compliance with the test results that are obtained for tests of large geometries. By this, it can be concluded whether or not the mechanical behavior of designed geometries can be predicted by extrapolating the elementary material properties towards the geometry form.

### 6.2.2 Tested Blocks

On Figure 124 the different blocks that are subjected to a bending test, are shown. The red lines again represent the direction of the printed lines.

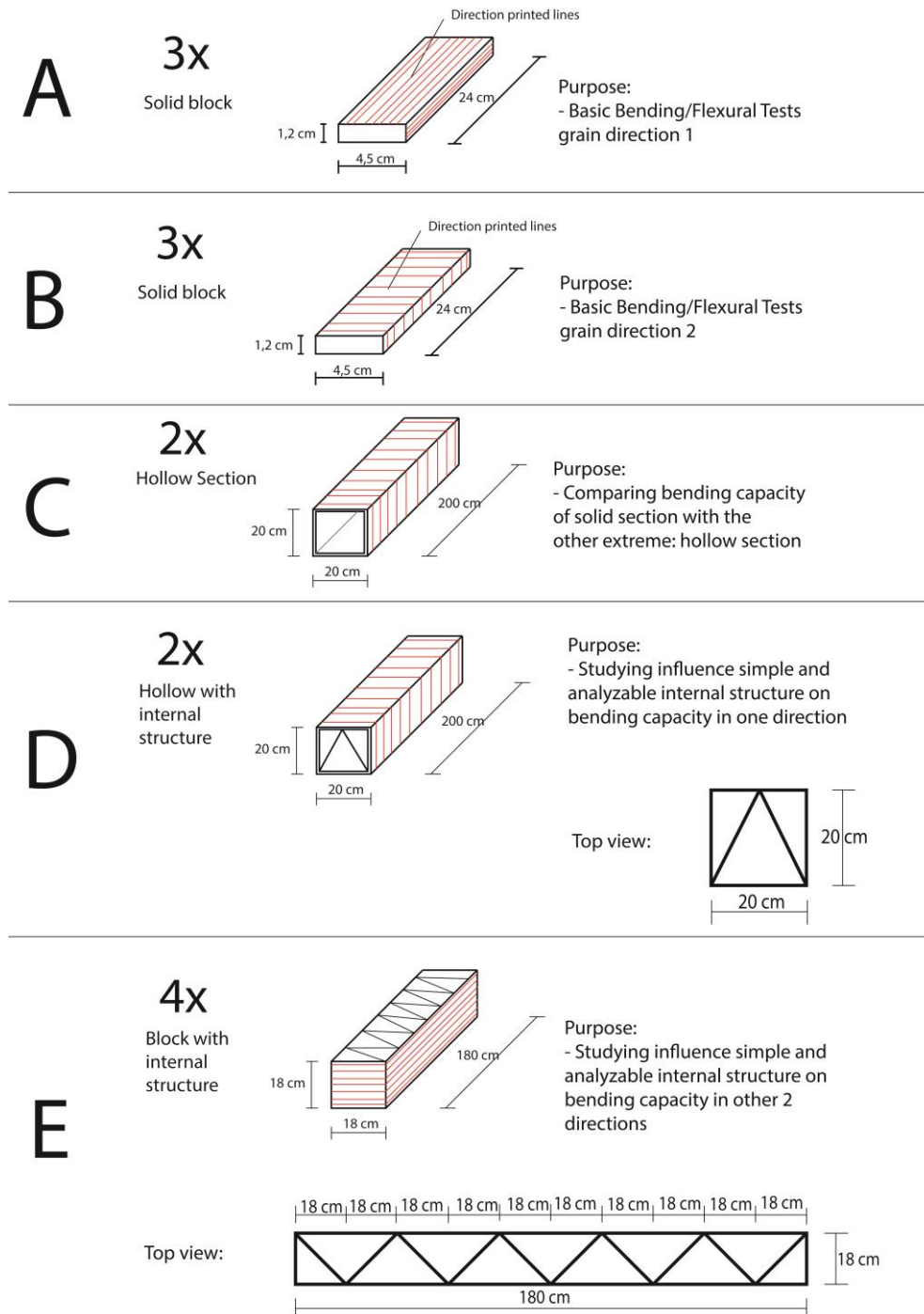


Fig. 124 Graphical representation of the tested bending blocks

Block A and B are completely solid blocks, with block A having its grain direction parallel to the direction in which the fibers will bend and block B having its printed lines perpendicular to the direction of bending. At first, it was desired to give the solid blocks the same dimensions as the 'open' blocks C-E, such that a better comparison between solid and open blocks would be possible. However, due to the long printing duration in combination with the high printing costs of solid blocks, it was decided in consultation with DUS to make these solid blocks as small as possible. The standards [NEN-EN-ISO-178, 2010] give dimensions of 8.0 x 1.5 x 0.4 cm as standard dimensions for the specimens of a flexural test. However, a height of 0.4 cm would mean that the height would only consist of two layers according to the printing line thickness of around 0.2 cm in the z-

direction. A sample height consisting of only two layers, probably would not lead to representative flexural test results. Therefore it is decided to multiply all the dimensions of this standard test specimen by a factor 3, such that the dimensions become 24x4.5x1.2 cm. By this the mutual ratios are still in accordance with the standard, while the height now consists of enough printing layers to obtain proper testing results.



**Fig. 125 The solid bending blocks – type A and B**

Blocks A and B, fully closed blocks, can be seen as an extreme/upper boundary for the amount of applied material within the block composition. Block C forms the opposite extreme, as a fully open block composition can be seen as the lower boundary of material use.

The walls of block C consist of one printed layer, because this is in line with the way geometries so far are designed and printed by DUS. This means that the wall thickness is defined by the possible resolution-range within the horizontal plane, leading to a wall thickness of between 4-6 mm.

The outer dimensions of block C are adapted to the available testing equipment for the 4 point flexural test. The upper tool that compresses with two points at the top of the block, has a fixed distance between the two point loads of 60 cm. For the spacing between the two points of support of the tool beneath there can be chosen between a distance of 0.6 m, 1.4 m and 1.8 m. For obtaining proper results, the heart-to-heart distance between the two supports needs to be between 2.0-3.0 times the distance between the point loads. This means that both the support spacing of 1.4 m and 1.8 m are possible. At both sides of the supports, the block has to cantilever enough to prevent the block from slipping of the supports. For this reason it is recommended that the length of the block becomes about 2.2-3.3 times the distance between the point loads, which leads to a possible block length between about 1.3 and 2.0 meters.

Another requirement for obtaining proper results from the bending test (which means, failure on bending and not on shear), is that the height and width of the tested block is about  $1/10^{\text{th}}$  of the block length. To increase the relationship between the bending blocks and the geometries that are designed printed so far by DUS, it is desired that the height and width of the bending blocks come as close as possible to the dimensions of the DUS-geometries. Most of the designed geometries of DUS have a width of about 30 centimeters. To come to a block height and width as close as possible to this 30 centimeters, the maximum possible block length of 2.0 meters has been chosen, such that the block height and width are maximized as well and become 20 centimeters in accordance with the h/l-ratio of 1/10.



**Fig. 126** The beams of type C with a square hollow section

By testing the blocks A, B and C, the upper and lower boundary for the amount of material use, and probably therefore also for the bending strength performance, are set. In practice, the printed geometries often will be somewhere in between the presented extremes of a completely closed block and a fully open one. This because a fully closed geometry conflicts in a way with the application of 3D printing technologies and therefore will not be cost-effective. A fully open geometry however, will have a non-optimized strength performance.

Block D and E are examples of geometries that fall in between the presented extremes. Due to the inner structures, it is likely that higher strength performances will be obtained than for a fully open structures and that the strength/cost-ratio will be better than for the completely closed geometry.

Block D is the same bending Block as Block C with the addition that this time a simple inner construction is applied. Because block C and D have the same outer dimensions, it will be possible to directly observe the effect of adding an inner structure within the hollow section. Because the printer only can print continuous lines and no interruptions are possible, one is limited in the design of the cross-section and therefore in the choice of the inner structure. It for example is not possible to have an inner structure in the form of a cross, as this cross section could not be obtained with a continuous line. The chosen inner structure of two diagonal lines that meet each other in the middle of the top-layer therefore was chosen as a feasible and structurally effective cross-section.



**Fig. 127** Beams of type D – Square hollow section with inner structure

Block E is a hollow bending block with an inner structure like block D, but this time the inner structure, consisting of diagonals, is oriented in the other direction. As a consequence, the direction of the printed lines and the sides of the block that are open (long side faces instead of end faces), automatically need to be changed along with the changed structural direction. This is due to the fact that the printer is not able to print spans and cantilevers and therefore non-solid geometries can only be printed in one way, with the vertical z-direction in the direction of the open face. Hence, block D and E are the only possible two orientations in which

## 6. Material Tests – Block/Geometry level

an inner structure can be obtained within the geometry of a bending beam.



**Fig. 128** Beam types E, laid down in the orientation in which they will be tested

There are four pieces created of Block E instead of two pieces like was the case for Block C and D. This is because for block E it is interesting to look at the bending behavior of the beam in two different orientations. Therefore, for two of the blocks the point loads will be applied on the closed faces of the block and for the other two blocks on the open faces.

The dimensions of Block E all are 10% smaller than the dimensions of block C and D. This was necessary because the long side of the beam is oriented in the horizontal printing direction, for which the maximum printing space is limited to 180 cm. This while in the vertical z-direction, to which the long side of beams C and D is oriented, the maximum printing space is 300 cm.

As can be noticed, the geometry of bending Block E comes quite close to the geometry of most of the wall-blocks that are printed so far by DUS, as the printed DUS-walls somewhat form an extrusion of block E in the z-direction.

The print quality of the four E-blocks is relatively high. No local inaccuracies can be observed.

### 6.2.3 Test Setup

#### Block A and B

For the 4 point bending test of block types A and B a Zwick testing machine is used from the faculty of Mechanical, Maritime & Materials Engineering (3mE) that can apply compressive forces up to 10 kN. The bottom tool consists of two supporting points, of which the spacing can be adapted freely within the range of the tool. Center-to-center, a spacing of 175 mm is chosen here, such that enough space (2x sample height) for cantilevering of the sample was left at both sides. The top of the supports is circular formed, such that the material sample does not fail on toughness of the surface. The upper tool is somewhat the same as the bottom tool, with the difference that the possible spacing range between the two vertical pieces that deliver the point loads on top of the sample, is smaller than the distance between the supporting points. For the center-to-center distance between the two point loads, a spacing of  $1/3^{\text{rd}}$  of the length is chosen, which is 80 mm.



**Fig. 129** Test setup for blocks A and B

Within the Zwick TestXpert II software, it is set that a flexural test will be performed with a rectangular test sample. The following test settings are entered into the program:

Test settings
Specimen width = 41.0 mm
Specimen thickness = 16.4 mm
Support separation = 175 mm
Maximum bending = 30 mm
Speed = 10 mm/min
Preload = 5 N

**Table 59** Test settings flexural test

### Block C and D

For the 4 point bending test of the blocks C and D, again a Zwick testing machine from the faculty of 3ME is used, but this time again the larger machine that can apply loads up to 100 kN. The upper tool that is connected to the moving head of the testing machine consists of a steel plate with two circular hollow tubes that transfer the load, delivered by the testing machine, towards the bending beam in the form of two points loads. The spacing between these point loads is fixed and amounts 60 cm. For the distance between the two supporting tools, there are four different possibilities: 60 cm, 100 cm, 140 cm and 180 cm. With a beam length of 200 cm, both a support spacing of 140 cm and 180 cm are possible for these blocks, as a regular support spacing measures 2-3 times the distance between the point loads. There is chosen for a spacing of 140 cm here, to gain more conformity with the testing of the E-blocks. For the E-beams, as it happens, 140 centimeter was the only option for the support distance, as the length of these beams is only 180 centimeters.



**Fig. 130** Test setup Block type C (left) and block type D (right)

Within Zwick TestXpert II, it again is set that a flexural test will be performed on a rectangular test sample. The following test settings are entered into the program:

Test settings
Specimen width = 200 mm
Specimen height = 200 mm
Support separation = 1400 mm
Maximum displacement = 100 mm (=1/2 x height), except for D2 were a max displacement of 150 mm was set.
Speed = 10 mm/min
Preload = 5 N

**Table 60** Test settings - geometry bending tests

## 6. Material Tests – Block/Geometry level

### Block E

The test setup and settings for the E-blocks are almost the same as for block C and D. Only the specimen width and height are now set to 180 x 180 mm.

As already explained under paragraph 6.2.2, two of the E-geometries will be tested in the orientation as shown on the left picture of Figure 131 and the other two E-blocks will be tested according to the orientation that is shown on the right picture.



Fig. 131 Test setup Block E1 and E2 (left) and Block E3 and E4 (right)

### 6.2.4 Test Results

#### Block A and B

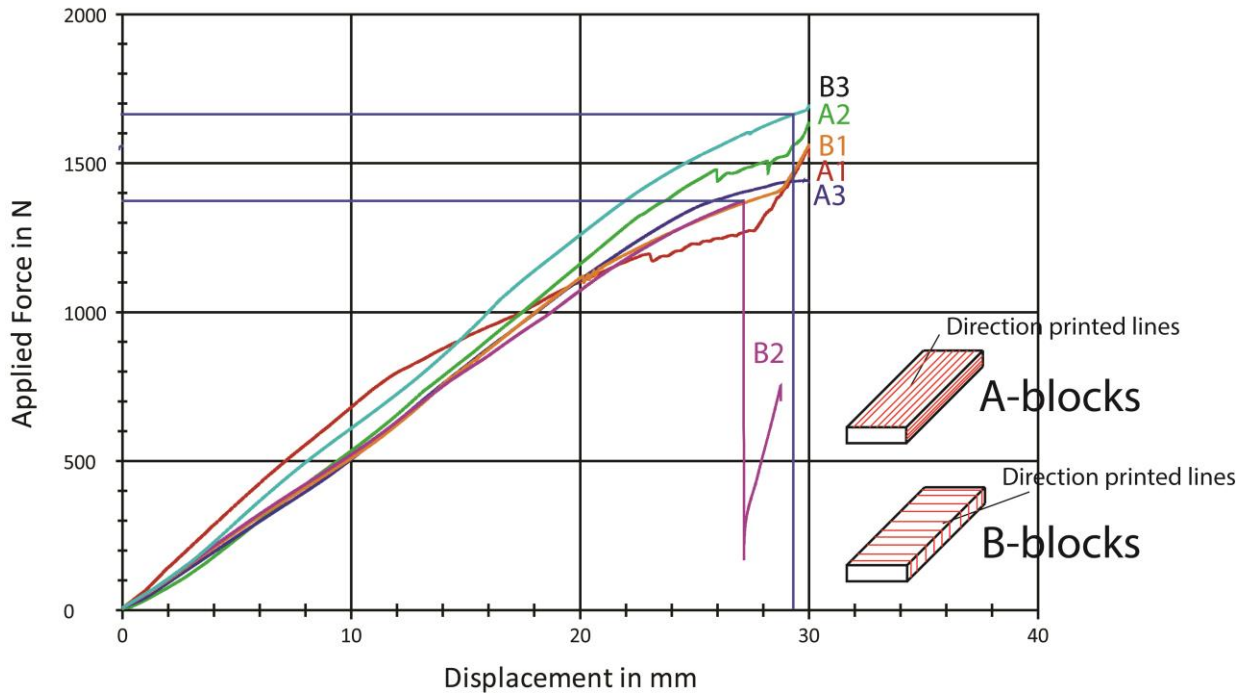


Fig. 132 Left: block type A in bending with its grain in the bending direction. Right: Block type B, which has its grain perpendicular to the direction of bending.



Fig. 133 Left: Permanent deformation of Block type A (left) and all the tested solid blocks (right)

The following Force-displacements diagrams were obtained from testing the 6 solid blocks:



**Fig. 134 Force-displacement curves block types A and B**

It is now the case to determine the required flexural properties, that are mentioned in paragraph 6.2.1, from these test-graphs. This can be done by using the following schematisations and formulas:

*Flexural Strength:*

Since the specimen graphs do not have a maximum and, apart from sample B2, do not have a breaking point either, according to [NEN-EN-ISO-178, 2010] the applied load that can be used for determining the flexural strength should be taken at a conventional deflection  $s_c$  of 1.5 times the sample height. This is shown in the graph below:

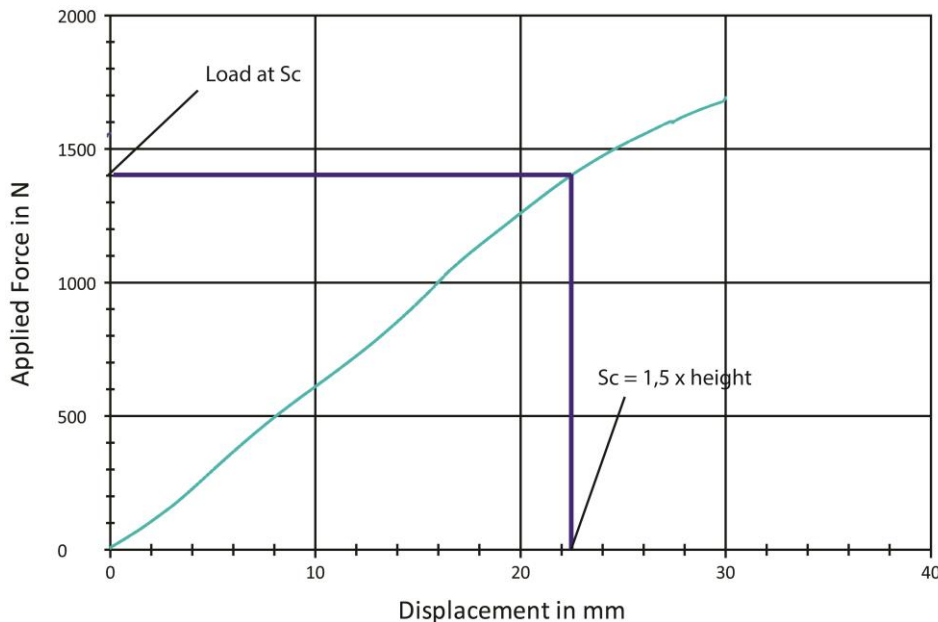


**Fig. 135 Determination of the Load at the conventional deflection  $s_c$**

For all the samples the load at  $s_c$  is taken, except for sample B2, for which the breaking load is taken. This is common for samples that break before reaching the maximum displacement.



The load case of this flexural test can be schematized in the following way:

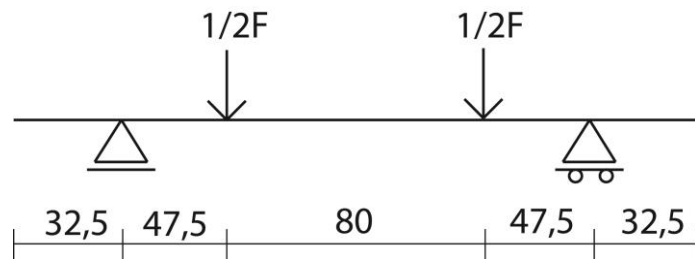


Fig. 136 Load case flexural test

From the load-case, it can be obtained that the maximum bending moment in the test sample is applied in the area between the two point loads. As explained earlier on, this is one of the main reasons for applying a four point flexural test instead of a three point flexural test, because with the four point test an area is exposed to the maximum bending load instead of only one single point as is the case in the three point test.

Based on this maximum bending moment, the flexural strength of the test sample now can be determined. This is done by calculating the maximum bending stress that occurs in the test sample. As the figure below shows, the symmetry of the test sample leads to a bending stress distribution where the maximum positive and negative stress are equal, with the maximum positive (tensile) stress working in the bottom fiber of the sample and the maximum negative (compressive) stress in the top fiber. Since from chapter 5 it is known that the compressive strength is significantly larger than the tensile strength, the strength in the bottom fiber of the test sample will be normative.

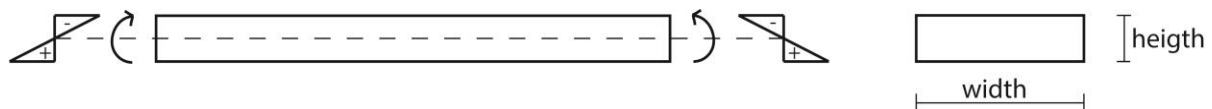


Fig. 137 Flexural stress in the solid block, caused by the drawn bending moment

The flexural strength, which is equal to the bending stress in the bottom fiber, can now be calculated in the following way:

$$f_f = \frac{M \cdot z}{I} \quad (6.3)$$

with 'M' is the maximum bending moment that works between the two point loads, z is the distance between the central and the outer fiber, which is:

$$z = \frac{1}{2} \cdot height \quad (6.4)$$

and 'I' is the moment of inertia which, for a rectangular solid section is equal to:

$$I = \frac{1}{12} \cdot b \cdot h^3 \quad (6.5)$$

*Flexural Modulus:*

The deflection equations for a four-point bending test are given below. The deflection that is measured in the flexural test concerns the deflection directly below a point load, since the displacement of the moving compressive head of the test machine is the displacement that is measured. So on figure 138, the deflection at a distance 'a' from the support, is the deflection that is measured. This deflection at a distance 'a' from the support and below the point load, can be calculated with the first of the three given formulas.

$$w(x) = \begin{cases} \frac{Px(3a^2 - 3La + x^2)}{6EI} \\ \frac{aP(a^2 + 3x^2 - 3Lx)}{6EI} \\ \frac{P(L-x)(3a^2 - 3La + L^2 + x^2 - 2Lx)}{6EI} \end{cases} \quad (6.6)$$

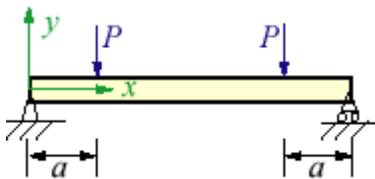


**Fig. 138** Load scheme of the performed 4-point bending test

Deflection at a distance 'a' from the support:

$$w(a) = \frac{(Pa(3a^2 - 3La + a^2))}{6EI} \quad (6.7)$$

This formula can be rewritten to:

$$E = \frac{(Pa(3a^2 - 3La + a^2))}{6I \cdot w(a)} \quad (6.8)$$

Because  $w(a)$  can be measured from the obtained force-displacement diagram (this again is the conventional deflection  $s_c$ ),  $w(a)$  is known from the test and can be filled in. Furthermore, the moment of Inertia  $I$  is already known from the determination of the flexural strength, the distance  $a$  is 47.5 mm and  $L=175$  mm (Figure 136). Now the Flexural Modulus can be determined making use of this rewritten formula of the deflection.

*Flexural Strain:*

Since the flexural strength and flexural modulus are already determined, the flexural strain can now be simply calculated by making use of Hooke's law:

$$\varepsilon = \frac{\sigma}{E} \quad (6.9)$$

Now the flexural properties can be determined from the force-displacement curves, leading to the following table of results:

## 6. Material Tests – Block/Geometry level

Specimen Name	length [mm]	width [mm]	height [mm]	CS Area [mm <sup>2</sup> ]	Conventional deflection (Sc) = 1.5 x height [mm]	Load at Sc* [N]	Flexural Strength [MPa]	Flexural Modulus [MPa]	Flexural Strain [%]
A1	240	50	16.4	820	24.6	1210	12.8	337.1	3.80
A2	240	50	17.0	850	25.5	1480	14.6	357.2	4.09
A3	240	50	16.4	820	24.6	1330	14.1	370.6	3.80
B1	240	43	17.5	752.5	26.25	1350	14.6	337.4	4.33
B2	240	43	19.0	807.5	28.5	1380	12.8	251.1	5.10
B3	240	42	19.6	823.2	29.4	1670	14.7	271.5	5.43

Table 61 Results table flexural test - solid blocks

\*Accuracy = 10 N

Material Properties	Symbol	Unit	Average	Standard Deviation	Characteristic
Flexural strength //	$f_{f,0}$	MPa	13.8	0.93	12.1
Flexural strength $\perp$	$f_{f,90}$	MPa	14.0	1.07	12.0
Flexural Modulus //	$E_{f,0}$	MPa	355.0	16.86	323.1
Flexural Modulus $\perp$	$E_{f,90}$	MPa	286.7	45.10	201.4
Flexural strain //	$\epsilon_{f,0}$	%	3.9	0.17	3.6
Flexural strain $\perp$	$\epsilon_{f,90}$	%	5.0	201.4	3.9

Table 62 Flexural properties parallel and perpendicular to the grain, as obtained from the test

## Block type C



Fig. 139 Testing of block C1, failure probably occurs due to local bending of the top flange or local buckling of the web, around the area where the line load is applied

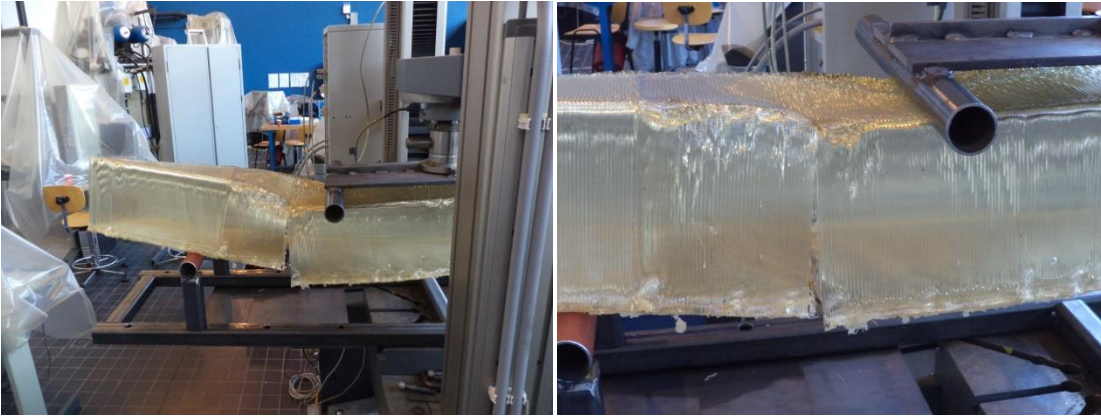


Fig. 140 Testing of Block C2, as can be observed the block ruptures at the connection between two printed lines.

#### Block type D



Fig. 141 Testing procedure of block type D



Fig. 142 Testing of blocks E1 and E2, the beam bends as whole but shows local buckling of the webs



Fig. 143 Testing of blocks E3 and E4, only a small load can be applied due to local bending of the top-flange

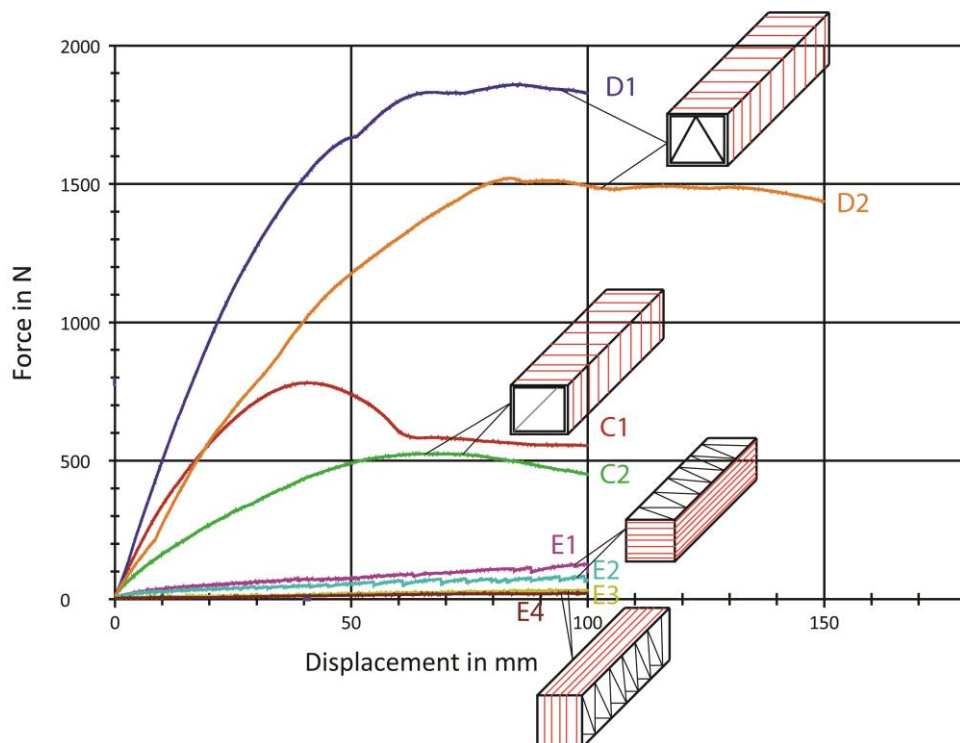


Fig. 144 Force-displacement curves of the tested geometries C to E

The flexural properties for the tested geometries/beams C, D and E are determined in about the same manner from the obtained force-displacement curves, as is done for the solid blocks A and B. An important difference is that the determination of the moment of inertia is more complex now. For block D it was necessary to first determine the static moment  $S_z$  and coordinate of the center of forces  $z_c$ , because this cross section is not symmetrical. Furthermore, for the blocks of type C and D it holds that the bending strength is determined for the maximum load, as these curves show a clear maximum this time. For the blocks of type E, the bending strength is just determined for the force at the maximum set displacement.

In table 63 the cross sectional area, static moment, moment of inertia and basic dimensions are given. Table 64 gives the calculated flexural properties.

Specimen Name	length [mm]	width [mm]	height [mm]	Wall thickness [mm]	CS Area [mm <sup>2</sup> ]	Sz [mm <sup>2</sup> ]	Zc=Sz/A [mm]	Izz [mm <sup>4</sup> ]
C1	2020	200	200	4.8	3747.84	/	100 mm	21054110.11
C2	2020	200	200	4.7	3671.64	/	100 mm	20642215.69
D1	2030	200	200	4.3	4286.20	414112.87	96.615	26502712.81
D2	2030	200	200	4.5	4479.95	418310.04	93.374	27755767.32
E1	1800	180	180	5.0	2700	/	/	8662741.70
E2	1800	180	180	4.5	2430	/	/	8482267.91
E3	1800	180	180	4.5	2430	/	100	12477801.53
E4	1800	180	180	4.3	2322	/	100	11950108.14

Table 63 Size and dimensional properties of the tested geometries

Specimen Name	Max deflection [mm]	Max Load [N]	'Flexural Strength' [MPa]	'Flexural Modulus' [MPa]	'Flexural Strain' [%]
C1	40.7	782	0.74	97.3	0.76
C2	64.8	526	0.51	41.9	1.22
D1	84.8	1860	1.40	88.3	1.59
D2	83.7	1520	1.10	69.8	1.57
E1	99.7	127	0.26	15.7	1.68
E2	99.3	83.5	0.18	10.6	1.68
E3	96.5	32.5	0.05	2.9	1.63
E4	94.6	22.1	0.03	2.1	1.60

Table 64 Flexural properties of the tested geometries, as obtained from the test

## 6. Material Tests – Block/Geometry level

### 6.2.5 Conformity with results elementary tests

#### Block A and B

When looking at the obtained flexural properties of the solid blocks A and B, it is obvious that the obtained flexural strength and flexural modulus are significantly higher than the tensile strength and Young's Modulus that are obtained from the tensile tests in chapter 5.

Material Properties	Symbol	Unit	Average	Standard Deviation	Characteristic
Flexural strength //	$f_{f,0}$	MPa	13.8	0.93	12.1
Flexural strength $\perp$	$f_{f,90}$	MPa	14.0	1.07	12.0
Flexural Modulus //	$E_{f,0}$	MPa	355.0	16.86	323.1
Flexural Modulus $\perp$	$E_{f,90}$	MPa	286.7	45.10	201.4
Flexural strain //	$\epsilon_{f,0}$	%	3.9	0.17	3.6
Flexural strain $\perp$	$\epsilon_{f,90}$	%	5.0	201.4	3.9
Tensile strength //	$f_{t;0,xz}$	MPa	8.33	1.07	6.45
Tensile strength $\perp$	$f_{t;90,xz}$	MPa	5.16	1.62	2.28
E-modulus // (tensile test)	$E_{0,xz}$	MPa	160.2	14.14	131.8
E-modulus $\perp$ (tensile test)	$E_{90,xz}$	MPa	129.6	12.59	104.3
Elongation at tensile strength //	$\epsilon_{t;0,xz}$	%	17.8	n.a.	n.a.
Elongation at tensile strength $\perp$	$\epsilon_{t;90,xz}$	%	12.6	n.a.	n.a.

Table 65 Flexural properties solid blocks compared to tensile properties from chapter 5

This is a positive given, because it means that when the material is applied within a block geometry, the performance of the material is better than what could have been expected based on the elementary material properties.

An explanation for the fact that the strength of the material improves when applied within a block geometry, again can be found in the use of multiple printed layers in both the directions. By printing geometries with multiple printing layers in both directions namely, more internal connections are made between the material particles, leading to a higher strength.

Another explanation that the flexural properties for blocks A and B are higher than the elementary material properties is that according to a strength theory based on the Weibull-probability-distribution, the presence of a stress gradient in a cross section of a bending test compared to the uniform loaded cross section in a tensile test, in general leads to a higher tensile strength performance of the material within a bending test [Whitney, 1979].

#### Block type C

The flexural properties for beam C1 and C2 as determined in paragraph 6.2.4 are again given in the table below.

Specimen Name	Max deflection [mm]	Max Load [N]	Flexural Strength [MPa]	Flexural Modulus [MPa]	Flexural Strain [%]
C1	40.7	782	0.74	97.3	0.76
C2	64.8	526	0.51	41.9	1.22

Table 66 Flexural properties - block type C

It is obvious that the reached maximum stresses in the outer fibers of the cross section are significantly lower than the tensile and compressive strength of the printing material. This either means that the beam geometries

fail due to a local inaccuracy or that another strength mechanism is normative for the obtained maximum load value.

The first possible cause already is quite plausible, because since the beam walls of beam C have a thickness of only one printed layer and because these walls are loaded in tension perpendicular to the direction of the printed lines, one weak connection between two printed lines is enough for a failure of the whole beam. The bigger the geometry, the larger the chance is of the presence of an inaccurate printed line. Therefore it seems legitimate that a long beam with a thickness of only one layer, fails even at a lower strength than a small tested sample.

When having a look at the pictures that are made of block C2 during the test (Figure 140), it indeed seems that this block fails due to the initial presence of a local inaccuracy, as a clear cross section that ruptures is visible. On the picture that is made of block C2 before performing the test (Figure 145), some printed lines are visible that do not completely connect straight to the surrounding lines. Therefore the mutual connection between these lines probably is less, leading to a weaker spot in the beam geometry. As corners form the connection points between individual beam members, it is plausible that especially inaccuracies around corner points, may cause a normative failure mechanism. Figure 146 shows that quickly after applying the load, further rupture took place of the weak spot indicated in red. The spots indicated by blue circles also seemed weaker but did not lead to a local failure.



**Fig. 145** Local inaccuracies that were observable on the C-geometries, prior to the test. The red-circled spot on geometry C2 is the location where rupture would take place during the test.



**Fig. 146** Local inaccuracies in block C2, observable right after application of the load. As can be seen, the rupture process around the red-circled weak spot already starts right after the application of the load.

Although Figure 145 shows that some weak spots are present in block C1 as well, these inaccuracies did not cause the failure of the beam. This means for block C1 another failure mechanism was normative, above the failure due to rupture around a weak spot as was the case for beam C2.



## 6. Material Tests – Block/Geometry level

When taking a closer look at the exact tensile strengths perpendicular to the grain (table 67) the minimum obtained value during the tensile test in chapter 5 was 2.62 MPa, which is about three to four times larger than the maximum obtained strength in the beam. Because the bending strength of the printing material turned out to be higher than the tensile strength, it is most likely that the low obtained value for the maximum applied load is caused by another strength mechanism than overall bending of the beam.

Material Properties xz-direction	Symbol	Average	Standard Deviation	Characteristic
Tensile strength $\perp$ [MPa]	$f_{t;90,xz}$	5.16	1.62	2.28
E-modulus 90°-direction [MPa]	$E_{90,xz}$	129.6	12.59	104.3

**Table 67 Tensile strengths perpendicular to the grain as obtained in chapter 5**

As can be observed on the test photos in paragraph 6.2.4 already, beam C2 failed at a connection between two printed layers in the print z-direction, which can be caused by bending, shear or a combination of those two. Beam C1 seems to fail due to local bending and/or buckling of individual walls around the area where the load is applied. The bending mechanism of the overall beam is already looked at. Below a closer look will be taken on the other described mechanisms.

### *Shear load:*

As block C2 fails between two printed layers in the z-direction, shear might be a plausible cause of this failure. For calculating the shear stress in the cross section, first the maximum shear force along the beam length should be determined. The maximum shear force in the beam is found at two sides between the support and the point load and has the same value as the point load. This means that the maximum shear load is half times the total load that is applied by the testing machine:

$$V = \frac{1}{2} \cdot F \quad (6.10)$$

By filling in the maximum shear force obtained from the test in the formula below, the shear stress can be determined for every point in the cross section:

$$\sigma_{shear} = \frac{V \cdot S_z}{b \cdot I} \quad (6.11)$$

In this formula  $S_z$  and  $b$  are the static moment respectively the width of the shearing part. These properties vary for the different points within the cross-section.  $I$  is the moment of Inertia, which is constant and already determined during the determination of the flexural strength.

Calculating the shear stress in the maximum and minimum points of the cross section now leads to the following shear stress distribution:

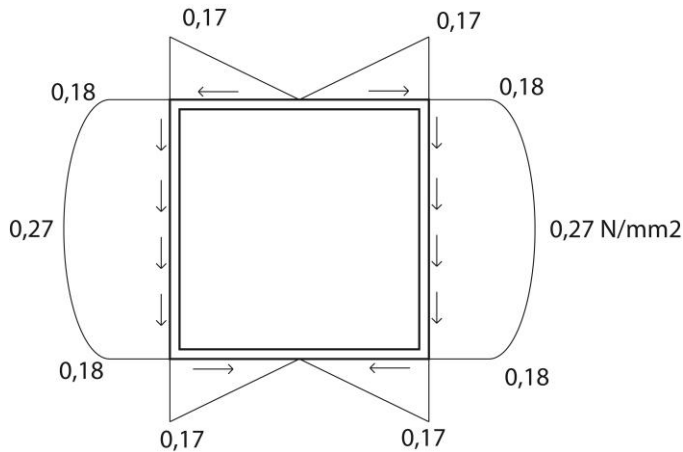


Fig. 147 Shear stress distribution in cross section of beam C

As can be observed, the maximum value of the shear stress, caused by the maximum obtained test load is 0.27 MPa. This is quite far below the shear strength that was obtained from the shear test in chapter 5, for which the results are given in the table below.

Material Properties xz-direction	Symbol	Average	Standard Deviation	Characteristic
Shear strength $\perp$ [MPa]	$f_{s,90,xz}$	5.8	1.19	3.7

Table 68 Shear strength perpendicular to the grain

This difference shows that the beam probably is not failed on shear alone. It can however be the case that a combination of shear and bending has caused the failure of the beam. This can be checked making use of the criterion of Von Mises:

$$\frac{1}{\sqrt{2}} \sqrt{[(\sigma_{xx} - \sigma_{yy})^2 + (\sigma_{xx} - \sigma_{zz})^2 + (\sigma_{zz} - \sigma_{xx})^2 + 6\sigma_{xy}^2 + 6\sigma_{yz}^2 + 6\sigma_{zx}^2]} > \sigma_v \quad (6.12)$$

Filling in this formula gives:

$$\frac{1}{\sqrt{2}} = \sqrt{(0.74 - 0)^2 + (0 - 0.74)^2 + 6 \cdot 0.1769^2} = 1.13 \text{ MPa}$$

This 1.13 MPa is still lower than both the tensile strength as the shear strength as obtained in chapter 5. However, for this 1.13 MPa it already becomes more likely that some inaccuracy has led to the failure of the beam.

The pictures in Figure 148 show the local bending mechanism of a horizontal beam flange and the buckling mechanism of a vertical beam web at the place where the point loads of the testing device are applied. These mechanisms also could cause the failure of the beam. Especially in case of beam C1, were no rupture was observed between two printed lines, it is plausible that the load capacity of individual beam members determine the overall beam strength.

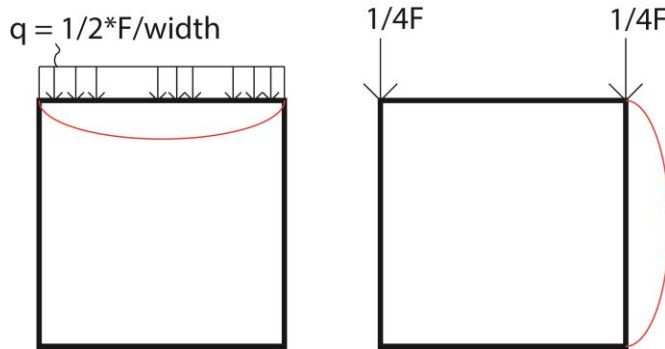


Fig. 148 left: local bending mechanism of horizontal top flange. Right: buckling mechanism of vertical beam web

The two point loads of the 4 point bending test are applied over the whole width of the beam, as the point loads have the form of two steel circular bars that cover the whole beam width. This means that in the width direction of the beam, the point load acts like a uniform distributed load on the top beam flange. The magnitude of this distributed load is equal to the point load divided by the beam width. Since one point load is half of the total applied load,  $q$  is calculated by dividing half of the measured maximum load by the beam width:

$$q = \frac{\frac{1}{2} \cdot F}{width} \quad (6.13)$$

This leads to a maximum moment in the beam flange of:

$$M_{max} = \frac{1}{8} \cdot q \cdot l^2 = 9775 \text{ Nmm} \quad (6.14)$$

By using the formula for the bending strength again, the local maximum stress in the beam top flange around the point of the applied load can be determined:

$$\sigma = \frac{M_{max} \cdot z}{I} \quad (6.15)$$

In the formula above, for the cross sectional width in the calculation of the moment of inertia  $I$ , a width of 300 mm in the longitudinal direction is taken which is half of the distance between the two point loads. This value is an estimate of the distance in the longitudinal direction over which the locally applied point load might have a local influence on the material.

Filling in the formula leads to a maximum stress in the flange of 8.48 MPa:

$$\sigma = \frac{9775 \cdot \frac{1}{2} \cdot 4.8}{\frac{1}{12} \cdot 300 \cdot 4.8^3} = 8.48 \text{ MPa}$$

Since this is more than the tensile strength of the material, it is quite likely that this local flange bending is the normative failure mechanism of the beam.

The local applied compressive force on the vertical web of the beam can be calculated by:

$$\sigma = \frac{N}{A} = \frac{\frac{1}{4} \cdot F}{A} = \frac{195.5}{4.8 \cdot 40} = 1.02 \text{ MPa} \quad (6.16)$$

In this formula, 40 mm is taken for the width as this is the width of the steel tube that applies the load on the beam.

The obtained value of 1.02 MPa is lower than the values obtained for the compressive strength in paragraph 5.3. However, since the length of the wall is bigger, it might be the case that this wall failed on buckling and therefore still forms a leading failure mechanism for this beam.

### Block type D

Specimen Name	Max deflection [mm]	Max Load [N]	Flexural Strength [MPa]	Flexural Modulus [MPa]	Flexural Strain [%]
D1	84.8	1860	1.40	88.3	1.59
D2	83.7	1520	1.10	69.8	1.57

Table 69 Flexural strength properties block type D

Performing a bending test on beams of type D, which are equal to the hollow beams of type C but then with a simple triangular structure inside, led to a flexural strength of about twice the strength of beam C. Although the inner structure leads to a far better transition of the forces from the point load towards the support, still the strength values are lower than the elementary strength values as obtained in chapter 5. Therefore, it probably is the case again that the beam fails locally around the applied point load due to bending of the top flange or buckling of the web. Due to the internal structure, the load is now divided over four webs instead of two, which leads to about a twice lower compressive force per web. This can be a plausible cause of the result that the maximum applied load was increased with a factor of about two.

For the bending load on the horizontal flange, about the same situation can be observed. Since the top flange spans only half of the beam width now, instead of the whole beam width as was the case for beam 2, the maximum bending stress in the flange will approximately be halved as well as the maximum bending moment will be halved too.

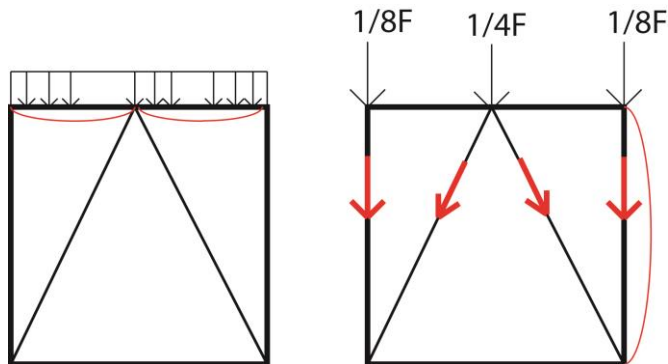


Fig. 149 left: the span of the top flange is halved compared to beam C. right: the compressive axial force within the webs is approximately halved as well

This again shows that it is plausible that the beam fails on local flange bending or local web buckling around the applied load. This was observed during the test, as the beam especially started to deflect around the load and also is confirmed by the doubling of the applied load, which is best explained by the halved load on individual beam walls.

## 6. Material Tests – Block/Geometry level

## Block type E

Specimen Name	Max deflection [mm]	Max Load [N]	Flexural Strength [MPa]	Flexural Modulus [MPa]	Flexural Strain [%]
E1	99.7	127	0.26	15.7	1.68
E2	99.3	83.5	0.18	10.6	1.68
E3	96.5	32.5	0.05	2.9	1.63
E4	94.6	22.1	0.03	2.1	1.60

Table 70 Flexural properties - blocks of type E

As can be seen in the table above, the obtained maximum load values for the E-type blocks are quite poor, especially for block E3 and E4.

Since the maximum load values, and the subsequent flexural strength values, are this low, it is quite likely that bending is not the governing failure mechanism for these blocks. This is confirmed by the photo's made during the test procedure (paragraph 6.2.4), on which can be observed clearly that the individual walls of the tested geometry buckle out or deflect by bending. Therefore, further on, a closer look is taken at these deflection mechanisms of individual walls.

Beam E1 and E2 are loaded in such a way that the applied compressive load is transmitted by three walls, as can be observed on the picture below where the red dots represent the places where the line load from the test device is transmitted to the three walls.

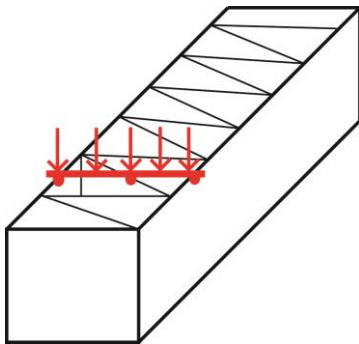


Fig. 150 The applied line load is transmitted by three walls/webs

Because one line load (is  $\frac{1}{2} \cdot F_{max}$ ) is divided over three walls, the load per wall is  $\frac{1}{6}$  of the measured maximum applied load.

The subsequent compressive strength per wall is equal to:

$$\sigma = \frac{N}{A} = \frac{\frac{1}{6} \cdot F}{A} = \frac{\frac{1}{6} \cdot 127}{180 \cdot 5} = 0.023 \text{ Mpa} \quad (6.17)$$

Although this obtained stress value is quite low, it can still be the cause of the failure. The length/width ratio of the wall actually is  $180/4.5 = 40$ , which might cause a buckling effect within the thin wall.

On the test photo's it can also be observed that beams E1 and E2 bend as a whole. This means that also for these beams, it holds that they are exposed to bending stresses leading to tension in the bottom fiber and compression in the top one. This compression in the top fiber can cause a buckling effect in the side wall as shown on Figure 151.

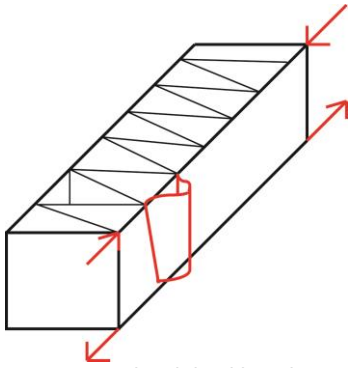


**Fig. 151** Local web buckling due to the compressive force that is caused by the overall bending of the beam

The compressive force working in the top fiber, has a magnitude of:

$$F = \frac{M_{max} \cdot z}{I} \cdot A = 0.26 \cdot 180 \cdot 4.5 = 211 \text{ N} \quad (6.18)$$

This compressive force forms a higher buckling force than the buckling force in the previous load case. As the length/width ratio again is 40, it is quite likely that this buckling effect, together with the previous one described, causes the failure of this beam at low stress levels.

When having a close look at the pictures made during the test performance, both the described buckling effects can indeed be observed.

For the block orientation of block E3 and E4, the obtained maximum load was the lowest of all beam types. When looking at the photos that were made during this test, it is clearly noticeable that the beam hardly buckles as a whole, but directly fails on the bending of the individual flange members below the applied line load. This process is shown on the following picture:

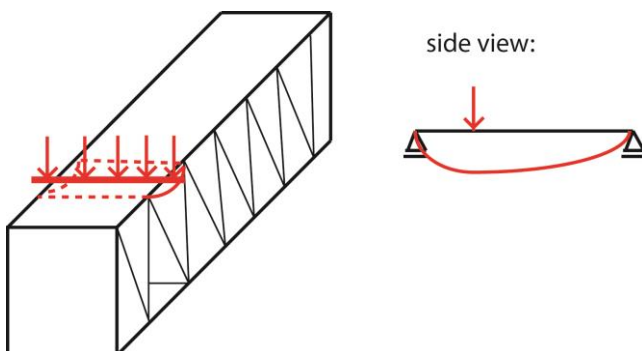


**Fig. 152** The applied line load causes local bending of the top flange of the beam

The load is applied at a distance of about 36 mm from a point where the inner structure supports the flange. The overall span of the flange is 360 mm. This leads to a maximum bending moment in the flange of 527 Nmm, which leads to a compressive stress in the top fibre of the flange of 0.702 MPa and a compressive force of 631.8 N. As this is about three times larger than the local forces in the members of blocks E1 and E2, it can be explained why the maximum overall beam load within the load orientation of E3 and E4 is about three times lower than for E1 and E2.

### 6.2.6 Test Evaluation and Conclusions

For the performed flexural tests, it unfortunately was not feasible to test fully closed blocks with the same dimensions as the 'open' blocks/geometries, as fully closed blocks of these dimensions would have led to an undesirable long printing duration and high printing costs. For this reason, the comparison between the flexural properties of the small closed blocks A and B and the large open geometries C, D and E, probably is not as accurate as would have been the case when the same size would have been used. First of all a bigger solid block would have led to a more homogeneous geometry, as the amount of printed lines in all directions would have been larger and the effect of one individual line would be less. Furthermore the test setup for blocks A and B was of course performed with other tools than was the case for the blocks C to E, which also might have an influence on the outcome.

Where the closed geometries A and B actually failed on bending, such that the flexural strength properties could be obtained from these tests, the open geometries C to E all failed on other failure mechanisms than the reach of the flexural strength. This is partly caused by the chosen dimensions of the tested open geometries. The ratio between the cross-sectional height of the geometries and the distance between the applied point load and the support turned out to be unsuitable for a failure of the geometry solely by bending. Instead, a geometry with these proportions is more likely to fail on shear or a combination of bending and shear. The reason that there still was chosen for these dimensions is that a cross sectional height of 200 mm is in accordance with the width dimension of the blocks that are so far printed by DUS Architects. So testing blocks with these dimensions would lead to a better insight in the failure mechanisms that can be expected for the design of DUS Architects.

From the results of the tested closed geometries A and B, it turned out that the flexural strength is higher than the tensile strength that was obtained in chapter five. This result leads to the conclusion that when the material is applied within a block geometry, the performance of the material is better than what could have been expected based on the elementary material properties. This is partly because in general, the flexural strength often is higher than the tensile strength. Furthermore this can be explained by the earlier mentioned theory that printing multiple layers in both directions leads to more internal connections and therefore a higher strength.

From the flexural test of blocks A and B the conclusion can be drawn that it is recommended to load geometries in bending in the direction of the printed lines, as block B2 showed that bending perpendicular to the grain direction, can lead to sudden brittle failure between the printed layers.

The tested Block C2 seemed to fail between two printed layers as well. Because of the low maximum stress value that was obtained it is more likely that this block failed on shear instead of bending. However, the obtained stress value still turned out to be lower than the shear strength that was found in Chapter 5. This probably is caused by failure in a point where the connection between two printed layers was weaker than on an average. This leads to the conclusion that the chance of presence of local inaccuracies becomes bigger for larger geometries and therefore the factored strength should become lower than the obtained strength values from chapter 5, when applying this material in practice. Especially when the material is applied in geometries with wall thicknesses of a single printed layer. The influence of local inaccuracies can be limited by creating multicarrier roads within an element. In this way, a local inaccuracy at the location of a connection between two members, will not be crucial.

The other open geometries C2, D1, D2, E1, E2, E3 and E4 all failed due to local mechanisms. Block C2 probably failed due to local bending of the horizontal flange on which the line load is applied. For the blocks D hold the same, but since the span of the flange is halved here, the applied maximum load is approximately doubled. This, while the applied amount of material is less than twice as much as the material use for blocks C. This means the applied inner structure of blocks D relatively is a more efficient solution than an entirely open tube. The blocks E, that come the closest to the geometries printed so far by DUS Architects, failed by local bending of the horizontal flange (block orientation E3 and E4) or by local buckling of the vertical web (block orientation E1 and E2) at very low stress values. Although the printing quality of these blocks was the highest (no local inaccuracies were visible), the orientation in which these blocks needed to be printed, led to a very poor strength performance. Because both the top and the bottom surface are open, the mutual support of the different walls is limited to the places where the inner triangular structure is connected with the outer walls. The geometries C and D on the other hand, have their open sides at the small surfaces of the rectangular. This leads to a tube-form where the four equal outer walls support each other over their full length, leading to a stiffer behavior.

The strength performance of the closed geometries A and B turned out to be much higher than the strength of the open geometries. Furthermore the open geometries all failed on local effects, which in some cases led to poor overall strength performances.

For these reasons, again the conclusion is confirmed that geometries should be build up by walls consisting of multiple layers. By this, the individual walls will act stiffer, the local and overall strength of geometries will become higher and the material will be more homogeneous and less dependent on local inaccuracies.

From the block bending tests also another important lesson is learned: When there is chosen for a geometry which is not completely closed, this automatically means for a rectangular geometry that it has to stay open on at least two of its six sides, as the printer is not able to print spans. One should make smart decisions here such that the amount of mutual connections between the printed walls is as large as possible. This namely increases the stiffness of the local members, which turned out to be the crucial property of the tested geometries.



## 7. Overview of Test Results, Grading and Qualification

### 7.1 Overview of Test Results

In chapter 3 an analysis and selection was made of the elementary material properties that were most important to obtain for being able to deliver a proper structural analysis and design for this phase of the 3D Print Canal House. After performing the nine elementary material tests that are described throughout chapter 5 and the block-tests of chapter 6, all of the required properties are indeed obtained. This leads to the numerical results tables that can be found under Appendix I.

The danger of using such a numerical table for structural design is that one completely relies on the values that are in. This, while a number cannot express additional information concerning the research method, which sometimes is essential to take notice of when applying the values or evaluating them. It therefore is recommended to at least have a quick look at the overall discussion and conclusions in chapter 9 respectively chapter 10 before applying the values for structural design. Or even better, have a quick read through the paragraph in which the particular test is described.

Below a summarizing description is given of the most important results per test. Most of the conclusions and (design) recommendations in the following chapters, are based on these results.

#### Tensile and Shear Test

1. The tensile strength on an average is twice as high parallel to the 'grain' than perpendicular to the grain.
2. Parallel to the grain, in most cases a large elongation is noticed before the material breaks. If the material however is loaded under a large angle or perpendicular to the grain, the material fails in a brittle manner at the adhesion between two printed layers.
3. Brittle failures for material that is loaded within the grain direction cannot be excluded, due to the fact that the material is very sensitive to local inaccuracies that can be present in the material.
4. Material that is printed within the xy-plane shows more isotropic behavior than material that is printed in the xz-plane, due to more and better adhesive connections between the different layers in the xy-plane than in the xz-plane.
5. The shear strength within the grain direction of the xz-plane on an average is about 14% higher than the shear strength perpendicular and 45 degrees to the grain.

#### Compressive Test – Solid Blocks

6. The compressive strength, on an average is about 2.0-2.5 times larger than the tensile strength.
7. There is not much difference in compressive strength between the three different orientations. The compressive strength in the grain-direction is only a little higher than in the other two directions.

#### Determination Young's Moduli

8. The Young's modulus is the biggest for samples that are printed within the xz-plane and loaded within the direction of the printed lines.
9. The deviations between the different E-values of identical tested specimens, are in the order of 13-20%, which is large. This probably means that the material is non-homogeneous and therefore shows inconsistent behavior. However, the large differences can also be caused by a combination of insufficient test results and a low amount of tested samples.

#### Absorption and Drying Test

10. The amount of water that is absorbed by the material is, with a mass-percentage of 0.081%, negligible.

#### Temperature – Strength Test

11. At a surface temperature of 40 degrees Celsius, the material has lost about 70% of the material strength it has at room temperature. At a surface temperature of about 70 degrees Celsius, the material has lost almost all its strength. This, while surfaces exposed to the sun in The Netherlands, can be heated up to temperatures of about 80 degrees.

#### DSC Test

12. As the softening temperature lies around 60 degrees, this temperature can be seen as the maximum temperature at which the material just has some mechanical strength left.
13. The melting temperature lies around 85 degrees, which means no melting of the material is expected under regular weather conditions. However, in case of a fire, the material will melt and even vaporize quickly.
14. The specific heat capacity of the printing material is relatively low, which means that the material insulates air heat well.

**Creep Test**

15. Failure due to creep already occurs after a short period of time, in case of a small exceeding of the characteristic strength.
16. Based on a material sample that is loaded to about 50% of the average tensile strength (and about 80% of the characteristic tensile strength) during one week, it can be concluded that the maximum deformation due to tensile creep is acceptable.

**Flexural Tests**

17. When the printing material is applied within a solid block geometry, the performance of the material is better than what could have been expected based on the elementary material properties. This means that the flexural strength of a block loaded in bending is higher than the material's tensile strength.
18. Also in case of printing multiple layers in both the vertical as the horizontal printing direction, the material can still fail in a brittle manner between two printed lines when loaded in tension.
19. The larger the printed geometry is, the bigger becomes the chance of presence of local inaccuracies that lead to normative failure modes. This means that for larger geometries, the chance increases that the maximum bearable stress is lower than the strength values that are determined within the elementary material tests of this research.
20. Geometries consisting of members with a thickness of a single printed layer are very sensitive for local failure mechanisms. Local failure mechanisms are buckling and bending of individual members or failure at the location of a local inaccuracy.

**Compressive/buckling test hollow sections**

21. The obtained compressive strength performance of thin-walled hollow cubes consisting of one printed layer is significantly (about 8-9 times) lower than the compressive strength of solid cubes. This is caused by the fact that thin-walled geometries behave less homogeneous and isotropic, because individual walls of the thin-walled structures can buckle and because thin-walled geometries are more sensitive to local inaccuracies.
22. Although geometries sometimes seem to completely form back to their original shape after removing the load, one can assume that the capacity of the geometry has been decreased, once this geometry is tested to its full plastic capacity.
23. Buckling of individual members/walls often is a normative failure mechanism for axial loaded geometries.

**7.2 Strength Grading and Safety Factors**

Throughout chapter 5 and 6, characteristic strength values are determined that take into account the relative low amount of tested samples. Still, application of the characteristic strength values cannot guarantee a safe structural design, as the chance of failure when loading a structure towards the characteristic strength limit still is 1% [Kamerling, 2004], which is a too high chance of failure for a building. Furthermore, inaccuracies in material samples printed in the xz-direction, were prevented as much as possible by cutting the test samples from parts of the plate that were free of inaccuracies. This, while the tested blocks in chapter 6 showed, the presence of inaccuracies in large geometries cannot be excluded for the current quality of the printing process. For these reasons, it is recommended to reduce the characteristic strength of the printing material, by a factor of safety.

The tested geometry C2 (paragraph 6.1) probably failed on shear at a percentage of 22% of the characteristic shear strength perpendicular to the grain. Based on this example, it can be concluded that the performance of a geometry with a clear observable inaccuracy around a connective point is about 20% of the characteristic strength in case of thin-walled geometries. As this would lead to a significant degradation of the material strength and therefore to a significant limitation of the load and application possibilities, it again is strictly recommended to apply multiple layers as this reduces the chance of presence of inaccuracies. Furthermore, it is advised to perform a visual strength grading of printed geometries before they actually are applied within a structure. An advantage of the printed material is that inaccuracies can be clearly observed. Therefore the following conceptual grading system is recommended:

**A. Contribution local inaccuracies****1. For geometries with members consisting of one printed layer:**

- a. In case one observes one or a few printed lines that are not connected completely straight to the surrounding lines, it is recommended to apply an inaccuracy factor of 2. This is based on the performance of block C1 which failed on another mechanism (local member bending), while some poor connecting lines actually were present.
- b. In case one observes one or a few holes in a member that are not located close to a connection with another member, it is recommended to apply an inaccuracy factor of 3.
- c. In case one observes one or a few small holes in a member that actually is located close to a connection with another member, it is recommended to apply an inaccuracy factor of 5. This is based on the 20% strength performance of block C2 in paragraph 6.1, where it was the case that a small hole was present around a corner point between a horizontal and vertical member.

**2. For geometries with members consisting of 2-4 printed layers:**

- a. In case one observes one or a few printed lines that are not connected completely straight to the surrounding lines, it is recommended to apply an inaccuracy factor of 1.5. This is based on some of the tested shear samples in the xy-direction that became stronger when multiple layers were printed on each other by accident.
- b. In case one observes one or a few holes in a member that are not located close to a connection with another member, it is recommended to apply an inaccuracy factor of 2. This is significantly lower than for single printed lines, as the chance of rupture will firmly decrease in case of printing multiple layers.
- c. In case one observes one or a few small holes in a member that actually are located close to a connection with another member, it is recommended to apply an inaccuracy factor of 3. This again is lower than in case of one-layered geometries because the chance of rupture decreases.

**3. For geometries with members consisting of >4 layers:**

- a. When one observes a printed line that is not connected completely straight to the surrounding lines, it is recommended to apply an inaccuracy factor of 1.1. This is based on some of the tested shear samples in the xy-direction that became stronger when multiple layers were printed on each other by accident.
- b. When one observes a hole in a member that is not located close to a connection with another member, it is recommended to apply an inaccuracy factor of 1.2. This is significantly lower than for single printed lines, as the chance of rupture will firmly decrease in case of printing multiple layers.
- c. When one observes a small hole in a member that actually is located close to a connection with another member, it is recommended to apply an inaccuracy factor of 1.5. This again is lower than in case of one-layered geometries because the chance of rupture decreases.

**4. For all geometries:**

- a. In case large holes are observed, it is recommended to not use the element for structural purposes, at all. 'Large' applies here to the size of the holes reasonably related to the dimensions of the geometry and its members.

**B. Contribution temperature and long-term loading**

Besides the safety factor that should be applied for taking into account the local inaccuracies of the material, the tests in chapter 5 also proved that the circumstances under which stresses are applied on the material, also have a significant influence on the material strength. More specific, the temperature of the material and the duration of the load affect the actual strength performance of the material. Therefore, strength factors that take into account the temperature and load duration should be applied as well.

From the creep test that is described in paragraph 5.9.6, it was concluded that a strength reduction of 50% is recommended, in order to take into account the creep behavior. This means a creep factor of 2.0 should be applied on the strength. Because the majority of the stresses will be applied on a long-term (as most of the load on the printed house will be formed by own weight), this creep factor should be applied in any case.

For the thermal behavior it, first of all, holds that according to design recommendation 6 of paragraph 8.1.1, it is obligatory to add a cover material onto the printed polymer, in case the printed polymer is applied in a geometry that is facing the east, south or west. Omitting this measurement simply is unacceptable, since the printed polymer is not able to resist the thermal load that can be caused by direct sunlight.

In case this measurement is indeed taken, it depends on the type and thickness of the protecting materials, what further factors of safety should be applied to take into account the thermal behavior. The highest air temperature that has ever been measured in the Netherlands is 38.6 degrees [KNMI, 2014], say 40 degrees. According to the results of the strength-temperature test (paragraph 5.7), the strength reduction at this temperature already is 70%. This means a strength factor of 3.3 should be taken into account by all means. In case the sun protection layer is not able to prevent further heating of the printed material to temperatures higher than the air temperature, then this strength factor should become even higher. A building physical analysis is needed to judge whether or not the applied covering layer is able to protect the printing material against heating up by direct sunrays.

So, to summarize:

- Contribution long-term loading: 2.0 -> This creep factor should be applied in any case.
- Contribution thermal behavior:
  - 3.3 -> In case a covering layer is added to the printed material that prevents the printed layer from heating up due to direct sun rays, or in case a surface is facing the north.
  - 5.3 -> In case a covering layer is added that prevents the printing material from becoming warmer than 55 degrees.
  - $\infty$  -> In case a covering layer is not able to prevent the printing material from becoming warmer than 55 degrees.

### **C. Other contributions [Ullman, 2003]**

Apart from the contribution that takes into account the local inaccuracies, the temperature and the duration of the load, the overall material factor of safety should be further build up by the following other contributions:

- Contribution material familiarity: 1.2 -> The material is researched, although the number of performed tests is relatively low and tests are only performed within this sole research (no second opinion)
- Contribution of geometry: 1.1 -> The dimensions of printed geometries are not closely held.
- Contribution for failure analysis: 1.3 -> Failure analysis is not well developed as the amount of tested geometries is limited and no geometries of this material have been applied structurally in practice.
- Contribution for reliability: 1.2 -> average reliability demanded

As an example, if a single-layered geometry is applied that contains a hole around a corner-point (worst-case scenario) then the following factor of safety should be applied:

$$\gamma = 5.0 \cdot 2.0 \text{ (creep)} \cdot 3.3 \text{ (thermal behavior)} \cdot 1.2 \cdot 1.1 \cdot 1.3 \cdot 1.2 = 68.0 \quad (7.1)$$

In case a geometry is applied containing walls of five layers thick, without any holes or skew lines (best-case scenario), then the following factor of safety should be applied:

$$\gamma = 2.0 \text{ (creep)} \cdot 3.3 \text{ (thermal behavior)} \cdot 1.2 \cdot 1.1 \cdot 1.3 \cdot 1.2 = 13.6 \quad (7.2)$$

This means that a factor of safety ranging between 13.6 and 68.0 has to be applied for the printing material. The design value for the strength finally can be obtained by dividing the characteristic strength by the factor of safety that applies to the given geometry:

$$f_d = \frac{f_{kar}}{\gamma} \quad (7.3)$$

Note that the determination method for inaccuracy factors is purely based on the findings of this research project. For that reason, the chosen factors are conservative. By performing more research and by applying this material in practice, the given factors can be validated and made more accurate.

## 7. Overview of Results, Grading and Qualification

### 7.3 Comparison with other (building) materials

#### 7.3.1 Comparison with traditional structural materials

In the four figures below, the strength properties of the printing polymer that are determined during this research project, are compared with the strength properties of the more traditional structural materials steel, concrete and timber. This is done by means of the software package CES EduPack 2014, so the material properties of the materials of comparison, are defined according to the data from the databases of this software program. [Granta Design, 2014]

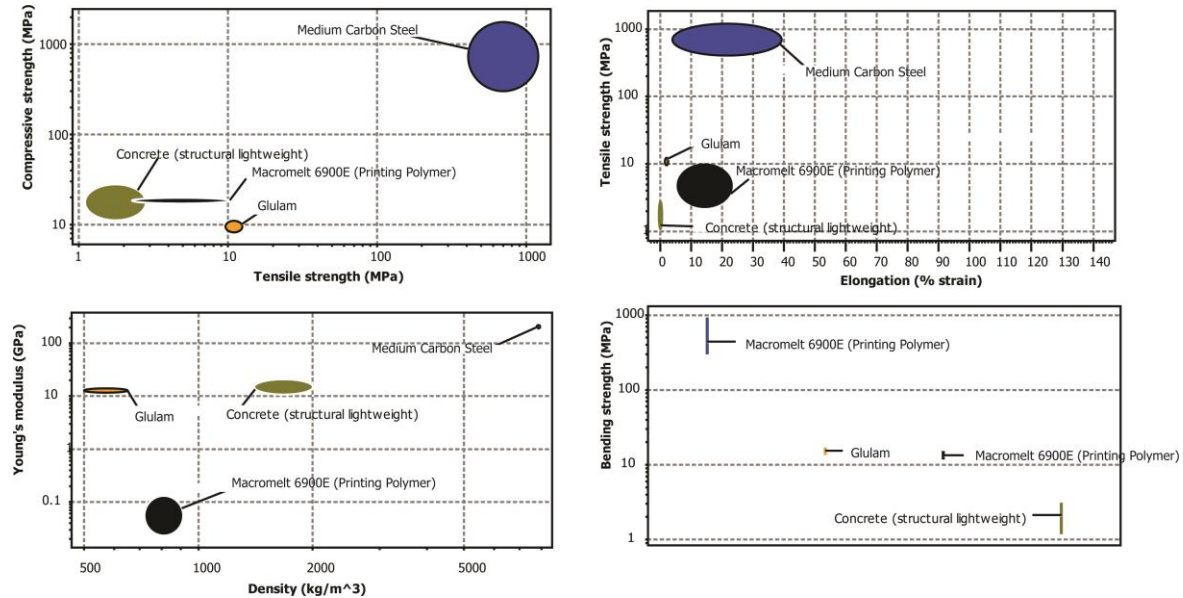


**Fig. 153 Comparison between the printing polymer and general applied structural materials. Above left: comparison of the tensile and compressive strengths, above right: comparison of tensile strengths and elongations, below left: comparison of Young's Moduli and densities, below right: Comparison of the bending strengths**

For the printing polymer Macromelt 6900 E, the characteristic strength is set as the lower boundary of the strength value and the maximum obtained test strength is chosen as the upper boundary.

In the graph at the above left corner of Figure 153, the compressive strength range of the different structural materials is set against the tensile strength. As can be observed, the compressive strength of the printing polymer is comparable to the compressive strength of concrete. For the tensile strength it holds that the performance of the printing material is about twice as good as the tensile strength of concrete. However, the tensile strength of the polymer is less than the strength of glulam.

The graph at the above right corner shows the tensile strength against the tensile strain. For the strain range of the printing polymer, the range of measured strains at the maximum stress level, is taken. Of course in the plasticity phase, the elongation often was much higher, but this is irrelevant for the structural application of the material. When looking at the graph it is interesting to see that the stretch ability of the printing polymer in the elastic phase, is not higher than the strain of steel. Of course these strain levels are for steel reached at much higher stress levels, but it is positive that that the strain level of the printing material is not unusual. Still, the strain levels of the materials of comparable strength, timber and concrete, are much lower which makes them more suitable for structural use.

The graph below left shows the young's modulus of the materials against the density. It is obvious that the young's modulus of the printing material is poor in comparison to the other building materials. This is mainly caused by the high strain-level of the printing material in comparison to the strain-range of timber and concrete.

The graph below right finally shows the bending strengths of the different materials. The flexural strength of the printing material is quite good as it can compete with the flexural strength of glulam and is much higher than the bending strength of concrete.

In Figure 154, the other material properties that are determined throughout the tests of this research are compared with the values of the common structural materials. These are the Melting point against the specific

heat capacity in the figure right and the water absorption against the density in the figure left.

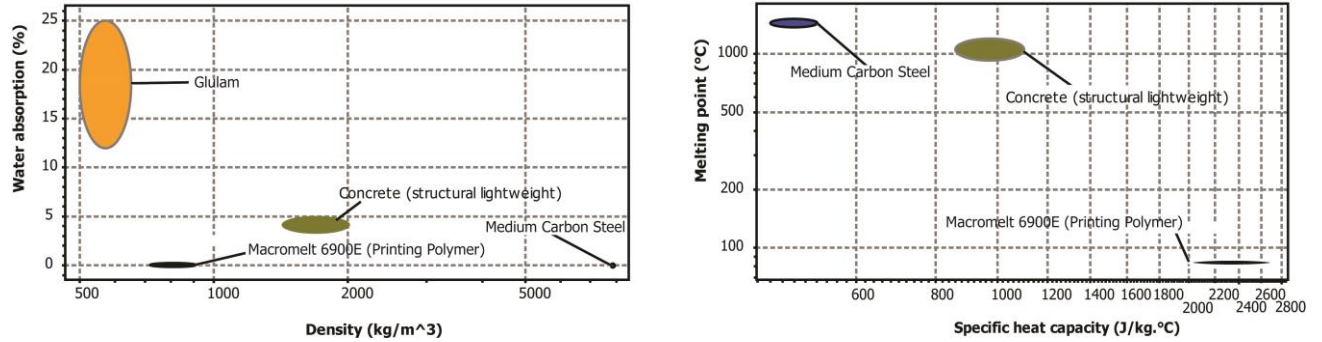


**Fig. 154** Left: comparison between printable polymer and general structural materials on the water absorption versus the density. Right: comparison on the melting point and specific heat capacity

The fact that the absorption of the printing material is negligible, is a positive characteristic of the material. Especially when it is compared to the high absorption percentages of concrete and wood. Of course concrete and timber, despite of their high absorption percentages, are capable of dealing with water, but still it seems to be a positive given that the printing material is watertight.

As can be seen on the horizontal axis of the right figure, the specific heat capacity of the printing material is relatively high compared to generally applied structural materials. As already concluded at the end of the DSC-test (paragraph 5.7) this is one hand a positive give, because the climate inside and outside can be separated well with this material. On the other hand this means, that once the inner side of a building is heated up, it will be difficult to cool it down again. Especially during the summer this might lead to undesirable warm rooms. The vertical axis of the picture right, demonstrates that the melting temperature of the printing material is very low compared to the melting points of concrete and steel. This again shows that the behavior of the printing materials at low temperatures forms the most important barrier for structural application of this material. It is obvious that improvement especially is required for the thermal behavior of the material, because the other properties, apart from the young’s modulus, are able to compete quite well with concrete and timber.

**7.3.2 Comparison with other polymers**

In Figure 155, the structural properties of the printing polymer (Macromelt 6900E) are compared to the properties of other polymers that are applied in the building industry. There is chosen for a comparison with PC, PVC and CFRP (carbon fiber reinforced plastic). PC and PVC because although they are not applied structurally, these actually are the most used materials in the building industry. To also compare the printing polymer to an actual structural polymer, CFRP is added to this comparison as well.

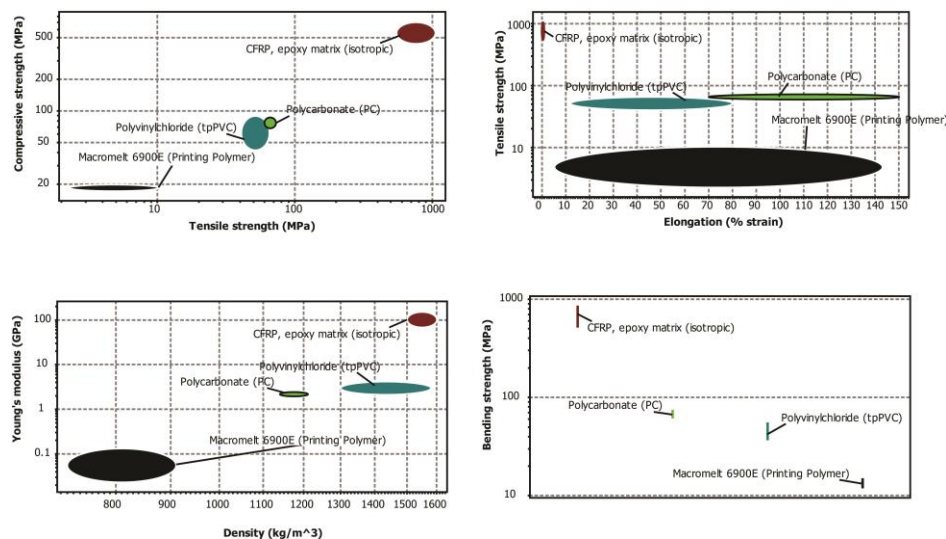


**Fig. 155** Comparison between the printing polymer and polymers that are commonly applied in the construction industry. Above left: comparison of the tensile and compressive strengths, above right: comparison of tensile strengths and elongations, below left: comparison of Young’s Moduli and densities, below right: Comparison of the bending strengths

## 7. Overview of Results, Grading and Qualification

The graph above left shows that the compressive and tensile strength of the printing polymer are significantly lower than the strengths of the compared polymers. This while PVC and PC are not even applied within structures. For the graph above right, which shows the tensile strength against the elongation, there is chosen this time to plot the full range of measured strains of the printing polymer. So also the ultimate strain levels that were obtained in the plasticity phase. This is done because the plotted strain ranges of PVC and PC also seemed to cover the plasticity area. The figure shows that the elongation range is comparable to PC. However, the strain range of CFRP shows that for a structurally applied polymer, very low strain-levels are demanded. The figures below left and right with respectively the Young's Modulus and the bending strength plotted, show again that the mechanical/strength performance of the printing polymer can by far not compete with the performances of generally applied polymers. This probably means that the advantages of the current usage of polymers in construction works are only utilized for plastics of these strength ranges. However, as the arrival of the 3D-printer brings in a new argument for applying polymers within construction works, it is not necessarily the case that a printable polymer needs to have the same strength performance as polymers that are currently applied in the construction industry.

In Figure 156 the absorption and thermal characteristics of the printing material are compared with these properties of PC, PVC and CFRP.

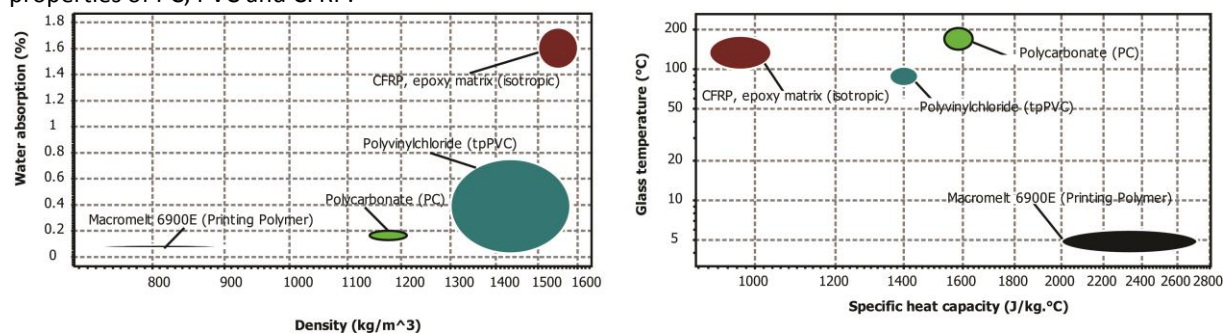


**Fig. 156 Comparison between printable polymer and polymers that are commonly applied in the construction industry. Left: comparison on the water absorption versus the density. Right: comparison on the melting point and specific heat capacity**

Although the absorption percentages of all polymers are relatively low, the negligible absorption of the printing material turns out to be quite an unique property for polymers applied in the construction industry. In the figure right this time the glass temperatures are compared instead of the melting temperatures, as the melting temperatures were not available for, or applicable to all of the other plastics (CFRP is not a thermoplastic). The low glass temperature of the printing polymer compared to the glass temperatures of the other polymers, demonstrates that the printing polymer is commonly applied in the rubber phase as the glass temperature of the printing material lies below room temperature. This while the other plastics clearly are applied in the solid phase, as their glass temperatures lie above the maximum temperature of sun-heated parts in The Netherlands (80 degrees). Applying a polymer in its rubber phase structurally is unfeasible, as the low Young's Modulus and poor temperature behavior already evidenced. The low glass temperature of the printing polymer compared to other plastics, confirms this once more.

When diving a little deeper into this topic, comparison of the molecular weights (or weight distributions) can deliver more insight in the printing material's characteristics and expected behavior. The green curve in the picture below shows the molecular weight distribution of the applied printing polymer Macromelt 6900E. This curve is determined by Henkel by means of a liquid chromatography technique.

Because the software package CES EduPack did not contain molecular weight or weight distribution data, other sources have been consulted to make a comparison possible. The number average molecular weight  $M_n$  of the printing polymer can compete with the molecular weight of Polycarbonate, however it is inferior to the  $M_n$  of PVC and CFRP. It is surprisingly to see that the weight average molecular weight is in the same range of the molecular weight of CFRP. Although the number average molecular weight is a fairer representation of the average weight of molecules in practice [Agilent technologies, 2014], it is remarkable that there actually are molecules within the printing material that have the same weight as molecules of structural polymers. An important difference here probably is that for the CFRP values, it holds that the found molecular mass range forms a fair representation of the actual average molecular weight. This, while for the printing polymer, the

molecules with high weights form outliers. This theory is supported by the number average weight of the printing polymer, which is relatively low in comparison to its weight average molecular weight.

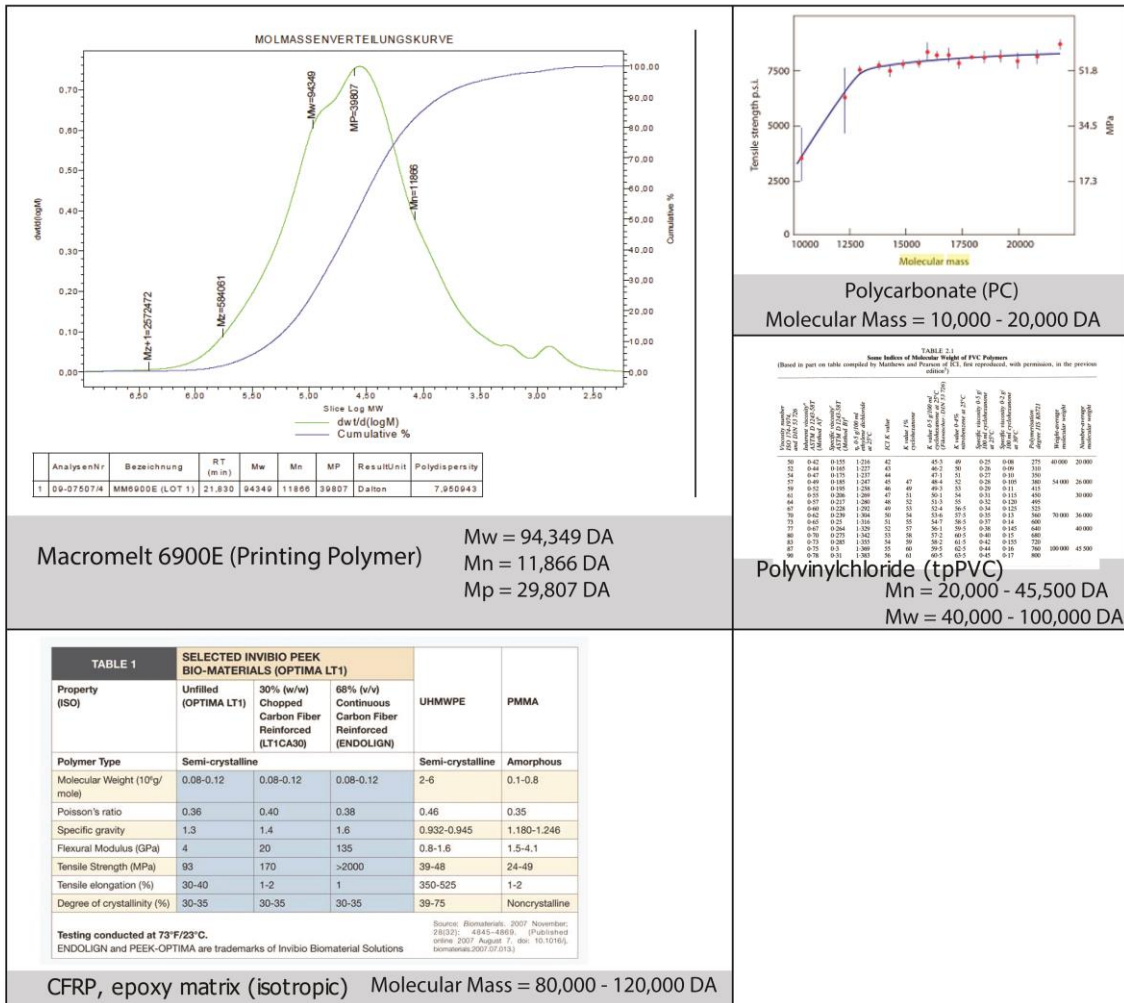


Fig. 157 Above left: Weight distribution curve of the printing polymer [Marchese, 2014], Above right: common molecular mass rates of PC set against the associated tensile strength [Gilmore, 2014], Below right: table showing average molecular weights and number molecular weights of common applied PVC's [Titow, 1984], Below left: table showing molecular masses of common applied CFRP's. [Composites world, 2014]

### 7.3.3 Cost Comparison

On Figure 158, the costs per kilogram of the printing polymer is compared to the price per kilogram of the traditional structural materials. The current price per kilogram of Macromelt 6900E is about 20 euros. However, because Macromelt 6900E is especially created for applications in the medical industry, Henkel expects that less filtering processes will be needed once a material like this will be applied in the construction industry. This, because the specific quality demand for the building industry probably is more roughly. Application in the building industry of a material like this, will therefore probably be possible against a lower price. Furthermore, the demanded quantity for construction works will be much higher than for the current industries that purchase this material. For higher quantities, Henkel can deliver materials like this for a better price. This is a second reason for which Henkel expects that the actual price when applying a material like this in the building industry, will turn out lower than the current price of 20 euro. For the two reasons mentioned above, Henkel estimated that the actual price will lie around 5-10 EUR/kg, when a polymer like this will be applied in the building industry. This range is plotted in the graph below:



## 7. Overview of Results, Grading and Qualification

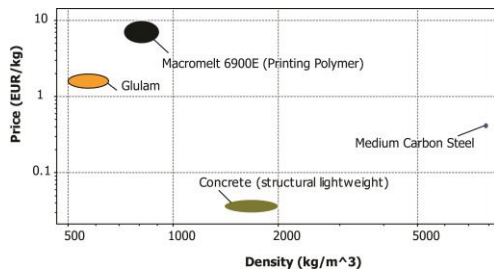


**Fig. 158** Cost comparison between the printing polymer and commonly applied structural materials

In the experimental phase where the 3D printing project is currently in, the material costs do not form a crucial property as the technological feasibility will not depend on it. In the long run however, the material costs actually will form an important parameter. This because the material price is one of the characteristics that at the end determine whether the 3D-printing technique and appurtenant printing material can become a successful addition to the current building industry. When 3D-printing in the future has lost its initial value of 'novelty', it needs to become a price-competitive construction technique to survive and be commercially feasible on the long run. Of course there are costs that can be saved by 3D-printing, as the amount of man-hours and building time probably can be reduced when applying this technique. Furthermore application of the 3D-printing technique in the construction industry probably means a safer working environment, which increases the value. Also the major property, that by 3D-printing it probably will become possible to create complicated forms in a simple manner, will probably increase the value and decrease the costs. Another advantage is that the amount of wasted material probably will be lower with 3D-printing, as the building method is less gross and more accurate than current construction methods. Still, besides all these advantages, the estimated price per kilogram of the printing material is significantly higher than the price of the current applied structural materials. Based on solely the price per kilogram, it therefore is hard to estimate whether 3D-printing with polymers can become a price- or value-competitive addition to the current construction industry.

When comparing the price of the printing polymers with the polymers that are commonly applied in the construction industry, then the result is more positive than was the case for the comparison with the traditional structural materials. This can be observed in the figure below:

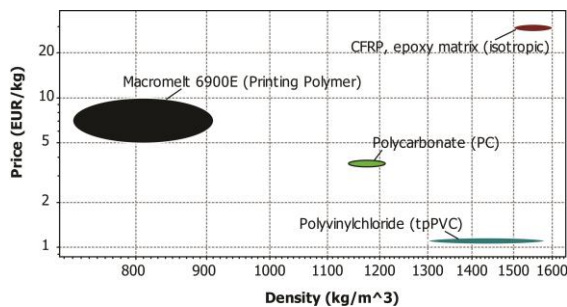


**Fig. 159** Cost comparison between the printing polymer and polymers that are commonly applied in the construction industry

The price of structural applicable CFRP is even higher than the expected price of the printing polymer. Still, as the estimated price of the printing polymer is based on its current properties, it probably is the case that the price will increase once this material will become structurally applicable like CFRP. A price-comparison with PC and PVC therefore is fairer as the current properties of the printing polymer come closer to the property ranges of PC and PVC. In this latter comparison, the price of the printing polymer is higher than PC and PVC while it satisfies less good to the demands of applicability within a building project. It therefore seems that the extra requirement of printability, in the end will lead to a higher price for the printing material. As mentioned above, this does not automatically needs to be a problem, because 3D-printing in the construction industry can lead to other cost-reductions and value-additions. Furthermore, once 3D-printing in the building industry might become more common, it is expected that the price will be further reduced, because competition will then grow and supply increase.

## 7.4 Other important properties

Part of the material properties that are mentioned in table 2 of paragraph 3.3.1 are not studied within the scope of this research, which is a conscious choice. As mentioned before, for all these properties it holds that they actually should be known to guarantee a safe application of the material for a general housing project. However, given the experimental character of the particular 3D Canal House project, studying all properties already in this phase would be unnecessarily profound for the early stage the project is in during the performance of this research. For this reason, the choice is made to emphasize the material research within this graduation project on the properties that are essential to be known to be able to set next steps within the 3D print canal house project.

The emphasis here lies on the basic mechanical properties and the orientation behavior, temperature behavior and creep behavior, as the hypotheses is that these are the most crucial properties to be known for preliminary structural design. However, when in future the designing parties continue with designing geometries that are thin-walled, the indentation hardness (surface hardness) is a property that becomes important to be known as well. This, because in case a printed geometry consists of only one or a few layers, the chance is high that dents and scratches that arise on the surface, might influence the strength performance of the material. For solid geometries consisting of large numbers of printed layers, the influence of dents and scratches on the strength probably is negligible.

So once the designing parties decide to continue building up geometries by thin walls, it is highly recommended to perform research on the hardness of the printing material.

Another mechanical property that is not studied within this research but can become important under certain circumstances is the low cycle fatigue behavior of the material which can be expressed in a fatigue strength limit. In practice, fatigue in buildings especially occurs around connections that are exposed to repetitive and/or strongly fluctuating loads. These loads for example can be caused by wind, especially when there are a lot of surrounding buildings that interfere the wind, or by earthquakes. From the creep test, the conclusion is earlier drawn that the printing material is sensitive for locally applied loads by stronger elements. Therefore the recommendation is made that one should prevent to design connections with steel connective elements as much as possible. This recommendation probably will also benefit for the fatigue resistance of the construction, as connections normally are the building parts that are most sensitive to fatigue. Still, it is recommended for future research to study the fatigue behavior of the printing material, because also in case of proper detail designs, fatigue can still become a normative failure mechanism. Not that a lot of surrounding buildings or earthquakes are expected on the initial location of the 3D print canal house, but as the material is light weight, still vibrations due to wind loads and other variable loads can be expected.

This also means that besides studying the fatigue properties of the material, the vibration behavior of the house is an important aspect to check. Not only for the purpose of fatigue, but also for the maximum allowable vibration that is perceptible for users.

The weight of the material, expressed in the measured density, is relatively low compared to, for example, concrete. Therefore problems can be expected concerning the sound insulation capability of walls and floors composed of the printing material. For house separation walls and floors, the minimum required air-sound insulation is 52 dB [NEN 5077].

$$D_{nT,A,k} \geq 52 \text{ dB} \quad (7.4)$$

If one would apply solid walls consisting of solely the printing material, then with formula 7.5 the minimum required wall and floor thickness can be determined by the practical mass-law:

$$R_{wand} = 17.5 \cdot \log m + 3 \quad [\text{Boveldt, 2014}] \quad (7.5)$$

$R_{wand} \geq 52 \text{ dB}$  gives for the density of  $0.98 \text{ gcm}^{-3}$  for solid blocks a wall and floor thickness of 0.64, say approximately 0.70 m. [NEN 5077]

This means that if houses that are solely composed of the printing material, would be connected to each other, the walls and floors between different houses should at least have a thickness of 0.70 m. This probably means that the sound insulation requirement is normative and leads to, for housing, unusual and inefficient wall and floor thicknesses.

## 7. Overview of Results, Grading and Qualification

For detached houses, the sound insulation requirement is lower, namely  $\geq 37$  dB [NEN 5077].

In this case, the thickness of a solid façade or roof would become only about 0.10 m. A thickness that probably already will be reached by structural and/or heat insulation requirements. Therefore when this material would be applied in detached houses, the sound insulation requirement probably would not be normative.

(In this reflection, the contact sound insulation is omitted because this value need to be measured in practice and furthermore is assumed not to be normative for the thickness of walls and floors.)

To indeed check if the heat insulation requirement leads to a wall thickness already higher than 100 mm, the wall thickness is determined by means of the requirement that the thermal resistance  $R_c$  needs to be at least:

$$R_c = 2.5 \text{ m}^2 \cdot \frac{K}{W} \quad (7.6)$$

And that  $R_c$  can be determined with:

$$R_c = \frac{d}{\lambda} \quad (7.7)$$

Since the thermal conductivity  $\lambda$  is unknown, the heat conductivity of PVC, which is about 0.13, is taken as a reference.

This leads to a wall thickness of about 0.3 meters. Which indeed is already significantly higher than the façade thickness that is required to meet the sound insulation standards.

It can be concluded that for house separating walls between connected houses, the sound insulation requirement is normative and leads to separating walls and floors of about 0.70 m. Although the required wall thickness to meet structural requirements depend on the applied form and dimensions of the particular structure, it is reasonable to assume that the required wall thickness to meet the structural requirements will turn out to be lower than 0.70 m.

For façade thicknesses of detached houses, the heat insulation requirement, that leads to a façade-thickness of about 0.30 m, is normative above the sound insulation requirement. Whether the heat insulation requirement for facades also is normative above the structural requirements will depend on the applied dimensions and form of the particular structure.

## 8. Design Recommendations

Based on the performed material research that is described under the chapters 5, 6 and 7, the following design recommendations can be given:

### 8.1.1 Overall design

1. One should always try as much as possible to load the material in the direction of the printed lines, especially when the material is loaded in tension or bending. This because, the material is significantly stronger in this direction and, in most cases, fails after an initial deformation instead of in a brittle manner.
2. It is advised not to judge the structural performance of geometries with one's bare eyes, as structural degradation is not always visible in the form of permanent deformations.
3. One should never conclude for a geometry which initially can resist a load, that this geometry therewith is capable of actually resisting that load on a longer-term.
4. It is recommended to apply safety factors over the applied load according to the scheme that is presented in paragraph 7.2.
5. Inspection of loaded geometries needs to be performed on a regular base to check if failure of individual parts has been taken place.
6. When the tested printing material is applied in elements that are facing the east, south or west, one should always apply a material that blocks the direct sunray to cover up the printing material.
7. It is advised to give the material a color which is as close as possible to white, as this increases the sun-resistance and decreases the temperature inside of the house.
8. For heat-insulation purposes, it is likely that an insulating and/or air layer is required, especially for preventing the inside of the house from becoming too warm during the summer. As the material can resist the possible frost-circumstances in The Netherlands, insulating layers can be located both at the outside as on the inside of the printing material. It actually is advised to place the insulating layer on the outside, such that it can (partly) function as a protection-layer for direct sunlight as well.

### 8.1.2 Design of single blocks/printable geometries

1. It is recommended to experiment in creating building blocks that exist of multiple printed layers that are connected to each other within the xy-direction instead of blocks that are built up by only single layers, which so far has been the case. Using multiple layers within the xy-direction leads to a stronger, stiffer, more isotropic, more homogeneous and therefore better predictable material behavior. Another good reason to apply multiple layers in the xy-direction is that the building blocks will become waterproof, that the material becomes less sensitive to local inaccuracies and that the material can easier meet the heat and sound insulation requirements for housing.
2. Recommendation 1 means that all individual walls/members of printed geometries should consist of multiple printed layers in the horizontal direction. By this, the individual members become stiffer and the local and overall strength of geometries will become higher.
3. One should build up geometries such that the amount of mutual connections between the individual geometry-members is as large as possible and spans of the individual members will be minimized.
4. The influence of local inaccuracies can be limited by creating multicarrier roads within a printed geometry. In this way, a local inaccuracy at the location of a connection between two members, will not be crucial.
5. For geometries to which long-term loads are applied, it is recommended to create multicarrier roads within these geometries and also between different geometries.
6. For water-tightness of geometries, a minimum wall-thickness of 3 printed layers is suggested. In case of printing geometries consisting of only one layer, one should check these geometries on permeable holes and cracks.
7. An example of a satisfactory structural composition of a 3 meter-high printable façade wall can, for example, look as shown on figure 160: The total wall thickness is 400-500 mm and is build up by thin outer walls consisting of 10 printed layers, with inner 10-layer thick orthogonal members between those two walls at every 200-250 mm. Between the orthogonal members, diagonal, 10-layer-thick, members connect the top of one orthogonal member with the bottom of the other. The wall is printed with its long direction in the z-direction (vertical direction) of the printer.

## 8. Design Recommendations

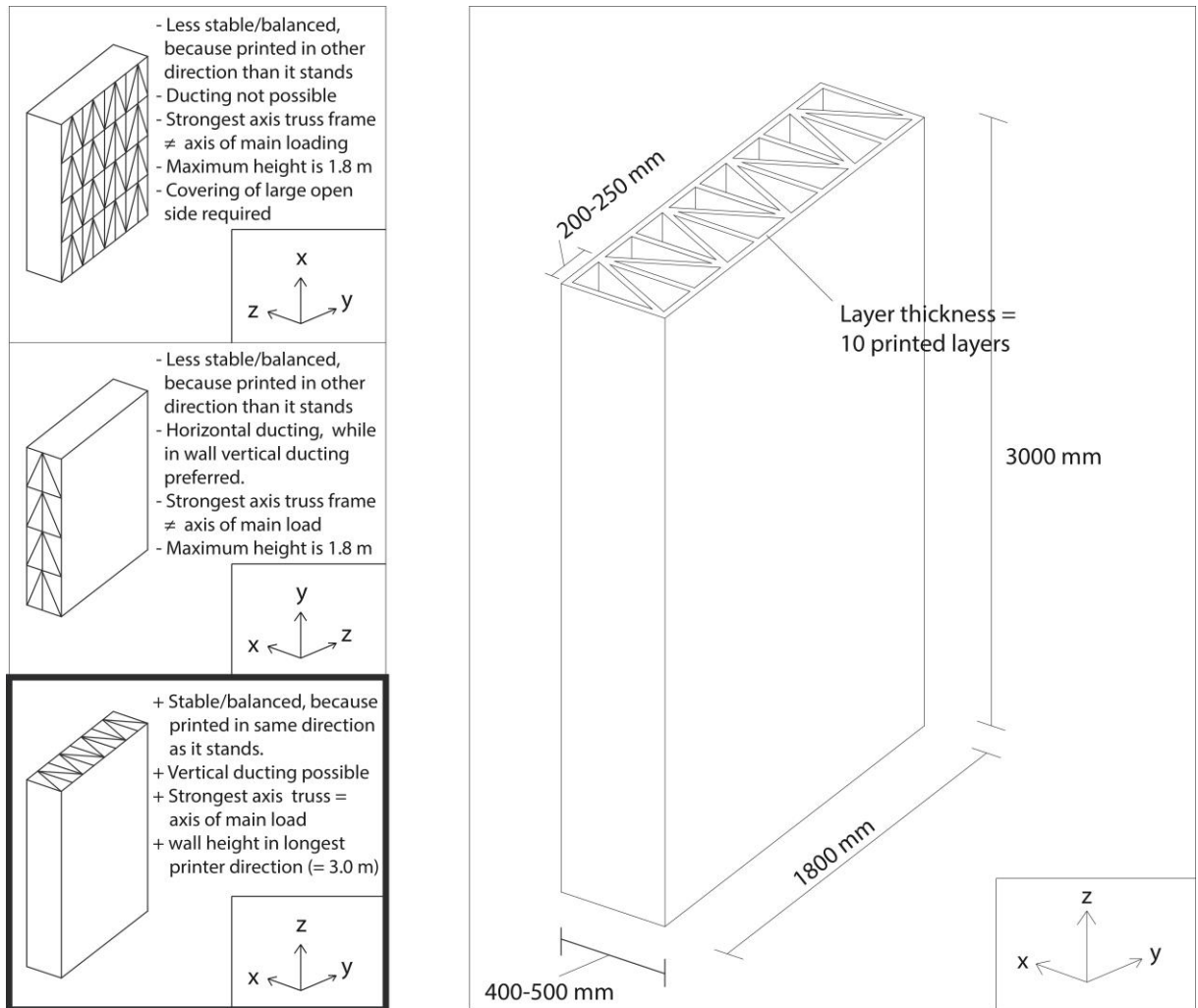


Fig. 160 Example of a satisfactory structural composition for a 3 meter-high printable wall

8. An example of a satisfactory structural composition of a 3 meter-spanning printable floor can look as in figure 161: The total floor thickness is 300 mm and is build up by thin outer layers consisting of 10 printed layers. 10-printing-layers-thick vertical members are placed between the two outer layers at every 180 mm. Between two vertical members, diagonal members with a thickness of 10 layers connect the top of one vertical member with the bottom of the next one. The floor should span in the direction perpendicular to the z-direction of the printer, such that the material is not loaded in tension perpendicular to the direction of the printed lines. A disadvantage for choosing the floor design alternative in the center above the design alternative at the left, is that the span of the floor is limited to 1.8 m according to the current dimensions of the 3D-printer. However, since the design alternative at the left is loaded in tension perpendicular to the 'fiber'-direction, this solution, that enables a span of 3m instead of 1.8 m conflicts with design recommendation 1 of paragraph 8.1.1 and therefore leads to a lower strength performance.

When these floors are situated inside, no further measures for physical matters are required. For the top slab (roof) of the house however, again a heat-resistant layer needs to be added on top and an insulation layer right underneath the top thin-wall of the floor composition.

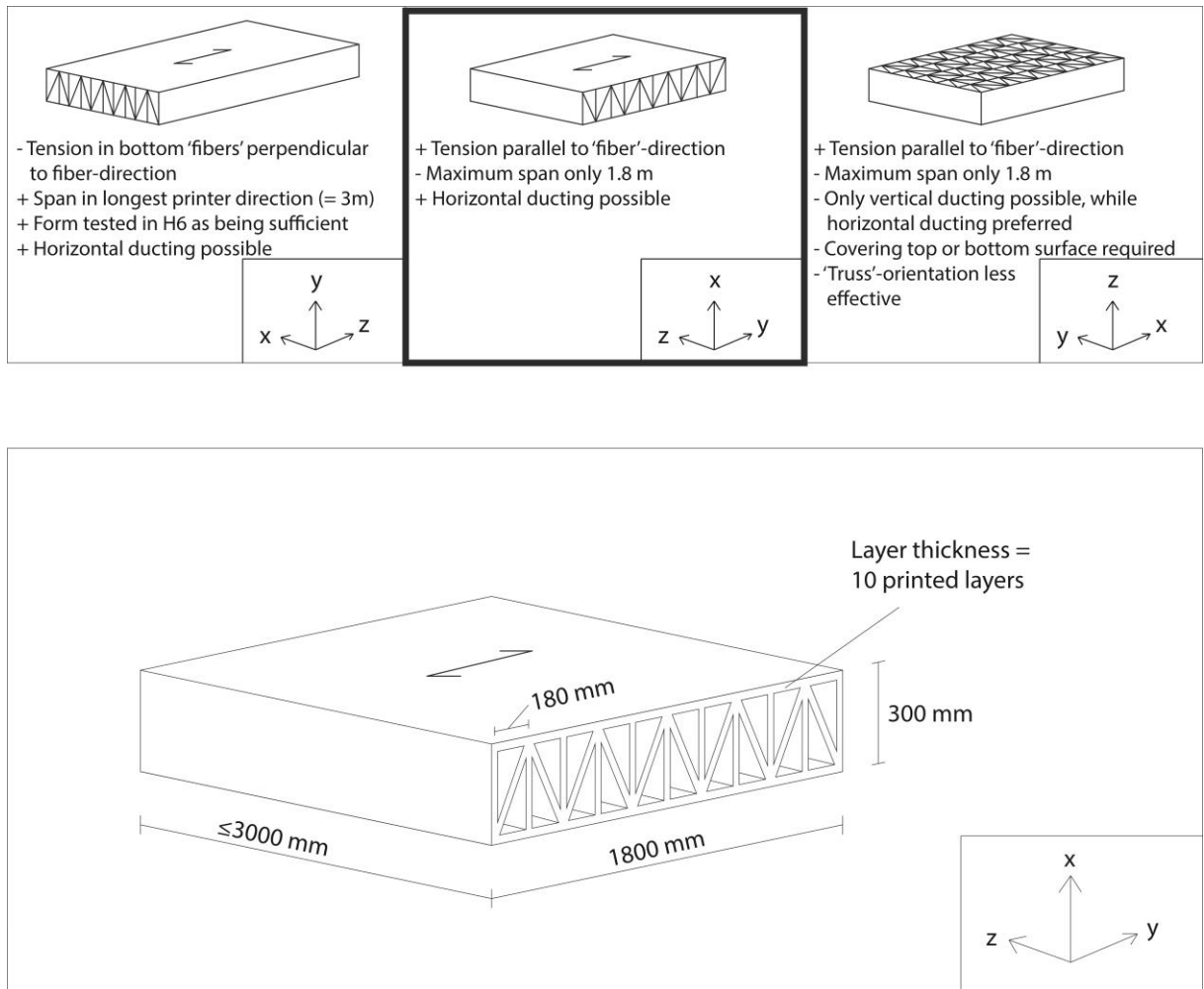


Fig. 161 Example of a satisfactory structural composition of a 1.8 meter-spanning printable floor

9. Instead of the described structural floor composition, it is also possible to give a floor slab an inner composition comparable to a concrete hollow core slab. Although this probably would mean a more optimized (strength/material-ratio) structural floor composition, a disadvantage of this floor design would be that the addition of the inner insulation layer is not possible. Furthermore, less space is available for other ducts and installations, while it is an architectural desire to integrate as much services as possible within the floors and walls.
10. It is also possible to create elements that consist both of a cantilevering floor part and a wall-part. In this way, a printed and thus seamless connection between the wall and floor is obtained, that can be connected to similar elements via a vertical connection between the wall parts and a horizontal connection between the floor-parts. An advantage of applying this 'corner'-geometries in the overall design of the house, is that only floor-floor and wall-wall connections are required instead of more complicated wall-floor connections. Furthermore the corner-element can lead to a much stiffer overall structure than individual floors and walls. In this case a proper printed floor-wall element would look as follows:

The inner floor composition remains unchanged compared to figure 161. The wall composition now will be printed with its long axis in the horizontal direction (xy-plane), which means that the wall composition is rotated 90 degrees compared to the design of the individual wall in figure 160. Between the vertical wall part and the horizontal cantilevering floor part, a triangular corbel-like part is present that enables a gradual transition between wall and floor and therefore forms a stiff corner. It is important to notice that this whole geometry can and should be printed in one run, such that no corner-connection is required when applying this block. A disadvantage of this geometry compared to the presented wall-block in figure 160 is that this 'corner-block' does not enable the opportunity to integrate vertical-lined services within the wall part.

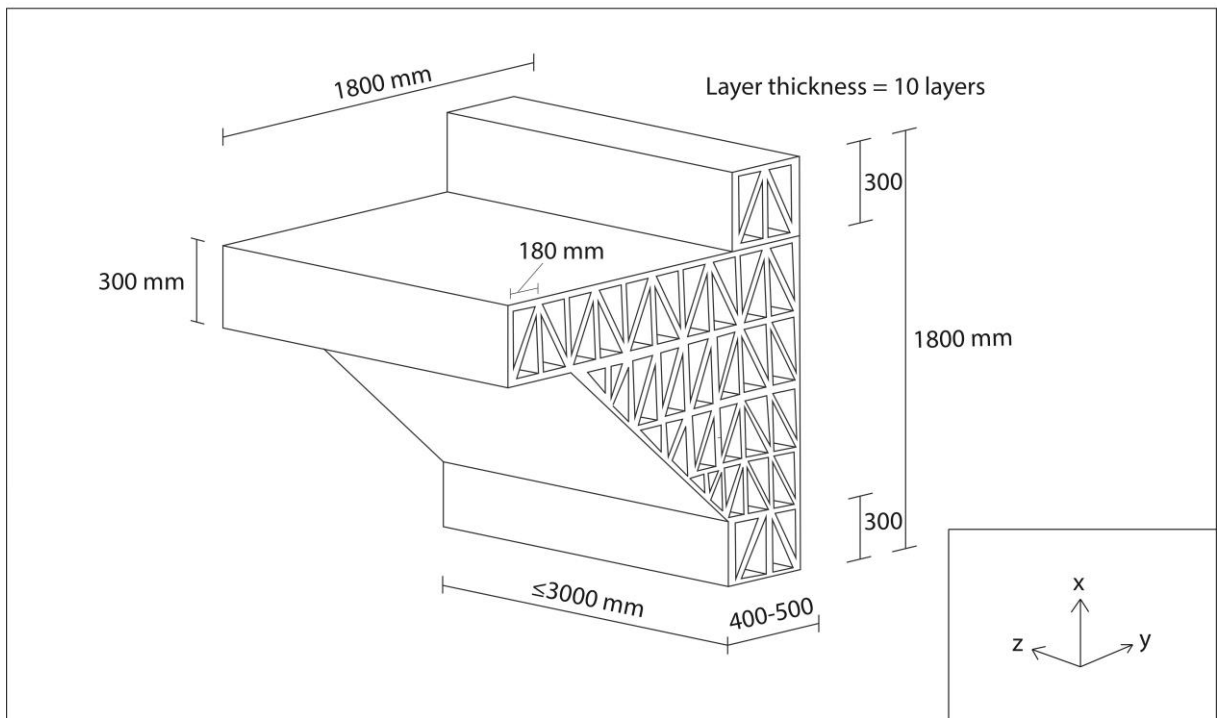
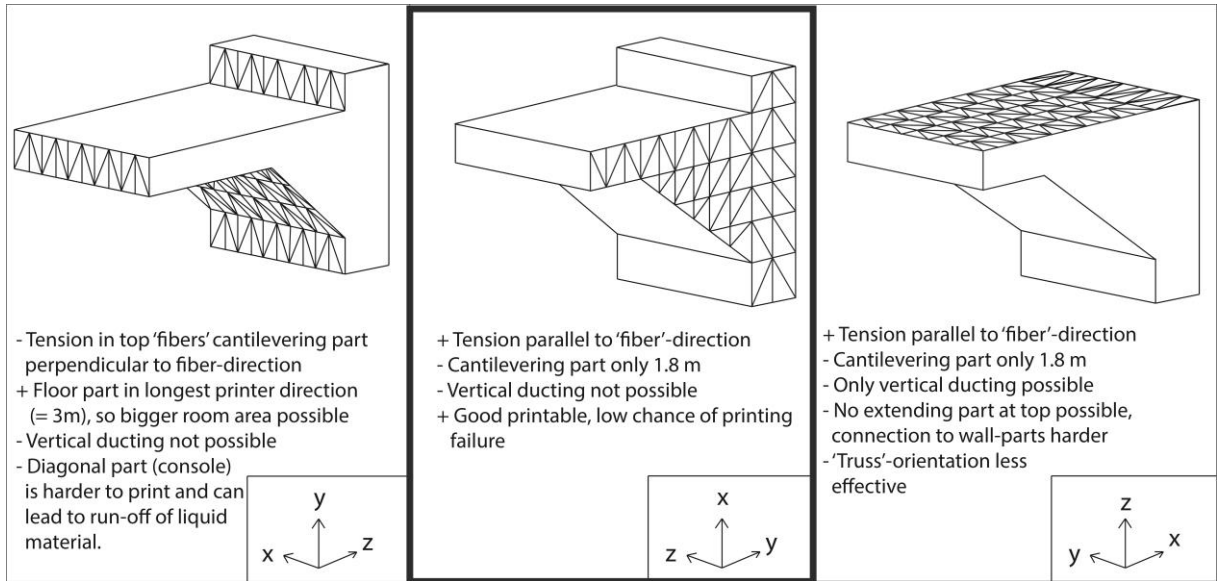


Fig. 162 Example of a satisfactory geometry in which floor and wall are combined in one printable block. In this way, no complex connections are necessary between horizontal and vertical oriented elements.

### 8.1.3 Design of connections between printable blocks

1. Because the material is very sensitive to locally applied forces, these should be prevented. This in particular has consequences for the design of connections between geometries, as connections often are points where stresses are transmitted over a small area. One should therefore design connections such that stresses are distributed over an area which is as large as possible. For floor-wall connections it is recommended to print a wall with a cantilevering corbel, such that the floor can be placed on this corbel. A measure should be taken here to prevent the floor from sliding or lifting. For wall-wall connections it is recommended that the head and bottom of the walls are designed such that these can be placed over each other. After placing the walls, the connection can be made definite by heating up the material around this connection to a temperature just above the melting temperature. In this way mutual definite connections between the two walls will be created, leading to a moment-resistant wall-wall-connection. This process can be compared to steel-welding. A floor-floor connection can be designed in the same way as a wall-wall connection.
2. By all means, connecting different elements with bolts should be avoided.



## 9. Discussion

### 9.1 Scope and limitations of overall Research

On the moment a material is applied within a building, especially when this material basically forms the only applied material of this building, then this material should not contain any surprises or unknowns. Unfortunately the scope of this material research was not sufficient to get to know the material in all its details. It is for example unknown how this material will react when exposed to electricity, to repetitive loads or how it chemically interacts with other building materials. Of course, reasonable assumptions can be made for these properties, but still the obtained knowledge after this research might not be sufficient enough to apply the material within a house with a residential function. However, the properties that actually are studied within this research, do form the most important material properties to be known for the application of this particular material within this particular building project. So the choice of focusing this research on the combination of thermal properties and mechanical properties has led to acquisition of the material properties that are most essential to be known, in order to set further steps within the 3D Print Canal House Project.

Another limitation of this research one should be aware of is that, in consultation with DUS Architects, the decision is made to not study the influence of the chosen print-resolution on the mechanical properties of the material. Instead, the mechanical properties are only obtained for the resolution that was found by DUS as being optimal for the printing process, taking into account the printing speed, minimization of the failure chance and connectivity between the layers. It therefore is important to be aware of the fact that the exact quantitative relationship between resolution and strength is an unknown factor in this project, only hypotheses can be made here.

Furthermore one should notice that the specimens that are made within the vertical xz-printing-plane are produced in a different manner than the samples that are obtained within the horizontal xy-printing plane. As described in chapter 4 the samples within the xy-plane are printed directly, while the samples within the xz-plane are produced by first printing plates and later on cut the samples from these plates. Samples that are printed directly within the xy-plane might lead to behavior of these samples that is closer to the real material behavior when applied within building blocks. This, because in reality everything is printed within the xy-plane in a continuous line, so without interruptions as well, while laser cut samples lead to line interruptions that are not present in reality.

Still, it might be true that a fairer comparison between the xy- and xz-plane would be obtained on the moment the specimens are fabricated in the same way. Since direct printing of 2-dimensional tensile- and shear-specimens is not possible within the xz-plane, the samples should in that case be laser cut from plates for both the xz- and xy-printing-plane.

Finally, it is important to notice that for most of the performed tests it holds that the amount of tested specimens, probably is not sufficient for drawing conclusions with a full certainty. The reason for the low amount of tested samples lies in the lack of availability of the 3D-printer for the purpose of this material research. Of course the test results offer a good insight in the material behavior and therefore are useful for preliminary (structural) design and as input for further improvement of the material. However, on the moment one would use the material results, for example, for reporting to 'Bouwbesluit' or to actually build structures, it is advised to first validate the obtained material properties by repeating the performed tests.

### 9.2 Usefulness of Individual Research Results

#### *Tensile test and Shear test*

The results that are obtained from the tensile and shear tests for the specimens that are printed within the xz-plane, are useful to compare the strengths of the material parallel, perpendicular and 45 degrees to the grain. The results obtained for specimens printed within the xy-plane however might not be completely appropriate for this purpose, since the obtained samples within this plane are quite isotropic. This is partly caused by the way these samples are produced within the xy-plane, but also because the behavior of the material in the xy-plane is more isotropic by all means, as more adhesive connections between different lines are made within this plane.

### ***Compressive test***

It might be the case that the test samples that are used for the compressive test are not representative for the printed house-blocks as they are designed by DUS Architects so far. The reason for this doubt lies in the fact that the use of a solid cube-formed 3D sample leads to an almost homogeneous material composition and behavior, due to gluing/sticking together of the material in directions perpendicular to the grain direction. This, while in practice so far it never occurred that DUS printed building blocks such that multiple layers were attached to each other in multiple directions. In fact, all blocks are composed from 2d-surfaces of one layer thick. Therefore, there is no complete certainty if the strength results of this compressive test can be extrapolated towards these kinds of 'DUS'-geometries. For that reason, a compressive test has been performed on hollow tubes as well in chapter 6, to compare the solid blocks of this test, with open geometries. On the other hand, the obtained positive results of the compressive test also might form a trigger for the involved parties DUS and Tentech, to consider a different way of block-designing.

### ***Young's Moduli***

For the extensometer tensile-test that is performed to determine the Young's Moduli, it unfortunately holds that the number of tested specimens is not sufficient to come to proper conclusions. The results of this test however can be used to get a feeling of the order of magnitude of E and for validation of earlier obtained results within the compressive test.

For both the Young's Moduli that are obtained within the tensile test with the use of an extensometer as for the Compressive Moduli as determined from the compressive test curves, it holds that the obtained differences for identical samples are relatively large. This means on one hand that the material behavior is unpredictable since different values are obtained for the same test within a large range. On the other hand will the material become better predictable on the moment that a higher number of samples are tested, because deviations and averages could be better mapped then.

### ***Absorption and Drying test***

The result of this test was that the amount of water that was absorbed by the tested samples was negligible. However, one should be aware of the fact that the tested solid cube samples, are not representative for the way in which the material is applied in practice. The material in the form as it is applied within the printed geometries so far, actually is permeable. This, because all the blocks that are printed so far, are built up by 2d-plates of one layer. Due to local inaccuracies that are often present within these plates and layers that don't connect properly, the building blocks will not be waterproof. When printing multiple layers next to each-other in the xy-direction, the permeability will be reduced for every extra layer that is added, as the layers will melt together and holes will be filled.

### ***Temperature-Strength Test***

The results of this test might not be accurate, mainly because during certain tests an estimation of the surface temperature needed to be made due to the use of an insufficient measurement method of the surface temperature. During the last six measurements, the measurement methods were improved, but for these measurements, different sample forms were used than for the earlier tests.

For these reasons it is recommended to repeat this test a few times, such that the results can be validated, especially around the critical area between 30 and 80 degrees. Unfortunately due to the lack of availability of the testing equipment and funds, there was no option to repeat this test within this research.

Although the execution of the test might not have been optimal and therefore the results not accurate, the obtained strength-temperature curves from this test still give a good insight in the reduction of the strength under an increasing temperature, as the inaccuracy-range of about 10 degrees is sufficient for getting an idea of the material behavior under different temperatures.

### ***Creep Test***

Because this test failed at the first two attempts, it can be concluded that the first applied test setup is not suitable for performing a tensile creep test on this material. This is due to the fact that the printing material is very sensitive to locally applied forces and therefore failed at the connection points instead of at the middle part of the specimen, which was the intention.

The second applied test setup turned out to be sufficient for performing a proper creep test. However, the first tested sample unfortunately was loaded with a stress-level higher than the characteristic material strength. As

## 9. Discussion

a consequence, quick plastic deformation appeared. Although a quick plastic deformation might not be the result one wants to obtain with a creep test, this test result still lead to an important conclusion. Namely that the strength boundaries that are set by the tensile test are narrow.

The second tested sample, on which a stress of about 80% of the characteristic strength level was applied, lead to successful testing results in the form of elastic deformation. However, since a creep test can't last forever and is bound to an end, it still is hard to say if and when a plastic deformation stage would have been reached. Therefore, although the performed 800N- and 500N-test enabled some initial valuable insights in the creep behavior of the material, more extensive research on the creep behavior of the material is required before it can be applied structurally with full safety.

### **Flexural Tests – block geometries**

For the flexural test, it unfortunately was not feasible to test completely closed blocks with the same dimensions as the 'open' blocks/geometries, as fully closed blocks of these dimensions would lead to a undesirable long printing duration and high printing costs. For this reason, the comparison between the flexural properties of the small closed blocks A and B and the large open geometries C, D and E, probably is not as accurate as would have been the case if the same size would have been used.

The closed geometries A and B actually failed on bending, while the open geometries C to E all failed on other failure mechanisms than the reach of the flexural strength. Therefore, the flexural properties of the printing material could be determined by the results of the tested blocks A and B while bending of the open blocks led to further insight in the failure mechanisms of open geometries. The choice for performing bending tests on both solid blocks as open geometries turned out to be a good one which led to valuable complementary insights on the material behavior. The boundaries of possible printable geometries were set by printing completely solid and completely open sections. By subsequently testing blocks with small inner structures, the behavior of intermediate forms between those two outer boundaries is studied as well. This has led to proper insights in the behavior of current printed and designed geometries of DUS Architects and delivers the required knowledge to give recommendations for improvement of the designs. The only possible shortcoming in the range of tested geometries, possibly is the absence of a test-geometry that already was printed with multiple layers in the horizontal direction. This would have definitely confirmed and validated the conclusion that printing multiple layers leads to a significantly better structural performance.

### **Compressive/buckling test hollow sections**

The presence of a locally thinner wall around one of the corners of all the compressive samples was unfortunate, because this led to an unilaterally insight in the possible failure mechanisms of a hollow square cube tested in compression, as all the samples failed in this weak corner. On the other hand this outcome at least did confirm the earlier conclusion that thin-walled geometries are sensitive for local inaccuracies. This is an important conclusion, because since the current printing process cannot guarantee a constant and uniform printing quality, there always is a chance of presence of local inaccuracies.

Fortunately the cross-section of the tested square hollow columns had a uniform wall thickness, such that these columns failed on local wall-buckling instead of failure on local inaccuracies. In this way, still different failure mechanisms were studied, such that a good insight is obtained in thin-walled geometries that are tested in compression. Therefore these tests formed a good addition to the earlier performed compressive test of solid cubes (paragraph 5.3), because now for both open as closed geometries, the behavior under axial compressive forces is known. The comparison between the results of the compressive test on closed versus open geometries, furnishes valuable knowledge for recommendations on the design of DUS Architects.

### 9.3 Future potential of printing houses in polymers

Based on the performed research that is described throughout the previous chapters, it is possible to judge the general future potential of printing houses and other structures with the use of printable polymers. In the first two subparagraphs (9.3.1 and 9.3.2), advantages and disadvantages of printing structures in the currently applied polymer are given. These advantages and disadvantages are found during this research project. The advantages and disadvantages lead to statements regarding the general feasibility of 3D-printing houses using printable polymers, which are described in subparagraph 9.3.3.

#### 9.3.1 Advantages of 3D-printing houses in the current applied polymer

1. The negligible water absorption of the printing material is a positive characteristic of the material in comparison to regular used structural materials (concrete, steel, timber), because it means that no protective measures need to be taken to make the material water resistant.
2. Except for the temperature-strength and stiffness, it holds that the strength performance of the printing material can compete quite well with the strengths of timber and concrete.
3. Application of 3d-printing techniques in the building industry can lead to cost savings and value additions on different parts of the design and building process.

#### 9.3.2 Disadvantages of 3D-printing houses in the current applied polymer

1. The mechanical behavior under high temperatures of the printing material is much less than for traditional structural materials.
2. The Young's Modulus and thus the material stiffness are poor compared to common structural materials.
3. The strength and stiffness of the printing material is significantly lower than for polymers that are commonly applied in the construction industry (PC, PVC and CFRP). This while PC and PVC are not even applied structurally.
4. Under regular circumstances, the printing material is applied in the rubber phase as the glass temperature lies around 5 degrees. This while other plastics in the construction practice are applied in the solid phase, as their glass temperatures lie above the maximum temperature of sun-heated parts in The Netherlands (80 degrees). Applying a polymer in its rubber phase structurally is unfeasible, as the low Young's Modulus and poor temperature behavior already evidenced. The relatively low glass temperature of the printing polymer confirms this once more.
5. The estimated price per kilogram of the printing material is significantly higher than for current applied structural materials and plastic materials.

#### 9.3.3 Statements and advises regarding the feasibility/future potential of 3D-printing houses in polymers

1. It is unfeasible to fully compose a house out of the current used printing material. This, because the material is applied in its rubber phase, which lead to a softening point and a stiffness that are too low to make the material structurally applicable. Improvement of the thermal and mechanical behavior of printable polymers is required to be able to apply a printed polymer within housing structures.
2. A house fully composed of the current printing material will by far not be able to meet the requirements as stated by the building code (Dutch: 'Bouwbesluit'), because the thermal behavior of the material is unsafe and insufficient. As DUS Architects does not have made a definite choice for the function of the building, it is recommended to define the end-product not as a 'house' but as a 'pavilion' for temporary use. This suits the probable function of the end-product better as the house will especially be built to learn and to expose. An important advantage of this change in destination is that the requirements will become much lower. As it triggers the imagination more to speak about a 'printed house' instead of a 'printed pavilion', to the outside world the sculpture of course can still be presented under the name '3D Print Canal House'. To regulators, contractors and structural engineers however, it is better to define the end-product as being a 'pavilion'.
3. When changing the destination from 'house' to 'pavilion', this also means that sound and heat insulation requirements do not play a role anymore. This means that required wall and floor thicknesses will be determined by structural requirements only.
4. In case one actually wants to build a house with the current material, the material is only applicable as a permanent mold for concrete. In that case, the inner holes of a printed geometry can be filled with reinforced concrete and insulating materials. On the outside of the permanent formwork, at least a heat-resistant façade-covering needs to be added. Although this solution might be undesirable, as one can hardly speak of a 'printed house' when only a mold is actually printed, this solution still has two

important advantages. At first, less material improvement is required for the printing material. As it might be the case that applying a printable polymer that is structurally feasible will take a long time or maybe will not be feasible at all, using the printing polymer as a formwork for additives forms a quick solution to obtain a house. Secondly, using the printable polymer as a mold for concrete still forms an innovative solution and a valuable addition to the current formwork techniques. Especially the opportunity to create free-formed molds forms a big advantage compared to techniques which are currently applied to obtain special concrete forms. Using a 3d-printer for fabricating molds therefore might be the first commercially feasible application of 3d-printing techniques within the construction industry.

5. The estimated price per kilogram of the printing material is significantly higher than for current applied structural materials and plastic materials. However, application of 3d-printing techniques in the building industry can lead to cost savings and value additions on other parts. Based on solely the price per kilogram, it therefore is hard to estimate whether 3D-printing with polymers can become a price- or value-competitive addition to the current construction industry.

## 9.4 Next steps

This thesis research, in which the structural feasibility of 3D-printing (housing) structures using printable polymers is studied, forms the first elaborate research that is performed around the 3D Print Canal House project. Although an important conclusion of this research is that printing structures with the current applied printing material is unfeasible, this of course does not mean that the project has to end because of this conclusion. By the performance of this study, insights are gained in next steps that need to be taken in order to work towards a future situation in which printing (housing) structures in polymers can become structurally feasible. These next research steps are presented in paragraph 9.4.1 of this paragraph. After this, in paragraph 9.4.2, some practical advises are given that can come in hand for performing future research.

### 9.4.1 Next research steps

1. Further research on the improvement of the temperature behavior of printable materials should be performed. For the application of the material within a building, the minimum performance should actually be such that the material retains much of its strength under normal circumstances. Later on, the material should be further improved such that it also behaves well under special (fire) conditions. Also, the stiffness (Young's Modulus) of the applied printing material needs to be increased. These improvements can probably be made by experimenting with printing of materials that are in a solid state under normal circumstances. The current applied material is in a rubber phase, which leads to the low stiffness and poor strength-temperature behavior.
2. For printability of a material, a low glass, softening and melting temperature and a low molecular weight are preferred. However, for structural application of a material, high temperatures and a high molecular weight are required. The most important challenge for enabling 3d-printing of houses with polymers, is to solve this contradistinction and find an optimum material that is printable and structurally applicable. As carbon fiber reinforced plastics form the most common plastics that are structurally applicable, one probably needs to search for a solution in this field. First achievements are made in printing fiber reinforced plastics [3ders, 2014]. A next step would be to make this combination of printing technique and material use, applicable and affordable to the scale of a house. So it can be concluded that obtaining a combination of a printing technique and material that enables printing of structural applicable materials, forms the most important aim for the feasibility of printing a house. It therefore is strongly advised to focus future research on the feasibility of 3d-printing with structural applicable polymers. The test results and conclusions of this report can be used as a starting point for this future research.
3. To improve the strength perpendicular to the grain, and to make the material less anisotropic, it also can be recommended that the adhesive properties of the material are further optimized by Henkel. It might be the case that by decreasing the hardening speed, the connection between two layers in the vertical z-direction becomes better. This because the previous layer is not dried yet when the next layer is printed on top of it, which might lead to a better adhesion between the layers.
4. Although improvement of the material to make it structurally feasible has the highest priority, this does not necessarily mean that the design process cannot be continued synchronously to the material development. It still is possible to structurally design geometries, connections, chambers and a full house composition under the assumption that the applied material fulfills certain requirements. A study like this would have three important purposes: at first, it further explores new opportunities

that 3d-printing techniques can bring for structural geometry design. Secondly, a feasible structural design can be obtained parallel to the material development such that optimized housing structures directly can be printed once the material properties are improved. And last, structural design helps in defining the minimum requirements for the material that needs to be developed. So apart from the essential material research, there still are good reasons to continue with the structural design research as well.

5. In case one decides to continue the structural design study, at first further research is required for designing the most optimum structural composition of wall-, floor- and combined elements. The design recommendations of chapter 8 together with the conceptual design examples in this same chapter, can be used as a starting point for a further study to the optimization of printable housing elements. An optimization need to be found here between structural, physical, esthetical and economical requirements.
6. After this, connections need to be designed to enable a proper conjunction between the printable geometries. The given design recommendations for detail-designs can be used here as a starting point.
7. Once optimal geometries and proper connections are designed, it is possible to compose individual chambers and after that a full house out of printable geometries. As the house probably will be build up element by element, and after that room by room, an important challenge here is to enable structural safety during the different phases of construction. Individual elements need to cooperate with each other to form a satisfying structural entity. On a higher level, connected rooms need to work together as well such that the complete house also forms a structural unit. Increasing the size of the printer would simplify these processes. Increasing of the printer dimensions therefore is recommended.
8. It is also advised to perform research on how to realize the foundation of the intermediate printed parts and the end-product. It is recommended here to first study the possibilities for creating a 3d-printed foundation. Although foundations often do not fall under the attention of architectural designers and neither under the attention of the public, foundations still form an indispensable part of every building. Performing a study to 3d-printed foundations therefore first of all completes the desire of a fully 3d-printed house and also might lead to interesting new insights. Perhaps 3d-printing techniques can have an added value for foundation designs as well.
9. On the moment it would turn out not to be feasible to print structural applicable polymers within a desired time span, then it is recommended to change the focus of the 3D Print Canal House Project from printing a complete house with printable polymers to the printing of formwork using printable polymers. In that case, the material and printing technique would need to be optimized for printing molds for which the requirements are significantly lower and therefore simpler achievable than the requirements for structural application.
10. Nowadays both architectural design and structural design for an important part are performed digitally, because it simplifies the design process and enables the creation of more complicated building forms. Under the designing parties, there is a big desire to create a single platform in which all the different parties can add content according to their expertise. By this, an integrated design could then be reached in a clear and fast manner. Although different attempts are ongoing to create such a platform, the arrival of 3d-printing techniques in the construction industry might speed up this process. This, because an integrated design platform becomes essential when using 3d-printing, as the design must be integrated into a single printing file.  
Normally the architect and structural engineer are the parties that work together the closest. Furthermore it is more realistic that the designs of structural engineers and architects are printable than, for example, the design part supplied by the installation engineer. For these reasons, coming to integrated designs is most essential for the architectural and structural parties. Therefore, the particular situation of the 3D Print Canal House project can act as an interesting case study for performing next steps towards an integrated computer model for architectural and structural design.
11. Apart from the practical applicability of a building material, nowadays sustainability of materials forms an important factor as well in the decision process of which material to apply. The difficulty of the sustainability characteristic, compared to most other characteristics, is that sustainability is hard to express in unambiguous numbers. Sustainability cannot be expressed in a single unit, but is formed by a combination of factors over the whole lifetime of a material. It is for that reason, that it is hard to come to a proper statement about the sustainability of a material, without performing elaborate research taking into account all these factors. A quick analysis learns us that applying the printing polymer as a construction material at least is promising when it comes to sustainability. Henkel states

that the printing polymer for an important part is manufactured from natural oils instead of traditional petroleum-based oils where plastics often are made from. Furthermore the 3D-process includes that the material waste is minimised, because only material is laid down there where it is needed. Also, the involved parties claim that the applied material is almost fully reusable after shredding it back to granulate form after use. These three characteristics are positive with regard to the overall sustainability of the material. However, no analysis is made between the scarcity of commodities of bio-plastics compared to common construction materials or to the emission of CO<sub>2</sub> during the production process of the printing polymer in comparison to general construction materials. It is also unknown how much energy is required for 3D-printing structures in comparison to the energy use of general construction methods. Furthermore, the CO<sub>2</sub> footprint of the recycling process of the printing material is not known and it is unclear what the lifetime of a printed structure will be.

For these reasons, elaborate research on the sustainability of the printable polymer, taking into account all these factors, is needed in order to come to a proper statement about the general sustainability of the printing material in comparison to common construction materials. It is worth to perform such a research, because if it turns out that 3D-printing structures by means of polymers indeed is more sustainable than using other building materials and construction methods, then this positive outcome can stimulate the further development of material and 3D-printing methods. This, because the more advantages this construction method has, the higher the chance becomes that this construction method will be further developed.

12. Finally it can be interesting to perform a study to the economical/commercial feasibility of 3d-printing houses and other structures, by using printable polymers. Independent of all the technical possibilities, money in the end is the leading quantity that determines whether this new technique can be implemented successfully in the construction industry. If there is no added value for implementing a new innovation in an existing situation, then in the rule, this innovation will not be implemented. The commercial prospects are hopeful, as different advantages for implementing this technique in the construction field can be thought of. Think for example of saving costs on time, labor and material quantity and the added value of free-form architecture. However the added value and cost savings that come with these advantages must outweigh possible disadvantages like technical development costs, implementation costs and material costs. Although a study to the commercial feasibility involves quite a lot of assumptions when performed in this early stage of the technique, such a study still can be already valuable in the current phase. A study like this can actually help in clarifying the future prospect and therefore can give direction to the technical development. Furthermore, it can help in convincing parties to get involved in the further development of this project and of this technique.

#### 9.4.2 Practical advises that support future research

1. In general, if one has available an accurate 3D-printer, it is considerable to use a 3D-printer to print out test specimens directly, because it forms a fast and non-labor intensive way to obtain complex-formed samples. For future material research of materials printed by the 'Kamermaker', it however is recommended to fabricate test specimens for both the xy- as the xz-plane by laser cut the samples from plates. This because the resolution of the 'Kamermaker' is not sufficient for direct printing test specimens of a required quality. By laser-cutting, more uniform test specimens are obtained with more accurate dimensions.
2. For future new or adapted 3D-printers, it is recommended to increase the length and the width of the printing area such that they become (at least) equal to the height. In the current situation, blocks can be printed 3 meters high in the z-direction and only 1.8 m width in the horizontal directions. In this situation, rectangular blocks will be printed with their long direction in the z-direction. As a consequence, these blocks often will be loaded perpendicular to the printed lines, especially in case of floors. This, while the material is stronger parallel to the direction of the printed lines. Increasing the width and length of the printing area, increases the design freedom and opens more possibilities to create blocks that are loaded in the strong direction of the material.
3. Data-values on factsheets that are provided by Henkel, should not be used directly for structural design. This because the property values of the material, once it is printed, differ significantly from the values on the Henkel-sheets. When one wants to use the Henkel-sheets for obtaining a quick indication of the capability of a new material, it is advised to multiply the mechanical properties on the Henkel-sheet with a factor 0.5 and the thermal properties with a factor 0.4.

4. It is advised to study the influence of the printing resolution on the strength properties of the material. The resolution now is optimised taking into account the printing speed, minimization of the failure chance and connectivity between the layers. It might be useful to optimise the resolution-settings, purely taking into account the adhesive connections between the printing layers and therefore the strength. This can be quite important since the performed tests show that the strength between layers, so perpendicular to the grain, is poor.
5. It is recommended to experiment with printing perpendicular printed layers on top of each other. This means that if a certain layer is directed to the x-direction, the layer on top of it is directed in the y-direction (other horizontal direction) and the next layer again in the x-direction etc. In this way, it might be the case that the anisotropic behavior of the material will be reduced or even eliminated.
6. More extensive research on the creep behavior of the material is required before it can be applied with full safety.
7. It is recommended for future research to study the fatigue behavior of the printing material, because this can be a normative failure mechanism, especially around connections.
8. Once the designing parties decide to continue building up geometries by thin members consisting of only one printed layer, it is highly recommended to perform research on the hardness of the printing material.
9. On the moment a new printing material is developed, it is recommended to first and foremost perform the strength-temperature test (paragraph 5.7) on this new material. This, because the temperature behavior is the weakest and therefore most critical characteristic of the current printing material so new materials should especially show improvement for this property.



## 10. Conclusions and Recommendations

The most important conclusions that can be drawn from the performed research, are given in paragraph 10.1. Paragraph 10.2 gives the most important recommendations that can be given based on the research performed in this thesis study. Although the conclusions and recommendations in this chapter give a good insight in the most important findings of this research project, it is strongly recommended to at least read paragraph 7.1, chapter 8 and chapter 9 for a more complete overview and better understanding of the results, conclusions and recommendations that are obtained from this thesis study.

### 10.1 Conclusions

1. The behavior of the printing material under high temperatures is much less than for traditional structural materials. A softening point of only 60 degrees Celsius and a strength degradation of 70% at a temperature of 40 degrees are unacceptable low properties for structural applications. Also, the Young's Modulus and thus the material stiffness are poor compared to common structural materials. These poor thermal behavior and low stiffness are caused by the fact that the printing material is applied in the rubber phase as the glass temperature lies around 5 degrees. This while other plastics in the construction practice are applied in the solid phase, as their glass temperatures lie above the maximum temperature of sun-heated parts in The Netherlands (80 degrees). Applying a polymer structurally in its rubber phase, is unfeasible, as the low Young's Modulus and poor temperature behavior already evidenced. Therefore the current printing material cannot be applied to create (housing) structures.
2. It can be concluded that within the 3D Print Canal House Project, there is far more expertise for printing within the vertical xz-plane than for printing in the horizontal xy-plane. Probable improvements can be made within the project by acquiring more knowledge for printing within both the planes.
3. The printing material shows clear anisotropic behavior, which means that the strength properties parallel and perpendicular to the direction of the printed lines differ significantly.
4. No problems are expected for the material being exposed towards rain and frost, as the printing material blocks almost all the water. A requirement for the water tightness of the material however is that the printed elements are build up with at least 3 printed layers in the horizontal direction, as often present holes in single printed layers will be filled in that case with a high certainty.
5. The specific heat capacity of the printing material is relatively low, which means that the material insulates air heat well. For a winter situation this is a positive given, but for the situation in the summer it means that measurements need to be taken to prevent the inner of the building for becoming too warm.
6. As the softening point of the material lies on 60 degrees, elements made of the printing material should never be directly exposed to the sun. This means for The Netherlands that this material may never be located in the outer layer of facades that are directed to the East, South or West.
7. The printing material is very sensitive for locally applied forces. This in particular has consequences for the design of connections. Connecting by means of bolts should be avoided.
8. Geometries consisting of members with a thickness of a single printed layer are very sensitive for local failure mechanisms. Local failure mechanism are buckling and bending of individual members or failure at the location of a local inaccuracy. By building up geometries by members consisting of multiple layers instead of one layer, the members will become stiffer, the local and overall strength of geometries become higher and the material is more homogeneous and less sensitive to local inaccuracies.
9. Keeping the span of the individual members within a geometry low, is crucial for increasing the structural performance, because the local spans often form the normative property for structural failure of geometries.
10. For house separating walls between connected houses, the sound insulation requirement is normative and leads to separating walls and floors of about 0.70 m. For façade thicknesses of detached houses, the heat insulation requirement, that leads to a façade-thickness of about 0.30 m, is normative above the sound insulation requirement. Whether the heat insulation requirement for facades also is normative above the structural requirements will depend on the applied dimensions, form and loads of the particular structure.

## 10.2 Recommendations

### General Recommendations

1. It is recommended to define the end-product not as a 'house' but as a 'pavilion' for temporary use. An important advantage of this change in destination is that the requirements will become much lower.
2. For future new or adapted 3D-printers, it is recommended to increase the length and the width of the printing area such that they become (at least) equal to the height. Increasing the width and length of the printing area, increases the design freedom and opens more possibilities to create blocks that are loaded in the strong direction of the material.
3. In case one actually wants to build a house with the current applied printing material, the material is only applicable as a permanent mold for concrete. In that case, the inner holes of a printed geometry can be filled with reinforced concrete and insulating materials. On the outside of the permanent formwork, at least a heat-resistant façade-covering needs to be added.

### Design Recommendations

1. One should always try as much as possible to load the material in the direction of the printed lines, especially when the material is loaded in tension or bending. This because, the material is significantly stronger in this direction and often fails after an initial deformation instead of in a brittle manner.
2. It is strongly recommended to create building blocks that exist of multiple printed layers that are connected to each other within the xy-direction instead of blocks that are built up by only single layers, which so far has been the case. Using multiple layers within the xy-direction leads to a stronger, stiffer, more isotropic, more homogeneous and therefore better predictable material behavior. Another good reason to apply multiple layers in the xy-direction is that the building blocks will become waterproof, that the material becomes less sensitive to local inaccuracies and that the material can easier meet the heat and sound insulation requirements for housing. This means that all individual walls/members of printed geometries should consist of multiple printed layers in the horizontal direction. By this, the individual members become stiffer and the local and overall strength of geometries will become higher. It is advised not to continue with printing single-layer-walled blocks, as these geometries are sensitive to local failure mechanisms. Due to these local failure mechanisms, the material by far is not loaded to its strength capacity. By building up geometry walls with multiple layers, the material capacity is better utilized.
3. One should build up geometries such that multicarrier roads are created within a printed element and spans of the individual members are minimized.
4. It is recommended to apply safety factors over the applied load according to the scheme that is presented in paragraph 7.2.

### Recommendations – Next Steps/Future Research

1. Further research on the improvement of the thermal behavior of printable materials should be performed. Also, the stiffness (Young's Modulus) of the applied printing material needs to be increased. These improvements can probably be made by experimenting with printing of materials that are in a solid state under normal circumstances. The current applied material is in a rubber phase, which leads to the low stiffness and poor strength-temperature behavior.
2. For printability of a material, a low glass, softening and melting temperature and a low molecular weight are preferred. However, for structural application of a material, high temperatures and a high molecular weight are required. The most important challenge for enabling 3d-printing of houses with polymers, is to solve this contradistinction and find an optimum material that is printable and structurally applicable. It therefore is strongly advised to focus future research on the feasibility of 3d-printing with structural applicable polymers. The test results and conclusions of this report can be used as a starting point for this future research.
3. Although improvement of the material to make it structurally feasible has the highest priority, this does not necessarily mean that the design process cannot be continued synchronously to the material development. A proposal for next steps that can be taken in the structural design process as a follow-up to this thesis research, is given under points 4-8 of paragraph 9.4.1.
4. On the moment it would turn out not to be feasible to print structural applicable polymers within a desired time span, then it is recommended to change the focus of the 3D Print Canal House Project

## 10. Conclusions and Recommendations

from printing a complete house with printable polymers to the printing of formwork using printable polymers. In that case, the material and printing technique would need to be optimised for printing molds. For formwork, the requirements are significantly lower and therefore simpler achievable than the requirements for structural application.

5. The particular situation of the 3D Print Canal House project can act as an interesting case study for performing next steps towards an integrated computational design tool for (at least) architectural and structural design.
6. Finally it can be interesting to perform a study to the economical/commercial feasibility of 3d-printing houses and other structures, by using printable polymers.

### **Practical recommendations that support future research**

1. Data-values on factsheets that are provided by Henkel, should not be used for structural design. This because the property values of the material once it is printed, differ significantly from the values on the Henkel-sheets. When one wants to use the Henkel-sheets for obtaining a quick indication of the capability of a new material, it is advised to multiply the mechanical properties on the Henkel-sheet with a factor 0.5 and the thermal properties with a factor 0.4.
2. On the moment a new printing material is developed, it is recommended to first and foremost perform the strength-temperature test (paragraph 5.7) on this new material. This because, the temperature behavior is the weakest and therefore most critical characteristic of the current printing material so new materials should especially show improvement for this property.
3. It is advised to study the influence of the printing resolution on the strength properties of the material.
4. It is recommended to experiment with printing perpendicular printed layers on top of each other. This means that if a layer is directed to the x-direction, the layer on top of it is directed in the y-direction (other horizontal direction) and the next layer again in the x-direction etc. In this way, it might be the case that the anisotropic behavior of the material will be reduced or even eliminated.
5. More extensive research on the creep behavior of the material is required before it can be applied with full safety.
6. Once the designing parties decide to continue building up geometries by thin members consisting of only one printed layer, it is highly recommended to perform research on the hardness of the printing material.
7. It is recommended for future research to study the fatigue behavior of the printing material, because this can be a normative failure mechanism, especially around connections.

**This page has been left blank intentionally**

# Appendices

## Appendix I – Determination method average value, characteristic value and standard deviation of test results.

For most of the tests that are described within this research report, it holds that from the obtained test results, the average value, the characteristic value and the standard deviation are determined. These values are determined according to the determination method that is described in [NEN-EN 1990+A1+A/C2, ch. 7, p. 106-107] and presented below:

[NEN-EN 1990+A1+A/C2, ch. 7, p. 106-107] gives the following formula for determination of the design value of a property X:

$$X_d = \eta_d \cdot \frac{X_{k(n)}}{\gamma_m} = \frac{\eta_d}{\gamma_m} \cdot m_x \{1 - k_n V_x\} \tag{I.1}$$

With:

- $\eta_d$  is the design value of the conversion factor, this factor depends on the testing method and material type. Because the standards EN 1992 to EN 1999, to which is referred within [NEN-EN 1990+A1+A/C2, ch. 7, p. 106-107] for determination of  $\eta_d$ , only include values for common applied structural materials, the value of  $\eta_d$  is included within the partial factor  $\gamma_m$ .
- $\gamma_m$  is a partial factor that needs to be chosen in accordance with the application area of the test results. This material factor of safety will be taken into account on the moment that the printing material will be applied within a structure. This factor then can be determined according to the rules of paragraph 7.2 of this report. For determination of the characteristic strength values, this factor is not taken into account yet and therefore chosen as 1.0 during the determination of the characteristic strength values.
- $m_x$  is the average value of the series of measured values
- $k_n$  is a factor for taking into account the effect of the amount of tested specimens on the characteristic values. The value of  $k_n$  differs for the different performed test within this research, because the amount of tested specimens also varies. For every test, a factor  $k_n$  that coincides with the amount of tested specimens  $n$  of the particular test, is picked from the table below:

$n$	1	2	3	4	5	6	8	10	20	30	$\infty$
$V_x$ bekend	2,31	2,01	1,89	1,83	1,80	1,77	1,74	1,72	1,68	1,67	1,64
$V_x$ niet bekend	-	-	3,37	2,63	2,33	2,18	2,00	1,92	1,76	1,73	1,64

**Table I.1 Table to determine the  $k_n$ -factor from the amount of tested specimens  $n$**

-  $V_x$  is the variation coefficient and can be determined with the formulas below:

$$V_x = \frac{s_x}{m_x} \tag{I.2}$$

with  $s_x$  is the standard deviation that can be found by formula I.3:

$$s_x^2 = \frac{1}{n-1} \sum (x_i - m_x)^2 \tag{I.3}$$

with:

- $n$  is the amount of tested specimens in the performed test.
- $x_i$  is an individual measurement value

By applying the formulas from [NEN-EN 1990+A1+A/C2, ch. 7, p. 106-107] that are described above, it is possible to determine the characteristic value (formula I.1) and the standard deviation (formula I.3) for the tests that are performed within this research.

## Appendix II –Inaccuracies in dimension measurements

In the result tables of the elementary mechanical tests of chapter 5, the width and thickness of the tested cross section are given. Multiplying this width and thickness leads to the cross-sectional area by which the force, that is applied by the testing device, is divided.

The width and thickness of the cross-section are measured by means of a caliper that is able to measure the dimensions with an accuracy of 0.1 millimeter. The accuracy of the measured thickness of the sample however is lower. This is caused by the given that the printed specimens do not have a uniform thickness.

This non-uniform thickness is a consequence of the FDM-printing-technology, that lays down the material layer by layer, which leads to a bumpy specimen profile as can be observed on the figure below:

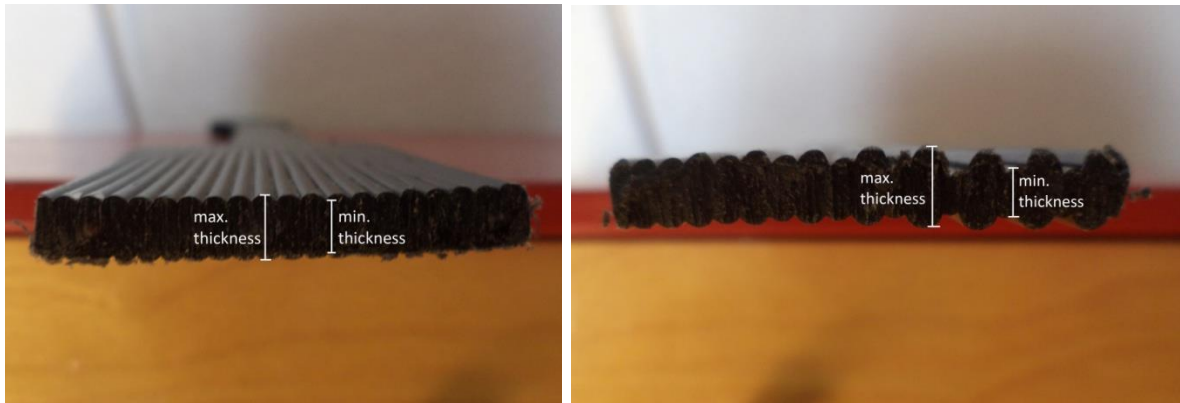


**Fig. II.1 Cross-sectional thickness variations in printed specimens**

As can be observed on the above pictures, the deviation of the thickness of a sample, differs per sample. For the most 'perfect' printed sample (like the picture on the left of figure II.1), printed in the xz-direction, the measured difference between the minimum and maximum thickness of the sample is 0.5 mm. For the 'untidiest' printed tensile sample in the xz-direction (like the picture on the right of figure II.1), this difference is 2.2 mm.

Because the pattern of the bumps for a single sample, is quite even, it might seem most logical to pick the average thickness of the sample for samples that are loaded in the grain direction. However, if one quickly measures the thickness of a printed element in practice, the chance is big that the maximum thickness of the element will be measured. This because when clamping the caliper around an element in the direction perpendicular to the direction of the printed lines, the maximum thickness of the sample will be measured. It is for that reason, that there is chosen to use the maximum thickness of a specimen as the actual thickness that is used for calculation of the cross-section and the strength. In this way it is certain that the strength values that are obtained from the mechanical tests, are on the safe side.

For samples that are loaded perpendicular to the grain direction, and therefore printed in the other direction, it would be most logical to choose the minimum thickness, because it is likely that the sample will fail over a cross-section where the thickness is minimal. However, also for these samples, the maximum sample thickness is taken, again to be on the safe side.

Because the maximum difference between the chosen maximum thickness and the average thickness of a sample is  $2.2/2 = 1.1$  mm and the minimum difference is  $0.5/2 = 0.25$  mm, the chosen margin for the thickness of samples that are printed in xz-direction and tested parallel to the grain lies between 0.25-1.1 mm. With an average sample thickness of about 6.0 mm, this means that this margin forms between 4.17-18.33 % of the thickness. This also means that the calculated strength values in practice can be 4.17-18.33% higher than measured, due to the chosen inaccuracy margin. For samples that are printed in xz-direction and tested perpendicular to the grain, this inaccuracy margin is 0.5-2.2 mm, which means an influence of the strength of between 8.35 and 36.67%. Again, as explained, it is wise that the maximum thicknesses are chosen for calculation of the strength, because in practice it is likely that the maximum thickness often will be measured as well.

In most cases, the laser cutter was not able to fully cut through the printed plate. Therefore these specimens partly needed to be sawn. Sawing of the samples lead to non-uniform specimen widths, because the samples

were not sawn completely straight and accurate. The maximum width range of a sample was 2.0 mm. Although the chance is high that a test sample fails in the cross-section with the minimum width, the average width of the sample is taken here, again to be on the safe side. This means that the inaccuracy of the presented width values is  $2.0/2 = 1.0$  mm. With an average width of 20.0 mm, this means that the influence of the chosen width margin on the actual width and strength is  $1.0/20 = 5\%$ .

If the width and thickness margin are put together for specimens that are tested parallel to the grain, the total influence of the chosen measurement margins on the cross sectional area and the strength lies between 9.4-24.2%. This is a relatively high margin, but necessary, as it is likely that inaccurate measurements will be performed in practice in the order of magnitude that is taken here.

For test specimens that were directly printed (these are the specimens that are printed in the xy-direction), the dimensional deviations are bigger than for the specimens that are cut from plates (samples printed in xz-direction). This is due to the given that direct printing of specimens led to more inaccurate samples than cut samples, as is mentioned in chapter 4. The deviations and subsequent inaccuracies of samples printed in the xy-direction are determined in the same manner as for xz-directed samples.

In the table below, an overview is given of the deviations and dimensional measurement inaccuracies of the different tested samples. It is important to repeat that the dimensions, that are chosen for calculation of the cross-sectional area and strength, are on the safe side.

Specimen type	Used in	Inaccuracy margin thickness	Inaccuracy margin width	Influence margin on strength
Dumbbell xz-printed, tested parallel to grain	Tensile test, Young's Modulus test, Strength-temperature test, Creep test	-0.25 to -1.1 mm	$\pm 1.0$ mm	9.4 to 24.2 %
Dumbbell xz-printed, tested perpendicular to the grain	Tensile test, Young's Modulus test	-0.5 to -2.2 mm	$\pm 1.0$ mm	13.8 to 43.5 %
Dumbbell xy-printed, tested parallel to grain	Tensile test, Young's Modulus test	-0.6 to -2.4 mm	$\pm 1.5$ mm	18.3 to 50.5%
Dumbbell xy-printed, tested parallel to grain	Tensile test, Young's Modulus test	-0.6 to -2.4 mm	$\pm 1.5$ mm	18.3 to 50.5%
Shear specimen xz-printed	Shear test	-0.25 to -1.1 mm	$\pm 0.3$ mm	10.4 to 25.4 %
Shear specimen xy-printed	Shear test	-0.5 to -2.5 mm	$\pm 1.0$ mm	51.6 to 70.0 %
Solid cube	Compressive test, Absorption and drying test	0.3 to 0.5 mm	0.5 to 1.0 mm	1.6 to 3.0 %

**Table II.1 Overview of dimensional measurement inaccuracies for the different tested samples**

In the table above, it can be observed that the samples of the compressive test can be measured most accurately. This is due to the fact that these samples are much thicker than the other samples and because multiple layers are printed in both directions. This leads to clotting of printed layers into a homogeneous composition, and therefore only relief on the surfaces and not within the blocks. By printing multiple layers in both directions, the influence of possible measurement inaccuracies due to bumps, therefore becomes lower. This again is an advantage of printing compositions consisting out of multiple printed layers.

## Appendix III – Obtained Material Properties



**Tensile Strength Properties**

Material Properties xz- direction (printed in vertical plane)	Symbol	Average Value	Standard deviation	Characteristic Value	Material Properties xy- direction (printed in horizontal plane)	Symbol	Average Value	Standard deviation	Characteristic Value
Tensile strength // [MPa]	$f_{t,0,xz}$	8.33	1.07	6.45	Tensile strength //	$f_{t,0,xy}$	7.03	1.83	3.78
Tensile strength $\perp$ [MPa]	$f_{t,90,xz}$	5.16	1.62	2.28	Tensile strength $\perp$	$f_{t,90,xy}$	8.19	0.73	6.90
Tensile breaking strength // [MPa]	$f_{f,0,xz}$	7.05	1.21	4.83	Tensile breaking strength //	$f_{f,0,xy}$	n.a.	n.a.	n.a.
Tensile breaking strength $\perp$ [MPa]	$f_{f,90,xz}$	5.16	1.62	2.28	Tensile breaking strength $\perp$	$f_{f,90,x}$	6.3	n.a.	n.a.
Yield strength // [MPa]	$f_{y,0,xz}$	7.3	0.97	5.6	Yield strength //	$f_{y,0,xy}$	6.6	1.72	3.6
Yield strength $\perp$ [MPa]	$f_{y,90,xz}$	4.8	1.55	2.1	Yield strength $\perp$	$f_{y,90,xy}$	7,5	8,2	6,6
Elongation at tensile strength // [%]	$\epsilon_{t,0,xz}$	17.8	n.a.	n.a.	Elongation at tensile strength //	$\epsilon_{t,0,xy}$	15.6	n.a.	n.a.
Elongation at tensile strength $\perp$ [%]	$\epsilon_{t,90,xz}$	12.6	n.a.	n.a.	Elongation at tensile strength $\perp$	$\epsilon_{t,90,xy}$	16.4	n.a.	n.a.
Elongation at break //	$\epsilon_{f,0,xz}$	90.2	n.a.	n.a.	Elongation at break //	$\epsilon_{f,0,xy}$	150	n.a.	n.a.
Elongation at break $\perp$ [%]	$\epsilon_{f,90,xz}$	12.6	n.a.	n.a.	Elongation at break $\perp$	$\epsilon_{f,90,xy}$	132.5	n.a.	n.a.

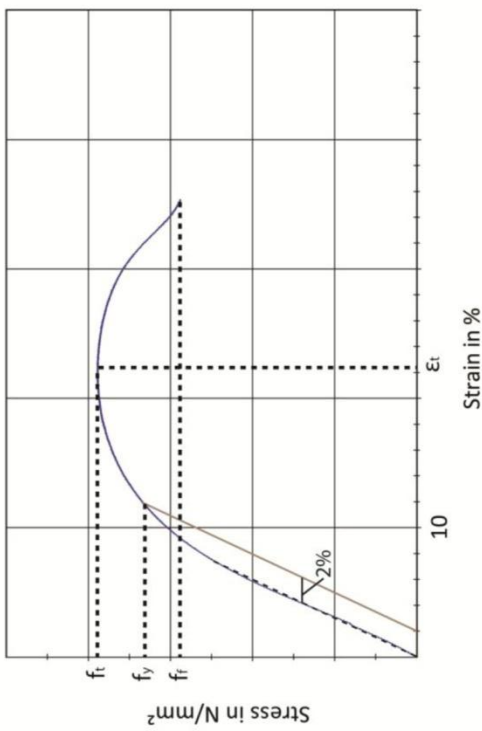


Fig. III.1 Tensile Properties as determined from Stress-Strain graph

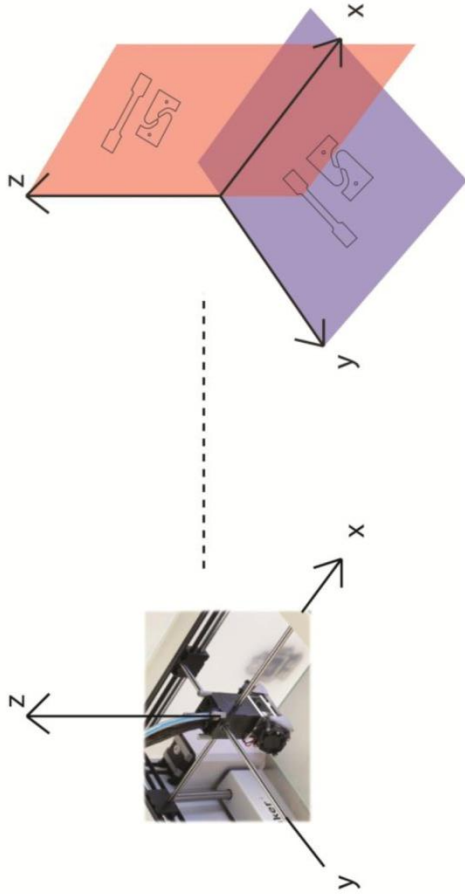


Fig. III.2 Vertical xz-plane and horizontal xy-plane

**Shear Strength Properties**

Material Properties xz-direction	Symbol	Average Value	Standard deviation	Characteristic Value	Material Properties xy-direction	Symbol	Average Value	Standard deviation	Characteristic Value
Shear strength // [MPa]	$f_{s,0,xz}$	6.9	1.68	4.0	Shear strength //	$f_{s,0,xy}$	5.0	1.28	2.7
Shear strength ⊥ [MPa]	$f_{s,90,xz}$	5.8	1.19	3.7	Shear strength ⊥	$f_{s,90,xy}$	5.0	2.29	0.9

**Young's Moduli**

Material Properties xz-direction	Symbol	Average Value	Standard deviation	Characteristic Value	Material Properties xy-direction	Symbol	Average Value	Standard deviation	Characteristic Value
E-modulus 0°-direction [MPa]	$E_{0,xz}$	160.2	14.14	131.8	E-modulus 0°-direction [MPa]	$E_{0,xy}$	121.3	11.53	98.1
E-modulus 90°-direction [MPa]	$E_{90,xz}$	129.6	12.59	104.3	E-modulus 90°-direction [MPa]	$E_{90,xy}$	129.6	24.54	80.2
E-modulus 45°-direction [MPa]	$E_{45,xz}$	121.4	13.72	93.8	E-modulus 45°-direction [MPa]	$E_{45,xy}$	119.4	47.66	23.6

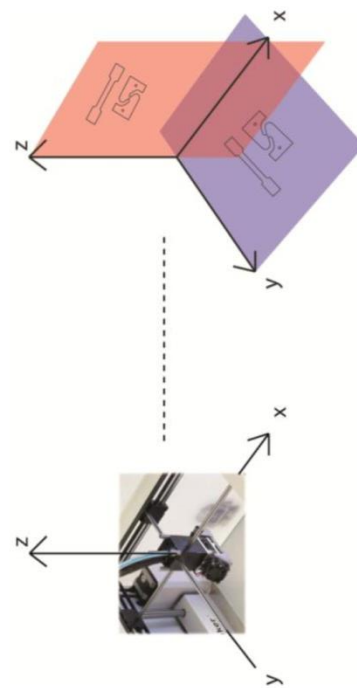


Fig. III.3 Vertical xz-plane and Horizontal xy-plane

**Compressive Strength Properties**

Material Properties	Symbol	Direction 1			Direction 2			Direction 3		
		Average Value	Standard deviation	Characteristic Value	Average Value	Standard deviation	Characteristic Value	Average Value	Standard deviation	Characteristic Value
Compressive strength [MPa]	$f_{c1}, f_{c2}, f_{c3}$	18.7	0.66	17.5	18.6	0.69	17.4	19.1	0.53	18.2
Compressive strain [%]	$\epsilon_1, \epsilon_2, \epsilon_3$	26.8	n.a.	n.a.	29.2	n.a.	n.a.	27.4	n.a.	n.a.
Compressive Yield Strength [MPa]	$f_{y1}, f_{y2}, f_{y3}$	13.7	0.92	12.1	13.8	0.61	12.7	14.4	0.18	14.1
Compressive Yield Strain [%]	$\epsilon_{y1}, \epsilon_{y2}, \epsilon_{y3}$	15.0	n.a.	n.a.	17.0	n.a.	n.a.	16.3	n.a.	n.a.
Compressive Modulus [MPa]	$E_{c1}, E_{c2}, E_{c3}$	135	8.66	120	122	10.27	104	145	17.17	114

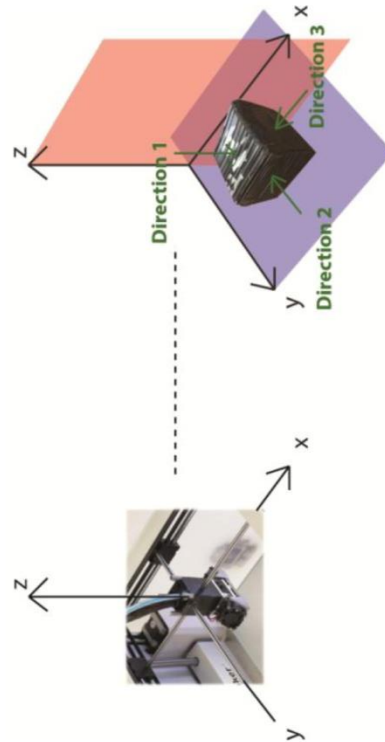


Fig. III.4 Directions Compressive Load in relation to print-planes

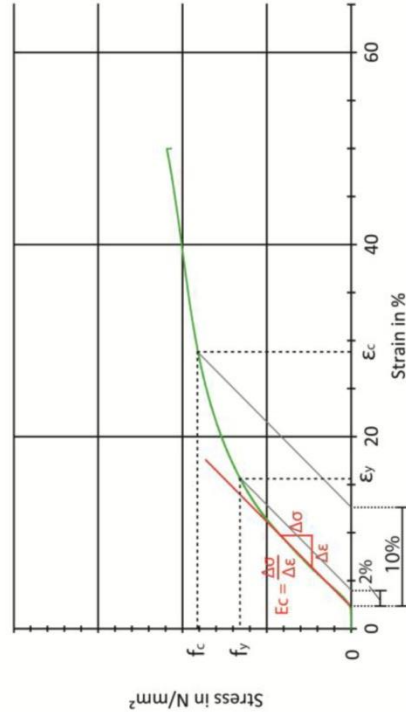


Fig. III.5 Determination of properties from stress-strain curve

**DSC Test Results**

Material Properties	Symbol	Unit	Test sample 1			Test sample 2			Average Value
			Average	Maximum	Room temperature	Average	Maximum	Room temperature	
mass	m	mg	15.12			9.04			
Specific Heat Capacity	c	J/g°C	2.33	2.72	2.2	2.34	2.71	2.0	
Softening point/temperature	T <sub>soft</sub>	°C	64			62			63.0
Melting point/temperature	T <sub>melt</sub>	°C	87			84			85.5
Solidification temperature	T <sub>solid</sub>	°C	42			45			43.5

**Density**

Material Property	Symbol	Value
Density Henkel-sheet [g/cm <sup>3</sup> ]	$\rho_{\text{Henkel}}$	0.98

**Water Absorption**

Material Property	Value
Maximum Absorption [weight %]	0.081

**Strength Properties under different temperatures**

Material Properties xz-direction												
Estimated actual surface temp. [°C]	-30	-19	-8	3	14	15-22	23-30	27-38	42	45	58	69
Ultimate tensile strength // [MPa]	19.07	20.27	16.21	14.69	11.59	8.33	8.25	4.93	2.77	1.64	1.65	0.57
Elongation at ultimate tensile strength // [%]	16.3	20.3	24.4	33.0	23.3	20.2	15.5	13.9	26.8	28.0	9.1	23.9

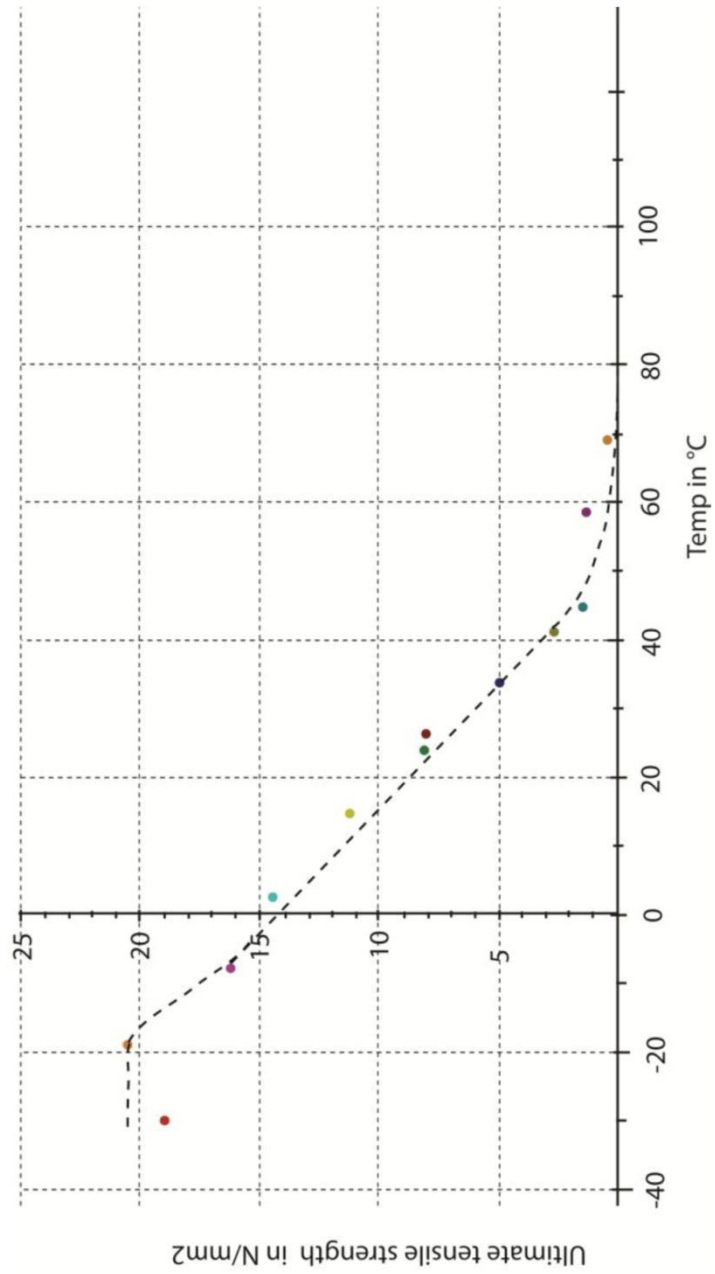
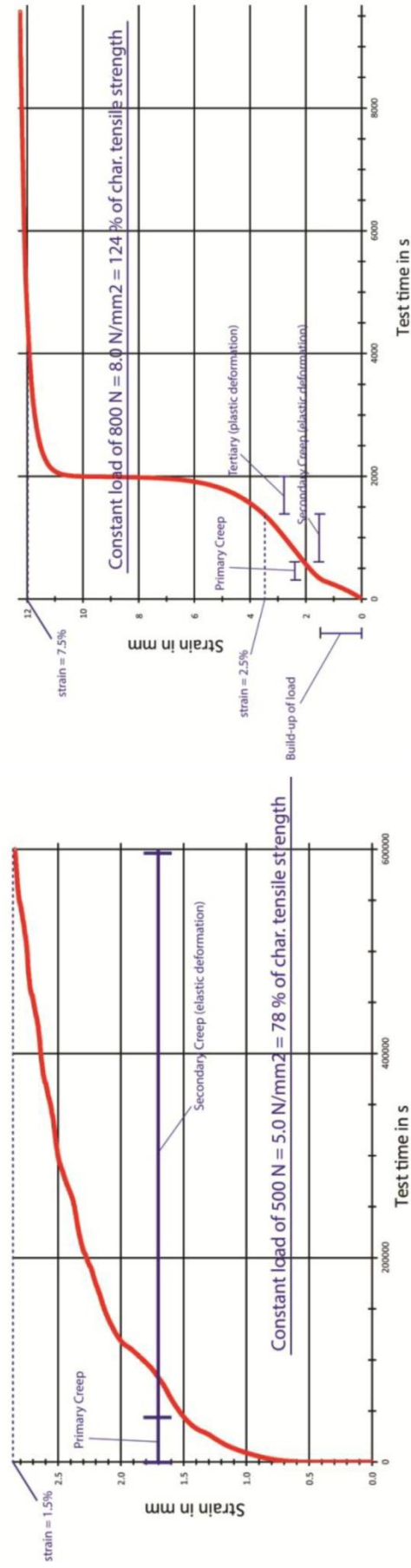


Fig. III.6 Strength-Temperature Curve

**Creep**

Material Property	Symbol	Value
Creep strain at approx. 80% of char. strength after 10.000 minutes [%]	$\epsilon_{\text{creep, end, 80\%}}$	1.5
Initial creep strain at approx. 80% of char. Strength [%]	$\epsilon_{\text{creep, init, 80\%}}$	0.94
Max. obtained strain at approx. 125% of strength [%]	$\epsilon_{\text{creep, end, 125\%}}$	7.5
Initial creep strain at approx. 125% of char. Strength [%]	$\epsilon_{\text{creep, init, 125\%}}$	1.3



**Fig. III.7 Left: Creep curve at 80% of char. strength; Right: Creep curve at 125% of char. strength**

### Compressive Strength – Square hollow sections

Material Properties	Direction 1			
	Symbol	Average Value	Standard deviation	Characteristic Value
Compressive strength [MPa]	$f_{cr,hollow}$	2.13	0.24	1.70
Compressive strain [MPa]	$\epsilon_1, \epsilon_2, \epsilon_3$	9.66	n.a.	n.a.

### Flexural Strength Properties

Material Properties	Symbol	Unit	Average Value	Standard Deviation	Characteristic Value
Flexural strength //	$f_{f,0}$	MPa	13.8	0.93	12.1
Flexural strength $\perp$	$f_{f,90}$	MPa	14.0	1.07	12.0
Flexural Modulus //	$E_{f,0}$	MPa	355.0	16.86	323.1
Flexural Modulus $\perp$	$E_{f,90}$	MPa	286.7	45.10	201.4
Flexural strain //	$\epsilon_{f,0}$	%	3.9	0.17	3.6
Flexural strain $\perp$	$\epsilon_{f,90}$	%	5.0	201.4	3.9



# Bibliography

## Articles

- Bao, Y., Wierzbicki, T., 2004, On fracture locus in the equivalent strain and stress triaxiality space. *Int J Mech Sci*, 2004;46, p. 81–98.
- Franks, F., 2003, Nucleation of ice and its management in ecosystems, *A Philosophical Transactions of the Royal Society* 361, p. 557-574.
- Middelton, J.C., Tipton, A.J., 2000, Synthetic biodegradable polymers as orthopedic devices, *Biomaterial* 21 (23), p. 2335-2346.
- Reyes A., Eriksson M., Lademo O.-G., Hopperstad O.S. and Langseth M., 2009, Assessment of yield and fracture criteria using shear and bending tests. *Materials and Design* 30, p. 596-608.
- Södergard, A., Stolt, M., 2002, Properties of lactic acid based polymers and their correlation with composition, *Progress in Polymer Science* 27 (6), p. 1123-1163.
- Tarigopula, V. et al., 2008, A study of large plastic deformations in dual phase steel using digital image correlation and FE analysis, *Exp. Mech.* 48, p. 181-196.
- Whitney, J.M., Knight, M., 1979, The relationship between tensile strength and flexure strength in fiber-reinforced composites, *SESA Spring Meeting*

## Books

- Betten, J., 2005, *Creep Mechanics: 3rd ed.* Berlin Heidelberg: Springer-Verlag.
- Domone, P., Illston, J., 2010, *Construction Materials: Their Nature and Behavior, Fourth Edition.* Boca Raton, Florida: CRC Press.
- Gilmore, C., 2014, *Material Science and Engineering Properties.* Boston, Massachusetts: Cengage Learning.
- Harrington, J.P., 1997, *SPE/ANTEC 1997 Proceedings.* Boca Raton, Florida: CRC Press.
- Hartsuijker, C., 2005, *Toegepaste Mechanica: Deel 2: Spanningen, vervormingen, verplaatsingen.* Den Haag: Academic Service.
- Hartsuijker, C., Welleman, H., 2007, *Constructiemechanica 3, deel 3 Bijzondere onderwerpen 1.* Den Haag: Academic Service.
- Hosein, A., 2009, *Creep of Fiber Reinforced Polymer (FRP) Pile Materials.* Ann Arbor: ProQuest LLC.
- Kamerling, M.W., Bakker H.E., 2004, *Jellema 7 Bouwmethodek.* Utrecht/Zutphen: ThiemeMeulenhoff.
- Kenneth, G., Budinski, 2009, *Materiaalkunde.* New Jersey: Pearson Education.
- Krusche, P. & Kruschke, M. & Althaus, D. & Gabriel, I., 1982, *Ökologisches Bauen,* Wiesbaden und Berlin: Umweltbundesamt, Bauverlag GMBH.
- Meyers M.A. and Chawla K.K., (1999), *Mechanical Behavior of Materials.* Cambridge: Cambridge University Press.
- McCrum, N.G, Buckley, C.P; Bucknall, C.B., 2003, *Principles of Polymer Engineering.* Oxford: Oxford Science Publications.
- Rosato, D. V., 2003, *Plastics Engineered Product Design,* Oxford: Elsevier
- Titow, W.V., 1984, *PVC Technology,* Dordrecht: Springer Science & Business Media.
- Ullman, D.G., 2003, *The Mechanical Design Process.* New York: McGraw-Hill.
- Verver, M.W., Fraaij, A.L.A., 2004, *Materiaalkunde.* Groningen: Noordhoff Uitgevers B.V.

## Internet Sources

- 3ders. <http://www.3ders.org/articles/20140324-arevo-labs-introduces-carbon-fiber-reinforced-polymers-to-3d-print-ultra-strong-parts.html>. Cited: 24 August 2014.
- 3D Printwereld. <http://www.3dprintwereld.com/41..> Cited: 24 August 2014.
- Agilent Technologies. <https://www.chem.agilent.com/Library/technicaloverviews/Public/5990-7890EN.pdf>. Cited: 24 August 2014.
- Biostruct. [http://www.biostructproject.eu/fileadmin/MEDIEN/Training/Material/1-New\\_eWPC\\_materials.pdf](http://www.biostructproject.eu/fileadmin/MEDIEN/Training/Material/1-New_eWPC_materials.pdf). Cited: 24 August 2014.
- Composites World. <http://www.compositesworld.com/articles/medical-applications-a-healthy-market>. Cited 24 August 2014.
- Contour crafting. <http://www.contourcrafting.org/>. Cited: 24 August 2014.

- D-shape. <http://www.d-shape.com/tecnologia.htm>. Cited: 24 August 2014.
- Engineering Archives. [http://www.engineeringarchives.com/les\\_mom\\_tensiletest.html](http://www.engineeringarchives.com/les_mom_tensiletest.html). Cited: 13 June 2014.
- Federal Highway Administration. <http://www.fhwa.dot.gov/publications/research/infrastructure/structures/06103/chapt3.cfm>. Cited: 13 June 2014.
- Granta. <http://www.grantadesign.com/education/edupack/edupack2014.htm>. Cited: 24 August 2014.
- Henkel. Macromelt, [http://henkel.com/com/content\\_data/248495\\_AG11038\\_FL\\_Macromelt\\_Biokunststoff\\_ENGL\\_Screen.pdf](http://henkel.com/com/content_data/248495_AG11038_FL_Macromelt_Biokunststoff_ENGL_Screen.pdf). Cited: 24 August 2014.
- Instron Glossary. <http://www.instron.us/wa/glossary/Yield-Strength.aspx>. Cited 24 August 2014.
- KNMI. [http://www.knmi.nl/cms/content/21416/tropische\\_dagen](http://www.knmi.nl/cms/content/21416/tropische_dagen). Cited 14 November 2014.
- Matweb. <http://www.matweb.com/reference/tensilestrength.aspx>. Cited: 13 June 2014.
- Mechmecca blogspot. [http://mechmecca.blogspot.nl/2012\\_03\\_20\\_archive.html](http://mechmecca.blogspot.nl/2012_03_20_archive.html). Cited: 13 June 2014.
- Mobiel.nu. <http://mobiel.nu.nl/gadgets/3482847/markt-rond-3d-printen-blijft-snel-groeien.html>. Cited: 24 August 2014.
- Octoprint. <http://www.octoprint.org>. Cited: 24 August 2014.
- Scielo Brazil. [http://www.scielo.br/scielo.php?script=sci\\_arttext&pid=S1516-14392010000100014](http://www.scielo.br/scielo.php?script=sci_arttext&pid=S1516-14392010000100014). Cited: 13 June 2014.
- Vircon Composites. [http://www.vircon-composites.com/4\\_1\\_4.asp/](http://www.vircon-composites.com/4_1_4.asp/). Cited: 13 June 2014.
- Virginia edu. <http://people.virginia.edu/~lz2n/mse209/Chapter15c.pdf>. Cited: 13 June 2014.

## Interviews

Marchese, L., Henkel, 2014

## Standards

- NEN-EN 12814-2 (en) (2000). Testing of welded joints of thermoplastics semi-finished products – Part 2: Trekproef.
- NEN-EN 15801 (en) (2009). Conservation of cultural property – Test methods – Determination of water absorption by capillarity.
- NEN 5077: 2006+C3 (2012). Geluidwering in gebouwen.
- NEN-EN-ISO 178 (en) (2010). Kunststoffen – Bepaling van de buigeigenschappen.
- NEN-EN 1990+A1+A1/C2 (nl) (2011), Eurocode: Grondslagen van het constructief ontwerp.

## List of Figures

Fig. 1 Composition of the building out of Chambers and printable Blocks/Elements .....	2
Fig. 2 Provisional Block Design in the form of a Honeycomb structure [source: DUS Architects] .....	2
Fig. 3 Visualisation of the structural problems within the Building project.....	6
Fig. 4 Research Methodology .....	8
Fig. 5 Due to gravity and consequential spreading of the material, different line thicknesses and resolutions are obtained in the xy-plane and the xz-plane.....	11
Fig. 6 The thickness of printed lines can be varied between 1.7 and 2.7 mm in the xz-plane and between 3.0 and 6.0 mm in the xy plane.....	12
Fig. 7 These three processes probably cause a difference in layer-connectivity between the xy-plane and the xz-plane .....	12
Fig. 8 A difference in strength properties is expected between the two printed planes and between the 'grain directions' .....	13
Fig. 9 Principle of the FDM-technique, which is the applied 3D-printing technique in the Canal House Project [Mechmecca blogspot, 2014] .....	14
Fig. 10 Common dimensions for a dumbbell specimen [NEN-EN 12814-2, ch. 6, p. 10-12] .....	20
Fig. 11 Due to the low printing resolution, the dimensions of the specimen shown in Figure 10 are enlarged to obtain more satisfactory specimen results.....	20
Fig. 12 Test setup of the tensile test [Engineering archives, 2014].....	20
Fig. 13 Common used specimens in a shear test [SciELO Brazil, 2014] .....	21
Fig. 14 Applying the usual shear specimens requires specific and complex tools [Vircon Composites, 2014].....	21
Fig. 15 Alternative shear specimen with a butterfly formed shear area. This specimen can be tested within a regular tensile test device, without the need of complex tools [Tarigopula, 2008] .....	21
Fig. 16 Dimensions of the shear test specimen [Reyes, 2009] .....	22
Fig. 17 Solid cube test specimen for the Compressive Test .....	22
Fig. 18 Test setup for the compressive test [Federal Highway Administration, 2014] .....	23
Fig. 19 Test setup for the determination of the Young's Modulus. An extensometer is applied to perform an accurate measurement over the gauge area [Mathweb, 2014] .....	23
Fig. 20 Common form of a temperature-strength curve.....	24
Fig. 21 Common form of a creep curve .....	24
Fig. 22 Overview of the required specimens for the different tests .....	25
Fig. 23 The original dimensions of the shear-specimens are doubled for the specimens that are printed within the xy-direction, since the resolution of the printer was not sufficient for printing the specimens in their original size .....	27
Fig. 24 3D-cad designs of the test specimens.....	28
Fig. 25 Cad-drawing of the path that need to be followed by the printer head .....	29
Fig. 26 Screenshot of Octoprint, the software-program in which the printer can be controlled. The printer resolution can be set in this program by adapting the printing parameters speed, pressure and height of the printer head.....	29
Fig. 27 Shear-specimens printed within the 'Kamermaker' .....	29
Fig. 28 Final result of the samples that are directly printed by the 'Kamermaker' within the xy-plane .....	30

Fig. 29 Within the building project, so far only single lines are printed within the xy-direction. So printing connecting parallel lines in the horizontal plane, like is done for the samples in Figure 27, was a novelty.....	30
Fig. 30 Efficient division of the specimens over the plates that will be printed within the xz-direction .....	31
Fig. 31 Printable structure consisting of the required plates out of which the specimens can be cut later on .....	31
Fig. 32 Internal curves and large inaccuracies on the plates, due to the absence of an internal structure in the printed block .....	32
Fig. 33 Laser cutting the specimens out of the plates that are printed within the vertical direction..	32
Fig. 34 Attempts to decrease the curvatures of the plates by placing weights on the plates and curving them in the opposite direction of the internal curve.....	33
Fig. 35 Left: in case of straight plates, the samples are perfectly cut out from the plates. Right: In case of curved plates, the laser did not fully cut through the plate, such that using a fretsaw was required to obtain the sample. ....	33
Fig. 36 End result of the laser cut specimens .....	33
Fig. 37 Left: the specimens that are directly printed within the xy-plane. Right: Specimens that are laser-cut from plates that are printed within the xz-plane.....	34
Fig. 38 Obtaining the different tensile properties from the stress-strain curve.....	35
Fig. 39 Applied test specimen.....	36
Fig. 40 Test setup of the tensile test. On the left a xz-sample is tested, on the right picture a xy-sample. ....	37
Fig. 41 Left: Specimens printed in the xz-plane and loaded in the grain direction, after they have been tested. Right: Curves of the tests specimens .....	37
Fig. 42 Left: Tested xz-samples that have their grains perpendicular to the load direction. Right: Stress-Strain curves of these tested samples.....	38
Fig. 43 Left: Samples that are loaded 45 degrees to the grain direction and their curves .....	39
Fig. 44 Comparison between the samples loaded parallel (0°), perpendicular (90°) and 45° to the grain.....	40
Fig. 45 Samples printed in the xy-plane after they are loaded parallel to the grain, and their stress-strain curves .....	41
Fig. 46 Samples that are printed in the xy-plane and loaded perpendicular to the grain direction....	42
Fig. 47 Samples that are printed in the xy-plane and loaded 45 degrees to the grain direction.....	43
Fig. 48 Left: Specimen dimensions of the xz-samples. Right: Specimen dimension of the xy-samples. ....	47
Fig. 49 Test setup for shear specimens that are printed in the xz-direction. These samples can be simply clamped within the same tools as used for the tensile test.....	47
Fig. 50 Left: A steel block is used to ensure that the shear area of the specimen falls in the same line as the middle point of the clamps. Right: A caliper is used to check that the specimen is placed fully straight in the two clamps.....	48
Fig. 51 Shear samples printed in the xz-plane and loaded in shear perpendicular to the grain direction .....	48
Fig. 52 Samples printed in the xz-plane and loaded in shear parallel to the grain. ....	50
Fig. 53 Specimens printed within the xz-plane and loaded 45 degrees to the grain .....	51

Fig. 54 Comparison between the shear specimens that are loaded such that the shear forces work perpendicular to the grain (0°), parallel to the grain (90°) and 45 degrees to the grain.....	52
Fig. 55 Test setup for shear specimens that are printed within the xy-plane.....	53
Fig. 56 Test specimens printed within the xy-plane and loaded in shear perpendicular to the grain direction .....	54
Fig. 57 Shear curves of the specimens loaded in shear perpendicular to the grain .....	54
Fig. 58 Tested specimens that are printed within the xy-plane and loaded in shear parallel to the grain.....	55
Fig. 59 Force-displacement curves of the specimens loaded in shear parallel to the grain .....	55
Fig. 60 Tested samples printed in the xy-plane and loaded in shear 45 degrees to the grain.....	56
Fig. 61 Shear curves of the tested samples that are shown on Figure 60.....	56
Fig. 62 Determination methods of the different compressive properties out of the stress-strain curve .....	58
Fig. 63 Different loading directions for the cubical compressive specimens.....	59
Fig. 64 Test setup compressive test .....	59
Fig. 65 Test specimens that are loaded in direction 1.....	60
Fig. 66 Stress-strain curves of the specimens that are loaded in direction 1 .....	60
Fig. 67 Test specimens loaded in direction 2 .....	61
Fig. 68 Stress-strain curves of the specimens tested in direction 2 .....	62
Fig. 69 Tested specimens that were loaded in direction 3.....	63
Fig. 70 Stress-strain curves of the specimens that were tested in direction 3, which is the direction parallel to the grain .....	63
Fig. 71 Specimen dimensions .....	65
Fig. 72 Test setup for the determination of the Young's moduli .....	66
Fig. 73 Stress strain curves of the specimens that are printed within the xz-plane. Specimens that are loaded parallel to the grain, perpendicular to the grain and 45 degrees to the grain, all can be found in this figure.....	67
Fig. 74 Stress-strain curves of the specimens that were printed within the xy-plane.....	67
Fig. 75 Tested specimen types for the density test.....	69
Fig. 76 Test setup density test.....	69
Fig. 77 By immersing the test sample and collecting the water that flows over the edge, the volume of the test specimen is determined .....	70
Fig. 78 Used test samples for the Absorption and Drying tests .....	71
Fig. 79 Test setup absorption test.....	72
Fig. 80 Test setup submersion/drying test.....	72
Fig. 81 Maximum and minimum surface temperature curves in the summer respectively winter [Source: Krusche et al., 1982].....	74
Fig. 82 Test setup Temperature-Strength test .....	76
Fig. 83 Tested specimens and their surface-temperatures during the test.....	77
Fig. 84 Stress-strain curves of all the tested specimens. The surface temperatures of the specimens during the test are indicated at the end of each curve.....	78
Fig. 85 Strength-temperature curve obtained from the curves of Figure 84.....	78
Fig. 86 Tested sample within aluminum cup.....	81
Fig. 87 Used DSC-7 device (left) and tested sample placed within device (right).....	82
Fig. 88 DSC curves of two tested samples – heating process.....	83

Fig. 89 DSC curves of two tested samples – process of cooling down .....	84
Fig. 90 Specific heat capacity curves for the two tested samples .....	85
Fig. 91 Tested samples Creep test and their dimensions .....	87
Fig. 92 Test setup creep test .....	88
Fig. 93 Working principle of the creep test setup. The arrows show the way in which the weight and loads are applied .....	88
Fig. 94 Calibration of the test setup, such that the desired tensile load is added to the sample .....	89
Fig. 95 Failed test specimens. As can be seen the specimens failed at the connection points .....	89
Fig. 96 Obtained creep curves .....	90
Fig. 97 Second attempt to create suitable test specimens for this test .....	91
Fig. 98 Test setup creep test .....	92
Fig. 99 Test samples - creep test 2 .....	93
Fig. 100 Local constriction due to plastic deformation .....	93
Fig. 101 Creep curve 800N-test .....	94
Fig. 102 Logarithmic creep curve 800N-test .....	94
Fig. 103 Sample 500N-test after test performance: no constriction is visible this time .....	95
Fig. 104 Creep curve 500N-test .....	95
Fig. 105 Logarithmic creep curve 500N-test .....	96
Fig. 106 Compressive and buckling test specimen as they came out of the printer .....	98
Fig. 107 Dimensions and print orientation of tested hollow cubes .....	99
Fig. 108 Compressive samples before testing .....	99
Fig. 109 Dimensions and print orientation of buckling specimen .....	100
Fig. 110 Buckling specimens before testing .....	100
Fig. 111 Left: Test setup. Right: direction of the applied load .....	101
Fig. 112 Test setup – buckling test .....	101
Fig. 113 Tested compressive samples .....	102
Fig. 114 Weak corner of hollow cube samples at which the samples failed .....	102
Fig. 115 Obtained Force-displacement curves of the compressive tests .....	103
Fig. 116 Test-Column F1, during the test and directly after the test .....	104
Fig. 117 Column F2 during and after the test. The sample seems to fold back completely. ....	104
Fig. 118 Testing the column F2 for a second time. This time a small permanent deformation at the side is visible after the test (picture right). ....	105
Fig. 119 Buckling curves for F1 and F2, of which the latter that is tested twice. Although sample F2 moved back to about its original form after the test, it is obvious that the strength performance has been decreased after the first test .....	105
Fig. 120 Left the tested solid cube (paragraph 5.3) and right the tested hollow cube of this paragraph .....	106
Fig. 121 Buckling mechanism of the overall column .....	108
Fig. 122 General buckling case that is best applicable to the test situation [Hartsuijker et al, 2007] .....	109
Fig. 123 Buckling mechanism of individual walls .....	110
Fig. 124 Graphical representation of the tested bending blocks .....	112
Fig. 125 The solid bending blocks – type A and B .....	113
Fig. 126 The beams of type C with a square hollow section .....	114
Fig. 127 Beams of type D – Square hollow section with inner structure .....	114
Fig. 128 Beam types E, laid down in the orientation in which they will be tested .....	115

Fig. 129 Test setup for blocks A and B.....	115
Fig. 130 Test setup Block type C (left) and block type D (right) .....	116
Fig. 131 Test setup Block E1 and E2 (left) and Block E3 and E4 (right) .....	117
Fig. 132 Left: block type A in bending with its grain in the bending direction. Right: Block type B, which has its grain perpendicular to the direction of bending. ....	117
Fig. 133 Left: Permanent deformation of Block type A (left) and all the tested solid blocks (right) .	117
Fig. 134 Force-displacement curves block types A and B.....	118
Fig. 135 Determination of the Load at the conventional deflection $S_c$ .....	118
Fig. 136 Load case flexural test .....	119
Fig. 137 Flexural stress in the solid block, caused by the drawn bending moment.....	119
Fig. 138 Load scheme of the performed 4-point bending test.....	120
Fig. 139 Testing of block C1, failure probably occurs due to local bending of the top flange or local buckling of the web, around the area where the line load is applied .....	121
Fig. 140 Testing of Block C2, as can be observed the block ruptures at the connection between two printed lines.....	122
Fig. 141 Testing procedure of block type D.....	122
Fig. 142 Testing of blocks E1 and E2, the beam bends as whole but shows local buckling of the webs .....	122
Fig. 143 Testing of blocks E3 and E4, only a small load can be applied due to local bending of the top-flange.....	123
Fig. 144 Force-displacement curves of the tested geometries C to E .....	123
Fig. 145 Local inaccuracies that were observable on the C-geometries, prior to the test. The red-circled spot on geometry C2 is the location where rupture would take place during the test. ....	126
Fig. 146 Local inaccuracies in block C2, observable right after application of the load. As can be seen, the rupture process around the red-circled weak spot already starts right after the application of the load.....	126
Fig. 147 Shear stress distribution in cross section of beam C .....	128
Fig. 148 left: local bending mechanism of horizontal top flange. Right: buckling mechanism of vertical beam web.....	129
Fig. 149 left: the span of the top flange is halved compared to beam C. right: the compressive axial force within the webs is approximately halved as well .....	130
Fig. 150 The applied line load is transmitted by three walls/webs.....	131
Fig. 151 Local web buckling due to the compressive force that is caused by the overall bending of the beam.....	132
Fig. 152 The applied line load causes local bending of the top flange of the beam .....	132
Fig. 153 Comparison between the printing polymer and general applied structural materials. Above left: comparison of the tensile and compressive strengths, above right: comparison of tensile strengths and elongations, below left: comparison of Young's Moduli and densities, below right: Comparison of the bending strengths.....	139
Fig. 154 Left: comparison between printable polymer and general structural materials on the water absorption versus the density. Right: comparison on the melting point and specific heat capacity .	140
Fig. 155 Comparison between the printing polymer and polymers that are commonly applied in the construction industry. Above left: comparison of the tensile and compressive strengths, above right: comparison of tensile strengths and elongations, below left: comparison of Young's Moduli and densities, below right: Comparison of the bending strengths.....	140

Fig. 156 Comparison between printable polymer and polymers that are commonly applied in the construction industry. Left: comparison on the water absorption versus the density. Right: comparison on the melting point and specific heat capacity .....	141
Fig. 157 Above left: Weight distribution curve of the printing polymer [Marchese, 2014], Above right: common molecular mass rates of PC set against the associated tensile strength [Gilmore, 2014 ], Below right: table showing average molecular weights and number molecular weights of common applied PVC's [Titow, 1984 ], Below left: table showing molecular masses of common applied CFRP's. [Composites world, 2014] .....	142
Fig. 158 Cost comparison between the printing polymer and commonly applied structural materials .....	143
Fig. 159 Cost comparison between the printing polymer and polymers that are commonly applied in the construction industry .....	143
Fig. 160 Example of a satisfactory structural composition for a 3 meter-high printable wall .....	147
Fig. 161 Example of a satisfactory structural composition of a 1.8 meter-spanning printable floor.	148
Fig. 162 Example of a satisfactory geometry in which floor and wall are combined in one printable block. In this way, no complex connections are necessary between horizontal and vertical oriented elements .....	149



# List of Tables

Table 1	Conditions to which the building material will be exposed to and the properties that describe the behavior of the material under these conditions .....	11
Table 2	Material Properties that actually should be known in order to guarantee a safe application of the material [Verver et al 2004, McCrum 2003, Kenneth et al 2009].....	16
Table 3	Henkel factsheet for the Macromelt 6900E polymer [Henkel, 2011] .....	17
Table 4	Overview of mechanical material properties that are essential to be known for this building project .....	19
Table 5	Overview of physical material properties that are essential to be known for this building project .....	19
Table 6	Different specimen-variations that should be made for the tensile- and shear-test in order to test the influence of the printing plane, the grain-direction and the resolution on the mechanical properties of the material .....	26
Table 7	The following resolution-variations should be studied for the compressive samples, in order to study the influence of the resolution on the compressive strength .....	26
Table 8	Properties to obtain within the Tensile test [Hartsuijker, 2005].....	35
Table 9	Available test specimens for the Tensile test .....	36
Table 10	Set dimensions for the gauge area within the control program .....	37
Table 11	Numerical results for the xz-specimens that are tested within the grain direction.....	38
Table 12	Numerical results of the tested xz-samples that have their grains perpendicular to the load direction. ....	39
Table 13	Numerical results of the samples that are loaded 45 degrees to the grain direction.....	40
Table 14	Comparison between the obtained tensile strengths for the different grain directions within the xz-plane .....	40
Table 15	Test results of the specimens that are printed within the xy-plane and tested in the grain direction .....	41
Table 16	Test results of the tensile specimens that are printed within the xy-plane and loaded perpendicular to the grain direction .....	42
Table 17	Test results for the specimens that are printed within the xy-plane and loaded in tensile, 45 degrees to the grain .....	43
Table 18	Comparison between the obtained tensile strengths for the all the different orientations	44
Table 19	Properties that need to be obtained within the Shear test .....	46
Table 20	Test specimens that are available for the shear test.....	46
Table 21	Set dimensions of the loaded shear area within the control program .....	48
Table 22	Test results of shear samples printed in xz-plane and tested in shear perpendicular to the grain direction .....	49
Table 23	Results of xz-specimens tested in shear parallel to the grain direction .....	50
Table 24	Test results of xz-specimens, loaded 45 degrees to the grain, in shear.....	51
Table 25	Comparison between the obtained test results of xz-specimens that are loaded in shear perpendicular to the grain (0°), parallel to the grain (90°) and under an angle of 45° to the grain .....	52
Table 26	Results of test specimens printed within the xy plane and loaded in shear perpendicular to the grain .....	54
Table 27	Test results of xy-specimens that are loaded in shear parallel to the grain direction .....	55

Table 28	Test results of specimens that are printed within the xy-plane and loaded 45 degrees to the grain.....	56
Table 29	Comparison of the shear strengths for all the different orientations.....	57
Table 30	Compressive properties that need to be found by means of the Compressive Test.....	58
Table 31	Available test specimens for the compressive tests.....	59
Table 32	Test results for specimens that are loaded in direction 1.....	61
Table 33	Test results for specimens that are loaded in direction 2.....	62
Table 34	Test results for specimens that are loaded in direction 3.....	63
Table 35	Different Young's Moduli to obtain within this test.....	65
Table 36	Test specimens that are available for this test.....	65
Table 37	Dimensions that are set in the control program for the gauge area.....	66
Table 38	Test results Extensometer-tests.....	68
Table 39	Test results density test.....	70
Table 40	Test results absorption test.....	72
Table 41	Test results Dry test.....	73
Table 42	Properties that need to be obtained within the temperature-strength test.....	74
Table 43	Specimens that are tested in the Temperature-Strength test.....	75
Table 44	Dimensions that are set for the gauge area.....	76
Table 45	Intended surface temperatures of the tested samples.....	76
Table 46	Test results Temperature-Strength test.....	79
Table 47	Properties to obtain within DSC Test.....	81
Table 48	Test setting DSC test.....	82
Table 49	Test results DSC test.....	85
Table 50	Test results 50kg creep test.....	90
Table 51	Test results 80 kg creep test.....	90
Table 52	Dimensions tested creep specimens.....	93
Table 53	Compressive strengths of the tested hollow cubes.....	103
Table 54	Test results – Buckling Test.....	106
Table 55	Test results – compressive tests performed on solid cubes (paragraph 5.3).....	107
<b>Table 56</b>	<b>Test results – compressive tests performed on hollow cubes. As can be read, the strength differences with the compressive tests performed on solid cubes (table 55) are significant.</b> .....	107
Table 57	Test results of tested square hollow columns.....	108
Table 58	Flexural properties to obtain.....	111
Table 59	Test settings flexural test.....	116
Table 60	Test settings - geometry bending tests.....	116
Table 61	Results table flexural test - solid blocks.....	121
Table 62	Flexural properties parallel and perpendicular to the grain, as obtained from the test.....	121
Table 63	Size and dimensional properties of the tested geometries.....	124
Table 64	Flexural properties of the tested geometries, as obtained from the test.....	124
Table 65	Flexural properties solid blocks compared to tensile properties from chapter 5.....	125
Table 66	Flexural properties - block type C.....	125
Table 67	Tensile strengths perpendicular to the grain as obtained in chapter 5.....	127
Table 68	Shear strength perpendicular to the grain.....	128
Table 69	Flexural strength properties block type D.....	130
Table 70	Flexural properties - blocks of type E.....	131





[Source: Dave de Vaal]